University of Alberta

Molecular and functional bases of coordination in early branching metazoans – insights from physiology and investigations of potassium channels in the Porifera

by

Gabrielle Jean Tompkins MacDonald

A thesis submitted to the Faculty of Graduate Studies and Research
in partial fulfillment of the requirements for the degree of

Doctor of Philosophy
in
Physiology, Cell and Developmental Biology

Biological Sciences

Fall 2010
Edmonton, Alberta

Examining Committee

Sally Leys, Supervisor, Biological Sciences

Warren Gallin, Biological Sciences

Andrew Waskiewicz, Biological Sciences

Peter Light, Pharmacology

Peter Anderson, External Examiner, Whitney Laboratory for Marine Bioscience

For my family, who have rallied around me

Abstract

Sponges are filter feeders that lack nerves and muscle but are nonetheless able to respond to changes in the ambient environment to control their feeding current. Cellular sponges undergo coordinated contractions that effectively expel debris. Syncytial sponges propagate action potentials through their tissue, causing immediate flagellar arrest. Understanding the basis of this coordination in sponges is of interest for the insight it provides on mechanisms of coordination in early branching animals. However, when I began this thesis no ion channels had been described from the Porifera. I adopted a multifaceted approach to studying the conduction system of sponges. This included cloning and characterizing potassium channels as a means to understanding the underlying ionic currents, and monitoring regulation of the sponge feeding current in response to environmental stimuli. The latter experiments provided a functional context. The glass sponges *Rhabdocalyptus dawsoni* and *Aphrocallistes vastus* arrest feeding in response to mechanical disturbance and to sediment in the incurrent water – suggesting a protective role. Monitoring patterns of feeding current arrests also revealed several features of the glass sponge conduction system: pacemaker activity, mechanosensitivity, distinct excitability thresholds, and tolerance to repeated stimuli. With access to the genome of the demosponge *Amphimedon queenslandica* I have also cloned and characterized the first sponge ion channels. Inward rectifier potassium (Kir) channels were prioritized for their role in regulating excitability. Kir channels cloned from *A. queenslandica* shared critical residues and a strong rectifying phenotype with Kir channels typically expressed

in excitable cells. A variety of potassium channels from *A. queenslandica* indicate great diversity and a foundation for coordination at the dawn of the Metazoa.

Acknowledgements

My sincere thanks to my supervisors Sally Leys and Andy Spencer, and committee members Warren Gallin and Andrew Waskiewicz for your feedback, guidance and patience. I am appreciative of additional support and/or training provided by Malcolm and April Hill and Linda Boland (University of Richmond), Declan Ali, Gary Ritzel, James Maclagan, Lorne LeClaire, George Braybrooke, Tara Klassen, Rheanna Sand, Donna Atherton and the staff of the Molecular Biology Service Unit (University of Alberta) and the Bamfield Marine Sciences Center. I am grateful for the mentorship in teaching offered by Louise McBain and Carla Starchuk. Thank you also to the members of the Leys lab. This research was funded by an Alberta Ingenuity Studentship and NSERC PGSD as well as NSERC grants to SP Leys and AN Spencer.

Table of Contents

CHAPTER 1: INTRODUCTION……1
1.1 Comparative approaches to the origin of the nervous systems 1
1.2 Selecting phylogenetically relevant animals from which to infer origins of nerves and coordination systems 3
1.2.1 Origin of nerves 3
1.2.2 Origin of coordination systems 4
1.3 Historical approaches to studying the origin of nerves.....6
1.3.1 Cnidarian neuroanatomy and the origin of nerves.....6
1.4 Cataloguing "nervous molecules" to gain insight into the origin of coordination systems.....7
1.4.1 Cnidarians.....7
1.4.2 Many molecules involved in active signalling predate the nervous system.....8
1.4.2.1 Neurotransmitters, neuropeptides and ion channels may mediate signalling in plants and unicellular eukaryotes 9
1.4.3 What were the mechanisms of coordination and underlying molecular mechanisms in ancestral metazoans?.....11
1.5 Sponges as model organisms to study the origin of Metazoan coordination systems.....12
1.6 Thesis outline.....14
1.7 References 23

CHAPTER TWO: ELECTRICAL CONDUCTION IN GLASS SPONGES: ENVIRONMENTAL REGULATION OF FEEDING CURRENT ARRESTS 35
2.1 Introduction 35
2.2 Materials and Methods.....39
2.2.1 In situ observations 39
2.2.2 Ex situ experiments.....40
2.2.3 Scanning electron microscopy.....44
2.3 Results.....45
2.3.1 In situ observations 45
2.3.2 Ex situ (tank) experiments.....46
2.3.2.1 Spontaneous arrests.....46
2.3.2.2 Responses to mechanical and sediment stimuli 47
2.3.2.3 Acclimation to small amounts of sediment.....48
2.3.2.4 Response to continuous sediment.....49
2.3.3 Composition of sediment and fine structure of the aquiferous system.....50
2.4 Discussion 51
2.4.1 Physiological significance of feeding current arrests 52
2.4.2 The function of the arrest response.....54
2.4.3 Ecological implications of sensitivity to sediment 56

2.5 Concluding remarks 58
2.6 References 69

CHAPTER THREE: CLONING AND CHARACTERIZATION OF INWARD RECTIFIER POTASSIUM CHANNELS FROM THE DEMOSPONGE *AMPHIMEDON QUEENSLANDICA* 76
3.1 Introduction 76
3.2 Materials and Methods 82
3.2.1 Isolation of cDNAs and DNA sequencing 82
3.2.1.1 RNA extraction 82
3.2.1.2 cDNA synthesis 83
3.2.2 Amplification of ion channel sequences 86
3.2.3 Inverse and RACE-PCR 89
3.2.4 Amino acid sequence and phylogenetic analysis 91
3.2.5 Functional Expression in Oocytes 92
3.2.5.1 Ligation into expression vector 92
3.2.5.2 cRNA synthesis 93
3.2.5.3 Oocyte preparation 94
3.2.5.4 Electrophysiology 95
3.3 Results and Discussion 97
3.3.1 Cloning and sequencing AmqKirA and AmqKirB 97
3.3.2 Phylogenetic Analysis and Primary Structure 98
3.3.3 Expression in oocytes 100
3.3.3.1 Electrophysiological properties 100
3.3.3.2 Selectivity for K^+ 102
3.3.3.3 Block by external Cs^+, *and* Ba^{2+} *and* Na^+ 104
3.3.3.4 Block by tertiapin-Q 106
3.4 Concluding remarks and directions for future research 107
3.4.1 Functional significance and mechanism of strong inward rectification 107
3.4.2 Future directions 110
3.5 References 132

CHAPTER FOUR: *AMPHIMEDON QUEENSLANDICA* POTASSIUM CHANNELS: EVIDENCE FROM CLONING AND ASSEMBLY FROM THE GENOME TRACE FILES 143
4.1 Introduction 143
4.2 Materials and methods 147
4.2.1 Searching the *Amphimedon queenslandica* genome for K^+ channel sequences 147
4.2.2 Two pore potassium (K2P) channels 149
4.2.2.1 Cloning K2P channels 149
4.2.2.2 Preparation of K2P complementary RNA 151
4.2.2.3 K2P functional expression in oocytes 152
4.2.3 Cloning of potassium tetramerization domain containing genes 154

4.2.4 Partial cloning of a putative cyclic nucleotide gated potassium channel....156
4.2.5 Attempted cloning of a putative slo family potassium channel....157
4.2.6 Amino acid sequence and phylogenetic analysis....159
4.3 Results and Discussion....159
4.3.1 Sequences retrieved by blast searches of *Amphimedon queenslandica* genome trace files....160
4.3.2 Sequences cloned from *A. queenslandica* cDNA....161
4.3.2.1 Two pore potassium channels....161
4.3.2.2 Potassium channel tetramerization domain containing (KCTD) proteins)....168
4.3.3 Putative *A. queenslandica* K channels. Partially cloned sequences....173
4.3.3.1 Cyclic nucleotide gated channels....174
4.3.3.2 Putative tetrameric potassium selective cyclic nucleotide gated channel (KCNG)....174
4.3.3.3 Functional and phylogenetic significance of tetrameric potassium selective cyclic nucleotide gated channels....177
4.3.4 Putative K^+ channel sequences from *A. queenslandica* trace files....179
4.3.4.1 Slo family of potassium channels....179
4.3.4.2 Putative voltage gated K channels....185
4.4 Summary and conclusions....186
4.4.1 The potassium channel complement of *A. queenslandica*....186
4.4.1.1 Summary of cloned potassium channel sequences....186
4.4.1.2 Summary of expected channels based on genome searching and partially cloned sequences....188
4.4.2 Directions for future ion channel research....188
4.5 References....209

CHAPTER FIVE: CONCLUSIONS AND DIRECTIONS FOR FUTURE RESEARCH....224
5.1 Sponges and the origin of conduction systems....224
5.2 Overview of multifaceted approach....224
5.3 Chapter 2 – Physiology of the glass sponge conduction system. Insights from the arrest response....226
5.4 Chapter 3 - Cloning and characterization of inward rectifier potassium channels....228
5.5 Chapter 4 - Two pore potassium channels and other channels – clues to the potassium channel complement of an early branching metazoan....229
5.6 Directions for future research....231
5.7 References....236

APPENDIX A:....240
A.1. Summary of attempts to clone sponge voltage gated potassium channel sequences....240

A.2. Primers used to amplify inward rectifier potassium channel sequences from *Amphimedon queenslandica.*.....245
A.3. Metazoan inward rectifier potassium channel protein sequences included in phylogenetic analyses. 247
A.4. Nucleotide sequences of inward rectifier potassium channels cloned from *Amphimedon queenslandica.*.....250
A.4.1. Nucleotide sequence of AmqKirA.....250
A.4.2. Nucleotide sequence of AmqKirB.....250

APPENDIX B: 251
B.1. List of sequences used to search *Amphimedon queenslandica* genome trace files for putative potassium channel sequences.....251

B.2. Predicted sequences of putative potassium channels compiled by Onur Sakarya and Ken Kosik, University of California at Santa Barbara.....254
B.3. Primers used to amplify putative potassium channel sequences from *Amphimedon queenslandica*.....259
B.4. *Amphimedon queenslandica* nucleotide sequences which match metazoan K channel sequences with expected values less than $1e^{-10}$.....261
B.5. Nucleotide sequences of cloned *Amphimedon queenslandica* two pore potassium channels. 271
B.6. List of two pore potassium channel sequences used in phylogenetic analyses 272
B.7. Cloned putative potassium tetramerization domain containing (kctd) protein 274
B.8. Evolutionary relationships of human potassium channel tetramerization domain containing proteins (kctd 1-21) and Amqkctd…….275

List of Tables

Table 3-1: Percentage amino acid identity of AmqKirA and AmqKirB with *Nematostella vectensis* (Nv) and vertebrate Kir channels..... 119

Table 4-1: Summary of partial putative potassium channel sequences assembled from the *Amphimedon queenslandica* genome trace files……....191

Table 4-2: Electrophysiological properties of mammalian two pore potassium channels adapted from O'Connell et al. (2002)..... 197

Table 4-3: Comparison of SubH_Kv and Sp-tetraKCNG sequences..... 206

List of Figures and Illustrations

Figure 1-1: Galen's views on human physiology, adapted from Ochs, 2004..... 18

Figure 1-2: Multiple proposed phylogenies for early branching metazoans. 19

Figure 2-1: Set up for in situ experiments, specimen collection and in tank experiments..... 60

Figure 2-2: Spontaneous arrests of pumping. 61

Figure 2-3: Arrest responses to mechanical and sediment stimuli. 62

Figure 2-4 :Incremental addition of 0.5 to 1 $g \cdot l^{-1}$ sediment to *R. dawsoni* (A) and *A. vastus* (B). 63

Figure 2-5: Gradual addition of sediment. 64

Figure 2-6: Long-term (2 to 4 h) addition of filtered (<25 μm) fjord sediment.... 65

Figure 2-7: Particles of fjord sediment from sponge collection sites viewed by SEM. 66

Figure 2-8: SEM of *A. vastus* (A to F) and *R. dawsoni* tissue (G). 67

Figure 3-1: Simplified map of PCR4®-TOPO® cloning vector adapted from www.invitrogen.com. 113

Figure 3-2: Simplified map of the pXT7 expression vector. 114

Figure 3-3: Simplified circuit for Two-Electrode Voltage Clamp of oocytes. ... 115

Figure 3-4: Ethidium bromide stained agarose gels (1%) showing AmqKir products. 116

Figure 3-5: LALIGN global alignment of predicted AmqKirA and AmqKirB amino acid sequences. 117

Figure 3-6: Kyte-Doolittle hydropathy plots for AmqKirA and AmqKirB..... 118

Figure 3-7: Multiple alignment of AmqKir with cnidarian and vertebrate Kir sequences. 120

Figure 3-8: Phylogenetic relationships between AmqKir channels and other metazoan inward-rectifier potassium (Kir) channels. 123

Figure 3-9: Ethidium bromide stained agarose gels (1%) showing procedure to obtain AmqKir cRNA. 125

Figure 3-10: Heterologous expression of sponge inward-rectifier potassium (Kir) channels. 126

Figure 3-11: Test of selectivity for K^+ over other monovalent cations. 128

Figure 3-12: Test of channel block of AmqKirA. 130

Figure 4-1: Summary of potassium channel types. 190

Figure 4-2: Ethidium bromide stained agarose gels (1%) showing AmqK2P products. 194

Figure 4-3: Primary structure and predicted topology of AmqK2P channel subunits..... 195

Figure 4-4: Partial clustalW alignment of predicted AmqK2P amino acid sequences with human K2P amino acid sequences. 198

Figure 4-5: Evolutionary relationships of metazoan two pore potassium channels inferred using Maximum Parsimony analysis in MEGA 4..... 199

Figure 4-6: Ethidium bromide stained agarose gel (1%) showing the initial AmqKCTD product. 201

Figure 4-7: Alignment of BTB domains of AmqKCTDA and group I human KCTD proteins with the tetramerization domains of Kv channels..... 202

Figure 4-8: Schematic representation of the *Strongylocentrotus purpuratus* tetrameric potassium selective cyclic nucleotide gated channel, Sp-tetraKCNG..... 204

Figure 4-9: Ethidium bromide stained 1% agarose gel showing putative Amq-tetraKCNG fragment..... 205

Figure 4-10: Proposed topology of large conductance (BK) calcium-activated potassium channels, adapted from Faber (2003). 207

List of Symbols, Abbreviations and Nomenclature

Symbol	Definition
Kir	Inward rectifier potassium channel
K2P	Two pore potassium channel
Kv	Voltage gated potassium channel
KCa	Calcium-activated potassium channel
KNa	Sodium-activated potassium channel
KCNG	Potassium selective cyclic nucleotide gated channel
KCTD	Potassium tetramerization domain containing protein
cRNA	Complementary ribonucleic acid
cDNA	Complementary deoxyribonucleic acid

Chapter 1: INTRODUCTION

1.1 Comparative approaches to the origin of the nervous systems

Nervous systems mediate many characteristic traits of animal life – including movement, the senses, and in some vertebrates, cognition. Biologists and philosophers alike have pondered the origin of the nervous system and its remarkable influence on the body. Reflecting a degree of awe at the complexity of animal faculties, early attempts to describe the basis of the nervous system took on mystical dimensions. Galen (200 AD) for example, saw nerves as narrow tubes which allowed animal spirits, the source of vitality, to circulate throughout the body (Figure 1-1) (reviewed in Ochs, 2004). These whimsical notions have been succeeded by modern perspectives and an appreciation of the importance of electrical signals in nervous function.

Comparative approaches have provided some of our most fundamental information on the physiology of the nervous system. Invertebrate models have been used as simplified correlates of signalling in vertebrates. For example, the squid giant axon was used in pioneering experiments unravelling the ionic basis of the action potential (Hodgkin et al., 1949). The sea slug *Aplysia californica*, which has large visible nerve cells, is a model organism for the study of learning-related synaptic plasticity (Roberts and Glanzman, 2003). Comparative approaches can *also* help us to infer the processes and selection steps that lead to the origin of neuro-sensory systems within the Metazoa and to their specialization within different phylogenetic groups. Working backward on an evolutionary

timeline this type of reasoning has been used to address some of the following questions. How did the chordate brain arise? How was the nervous system centralized? Where did nerves come from? And how did animals coordinate themselves before the advent of nerves? These questions can be addressed by comparing morphology, gene expression patterns, physiology and underlying molecules of metazoans that diverged before and after these major transitions.

As an example, ascidian (Urochordata) larvae are thought to closely resemble the hypothetical ancestor of all chordates and their nervous system is therefore considered a close approximation of a base model for chordate brain evolution (Arbas et al., 1991; Meinertzhagen and Okamura, 2001).

Similarly, the organization of cnidarian nervous systems may provide insight into the processes underlying centralization of the nervous system. Diffuse nerve nets are the most obvious feature of cnidarian nervous systems. However hydromedusae (Hydrozoa) have oral nerve rings interfacing with condensed neural tracts to form the functional equivalent of a central nervous system – integrating multiple synaptic inputs and serving a pacemaking role (Mackie and Meech, 1995a; Mackie and Meech, 1995b; Mackie and Meech, 2000; Mackie and Singla, 1975; Spencer and Arkett, 1984). There are a number of proposed scenarios for obtaining a ventralized (protostomes) or dorsalized (deuterostomes) central nervous system from a radial net (Holland, 2003). Nervous system asymmetry might have arisen when dorsal ventral patterning genes took on antineural activity. Body axis inversion would have had to occur secondarily in deuterostomes (Holland, 2003).

1.2 Selecting phylogenetically relevant animals from which to infer origins of nerves and coordination systems

1.2.1 Origin of nerves

Before selecting taxa in which to look for insights into evolution of nerves and coordination it is necessary to consider competing hypotheses on the relationships of early branching phyla. Each has different implications for the origins of neuro-sensory systems. For example, Dunn et al. (2008) compared expressed sequence tag (EST) data and found Ctenophores, animals with both a nervous system and striated muscle, to be the earliest diverging extant metazoans (Figure 1-2 A). Under this scenario, nerves would either have evolved twice – in the lineages giving rise to ctenophores and to a cnidaria-bilateria clade – or once, but have been lost from sponges and from placozoans. Phillipe et al. (2009) point out that the placement of ctenophores may be an artefact of long-branch attraction between ctenophores and the distantly related outgroup taxa. They improved resolution by more comprehensive species sampling and found instead that ctenophores and cnidarians form a coelenterate clade which is the sister group to the Bilateria (Figure 1-2B). In this more parsimonious scenario the nervous system evolved in the lineage giving rise to Eumetazoa (coelenterates and bilaterians). It makes sense then to explore properties and developmental origin of the coelenterate nervous systems to gain insight into the properties of ancient nervous systems. Research on cnidarians has been extensive. Select findings are summarized in sections 1.3 and 1.4.1.

Placozoans, small (1-4 mm in diameter) enigmatic metazoans which have only four known cell types but display an amoeboid-like creeping behaviour, (Grell and Ruthmann, 1991; Miller and Ball, 2005; Miller and Ball, 2008) may also be instructive in inferring the origin of nervous systems. Analyses by Philippe et al. (2009) (Figure 1-2B) indicate that placozoans diverged from the Eumetazoa before the advent of the nervous system. While placozoans lack nerves, homologues of genes expressed in the cnidarian nervous system which are thought to specify dorsal-ventral patterning of the nervous system are expressed in discrete cells in the margin of the placozoan *Trichoplax* (Hayward et al., 2001; Jakob et al., 2004; Miller and Ball, 2005). Marginal cells also express RFamide (Schuchert, 1993), an abundant cnidarian neuropeptide. These patterns are indicative of a sensory role. Some authors have suggested that placozoans are secondarily simple and the expression patterns are remnants of a nervous system in their ancestors (reviewed by Miller and Ball, 2005).

1.2.2 Origin of coordination systems

If we accept that the nervous system evolved in the lineage giving rise to coelenterates and bilaterians we also acknowledge the absence of a conventional nervous system in sponges and placozoans. Sponges have been described as colonial protozoans (Haeckel, 1874) or "long-lasting experiments in multicellularity far-removed from the main line of metazoan animals." (Hille, 2001). Counter to these views, phylogenetic analyses place both sponges and placozoans within the metazoan phylogenetic tree, and both lineages display

simple forms of behaviour (Leys and Meech, 2006; Pearse, 1989) – indicating that coordination systems predated the nervous system in the Metazoa. We cannot be sure of how the earliest multicellular animals sensed and responded to their environments. However we can formulate hypotheses based on the mechanisms and underlying molecular toolkits of the earliest branching extant metazoans.

Tree topologies based on mtDNA suggest that placozoans, not sponges, are the most basal metazoans (Dellaporta et al., 2006). Most phylogenies, including comparison of slowly evolving nuclear genes support the placement of placozoans as the sister group to the Eumetazoa (Cnidaria + Bilateria) (Srivastava et al., 2008), with sponges branching off earlier as the sister group to the Placozoa-Cnidaria-Bilateria clade. While Srivastava et al. (2008) did not include sequences from ctenophores to test the singular finding of Dunn et al. (2008) that ctenophores are the most basal, their analysis is consistent with the order of metazoan evolution deduced from numerous molecular phylogenies (Collins, 1998; Lavrov et al., 2005; Medina et al., 2001; Müller et al., 1998; Schütze et al., 1999); with sponges the most ancient lineage. The comprehensive phylogenomic data set assembled by Philippe et al. (2009) enriched in sequences from basal metazoans (placozoans, all four sponge lineages, ctenophores and cnidarians) drew the same conclusion (Philippe et al., 2009) (Figure 1-2B). Their analysis also contradicted previous 18S rRNA data which indicated that despite a common sponge body form, homoscleromorph sponges (Figure 1-2C) or calcareous sponges (Calcarea) are more closely related to eumetazoans than to siliceous sponges (Demospongiae and Hexactinellida). Were this true it would

suggest that a sponge-like animal gave rise to the Metazoa (Collins, 1998; Borchiellini et al, 2001; Sperling and Peterson, 2007). Analyses by Philippe et al. (2009) suggests the sponge body plan, including an aquiferous system and choanocyte chambers, evolved solely in the sponge lineage. Nonetheless, critical metazoan innovations, including mechanisms of coordination, will likely be reflected in extant sponges.

1.3 Historical approaches to studying the origin of nerves

1.3.1 Cnidarian neuroanatomy and the origin of nerves

A number of authors have looked to cnidarians to try to determine how nerves, the functional units of the nervous system, arose in the first place. Grundfest (1965) and Lentz (1968) proposed that neurons arose from cells that functioned in nutrient dispersal, either concurrent with or preceding sensory and conductive properties. Westfall believed primitive protoneurons had receptive, conductive and neurosecretory properties. In support of this, she described *Hydra* nerve cells with a sensory cilium at the receptor pole, a conducting segment and basal neurites that both synapse with effectors and contain neurosecretory material (Westfall, 1973). Others proposed an electrogenic origin of neurons. Parker (1919) proposed that the nervous system arose as pacemakers to coordinate independent effectors, such as groups of primitive muscle cells, while Pantin (1956) suggested that these pacemaking cells initially arose to coordinate existing diffuse networks. Mackie and Passano (1968) discovered that epithelial cells connected by low resistance pathways in hydromedusae were also excitable,

and Mackie (1970) went on to suggest that nerves arose from a similar tissue arrangement where cells are already connected for metabolic exchange and electrical current flow. Nerves with elongated conducting segments would have evolved out of the need to selectively excite subgroups of cells.

1.4 Cataloguing "nervous molecules" to gain insight into the origin of coordination systems

1.4.1 Cnidarians

The discovery of excitable epithelia coexisting with nerve cells, as well as the repeated occurrence of excitable epithelia throughout the animal kingdom (Mackie, 1970) highlights an important facet of evolution in nervous systems: that excitability can arise in different tissues, even within a single organism. Rather than attempt a gradual reconstruction of cellular movements and specializations underlying evolution of the nervous system, it seems more pertinent then to consider not which cell types gave rise to nerves but rather what neuronal molecules enable an electrically excitable phenotype when expressed under appropriate conditions (Mackie, 1990).

Interestingly, analyses of the finer details of the cnidarian nervous system show that although the nervous system is anatomically simple, cnidarian neurophysiology does not differ considerably from higher animals. *Nematostella* and *Hydra* genomes contain genes for axon targeting, synapse formation, vesicle transport and synaptic transmission (summarized in Watanabe et al., 2009). Peptidergic transmitter molecules have been localized to neurons and there is

evidence of cholinergic, serotinergic, dopaminergic, glutamatergic, taurinergic, nitrergic and monoaminergic transmitter pathways (Anderson, 2004; Arbas et al., 1991; Bouchard, 2004; Gillis and Anctil, 2001) and nitric oxide has been shown to modulate peristaltic contractions in the sea pansy *Renilla* (Anctil et al., 2005). Ionic currents and the structure of underlying ion channels - the so called "quintessential nervous molecules" (Kung, 1989) - are also largely conserved between cnidarians and higher metazoans. For example, Anderson and Greenberg (2001) compared cnidarian and mammalian L-type and non L-type voltage gated calcium (Ca_v) channels and found that the two cnidarian channels had greater identity with their mammalian counterparts than with each other, indicating that Ca_v channels diverged into the two subtypes prior to the origin of cnidarians. The Shaker family of voltage-gated potassium channels, which are critical to excitability throughout the Metazoa, are also diversified into subtypes in cnidarians (Jegla et al., 1995). Thus, it appears that many of the building blocks of higher metazoan nervous systems are already well established in cnidarians and thus were likely present in the ancestral eumetazoan or ureumetazoan. As Bullock and Horridge (1965) put it, cnidarians "give evidence of being too far along in evolution [of the nervous system] to aid directly in this question."

1.4.2 Many molecules involved in active signalling predate the nervous system

1.4.2.1 Neurotransmitters, neuropeptides and ion channels may mediate signalling in plants and unicellular eukaryotes

A brief survey of non-metazoan eukaryotes shows that analogues of many of the molecules which mediate active signalling in the nervous system pre-date the acquisition of a nervous system. Neurotransmitters – which in their simplest form are produced as a by product of cellular metabolism – are phylogenetically dispersed (Arbas et al., 1991). Neuropeptides and GABAergic and glutamatergic signalling pathways - which were thought until recently to be metazoan innovations (Prosser, 1989) – have now been identified in plants (Bouché et al., 2003; Davenport, 2002), and unicellular eukaryotes (Ramoino et al., 2003; Ramoino et al., 2010). These so called nervous molecules can be assembled into signalling systems reminiscent of the nervous system.

In plants electrical impulses are propagated over long distances at 2-20 $cm \cdot s^{-1}$ through long chains of phloem cells electrically linked by plasmodesmata (Fromm and Lautner, 2007). Action potentials trigger inhibition of photosynthesis (Koziolek et al., 2004), changes in gene expression (Stankovic and Davies, 1996; Wildon et al., 1992), upregulation of respiration following pollination (Fromm et al., 1995; Sinyukhin and Britikov, 1967) and downregulation following cold shock (Fromm and Lautner, 2007). In their most animal-like manifestation, plant action potentials trigger instant trap closure in the Venus fly trap (Sibaoka, 1969) and folding of leaflets in *Mimosa* (Fromm and Eschrich, 1988; Sibaoka, 1966; Sibaoka, 1969).

Homology with metazoan nervous systems has also been implied by the naming schemes used for plant ion channels. Pilot et al. (2003) borrowed the term Shaker from metazoan potassium channels that govern excitability, and applied it to a group of plant 6 transmembrane potassium channels in plants. However, the authors' phylogenetic analyses show that metazoan Shaker channels are one of the least related groups of metazoan 6 transmembrane K channels. Plant Shaker channels instead group more closely with metazoan KCNH (eag related), HCN (inward rectifier) and metazoan and plant CNG (cyclic nucleotide gated) channels.

Moreover, although plant action potentials are all-or-none with absolute and relative refractory periods like animals, the underlying ionic currents are fundamentally different with Cl^- efflux rather than Na^+ or Ca^{2+} influx depolarizing the membrane (Wacke and Thiel, 2001). Thus, although plants have evolved rapid conduction systems the underlying mechanisms differ, presumably from hundreds of millions of years of modification of molecular building blocks present in their unicellular ancestors.

Unicellular eukaryotes, despite their apparent simplicity, sense and respond to a variety of environmental stimuli – mechanical, thermal, chemical, photic and ionic – and have been variously described as "conscious cells" (Margulis, 2001) and free-swimming sensory cells (Mackie, 1990). In *Blepharisma* a transmitter molecule resembling serotonin is employed as a mating pheromone (Miyake, 1984) and changes in membrane currents modulate contractile and ciliary systems as in metazoans (Machemer, 2007; Saimi and

Kung, 1987). Ionic currents in *Paramecium* are surprisingly well characterized owing to the use of genetic dissection approaches. Mutants selected by swimming assays are easily cultured providing large amounts of starting material for electrophysiological and molecular characterization (Hennessey, 1989). A diversity of calcium and potassium currents contribute to calcium-based action potentials as seen in many invertebrates (Jan and Jan, 1997; Jeziorski et al., 2000). Comparison of protozoan and metazoan sequences, however, indicate that ion channels are not homologous. For example the Shaker family of voltage-gated potassium channels, which are critical to excitability throughout the Metazoa, had fully diversified in cnidarians (Jegla et al., 1995) is not present in *Paramecium* (Jegla and Salkoff, 1995).

1.4.3 What were the mechanisms of coordination and underlying molecular mechanisms in ancestral metazoans?

The previous section emphasized that many molecules we typically associate with mediating signalling in nervous systems, including neurotransmitters and ion channels can be organized into signalling systems in non-metazoan eukaryotes. However, phylogenetic comparisons indicate that ion channels in metazoans are distinct. The conservation of Shaker and voltage gated calcium channels between cnidarians and higher metazoans intimates that the complement of ion channels in the nervous system was established early in animal evolution and has changed very little. In asking how the nervous system arose then it makes sense to focus on understanding how the neuronal building blocks, including ion channels, were modified over time to yield rapid conduction

systems within the Metazoa. Understanding the basis of coordination in the most basal metazoans both helps in identifying the components enabling an excitable phenotype in the absence of nerves, and provides a baseline against which modified building blocks in more derived metazoans can be gauged.

1.5 Sponges as model organisms to study the origin of Metazoan coordination systems

I have already argued that sponges (Porifera) are the earliest branching extant metazoans and that they are therefore a phylogenetically relevant lineage from which to infer properties of the earliest animals. Sponges are sessile filter feeders. They have a unique body plan that is perforated by a water-filled canal system. Water currents are generated by flagella in chonaocyte chambers at the interface between incurrent and excurrent systems (Leys et al., 2005). Food entrained in water currents is processed by the tissue before water is expelled through a central osculum or oscula.

Sponges lack conventional nerves and muscle but display coordinated responses (reviewed by Leys and Meech, 2006), the bases of which may provide insight into the mechanisms and functional context of coordination systems in ancestral animals. Elliott and Leys (2007) and Nickel (2004 and 2007) have described coordinated full-body contractions in cellular sponges (Porifera: Demospongiae), which are thought to function in clearing the aquiferous system of particulate material. The mechanisms underlying sponge contractions have not been fully deciphered. Loewenstein (1967) recorded electric coupling between mechanically opposed sponge cells *in vitro*, however gap junctions or other low

resistance pathways for electric current flow have not been observed in intact tissues (Garrone et al., 1980; Green and Bergquist, 1979; Lethias et al., 1983). A second messenger pathway is implicated by the presence of glutamate/GABA-like metabotropic receptors and demonstration of glutamate induced contractions in demosponges (Elliott and Leys, 2010; Ellwanger et al., 2006; Perovic et al., 1999; Ramoino et al., 2007). External calcium was required for contraction in *E. muelleri* to propagate, suggesting involvement of a calcium wave. GABA inhibits contractions (Elliott and Leys, 2010), consistent with its role as an inhibitory neurotransmitter mediating muscle relaxation in other metazoans (Fagg and Foster, 1983). It thus appears that sponges coordinate behaviour using chemical messenger systems common to other animals.

Even more reminiscent of coordination in higher animals, is the presence of electrical signalling in glass sponges (Hexactinellida). These animals are unique in that the bulk of their tissue is a giant syncytium of fine strands draped over the skeleton (Leys, 1999; Mackie and Singla, 1983). This tissue conformation allows electric signals to propagate throughout the entire sponge, unimpeded by cell membranes, triggering flagellar arrest. Leys and Mackie (1997) confirmed the presence of all-or-none action potentials in *Rhabdocalyptus dawsoni* by recording from aggregates grafted to the body wall. Extracellular recordings indicate a Ca^{2+} potential with potassium repolarization (Leys et al., 1999). Intracellular recordings have not been obtained from any sponge due to the difficulty of penetrating the extremely thin cells or tenuous syncytial strands lining the surface. Patch recordings of isolated cells from a demosponge show

cation currents that are gated by arachadonic acid, suction and increase in temperature (Carpaneto et al., 2003; Zocchi et al., 2003; Zocchi et al., 2001) but due to the lack of electrical activity in that sponge's tissues, channel characteristics have not been further explored. Initial patch clamp recordings of aggregates of glass sponge tissue (*Rhabdocalyptus dawsoni*) show K^+ channels (Leys and Meech, unpublished). However, progress in recording from glass sponges is encumbered by the extreme difficulty of collecting and maintaining these deep water animals, along with the absence of poriferan ion channel information (Hille, 2001) on which to base pharmacological investigations.

1.6 Thesis outline

Understanding the functional context and mechanisms underlying coordination in sponges can help us to infer the nature of coordination in the earliest animals and can provide insight into the molecules conferring an excitable phenotype. As mentioned above, however, use of patch clamp or intracellular recordings to identify ionic currents regulating membrane physiology is complicated by the nature of sponge tissues. Moreover, glass sponges, the only sponges from which electrical signals are known, are located at great depth, are difficult to obtain on an ongoing basis (shallow populations at 30 m are sparse) and can only be maintained in good health in the Bamfield Marine Sciences Center seawater system.

The difficulty of the system necessitates a multifaceted approach wherein information on the functional context of sponge coordination systems is gleaned

from hexactinellids (*Rhabdocalyptus dawsoni* and *Aphrocallistes vastus*) and information on the molecules underlying membrane physiology gleaned by searching the genome of the demosponge *Amphimedon queenslandica* for ion channels sequences and basing cloning efforts on these sequences. This approach minimizes dependence on live animals while providing the first ion channel characterization for the Porifera.

Initial work included in tank experiments to test the arrest responses of the hexactinellid sponges *Rhabdocalyptus dawsoni* and *Aphrocallistes vastus* to natural stimuli including sediment. Since feeding current arrests coincide with the arrival of action potentials, recording arrests provides a convenient means of monitoring electrical activity and provides a functional context for the conduction system. This work forms the basis of Chapter 2, a version of which has been published (Tompkins-MacDonald and Leys, 2008).

I subsequently turned to the molecular basis of sponge coordination. I attempted degenerate cloning of ion channels from hexactinellids, prioritizing potassium channels. Potassium channels can be identified by a consensus "signature sequence" forming the selectivity filter in the pore domain –thr-X-X-thr-X-gly-tyr-gly-glu- (Heginbotham et al., 1992; Heginbotham et al., 1994) but are otherwise architecturally diverse. Generally speaking, channel families correlate to the stimuli that gate them, including voltage, cyclic nucleotides, ATP and G-proteins (Coetzee et al., 1999). Typically subunits have two, four or six transmembrane (TM) domains and functional channels form as dimers (4TM) or tetramers (2TM and 6TM), bringing together four pore-forming loops to line a

central ion conduction pathway. In metazoan nervous systems voltage gated potassium (Kv) channels from the Shaker family regulate action potential shape, duration and firing frequency (Hille, 2001). I had hoped to eventually correlate cloned Kv channels with ionic currents in the glass sponge action potential; however cloning efforts were unsuccessful. A survey of the genome of the demosponge *A. queenslandica* indicates the presence in sponges of a number of molecules typically associated with synapses. However, Shaker voltage-gated potassium channels, which were the target of my cloning efforts in hexactinellids, were not found (Sakarya et al. 2007).

Cloning efforts progressed however with the help of potassium channel sequences assembled from genome trace files of *A. queenslandica* by Onur Sakarya and myself. Using gene specific primers I have cloned several full-length potassium channels, including inward rectifier potassium channels (Kir) and two pore potassium channels (K2P) and present the electrophysiological characterization of Kir channels in Chapter 3. Electrophysiological experiments were completed in collaboration with Linda M. Boland at the University of Richmond, Richmond Virginia. A paper on the functional characterization of sponge inward rectifier potassium channels has been published (Tompkins-MacDonald et al., 2009).

Chapter 4 summarizes sequence data for *A. queenslandica* K2P channels, which were cloned but for which electrophysiological recordings were not possible. Additionally I present putative partial potassium channel sequences collected either through cloning or assembly of contiguous sequences from the *A.*

queenslandica genome. Together with Chapter 3 this information provides the first insight into the potassium channel complement of a sponge with insights into the molecular toolkit of ancestral metazoans.

Chapter 5 presents overall conclusions and suggestions for future research on coordination systems in the Porifera. My thesis provides functional insight into the conditions under which early metazoan coordination systems arose, and a view of the potassium channels available to mediate excitability within the Metazoa.

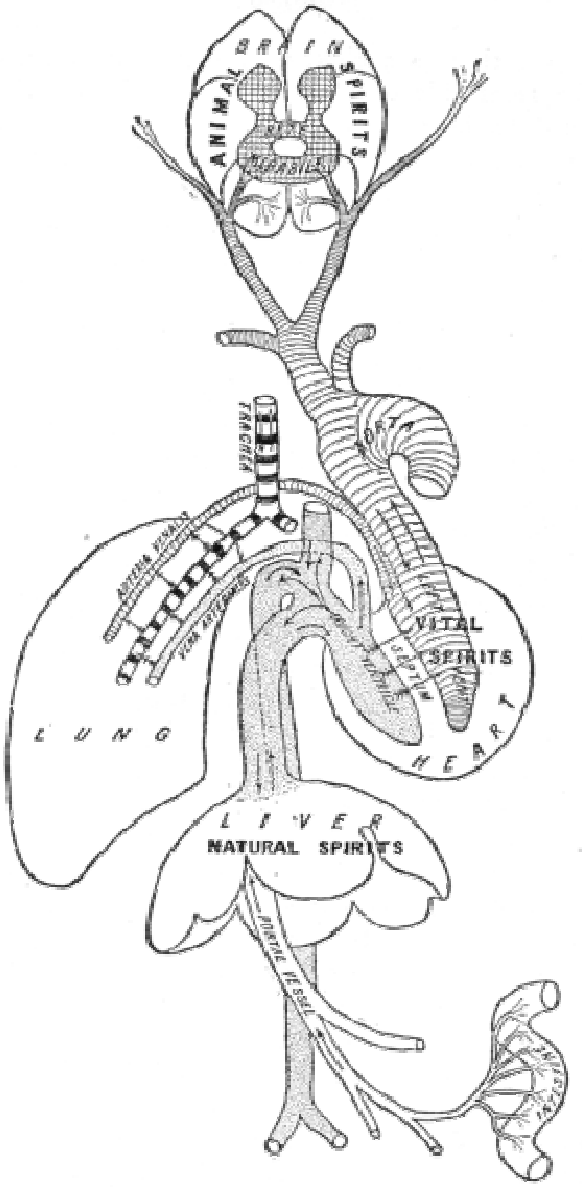

Figure 1-1: Galen's views on human physiology, adapted from Ochs, 2004.

Galen believed that nerves were hollow tubes that allowed the source of vitality, animal spirits, to circulate throughout the body.

Figure 1-2: Multiple proposed phylogenies for early branching metazoans.

Phylogenetic trees adapted from (A) Dunn et al., 2008, (B) Philippe et al., 2009 and (C) Sperling et al., 2007; showing a basal position of Ctenophora (A) or Porifera (B and C). (A) RaxML maximum likelihood analyses with 77 taxa and 1000 bootstrap replicates. Leaf stabilities (blue) are shown above each branch. (B) Bayesian analysis of 128 nuclear-encoded proteins using 100 bootstrap replicates. Bootstrap supports (BS) are indicated for analyses using three different outgroups: outgroup 1, pink; outgroup 2, blue; unrooted analysis, black. The tree obtained with outgroup 1 is shown. (C) Bayesian analysis of 30 eumetazoan taxa and 12 sponges rooted with the plant *Arabidopsis* and yeast *Saccaromyces*. The Porifera (dark grey box) are paraphyletic with the homoscleromorph *Oscarella* more closely related to eumetazoans than to other sponges. Calcisponges are more closely related to the epitheliozoans than to demosponges.

A

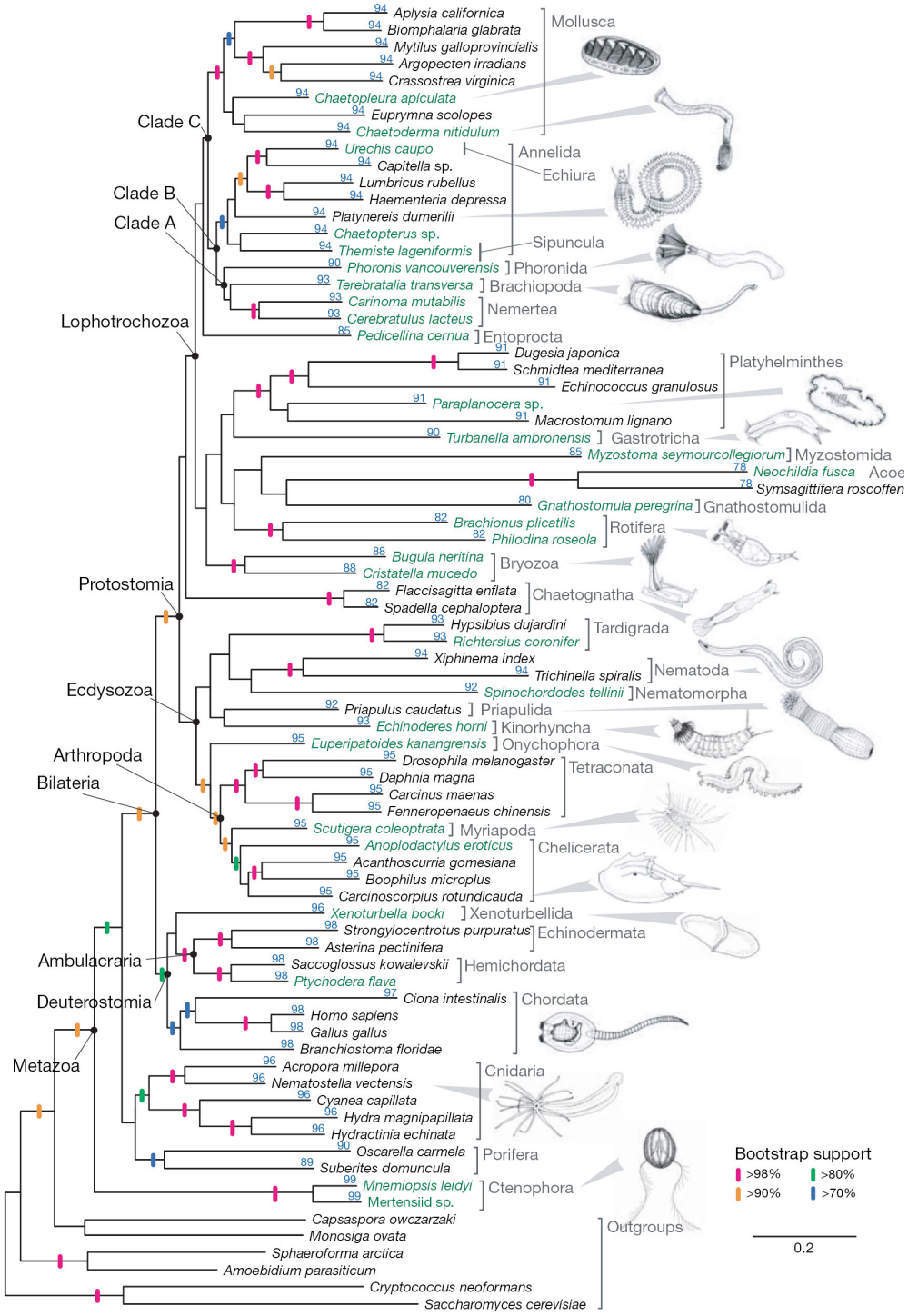
Aplysia californica
Biomphalaria glabrata
Mytilus galloprovincialis
Argopecten irradians
Crassostrea virginica
Mollusca
Chaetopleura apiculata
Euprymna scolopes
Chaetoderma nitidulum
Clade C
Urechis caupo
Capitella sp.
Annelida
Echiura
Lumbricus rubellus
Haementeria depressa
Clade B
Platynereis dumerilii
Clade A
Chaetopterus sp.
Themiste lageniformis
Sipuncula
Phoronis vancouverensis
Phoronida
Terebratalia transversa
Brachiopoda
Carinoma mutabilis
Cerebratulus lacteus
Nemertea
Lophotrochozoa
Pedicellina cernua
Entoprocta
Dugesia japonica
Schmidtea mediterranea
Platyhelminthes
Echinococcus granulosus
Paraplanocera sp.
Macrostomum lignano
Turbanella ambronensis
Gastrotricha
Myzostoma seymourcollegiorum
Myzostomida
Neochildia fusca
Acoe
Symsagittifera roscoffen
Gnathostomula peregrina
Gnathostomulida
Brachionus plicatilis
Philodina roseola
Rotifera
Bugula neritina
Cristatella mucedo
Bryozoa
Protostomia
Flaccisagitta enflata
Spadella cephaloptera
Chaetognatha
Hypsibius dujardini
Richtersius coronifer
Tardigrada
Xiphinema index
Trichinella spiralis
Nematoda
Spinochordodes tellinii
Nematomorpha
Priapulus caudatus
Priapulida
Ecdysozoa
Echinoderes horni
Kinorhyncha
Euperipatoides kanangrensis
Onychophora
Drosophila melanogaster
Daphnia magna
Tetraconata
Carcinus maenas
Fenneropenaeus chinensis
Arthropoda
Bilateria
Scutigera coleoptrata
Myriapoda
Anoplodactylus eroticus
Acanthoscurria gomesiana
Chelicerata
Boophilus microplus
Carcinoscorpius rotundicauda
Xenoturbella bocki
Xenoturbellida
Strongylocentrotus purpuratus
Asterina pectinifera
Echinodermata
Ambulacraria
Saccoglossus kowalevskii
Ptychodera flava
Hemichordata
Deuterostomia
Ciona intestinalis
Homo sapiens
Gallus gallus
Chordata
Branchiostoma floridae
Metazoa
Acropora millepora
Nematostella vectensis
Cnidaria
Cyanea capillata
Hydra magnipapillata
Hydractinia echinata
Oscarella carmela
Porifera
Suberites domuncula
Mnemiopsis leidyi
Ctenophora
Mertensiid sp.
Capsaspora owczarzaki
Monosiga ovata
Outgroups
Sphaeroforma arctica
Amoebidium parasiticum
Cryptococcus neoformans
Saccharomyces cerevisiae
Bootstrap support
>98%
>80%
>90%
>70%
0.2

B

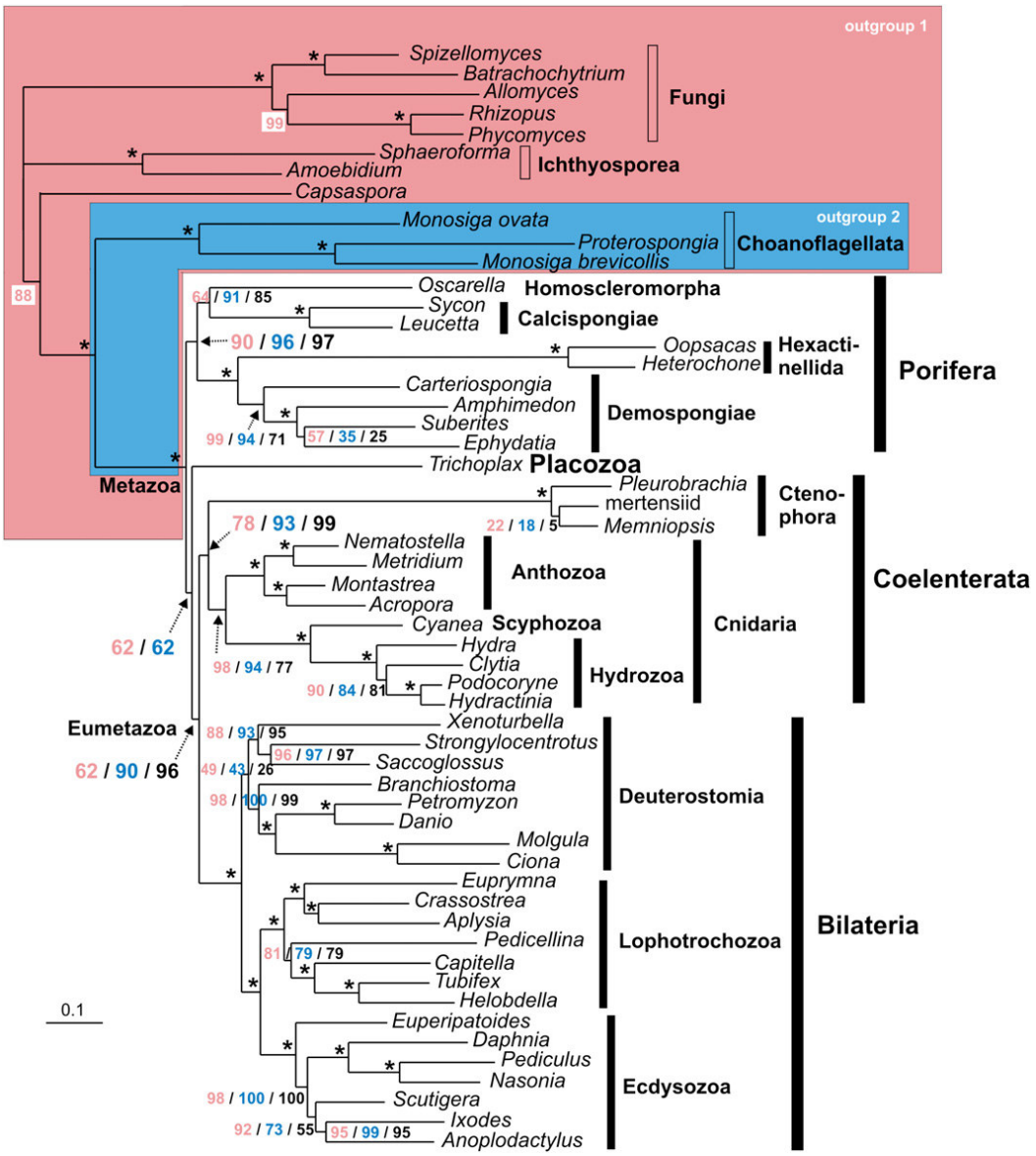
outgroup 1
Spizellomyces
Batrachochytrium
Allomyces
Rhizopus
Phycomyces
Fungi
Sphaeroforma
Amoebidium
Ichthyosporea
Capsaspora
outgroup 2
Monosiga ovata
Proterospongia
Monosiga brevicollis
Choanoflagellata
Metazoa
Oscarella
Homoscleromorpha
Sycon
Leucetta
Calcispongiae
Oopsacas
Heterochone
Hexacti-nellida
Carteriospongia
Amphimedon
Suberites
Ephydatia
Demospongiae
Porifera
Trichoplax
Placozoa
Pleurobrachia
mertensiid
Memniopsis
Cteno-phora
Nematostella
Metridium
Montastrea
Acropora
Anthozoa
Cyanea
Scyphozoa
Hydra
Clytia
Podocoryne
Hydractinia
Hydrozoa
Cnidaria
Coelenterata
Eumetazoa
Xenoturbella
Strongylocentrotus
Saccoglossus
Branchiostoma
Petromyzon
Danio
Molgula
Ciona
Deuterostomia
Euprymna
Crassostrea
Aplysia
Pedicellina
Capitella
Tubifex
Helobdella
Lophotrochozoa
Bilateria
Euperipatoides
Daphnia
Pediculus
Nasonia
Scutigera
Ixodes
Anoplodactylus
Ecdysozoa
0.1

C

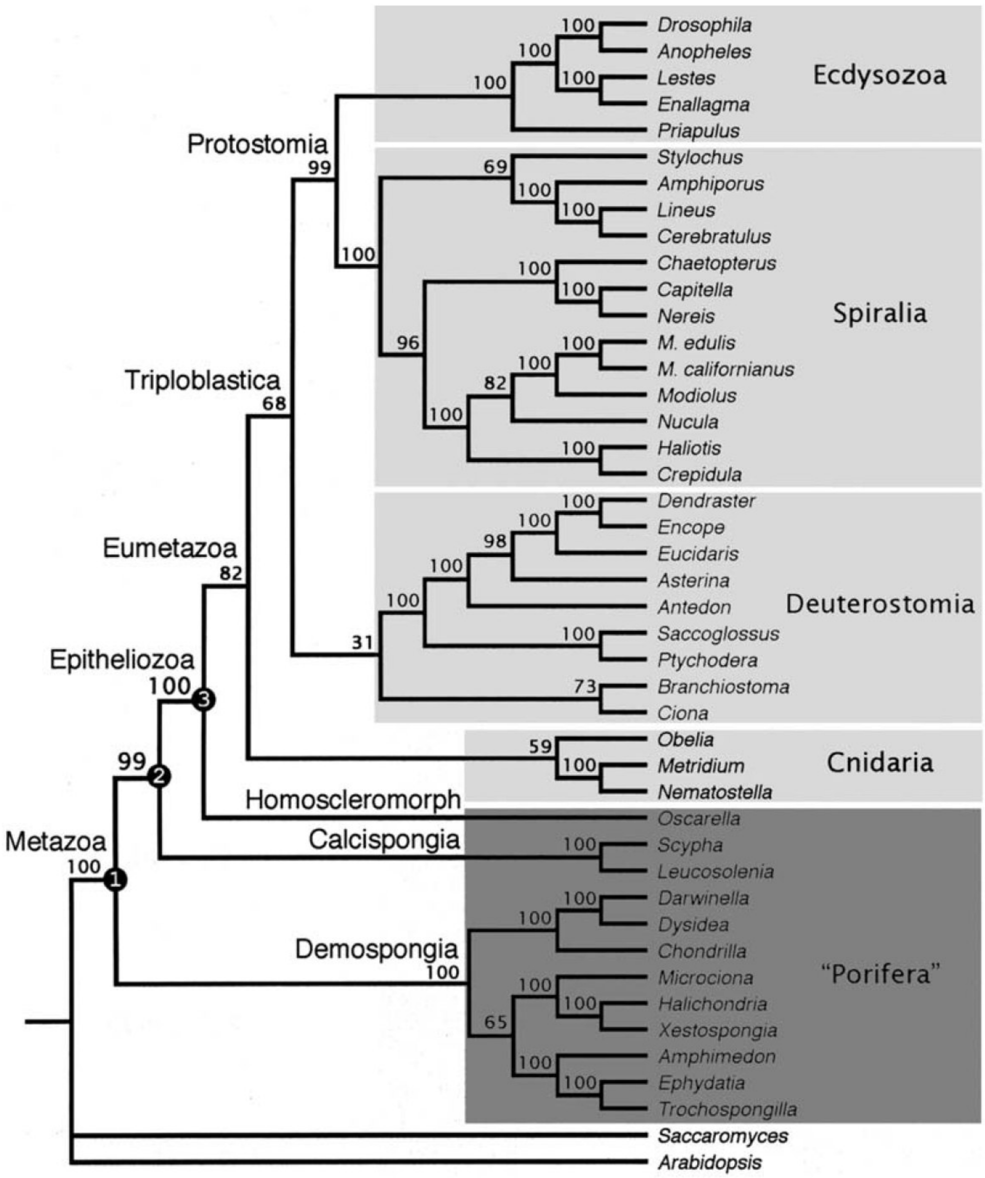
Drosophila
Anopheles
Lestes
Enallagma
Priapulus
Ecdysozoa
Protostomia
99
Stylochus
Amphiporus
Lineus
Cerebratulus
Chaetopterus
Capitella
Nereis
Spiralia
M. edulis
M. californianus
Modiolus
Nucula
Haliotis
Crepidula
Triploblastica
68
Dendraster
Encope
Eucidaris
Asterina
Antedon
Deuterostomia
Saccoglossus
Ptychodera
Branchiostoma
Ciona
Eumetazoa
82
Epitheliozoa
100
Obelia
Metridium
Nematostella
Cnidaria
99
Homoscleromorph
Oscarella
Calcispongia
Scypha
Leucosolenia
Metazoa
100
Darwinella
Dysidea
Chondrilla
Demospongia
100
Microciona
Halichondria
Xestospongia
"Porifera"
Amphimedon
Ephydatia
Trochospongilla
Saccaromyces
Arabidopsis

1.7 References

Anctil, M., Poulain, I. and Pelletier, C. (2005). Nitric oxide modulates peristaltic muscle activity associated with fluid circulation in the sea pansy *Renilla koellikeri*. *Journal of Experimental Biology* **208**, 2005-2017.

Anderson, P. A. V. (2004). Cnidarian neurobiology: what does the future hold? *Hydrobiologia* **530**, 107-116.

Anderson, P. A. V. and Greenberg, R. M. (2001). Phylogeny of ion channels: clues to structure and function. *Comparative Biochemistry and Physiology Part B* **129**, 17-18.

Arbas, E. A., Meinertzhagen, I. A. and Shaw, S. R. (1991). Evolution in Nervous Systems. *Annual Review of Neuroscience* **14**, 9-38.

Bouchard, C., P. Ribeiro, F. Dubé, C. Demers, M. Anctil. (2004). Identification of a novel aminergic-like G protein-coupled receptor in the cnidarian, *Renilla koellikeri*. *Gene* **341**, 67-75.

Bouché, N., Lacombe, B. and Fromm, H. (2003). GABA signaling: a conserved and ubiquitous mechanism *Trends in Cell Biology* **13**, 607-610.

Bullock, T. H. and Horridge, G. A. (1965). Structure and function in the nervous systems of invertebrates. San Francisco: W.H. Freeman & Co.

Carpaneto, A., Magrassi, R., Zocchi, E., Cerrano, C. and Usai, C. (2003). Patch-clamp recordings in isolated sponge cells (*Axinella polypoides*). *Journal of Biochemical and Biophysical Methods* **55** 179-189.

Collins, A. G. (1998). Evaluating multiple alternative hypotheses for the origin of Bilateria: An analysis of 18S rRNA molecular evidence. *Proceedings of the National Academy of Sciences* **95**, 15458-15463.

Davenport, R. (2002). Glutamate receptors in plants. *Annals of Botany* **90**, 549-557.

Dellaporta, S. L., Xu, A., Sagasser, S., Jakob, W., Moreno, M. A., Buss, L. W. and Schierwater, B. (2006). Mitochondrial genome of *Trichoplax adhaerens* supports Placozoa as the basal lower metazoan phylum *Proceedings of the National Academy of Sciences* **103**, 8751-8756.

Dunn, C. W., Hejnol, A., Matus, D. Q., Pang, K., Browne, W. E., Smith, S. A., Seaver, E., Rouse, G. W., Obst, M., Edgecombe, G. D. et al. (2008). Broad phylogenomic sampling improves resolution of the animal tree of life. *Nature* **452,** 745-750.

Elliott, G. R. D. and Leys, S. P. (2007). Coordinated contractions effectively expel water from the aquiferous system of a freshwater sponge. *Journal of Experimental Biology* **210**, 3736-3748.

Elliott, G. R. D. and Leys, S. P. (2010). Evidence for glutamate, GABA and NO in coordinating behaviour in the sponge, *Ephydatia muelleri* (Demospongiae, Spongillidae) *Journal of Experimental Biology* **213**, 2310-2321.

Ellwanger, K., Eich, A. and Nickel, M. (2006). GABA and glutamate specifically induce contractions in the sponge *Tethya wilhelma*. *Journal of Comparative Physiology A* **193**, 1-11.

Fagg, G. E. and Foster, A. C. (1983). Amino acid neurotransmitters and their pathways in the mammalian central nervous system. *Neuroscience* **9**, 701-719.

Fromm, J. and Eschrich, W. (1988). Transport processes in stimulated and non-stimulated leaves of *Mimosa pudica*. II. Energesis and transmission of seismic stimulations. *Trees* **2**, 18-24.

Fromm, J., Hajirezaei, M. and Wilke, I. (1995). The biochemical response of electrical signaling in the reproductive system of *Hibiscus* plants. *Plant Physiology* **109**, 375–384.

Fromm, J. and Lautner, S. (2007). Electrical signals and their physiological significance in plants. *Plant, Cell & Environment* **30**, 249-257.

Garrone, R., Lethias, C. and Escaig, J. (1980). Freeze-fracture study of sponge cell membranes and extracellular matrix. *Biol. Cell.* **38**, 71-74.

Gillis, M.-A. and Anctil, M. (2001). Monoamine release by neurons of a primitive nervous system: an amperometric study. *Journal of Neurochemistry.* **76**, 1774-1784.

Green, C. R. and Bergquist, P. L. (1979). Cell membrane specializations in the Porifera. *Colloq. Int. Cent. Natl. Rech. Sci.* **291**, 153-158.

Grell, K. and Ruthmann, A. (1991). Placozoa. In *Microscopic Anatomy of Invertebrates*, (eds. F. Harrison and J. Westfall), pp. 13-28. New York: Wiley-Liss.

Grundfest, H. (1965). Evolution of electrophysiological varieties among sensory receptor systems. In *Essays on physiological evolution*, (ed. J. W. S. Pringle), pp. 107-138. Oxford: Pergamon.

Haeckel, E. (1874). Die Gastraea-Theorie, die phylogenetische classification des thierreichs und die homologie der keimblätter. *Zeitschrift für Naturwissenshaft* **8**, 1–55.

Hayward, D. C., Catmull, J., Reece-Hoyes, J. S., Berghammer, H., Dodd, H., Hann, S. J., Miller, D. J. and Ball, E. E. (2001). Gene structure and larval expression of cnox-2Am from the coral *Acropora millepora*. *Development Genes and Evolution* **211**, 10-19.

Heginbotham, L., Abramson, T. & MacKinnon, R. (1992). A functional connection between the pores of distantly related ion channels as revealed by mutant K^+ channels. *Science* **258,** 1152-1155.

Heginbotham, L., Lu, Z., Abramson, T. & MacKinnon, R. (1994). Mutations in the K^+ channel signature sequence. *Biophysical Journal* **66,** 1061-1067.

Hennessey, T. M. (1989). Ion currents of *Paramecium*: effects of mutations and drugs. In *Evolution of the First Nervous System*, (ed. P. A. V. Anderson), pp. 215-235. New York: Plenum Press.

Hille, B. (2001). Ionic channels of excitable membranes. Sunderland, MA: Sinauer Associates, Inc.

Hodgkin, A. L., Huxley, A. F. and Katz, B. (1949). Ionic currents underlying activity in the giant axon of squid. *Archives des Sciences Physiologiques.* **3**, 129-150.

Holland, N. D. (2003). Early central nervous system evolution: an era of skin brains? *Nature Reviews Neuroscience* **4**, 617-627.

Jakob, W., Sagasser, S., Dellaporta, S., Holland, P., Kuhn, K. and Schierwater, B. (2004). The Trox-2 Hox/ParaHox gene of *Trichoplax* (Placozoa) marks an epithelial boundary. *Development Genes and Evolution* **214**, 170–175.

Jan, L. Y. and Jan, Y. N. (1997). Cloned potassium channels from eukaryotes and prokaryotes. *Annual Review of Neuroscience* **20**, 91-123.

Jegla, T., Grigoriev, N., Gallin, W. J., Salkoff, L. and Andrew N. Spencer. (1995). Multiple *Shaker* potassium channels in a primitive metazoan. *The Journal of Neuroscience* **15**, 7989-7999.

Jegla, T. and Salkoff, L. (1995). A multigene family of novel K^+ channels from *Paramecium Tetraurelia*. *Receptors and Channels* **3**, 51-60.

Jeziorski, M., Greenberg, R. and Anderson, P. (2000). The molecular biology of invertebrate voltage-gated $Ca^{(2+)}$ channels. *Journal of Experimental Biology* **203**, 841-856.

Koziolek, C., Grams, T. E. E., Schreiber, U., Matyssek, R. and Fromm, J. (2004). Transient knockout of photosynthesis mediated by electrical signals. *New Phytologist* **161**, 715–722.

Lavrov, D. V., Forget, L., Kelly, M. and Lang, B. F. (2005). Mitochondrial genomes of two demosponges provide insights into

an early stage of animal evolution. *Molecular Biology and Evolution* **22**, 1231-1239.

Lentz, T. L. (1968). Primitive nervous systems New Haven: Yale University Press.

Lethias, C., Garrone, R. and Mazzorana, M. (1983). Fine structure of sponge cell membranes: comparative study with freezefracture and conventional thin section methods. *Tissue and Cell* **15**, 523–535.

Leys, S., Mackie, G. and Meech, R. (1999). Impulse conduction in a sponge. *Journal of Experimental Biology* **202**, 1139-1150.

Leys, S. P. (1999). The choanosome of hexactinellid sponges. *Invertebrate Biology* **118**, 221-235.

Leys, S. P. and Mackie, G. O. (1997). Electrical recording from a glass sponge. *Nature* **387**, 29-30.

Leys, S. P. and Meech, R. W. (2006). Physiology and coordination of sponges. *Canadian Journal of Zoology* **84**, 288-306.

Leys, S. P., Rohksar, D. S. and Degnan, B. M. (2005). Sponges. *Current Biology* **15,** R114-R115.

Lowenstein, W. R. (1967). On the genesis of cellular communication. *Developmental Biology* **15**, 503-520.

Machemer, H. (2007). Cellular Behaviour Modulated by Ions: Electrophysiological Implications. *Journal of Eukaryotic Microbiology* **36**, 463-487.

Mackie, G. (1990). The Elementary Nervous System Revisited. *American Zoologist* **30**, 907-920.

Mackie, G. and Singla, C. (1983). Studies on hexactinellid sponges. I Histology of *Rhabdocalyptus dawsoni* (Lambe, 1873). *Philosophical Transactions of the Royal Society of London B* **301**, 365-400.

Mackie, G. O. (1970). Neuroid conduction and the evolution of conducting tissues. *Quarterly Review of Biology* **45**, 319-332.

Mackie, G. O. and Meech, R. W. (1995a). Central circuitry in the jellyfish *Aglantha digitale* I. The relay system. *Journal of Experimental Biology* **198**, 2261-2270.

Mackie, G. O. and Meech, R. W. (1995b). Central Circuitry in the jellyfish *Aglantha digitale* II. The ring giant and carrier systems. *Journal of Experimental Biology* **198**, 2271-2278.

Mackie, G. O. and Meech, R. W. (2000). Central circuitry in the jellyfish *Aglantha digitale*. III. The rootlet and pacemaker systems. *Journal of Experimental Biology* **203**, 1797-1807.

Mackie, G. O. and Passano, L. M. (1968). Epithelial Conduction in Hydromedusae. *Journal of General Physiology* **52**, 600-621.

Mackie, G. O. and Singla, C. L. (1975). Neurobiology of Stomotoca. I. Action systems. *Journal of Neurobiology* **6**, 339-356.

Margulis, L. (2001). The conscious cell. *Annals of the New York Academy of Sciences.* **929**, 55–70.

Medina, M., Collins, A. G., Silberman, J. D. and Sogin, M. L. (2001). Evaluating hypotheses of basal animal phylogeny using complete sequences of large and small subunit rRNA *Proceeding of the National Academy of Sciences* **98**, 9707-9712.

Meinertzhagen, I. A. and Okamura, Y. (2001). The larval ascidian nervous system: the chordate brain from its small beginnings. *TRENDS in Neurosciences* **24**, 401-410.

Miller, D. and Ball, E. (2005). Animal Evolution: The Enigmatic Phylum Placozoa Revisited. *Current Biology* **15**, R26-R28.

Miller, D. and Ball, E. (2008). Animal Evolution: *Trichoplax*, Trees, and Taxonomic Turmoil. *Current Biology* **18**, R1003-R1005.

Miyake, A. (1984). Blepharismone: A conjugation- inducing trypotophan derivative in the ciliate *Blepharisma*. In *Progress in tryptophan and serotonin research*, eds. H. G. Schlossberger W. Hocken B. Linzen and H. Steinhart), pp. 807-813. De Gruyter, Berlin.

Müller, W., Kruse, M., Koziol, C., Müller, J. and Leys, S. (1998). Evolution of early Metazoa: phylogenetic status of the Hexactinellida within the phylum of Porifera (sponges). *Progress in Molecular and Subcellular Biology* **21**, 141-156.

Nickel, M. (2004). Kinetics and rhythm of body contractions in the sponge *Tethya wilhelma* (Porifera: Demospongiae) *Journal of Experimental Biology* **207**, 4515-4524.

Ochs, S. (2004). A history of nerve functions from animal spirits to molecular mechanisms. Cambridge: Cambridge University Press.

Pantin, C. F. A. (1956). The origin of the nervous system. *Pubbl. Staz. Zool. Napoli.* **28**, 171-181.

Parker, G. H. (1919). The elementary nervous system. Philadelphia: Lippincott.

Pearse, V. B. (1989). Growth and Behavior of *Trichoplax adhaerens*: First record of the Phylum Placozoa in Hawaii. *Pacific Science* **43**, 117-121.

Perovic, S., Krasko, A., Prokic, I., Mueller, I. and Mueller, W. (1999). Origin of neuronal-like receptors in Metazoa: cloning of a metabotropic glutamate/GABA-like receptor from the marine sponge *Geodia cydonium*. *Cell and Tissue Research* **296**, 395-404.

Philippe, H., Derelle, R., Lopez, P., Pick, K., Borchiellini, C., Boury-Esnault, N., Vacelet, J., Renard, E., Houliston, E., Quéinnec, E. et al. (2009). Phylogenomics revives traditional views on deep animal relationships. *Current Biology* **19**, 706-712.

Pilot, G., Pratelli, R., Gaymard, F., Meyer, Y. and Sentenac, H. (2003). Five-group distribution of the Shaker-like K^+ channel family in higher plants. *Journal of Molecular Evolution* **56**, 418-434.

Prosser, C. L. (1989). Conclusions and speculations. In *Behavioral neuromodulators: cellular, comparative and evolutionary patterns*, vol. 29, pp. 1355-1357. New Orleans, Louisiana: American Zoologist.

Ramoino, P., Fronte, P., Beltrame, F., Diaspro, A., Fato, M., Raiteri, L., Stigliani, S. and Usai, C. (2003). Swimming behavior regulation by GABAB receptors in *Paramecium*. *Experimental Cell Research* **291**, 398-405.

Ramoino, P., Lorenzo, G., Paluzzi, S., Raiteri, L., Diaspro, A., Fato, M., Bonanno, G.,Tagliafierro, G., Ferretti, C. and Manconi, R. (2007). The GABAergic-like system in the marine demosponge *Chondrilla nucula*. *Microscopy Research Technique* **70**, 944-951.

Ramoino, P., Milanese, M., Candiani, S., Diaspro, A., Fato, M., Usai, C. and Bonanno, G. (2010). (gamma)-Amino butyric acid (GABA) release in the ciliated protozoon *Paramecium* occurs by neuronal-like exocytosis *Journal of Experimental Biology* **213**, 1251-1258.

Roberts, A. C. and Glanzman, D. L. (2003). Learning in *Aplysia*: looking at synaptic plasticity from both sides. *TRENDS in Neurosciences* **26,** 662-670.

Saimi, Y. and Kung, C. (1987). Behavioral Genetics of *Paramecium*. *Annual Review of Genetics* **21**, 47-65.

Schuchert, P. (1993). *Trichoplax adhaerens* (Phylum Placozoa) has cells that react with antibodies against the neuropeptide RFamide. *Acta Zoologica* **74**, 115–117.

Schütze, J., Krasko, A., Custodio, M. R., Efremova, S. M., Müller, I. M. and Müller, W. E. (1999). Evolutionary relationships of Metazoa within the eukaryotes based on molecular data from Porifera. *Proceedings of the Royal Society of London Series B - Biological Sciences* **266**, 63–73.

Sibaoka, T. (1966). Action potentials in plant organs. *Symposia of the Society for Experimental Biology* **20**, 49–73.

Sibaoka, T. (1969). Physiology of rapid movements in higher plants. *Annual Review of Plant Physiology* **20**, 165–184.

Sinyukhin, A. M. and Britikov, E. A. (1967). Action potentials in the reproductive system of plants. *Nature* **215**, 1278–1280.

Spencer, A. N. and Arkett, S. A. (1984). Radial symmetry and the organization of central neurones in a hydrozoan jellyfish. *Journal of Experimental Biology* **110**, 69-90.

Srivastava, M., Begovic, E., Chapman, J., Putnam, N. H., Hellsten, U., Kawashima, T., Kuo, A., Mitros, T., Salamov, A., Carpenter, M. L. et al. (2008). The *Trichoplax* genome and the nature of placozoans. *Nature* **454,** 955-960.

Stankovic, B. and Davies, E. (1996). Both action potentials and variation potentials induce proteinase inhibitor gene expression in tomato. *FEBS letters* **390**, 275–279.

Tompkins-MacDonald, G. J., Gallin, W. J., Sakarya, O., Degnan, B., Leys, S. P. and Boland, L. M. (2009). Expression of a poriferan potassium channel: insights into the evolution of ion channels in metazoans *Journal of Experimental Biology* **212**, 761-767.

Tompkins-MacDonald, G. J. and Leys, S. P. (2008). Glass sponges arrest pumping in response to sediment: implications for the physiology of the hexactinellid conduction system *Marine Biology* **154**, 973-984.

Watanabe, H., Fujisawa, T. and T. W. Holstein (2009). Cnidarians and the evolutionary origin of the nervous system *Development, Growth and Differentiation* **51**, 167-183.

Wacke, M. and Thiel, G. (2001). Electrically triggered all-or-none Ca^{2+}-liberation during action potential in the giant alga *Chara*. *Journal of General Physiology* **118**, 11-21.

Westfall, J. A. (1973). Ultrastructural evidencefor a granule-containing sensory-motor-interneuron in *Hydra littoralis*. *Journal of Ultrastructure Research* **42**, 268-282.

Wildon, D. C., Thain, J. F., Minchin, P. E. H., Gubb, I. R., Reilly, A. J., Skipper, Y. D., Doherty, H. M., Odonnell, P. J. and Bowles, D. J. (1992). Electrical signaling and systemic proteinase-inhibitor induction in the wounded plant. *Nature* **360**, 62–65.

Zocchi, E., Basile, G., Cerrano, C., Bavestrello, G., Giovine, M., Bruzzone, S., Guida, L., Carpaneto, A., Magrassi, R. and Usai, C. (2003). ABA- and cADPR-mediated effects on respiration and filtration downstream of the temperature-signaling cascade in sponges. *Journal of Cell Science* **116**, 629-636.

Zocchi, E., Carpaneto, A., Cerrano, C., Bavestrello, G., Giovine, M., Bruzzone, S., Guida, L., Franco, L. and Usai, C. (2001). The temperature-signaling cascade in sponges involves a heat-gated cation channel, abscisic acid and cyclic ADP-ribose. *Proceeding of the National Academy of Sciences* **98,** 14859-14864.

Chapter Two: ELECTRICAL CONDUCTION IN GLASS SPONGES: ENVIRONMENTAL REGULATION OF FEEDING CURRENT ARRESTS[1]

2.1 Introduction

In its simplest manifestation the coordination system of animals facilitates food capture, allowing for continued survival. To Albert (1999) the nervous system arose in a sessile hypothetical 'animat' similar to a nerve-free *Hydra*, with electrically coupled epithelia serving as anchoring points and conductive links to primitive muscle cells. In computer simulations, acquisition and increase in number of nerves, producing a cnidarian-like nerve net improves survival by increasing the effective range of food capture from the water column (Albert, 1999).

Sponges (Porifera) differ in that they draw food toward themselves by virtue of water currents generated by constant beating of flagella within the body wall. Food particles enter narrowing canals and are processed by tissue on the incurrent surface of flagellated chambers (Turon et al., 1998; Leys, 1999; Wyeth, 1999). Sponges, therefore, do not require a neuromuscular system to facilitate reaching for food; however continual perfusion of the aquiferous system can leave specimens susceptible to clogging in the presence of elevated particulates. In *Verongia lacunosa* pumping was depressed in the presence of clay (Gerrodette

---

1

A version of this chapter has been published. Tompkins-MacDonald and Leys 2008. Marine Biology 154: 973-984.

and Flechsig, 1979). Whether depression was a consequence of clogging or a mechanism to restrict sediment uptake is unclear. Recently, however, Elliott and Leys (Elliott and Leys, 2007) described coordinated contractions, triggered in the freshwater sponge *Ephydatia muelleri* by particulates in the incurrent water. The response commences with constriction of the osculum and finishes with a spastic expulsion of water and particulates, (as in a sneeze). It appears then, that at least in part, coordination systems in the Porifera will have evolved to sense and respond to the presence of excessive particulates.

Many suspension-feeding animals avoid being clogged with sediment by temporarily stopping or reducing feeding (e.g., Mackie et al., 1974; Bock and Miller, 1996; Ellis et al., 2002). Sensory systems, coordinated by the nervous system, allow quick responses to changes in water quality, such as ciliary arrest and constriction of incurrent siphons in the ascidian *Corella* (Mackie et al., 1974). Sponges lack neurons, yet they too selectively remove food from the water column (Leys and Eerkes-Medrano, 2006; Yahel et al., 2006) so they have evolved other ways of dealing with excessive particulates in their feeding current. Some cellular sponges (Demospongiae and Calcarea) can close the openings to their incurrent canals (ostia), constrict the size of their intake canals, and even carry out a series of slow contractions that expel unwanted material (Nickel, 2004; Ellwanger et al., 2006; Leys and Meech, 2006; Elliott and Leys, 2007). Syncytial sponges (Porifera, Hexactinellida), known as glass sponges for their

vitreous skeleton, have a different solution. Although they lack contractile tissues that would permit closure of ostia and canals to prevent the intake of suspended particulates (Mackie et al., 1983; Mackie and Singla, 1983), their syncytial tissues allow action potentials initiated at single or multiple sites to propagate through the entire animal, arresting the feeding current (Leys and Mackie, 1997). The impulses travel at 0.27 $cm \cdot s^{-1}$ (Leys and Mackie, 1997; Leys et al., 1999) - one order of magnitude slower than electrical conduction in cnidarian epithelia (Mackie, 1979).

The feeding current arrest in hexactinellids is similar to ciliary arrest in some suspension feeders, including the arrest of lateral cilia in lamellibranch gills of bivalves and the branchial cilia of ascidians (Mackie et al., 1974; Walter and Satir, 1978; Bergles and Tamm, 1992). In these cases particulate matter may trigger membrane depolarization; ensuing calcium influx into ciliated cells causes cilia to arrest. Extracellular recordings from the hexactinellid *Rhabdocalyptus dawsoni* suggest the glass sponge action potential is Ca^{2+} based (Leys et al., 1999). Arrests are thought to result from calcium influx into branched choanocytes (Mackie et al., 1983; Leys et al., 1999).

The initial observations of arrests are credited to G. Silver who noticed that pumping stopped in the presence of divers, but *in situ* observations suggest that natural stimuli are fish that disturb or resuspend sediment (Yahel et al., 2007). The physiology of feeding arrests has only been described for *R. dawsoni* because this species can be collected by SCUBA with some populations living as shallow as 20 m (Leys and Lauzon, 1998; Leys et al., 2004). Other species of hexactinellid

are found in deeper water and are difficult to collect in good condition (Bett and Rice, 1992; Barthel, 1995; Beaulieu, 2001), but all hexactinellids have syncytial tissues (Leys et al., 2007) and all are therefore presumed to propagate electrical signals that arrest the feeding current.

The relationship between hexactinellid sponges and sediment is complex. Few species are known to settle on soft substrates; most require something hard to attach to, but nevertheless the deep environment of glass sponges is sediment rich from the slow accumulation of marine snow (Bett and Rice, 1992; Conway et al., 2004; Leys et al., 2004). Specimens of *R. dawsoni* were found to arrest pumping in the presence of sediment (Leys et al., 1999), yet at the same time it has been implied that this species may extract organic matter from sediment resuspended in bottom currents and along fjord walls (Bett and Rice, 1992; Yahel et al., 2007). Furthermore, observations of 9000-year old reefs suggest that sediment is an important factor in cementing the reef structure together over time (Conway et al., 2001; Whitney et al., 2005). Thus there appears to be a conundrum between the sensitivity to and tolerance of the stimuli produced by sediment. Presumably this has shaped the properties of the glass sponge conduction system.

I examined the ubiquity of the arrest response in hexactinellids by testing whether the cloud sponge *A. vastus* (Order Hexactinosida) also arrests its feeding current in response to experimental and natural stimuli, including sediment. In *R. dawsoni* (Order Lyssacinosida) arrests are elicited immediately upon arrival of action potentials and therefore provide a convenient means of monitoring electrical activity (Leys, Mackie et al., 1999). Here I examine the effect of short

term sediment exposure on pumping sensitivity, and test the effects of long-term exposure to sediment to determine whether hexactinellids eventually tolerate repeated sediment stimuli and pump continuously. My findings have implications for the physiology of the hexactinellid conduction system, as well as for the sensitivity of hexactinellids and suspension feeders in general, to sediment.

2.2 Materials and Methods

2.2.1 In situ observations

The boot sponge *Rhabdocalyptus dawsoni* [Lambe, 1892] (Order Lyssacinosida) and the cloud sponge *Aphrocallistes vastus* [Schultz, 1886] (Order Hexactinosida) were observed *in situ* on vertical or near vertical walls at San Jose Islets and Hosie Islands, Barkley Sound, British Columbia using the remote operated vehicle ROPOS (Canadian Scientific Submersible Facility, Sidney, British Columbia). During a field study of feeding, fluorescein dye was squirted onto specimens to test for pumping. Specimens that were pumping took in the dye and exhaled it through the osculum (Figure 2-1A, B). Fluorescein was also squirted on dead sponges. Dye was not drawn through these specimens. Small (<20 cm) *R. dawsoni* were collected by SCUBA from 30 m at San Jose Islets and small (<30 cm) *A. vastus* were collected by ROPOS at 160 m. *A. vastus* has a fused siliceous skeleton that is fragile, but small specimens were detached from the wall intact by applying gentle pressure from below with a manipulator arm (Figure 2-1C). Specimens were brought to the surface in water from depth and transferred to darkened flow-through seawater tanks at the Bamfield Marine

Sciences Centre, British Columbia, Canada, where water is pumped directly from 30 m depth. Water temperature was 10°C but reached 12°C on several occasions in early August, reflecting warming of inlet waters from 9 to 11°C. While Leys and Meech (2006) found that specimens often did not pump below 7ºC and were less responsive to experimental stimuli at temperatures >12ºC, subsequent experiments have shown that many specimens will in fact continue to respond even at temperatures as high as 19ºC. Thus tank temperatures (10 to12ºC) were well within the range of tolerance of the animals.

Loose sediment that had settled on rock shelves on fjord walls was collected with specimens and kept in holding tanks for later use in experiments. Sediment was in part settled marine snow, a mixture of organic detritus, microorganisms and clay minerals (Alldredge and Silver, 1988). It is this sediment that would be resuspended by passing fish, or by semidiurnal tidal currents, which reach $1 m \cdot s^{-1}$ along the fjord walls where resuspension loops are thought to contribute the bulk of suspended material (Yahel et al., 2007). A core of sediment from the Hecate Strait BC sponge reefs that had been maintained at 4°C was obtained from K. Conway of the Pacific Geological Survey, Sidney BC, to test the difference of responsiveness of the reef-forming sponge *A. vastus* to this kind of sediment.

2.2.2 Ex situ experiments

Because of the fragility of *A. vastus* only three specimens of eight collected were completely undamaged and could be used for physiological work.

Others lacked portions of the osculum or body wall. Ten specimens of *R. dawsoni* were used in sediment trials. Specimens were placed in 0.5 to 2.5 l flow-through plexiglass chambers and attached with stainless steel insect pins to the underlying Sylgard coating (Dow-Corning, Midland, MI, USA) (Figure 2-1D). Unfiltered seawater was passed over bioballs (plastic spheres with high surface area for degassing) and passed through a cooling system that maintained the temperature at 9 to 10^{o}C. Flow through the chamber was approximately 250 ml$\cdot$ min^{-1}.

Excurrent flow from each specimen's osculum was recorded using a thermistor flow meter (see Mackie et al., 1983 for design) which provides a convenient means of recording small changes in flow; a reference thermistor compensated for temperature change in the chamber. Records were captured with a digital amplifier (Powerlab 8/SP, ADInstruments, Colorado Springs, CO, USA) using Chart 5. Arrests appeared as downward deflections in the flow record over 15 s – 2 min. The thermistor's response at very low flow velocities was linear (see Reiswig, 1971; Mackie et al., 1983). Previous use of this probe design with experiments on *R. dawsoni*, illustrated that after a stimulus to the sponge, flow takes at least 20 s to completely stop; the arrest waveform approximates slowing of water after sudden cessation of a pump driving flow through a smooth-walled pipe (Mackie et al., 1983). The lag, due to inertia of the water mass, is consistent with large Reynold's number flow ($R \approx$ 100-500 in the sponge oscula 1-5 cm diameter and approximate velocity at the osculum 1cm s^{-1}). The duration of arrest-recovery events for each specimen was calculated by measuring the time

from the start of one arrest (the first downward deflection of the trace) until the same level of pumping was recovered. The duration of the arrest phase only was considered the time from start of arrest until the lowest point in the flow record. Pumping was confirmed with fluorescein dye.

Specimens also arrested spontaneously. Because of this, experimental stimuli were applied after a minimum of 10 min, and usually 30 min, of uninterrupted pumping. The response of *A. vastus* and *R. dawsoni* to mechanical stimulation was tested by touch with a pipette and by inserting a metal probe into the body wall. Responsiveness to sediment stimuli was tested in three ways: 1) Fjord sediment collected together with the sponges was added directly into the chamber over specimens, similar to resuspension. 2) Fjord sediment was added gradually to the incurrent water via peristaltic pump at 3 $ml \cdot min^{-1}$ until the first arrest of feeding current was observed. Sediment concentrations that trigger arrests. Large aggregates – which settle out and clog peristaltic pump tubing – were excluded by filtering sediment through 25 μm Nitex mesh. In these experiments, because it is a reef-forming species,. I *A. vastus* was also treated with filtrate from a reef sediment core. 3) In a final set of experiments, long-term effect of sediment on pumping was tested by adding the 25 μm filtrate of fjord sediment continuously (at 3 $ml \cdot min^{-1}$) for 2 to 4 h after the first arrest of feeding current had occurred. Filtered sediment was added to the incurrent water of tanks containing each species. For each experiment only one flow record from each individual was analyzed, however up to 20 runs were carried out with each individual, and all records showed consistent results.

To determine the concentration of sediment in the chamber when the specimens first arrested, 20 to 60 ml water samples were collected by syringe. Small volumes were taken so as to avoid altering flow in the chamber, but as the amount of sediment in these samples was in fact too little to weigh (<0.001g), the concentration of sediment in the chamber was determined indirectly by comparing percent transmittance (660 nm on a Spectronic 20) of water samples taken at the time of arrest to that of a dilution series of stock sediment suspension of known concentration. Stock sediment concentration was determined by suction filtering samples through pre-combusted glass fibre filters (Whatman GF/F). Filters were rinsed with distilled water, dried to constant mass in a 70°C oven and weighed prior to use. Concentrations and numerical trends in pumping were expressed as mean ± standard error.

Sediment from the fjords and the reef core was also fixed in 2% glutaraldehyde in seawater for microscopy. Fixed sediment was suction filtered onto 0.45 μm Millipore filters and rinsed with 70% ethanol. Pieces of air-dried filters were mounted on aluminum stubs, coated with gold and viewed in a JOEL JSM-6301FXV scanning electron microscope (SEM). Composition of sediment in randomly selected regions was determined by Energy Dispersive X-Ray (EDX) analysis. Reef sediment was found to be finer with >75% of particles smaller than 3 μm; <50% of fjord sediment particles were smaller than 3 μm in diameter.

2.2.3 Scanning electron microscopy

To look for evidence of possible clogging of the aquiferous system, specimens were fixed after 20, 40 and > 60 min in tanks made opaque with fjord sediment (<50% transmittance). Before fixing tissues, sed iment had caused repeated arrests and a gradual decline in overall pumping level. Pieces of tissue (5 to 10 pieces, each <1 cm^3) were cut from different portions of the body wall and fixed in 1% OsO_4, 2% glutaraldehyde, 0.45 M sodium acetate buffer pH 6.4, with 10% sucrose, overnight (Leys, 1995). Samples were dehydrated to 70% ethanol, desilicified with 4% hydrofluoric acid in 70% ethanol for 2 days, dehydrated further to 100% ethanol and fractured in liquid nitrogen. Fractured pieces were critical point dried, mounted on aluminum stubs, coated with gold and examined by SEM. Control tissue was from specimens not treated with sediment. Tissue was desilicified because the glass skeleton does not fracture; for comparison, non-desilicified tissue was cut open with a razor blade and prepared as above for SEM, and EDX to determine the presence, location and composition of sediment inside specimens. To see where inert particles would lodge in the aquiferous system, a 10% solution of 0.1, 0.5 and 1 μm latex beads (Molecular Probes, Eugene, OR, USA) in seawater (approximately 1x 10^{10}, 1 x 10^9 and 1x10^6 beads respectively) was poured into the chamber with both species. Tissue became pink (the colour of the beads) within 5 min, and at that time pieces of the specimens were fixed and prepared for SEM as above.

To determine if any canals bypass the flagellated chambers, where the narrowest channels occur, liquid plastic (Batson's No. 17 Plastic Replica

Corrosion Kit, Polysciences, Warrington, PA, USA) was injected in to either incurrent or excurrent sides of live and Bouins-fixed tissue. Plastic was injected gently until it was just visible under the tissue at the side opposite injection; despite great care not to force the plastic into the sponge, in some instances the polymer traversed the entire body wall. After the casts had hardened, the sponge skeleton was dissolved in 4% hydrofluoric acid overnight, and tissue digested with sodium hydroxide. Hardened replicas were fractured with a razor blade, mounted on stubs, coated with gold, and examined by SEM as described previously (Leys, 1999; Bavestrello et al., 2003).

2.3 Results

2.3.1 In situ observations

Pumping of both *Aphrocallistes vastus* and *Rhabdocalyptus dawsoni* was tested with fluorescein dye at 160 m depth at San Jose Islets and Hosie Islands (Figure 2-1A, B). Here, both species grow on almost vertical (80 to 90°), brachiopod-covered walls. Suspended sediment largely in the form of 'marine snow' falls onto sponges, settles on abundant shelves on fjord walls and can reduce visibility to a few meters. On several occasions the rapid movements of fish attracted by lights of the ROV resuspended sediment that had settled on the wall.

Despite the continual fallout of sediment, the surface tissue of all specimens of *A. vastus* was largely clear of debris. In contrast, the outer spicule coat of *R. dawsoni* was invariably cloaked with brown debris. Crabs and fish were

usually in the oscula of both species, but despite these possible mechanical disturbances, all specimens of *A. vastus* that were squirted with fluorescein dye *in situ* drew the dye in and pumped it out of the osculum within 30 s. In contrast, 4 of 9 individuals of *R. dawsoni* tested with fluorescein did not take up dye. One specimen was repeatedly tested and only took up dye 30 min after the arrival of the ROV. Dye flow from the osculum of one specimen of *R. dawsoni* ceased abruptly when it was purposefully tapped with the manipulator arm. Similar knocks to *A. vastus* did not affect dye flow. Dye did not flow from the osculum of dead specimens.

2.3.2 Ex situ (tank) experiments

2.3.2.1 Spontaneous arrests

Thermistor records showed that both *A. vastus* and *R. dawsoni* could pump continuously for several hours; however, both species also arrested periodically in the absence of experimental stimuli (Figure 2-2). Because of this, sediment and mechanical stimuli were delivered only after a period of uninterrupted pumping (typically 30 min). As previously reported for *R. dawsoni* (Leys et al., 1999), neither species showed diurnal rhythmicity in pumping, nor were either sensitive to changes in ambient light. In the interval 30 – 60 min after putting a new specimen in the chamber, arrests occurred at mean intervals of 6.4 ± 2.0 min (n=3) in *A. vastus* and 10.3 ± 3.6 min (n=8) in *R. dawsoni*. Despite the lower frequency of arrests in *R. dawsoni*, arrests were longer and therefore these sponges were arrested a greater percentage of the time. Individual arrest-recovery

events – from start of arrest until return to full pumping level – typically lasted 1 to 4 min (2.7 ± 0.3 min, n=3) in *A. vastus* (Figure 2-2A, B) and 1 to 10 min (4.1 ± 0.5 min, n=7) in *R. dawsoni* (Figure 2-2C-E). However *R. dawsoni* could remain arrested up to 6 h. The arrest phase of each event (from start of arrest to base of arrest-recovery curve) was usually 0.5 to 1.5 min (71 ± 11 s, n=3 and 57 ± 12 s, n=7 for *A. vastus* and *R. dawsoni* respectively).

The two species differed in the way arrests occurred. While for both species the shape of the arrest-recovery record could be v-shaped (i.e. flow arrested and began immediately again) (Figure 2-2A, B, D), in *R. dawsoni* pumping normally resumed very gradually after an arrest, as described previously by Mackie et al., (1983) (Figure 2-2C, E). Given that the oscula through which flow was recorded were 1- 5cm in diameter, the Reynolds number in the atrium and osculum would be large and the thermistor would normally record a small lag in the time between the arrest of the chambers and the arrest of flow through the osculum. V-shaped records were more typical in *A. vastus*, suggesting that either pumping resumed before flow from the osculum had come to a full halt, or that not all of the chambers in the sponge arrest pumping.

2.3.2.2 Responses to mechanical and sediment stimuli

Mechanical and sediment stimuli both triggered arrests in *A. vastus* and *R. dawsoni* (Figure 2-3). Sponges stopped pumping when a metal probe was inserted into the body wall. However, consistent with *in situ* observations, light touches or knocks to the outer body wall caused arrests in *R. dawsoni* but not in *A. vastus*.

Arrest-recovery events in response to mechanical stimuli were of similar duration in both species: 1.7 ± 0.6 min in *A. vastus* and 1.8 ± 0.2 min in *R. dawsoni* (n=3) with arrest phases of 26 ± 7 s and 21 ± 3 s respectively. In one specimen of *A. vastus* in particular the recovery phase of the record was often, but not always, marked by a temporary plateau, which could reflect variations in the internal morphology of the sponge, or perhaps a second arrest that occurred during the recovery phase (Figure 2-3A).

Sediment stimuli induced arrest-recovery events were slightly longer for both species: 2.4 ± 0.1 min, n=3 in *A. vastus* and 2.4 ± 0.5, n=5 in *R. dawsoni* with arrest phases of 47 ± 10 s, n=3 and 36 ± 5 s, n=5 respectively. Small and large additions of sediment (i.e. 10 ml to 1000ml of 0.5 to 1 $g \cdot l^{-1}$) applied to the body wall caused one or more arrests in *A. vastus* (Figure 2-3E) and *R. dawsoni* (Figure 2-3F). Seawater alone poured onto the sponges did not cause arrests.

2.3.2.3 Acclimation to small amounts of sediment

Addition of gradually greater amounts of sediment produced an apparent reduction in sensitivity of the arrest response (Figure 2-4). The first small additions of sediment (2 to 10 ml) triggered arrests, suggesting that even a few particles may be a sufficient stimulus; however subsequent additions of 10 to 100 ml for *A. vastus* and 2 to 20 ml for *R. dawsoni* had no effect on pumping. Larger sediment doses (50 to 200 ml for *R. dawsoni* and 200 to 500 ml for *A. vastus*) triggered arrests and repeated 500 ml doses applied over 10 to 20 min – caused a series of arrest-recovery events of 2 to 4 min duration that lasted several hours.

Many of these events had a marked periodicity (e.g. Figure 2-4B inset). Periodicities of these long trains of repeated arrest-recovery events were 3.4 ± 0.9 min (n=3) in *A. vastus* and 3.3 ± 0.3 min (n=5) in *R. dawsoni*.

2.3.2.4 Response to continuous sediment

Fjord sediment added by peristaltic pump to the incurrent flow of experimental chambers caused both species to arrest. The first arrests occurred at sediment concentrations of 15 ± 5 $mg \cdot l^{-1}$, n=9 for *R. dawsoni* and 36 ± 12 $mg \cdot l^{-1}$, n=3 for *A. vastus*. Initial arrest responses were distinct in the two species. In *R. dawsoni* the arrest phase was consistently abrupt: 25 to 60 s (34 ± 6 s, n=6; Figure 2-5A). In *A. vastus* pumping declined over 50 s to 4.5 min (143 ± 66 s, n=3), often in steps (Figure 2-5B, C). Fine sediment from reef cores had a similar effect on pumping in *A. vastus* but reduction in flow rate took even longer (7.7 min ± 4.8 min, n=3); in one instance flow took 17 min to completely arrest (Figure 2-5D). If sediment was only added until the first arrest, pumping resumed within minutes; however sequential arrest-recovery events persisted for up to an hour afterwards in both species (Figure 2-5D, E). Arrest-recovery events were 1 to 3 min in duration (2.2 ± 0.3 min, n=3) at 1 to 4 min intervals (3.0 ± 0.6 min between arrests, n=3) in *A. vastus* and 1 to 7 min in duration (2.7 ± 0.3 min, n=5) at 1 to 10 min intervals (3.9 ± 0.8 min between arrests, n=5) in *R. dawsoni*.

Addition of fjord sediment (<25µm) continuously for 2 to 4 h reduced pumping to 50 to 80% of original pumping levels in *A. vastus* (n=3) and 5 to 70% in *R. dawsoni* (n=7) (Figure 2-6). In all runs with *A. vastus* and 5 of 7 trials with

R. dawsoni, pumping levels recovered only after sediment addition stopped. Responses by *R. dawsoni* were variable. Some animals arrested less than once an hour (Figure 2-6A), others arrested every 2 to 3 min (6 ± 1.7 arrests·h^{-1}, n=7). In *R. dawsoni* arrests became less frequent with ongoing sediment addition. In Figure 2-6A a single arrest was triggered at the start of sediment addition, but after recovering from the initial arrest the sponge continued pumping for some hours at a much-reduced level. Return to normal pumping was drawn out (3 to 25 h); pumping was minimal for hours after sediment addition (Figure 2-6A, B), and often arrest-recovery events interrupted return to normal pumping.

In *A. vastus*, continued addition of sediment triggered either a series of arrest-recovery events 1 to 3 min in duration or gradual oscillations in flow over 8 to 12 min. Arrests were never prolonged as they were in *R. dawsoni*. Pumping resumed immediately following each arrest, and the sponge arrested every 2 to 3 min until original pumping levels were reached 6 or more hours later (Figure 2-6C).

2.3.3 Composition of sediment and fine structure of the aquiferous system

SEM analysis showed fjord sediment consisted of clays, diatom fragments and calcareous and siliceous sponge spicules, often bound in an organic matrix (Figure 2-7). Large aggregates were over 100 μm in diameter (Figure 2-7A); however, more than 75% of the sediment pieces were smaller than 20 μm (Figure 2-7B), and most pieces of sediment were smaller than 10 μm, small enough to fit

through the pores in the dermal membrane of the sponges (10 to 20µm in diameter).

Clay (sediment containing aluminum and silica) was found in the aquiferous system of specimens of both species fixed after more than 40 min exposure to sediment, but chambers were not clogged by clay if only exposed to sediment for less than 40 min. In these specimens (n=8) neither incurrent nor excurrent surfaces of the flagellated chambers appeared to be obscured by debris (i.e. Figure 2-8A to E). Individual pieces of clay were found on the excurrent surface of fewer than 10% of flagellated chambers examined (e.g. Figure 2-8C to D); only bacteria – no clays – were lodged against the surface of the collar microvilli (Figure 2-8E). Latex microspheres were fed to sponges for 5 min to determine where in the aquiferous system particles of comparable size would lodge. Examination of fixed specimens showed these attached to the incurrent side of the microvilli collars; 1 µm spheres and most 0.5 µm spheres did not pass through the collar microvilli to the excurrent stream (Figure 2-8F).

In contrast, in specimens subjected to long-term exposure to sediment, the excurrent surfaces of flagellated chambers were covered in clays. Clay was found in 20% of chambers of *R. dawsoni* and in some areas of the tissue 10 or more chambers were completely clogged with clays and other sediments (Figure 2-8G).

2.4 Discussion

I have confirmed that the hexactinellid sponges *Aphrocallistes vastus* and *Rhabdocalyptus dawsoni* arrest pumping in response to sediment. Small discrete

doses of sediment from the natural habitat, added as though resuspended by ambient currents or fish, caused immediate feeding arrests in both species, although sponges appeared to arrest less frequently if at all to subsequent small doses. However prolonged perfusion of sediment caused reduced pumping in all specimens of both species, as though the canal system became clogged. Recovery was marked by repeated on-off events similar to those described by Mackie et al., (1983) and considered indicative of pacemaker activity triggered by "unsatisfactory" conditions.

Concentrations of sediment that caused instantaneous arrest were similar in the two species and were comparable to levels that caused reduced pumping in the demosponge *Verongia lacunosa* (Gerrodette and Flechsig 1979). This concentration was only slightly higher than the range of suspended particulate concentrations found during the summer months in the fjords when the specimens were collected (7 $mg \cdot l^{-1}$) (Yahel et al., 2007).

2.4.1 Physiological significance of feeding current arrests

The arrest of pumping in *R. dawsoni* is due to spreading of an action potential (AP) throughout the animal at 0.27 $cm\ s^{-1}$ (Leys and Mackie, 1997). The AP is thought to be calcium-based, and its arrival at any region would cause entry of calcium into the branched choanocytes, causing the arrest of flagella (Leys et al., 1999). Thus a point stimulus would generate an AP that would spread the length of a 20 cm long animal in approximately 1minute, arresting all choanocytes in that time.

The immediate nature of the arrest response in *A. vastus*, both to mechanical stimuli and to sediment applied topically, and the similarity in duration of the arrest and recovery phases in both species of glass sponge, suggest that arrests in *A. vastus* are responses to electrical events as in *R. dawsoni*. However, arrest-recovery responses were distinct in the two species, which can be taken to reflect underlying differences in the physiology of the action potential. Presumably this ultimately reflects different strategies for coping with sediment.

In situ observations showed that *R. dawsoni* was most often arrested (not pumping) after the arrival of the ROV which stirred up sediment; *ex situ* experiments showed that *R. dawsoni* arrested readily in response to light touch, small amounts of sediment added both topically and to incoming seawater, and to vibrations transmitted through the seawater from knocks to the aquaria. Furthermore, arrests were usually long. In contrast, pumping in *A. vastus* was more robust. *In situ*, all specimens took up dye and pumped it immediately out of the osculum; none were arrested. In *ex situ* experiments *A. vastus* arrested only in response to very strong mechanical stimuli, but not when touched with a pipette or when the aquarium was tapped. Mechanical stimuli from fine (<25 μm) sediment from the reef core also failed to elicit immediate arrests – instead pumping levels slowly diminished as sponges became clogged. *R. dawsoni* and *A. vastus* also responded differently to long periods of exposure to sediment. Although this treatment caused reduced pumping in both species, *R. dawsoni* spent longer off or barely pumping both during and after sediment addition – that

is, arrests could last up to several hours. In contrast, specimens of *A. vastus* began to pump immediately after each arrest, during and after sediment addition.

The fused skeleton of *A. vastus* could account in part for differences in sensitivity. Whereas the spicules of *R. dawsoni* are loosely held together by tissue and vibration of a long spicule can cause an arrest (Mackie et al., 1983), in *A. vastus*, all but very small spicules in the skeleton are fused into a rigid scaffold. It is likely however, that properties of the conduction system differ. In earlier work Mackie et al. (1983) suggested that slow recovery from arrests in *R. dawsoni* could be either because flagella beat weakly to start or because some beat earlier than others. The fact that *A. vastus* began to pump immediately after each arrest may indicate that flagella all begin to beat strongly and in unison. This difference between the two species could reflect differences in the ability to resequester Ca^{2+} after an arrest.

2.4.2 The function of the arrest response

Rapid arrests coordinated by electrical signalling presumably protect hexactinellids from taking in noxious or excessive particulates (Lawn, 1981; Mackie et al., 1983). It has been suggested that arrests serve as an early warning system to enable distant parts of the specimens to stop pumping before noxious water reaches them (Leys et al., 1999). Since uptake of sediment is slow (fluorescein-dyed water traverses the body wall in 30 to 40s – considerably slower than for most demosponges) an arrest spreading throughout the tissue in 30 to 60s could prevent sediment reaching pristine flagellated chambers deeper in the body

wall. However, records showed that even when sponges were in continually murky water, after initial arrests they kept on pumping – albeit at a weaker level. Thus, although hexactinellids can arrest their feeding current in response to small irritations, large amounts of sediment clearly clog the feeding apparatus.

Clogging may be a wide-spread problem among sponges. In the demosponges *Petrosia ficiformis* (Bavestrello et al., 1988) and *Tethya wilhelma* (Nickel et al., 2006) and in another hexactinellid (*Scolymastra joubini*, Bavestrello et al., 2003) it has been suggested that water and sediment may bypass flagellated chambers by special canals. In the hexactinellids *R. dawsoni* (Leys, 1999) and *Sericolophus hawaiicus* (Reiswig, pers. comm.) prosopyles (entrances to the flagellated chambers) can line up directly opposite perforations in the secondary reticulum, providing a direct 5 μm diameter passage into the flagellated chamber, but it is unlikely that enough sediment would pass through these to adequately clear the sponge. No direct connections between incurrent and excurrent canals could be found in any of 15 plastic replicas of the aquiferous system of *A. vastus* (data not shown).

Alternatively, if sediment is ingested, the inorganic component of sediment could be expelled into the excurrent stream after processing by the tissue. In support of this our SEM-EDX studies have shown phagocytic vacuoles containing lithic material within the trabecular tissue. It is even possible that arrests could facilitate processing of sediment. Ca^{2+} influx into the trabecular tissue could trigger endocytosis as in adrenal chromaffin cells (Chan et al., 2003).

Feeding experiments on the hexactinellid *S. hawaiicus* show relatively low retention of bacteria (47%) and autotrophic eukaryotes (54%) (Pile and Young, 2006). Similar experiments on *A. vastus* and *R. dawsoni*, however, show that small heterotrophic protists and up to 99% of the most abundant bacterial cells were retained, and inorganic sediment was excreted (Yahel et al., 2006). The high retention of bacteria by *A. vastus* and *R. dawsoni* is inconsistent with bypass routes; without a bypass system how do hexactinellids cope with clogging?

One possibility is the use of repeated on/off events. The very regular arrests that occur after prolonged exposure to sediment are reminiscent of the rhythmic contractions seen in demosponges that flush material out of the aquiferous system in *Tethya wilhelma* and *Ephydatia muelleri* (Nickel, 2004; Elliott and Leys, 2007). The on/off events in the glass sponges occurred during a gradual increase in pumping level during prolonged sediment addition, which suggests they may be effective in clearing sediment from the animal, but exactly how stopping and starting flow in the sponge would aid in clearing sediment is still unclear.

2.4.3 Ecological implications of sensitivity to sediment

Several demosponges have special adaptations for habitats with high sediment loads. *Biemna ehrenbergi* lives buried in coarse sand through which it draws in nutrient rich water (Ilan and Abelson, 1995); other sponges grow on shells of mobile invertebrates, which periodically dislodge sediment (van Soest, 1993; Burns and Bingham, 2002). Corals and bivalves have even been shown to

adopt more efficient particle feeding in a high sediment regime (Urrutia et al., 1997; Anthony, 2000). The distinct pumping patterns shown for the two hexactinellid species may reflect specializations for coping with sediment.

A. vastus is one of the three sponges that form reefs at 100-250m depths on the Pacific Coast of North America. Sponge reefs are exposed to chronic low levels of sediment and the reefs are thought to act as baffles trapping suspended sediment, which then cements the reef framework together (Conway et al., 2004; Whitney et al., 2005). Immediate attempts to pump after each arrest could allow this species to continue pumping in the presence of ongoing sediment, making it well adapted for reef habitats such as the Fraser Ridge reef where sedimentation from the Fraser River plume exceeds 2 $cm \cdot yr^{-1}$ (Conway et al., 2004). *R. dawsoni* is notably absent at Fraser Ridge. In contrast, the low threshold of arrests and their prolonged nature in *R. dawsoni* may be suitable for preventing clogging during temporary sediment loads, such as by resuspension events along the fjord walls.

Nevertheless, the progressive decline in overall pumping level, presumably due to clogging, indicates that sustained exposure to sediment is likely to be detrimental to both species. While short-term adaptation, a phenomenon known from many species including cnidarians (Josephson, 1985; Grigoriev and Spencer, 1995), could explain the sustained pumping under continued sediment exposure, under these conditions pumping levels are so low (and thus ineffective for feeding) that glass sponges living under higher sediment conditions might be expected to be energetically stressed in comparison to those areas less affected by sediment. It has been noted that sponges in sediment-rich

habitats have narrower oscula (Conway et al., 2004). Future studies should investigate the relative health of sponges at sediment rich and poor habitats, in relation to sediment, ambient current and biotic factors including competition and predation.

2.5 Concluding remarks

The response of different species of glass sponge to particulates in the natural environment can tell us much about the unique electrical conduction system that these animals have evolved for controlling their feeding current. This work provides a number of insights into the function of propagated electric signals in the Porifera. Sediment triggers arrests of the glass sponge feeding current, presumably by mechanically irritating the trabecular tissue. The ionic basis of this reaction is unknown. However graded depolarizations, also known as receptor potentials, are triggered mechanically in both plants and animals (Corey and Hudspeth, 1979; Shimmen, 2001). Presumably a sufficient mechanical stimulus depolarizes the membrane beyond threshold for a Ca^{2+}-based action potential which in turn triggers flagellar arrest. The expansive nature of the syncytial tissues allows the electrical impulse to spread globally, arresting flagella. This diffuse mode of propagation is appropriate as there is a need to slow uptake of particulates through the thousands of ostia spanning the body wall. Similarly in cellular sponges a diffuse non-electrical signal leads to coordinated ostia closure and contractions that effectively expel sediment.

In conclusion, although glass sponges lack nerves they have a functional conduction system that senses environmental stimuli, and exacts a response; in this case a flagellar arrest. Further, like in nervous systems the conduction system of hexactinellids appears to have pacemaker activity and adaptability to repeated stimuli, indicating that mechanisms underlying these properties predated origin of the nervous system. Analysis of the molecules underlying the hexactinellid conduction system is needed to determine the basis of electrical conduction in sponges, and how these molecules are modified in the nervous systems of early branching eumetazoans.

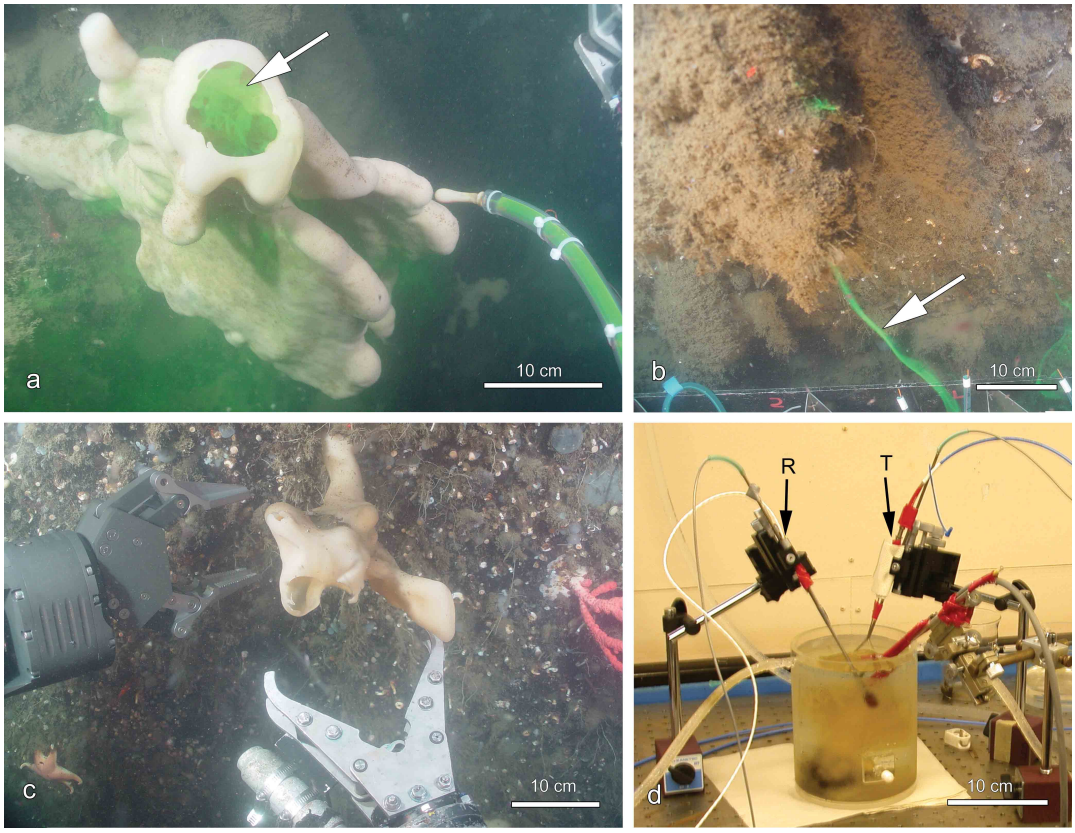

Figure 2-1: Set up for in situ experiments, specimen collection and in tank experiments.

Hexactinellid sponges *in situ* (A to C) and in flow-through experimental chambers (D). Fluorescein dye squirted onto (A) *Aphrocallistes vastus* and (B) *Rhabdocalyptus dawsoni* was pumped out through the osculum (arrows). (C) Specimens of *A. vastus* were collected with the Kraft Raptor manipulator arm (left). (D) In chambers a thermistor probe (T) recorded flow from sponges. Reference probe, R.

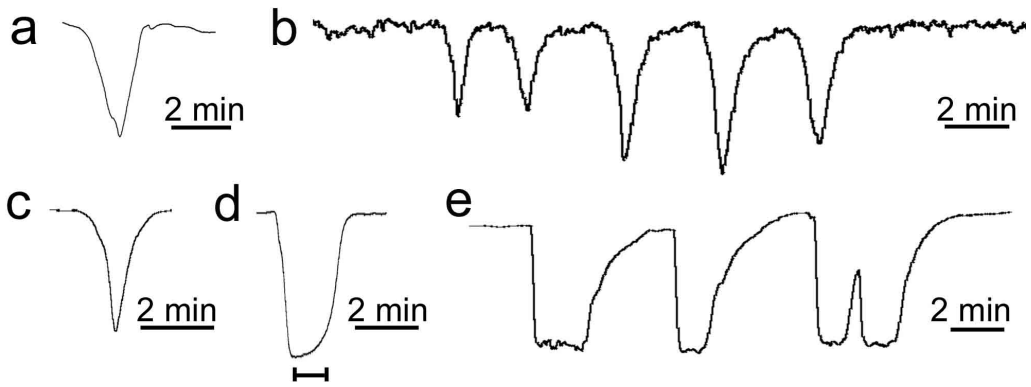

Figure 2-2: Spontaneous arrests of pumping.

Single or intermittent arrests appear as downward deflections in pumping records. (A, B) Arrest-recovery events in *A. vastus* were brief and V-shaped. (C, D) Arrests could be brief in *R. dawsoni* (C) but were often longer (D, E) and the initial phase of the recovery (D, bracketed) was more gradual than in *A. vastus*.

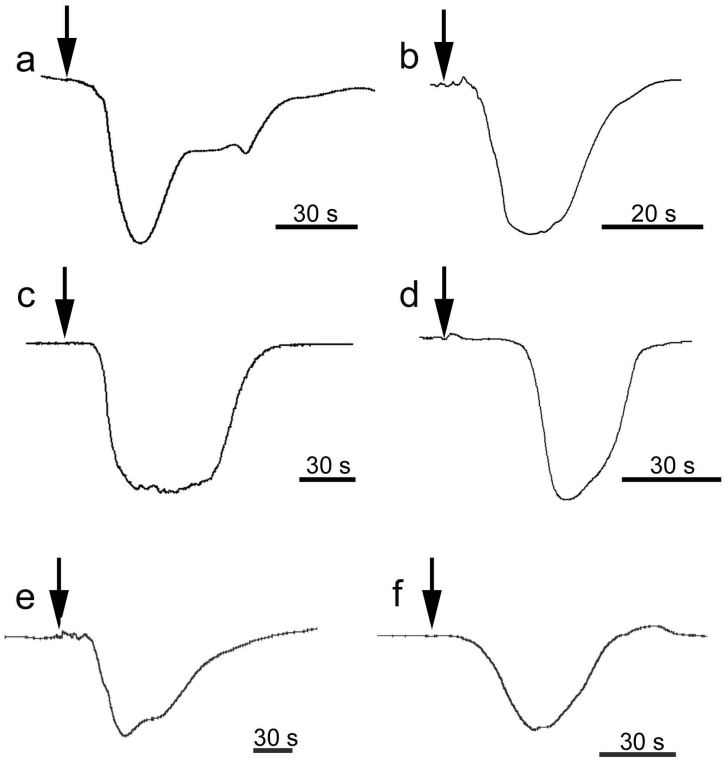

Figure 2-3: Arrest responses to mechanical and sediment stimuli.

Probes advanced into the body wall (arrows) of *A. vastus* (A, B) and *R. dawsoni* (C, D) induced arrests. Topical applications of sediment caused both *A. vastus* (E) and *R. dawsoni* (F) to arrest.

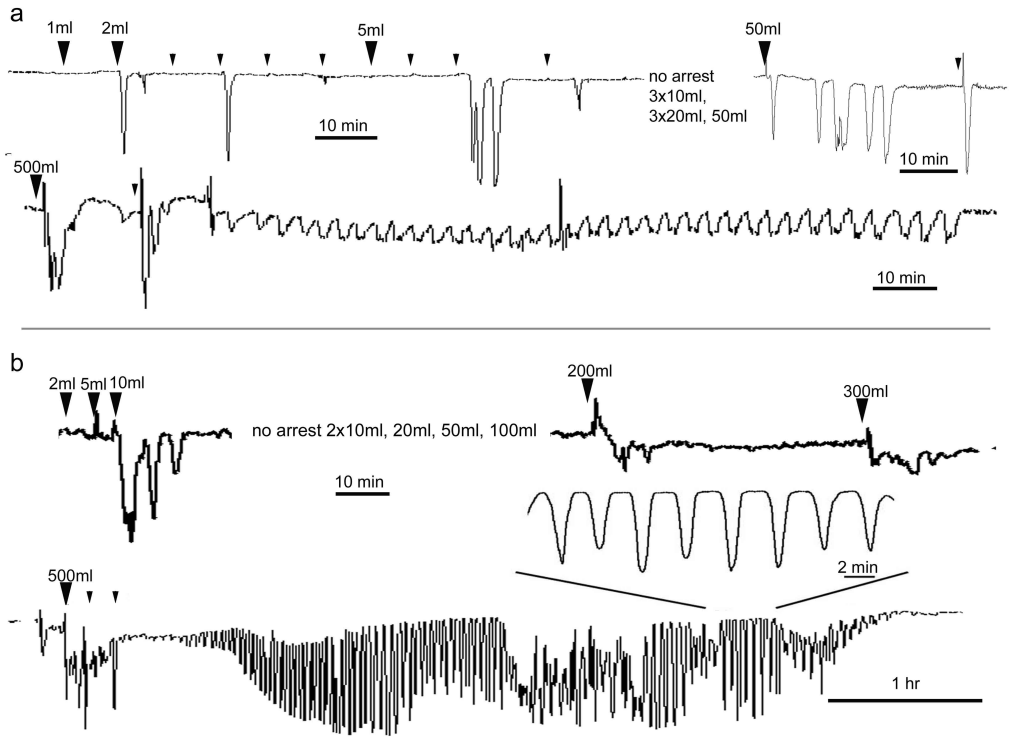

Figure 2-4 :Incremental addition of 0.5 to 1 g·l^{-1} sediment to *R. dawsoni* (A) and *A. vastus* (B).

Initial applications were more likely to trigger arrests than subsequent doses of the same or larger volumes. Much larger doses (here, repeated doses of 500ml) caused prolonged arrest-recovery cycles with marked periodicity (e.g., inset in B). Small arrowheads indicate repeated additions of the same volume.

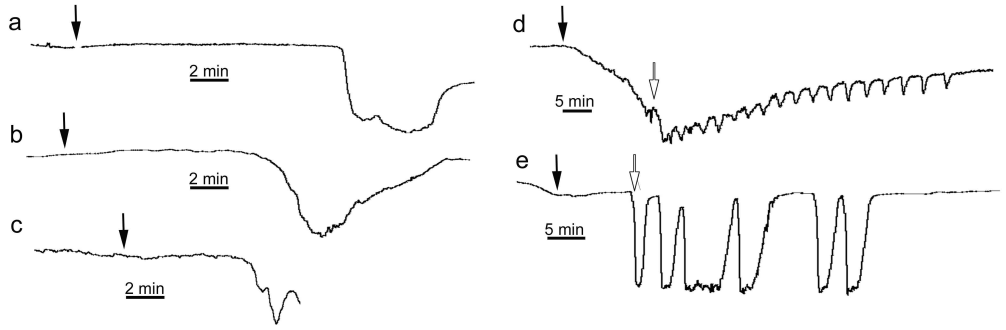

Figure 2-5: Gradual addition of sediment.

Gradual addition of (3 ml·min^{-1}) of 10 g·l^{-1} filtered (<25 µm) fjord sediment (black arrows) to *R. dawsoni* (A, E) and *A. vastus* (B, C) and reef sediment to *A. vastus* (D). (A) The arrest phase (time from start of arrest to full arrest) of *R. dawsoni* was 25 to 60 s, whereas in *A. vastus* (B, C) similar 'abrupt' arrests were not obvious; rather pumping level gradually declined over 50 s to 4.5 min in fjord sediment and over up to 17 min in reef sediment. Recovery after sediment addition stopped (white arrows) was marked by repeated arrest-recovery events in *A. vastus* (D) and *R. dawsoni* (E).

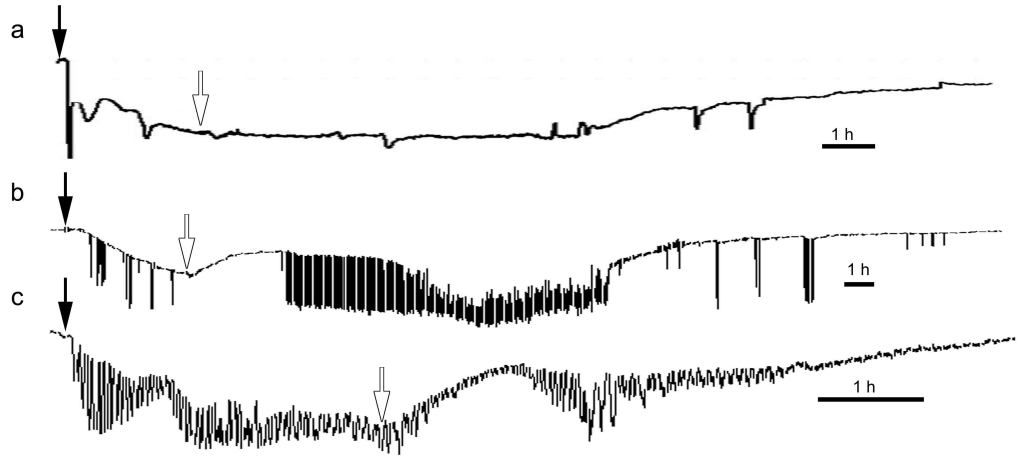

Figure 2-6: Long-term (2 to 4 h) addition of filtered (<25 µm) fjord sediment.

Sediment (10 $g \cdot l^{-1}$) added at 3 $ml \cdot min^{-1}$ (black arrow start, white arrow stop) to *R. dawsoni* (A, B) and *A. vastus* (C) triggered a gradual decline in pumping. (A, B) Arrests in *R. dawsoni* were less frequent with ongoing sediment addition. In (A) a single arrest was triggered at the onset of sediment addition; thereafter pumping level fluctuated and reached negligible levels within 1.5 h of start of sediment addition. Return to normal pumping was delayed by prolonged periods of negligible pumping (A, B) or repeated arrests lasting several hours (B). (C) In *A. vastus* pumping resumed immediately after each arrest during both sediment addition and return to normal pumping. Pumping levels remained low in both sponges as long as sediment was added.

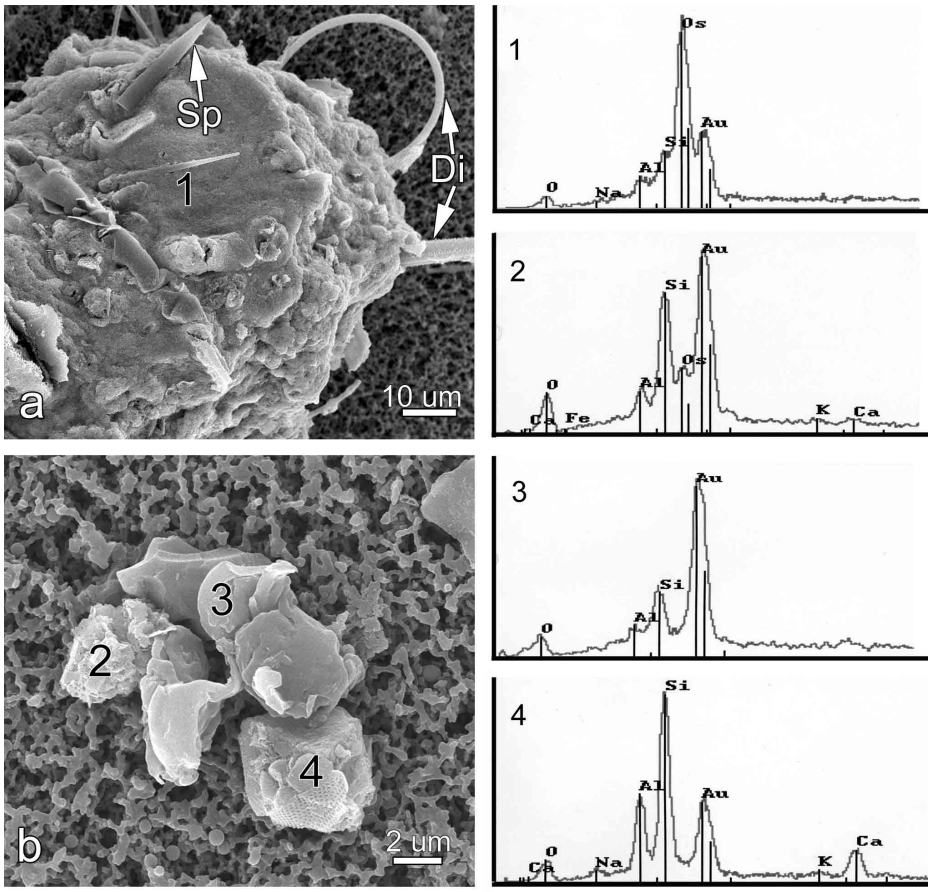

Figure 2-7: Particles of fjord sediment from sponge collection sites viewed by SEM.

(A) Aggregates of organic and inorganic material. (B) Small inorganic particles. EDX traces show the elemental composition of regions 1 to 4. Gold (Au) peaks are due to a gold coating applied in preparation for SEM. Osmium (Os) (applied during fixation) indicates organic material. Aluminum (Al) and silica (Si) indicate clays; (Si) could indicate sponge spicules (Sp) or diatom fragments (Di).

Figure 2-8: SEM of *A. vastus* (A to F) and *R. dawsoni* tissue (G).

Tisse is shown after either exposure to a heavy sediment suspension (A to E, G) or a mixture of 0.1 μm, 0.5 μm and 1 μm latex beads diluted in seawater (F). (A) A fracture through the body wall shows incurrent dermal (Dm) and excurrent atrial (At) surfaces, peripheral trabecular space (Pt) and juxtaposed incurrent (In) and excurrent (Ex) canals spanning the choanosome (Ch, bracket). (B) Inside of several flagellated chambers (Fch) containing organic debris and clay (Cl). (C) Incurrent surface of a flagellated chamber showing prosopyles (pores) in the primary trabecular reticulum (R1). The secondary reticulum (R2) can be seen arising from the primary reticulum. (D) Clay particle (arrow) on the trabecular tissue (R1) at the incurrent surface of a flagellated chamber. (E) Single collar body (Cb) of the branched choanocyte with a central flagellum (Fl) and rod-shaped bacteria (Ba) on the inner surface of the collar microvilli. (F) Branched choanocytes within the primary reticulum. Collar bodies arise from stolons (St) and collar microvilli are surrounded and supported by the secondary reticulum (R2). Latex beads (Lb, 1 μm and 0.5 μm) were found on the primary reticulum (R1) but were excluded from the inside of chambers by the microvilli mesh. (G) Clogged (1) and clean (2) flagellated chambers (Fch) of *R. dawsoni*. High aluminum content (Al) in EDX scan 1 indicates clogging by clays. Si indicates silica from clay or the glass skeleton.

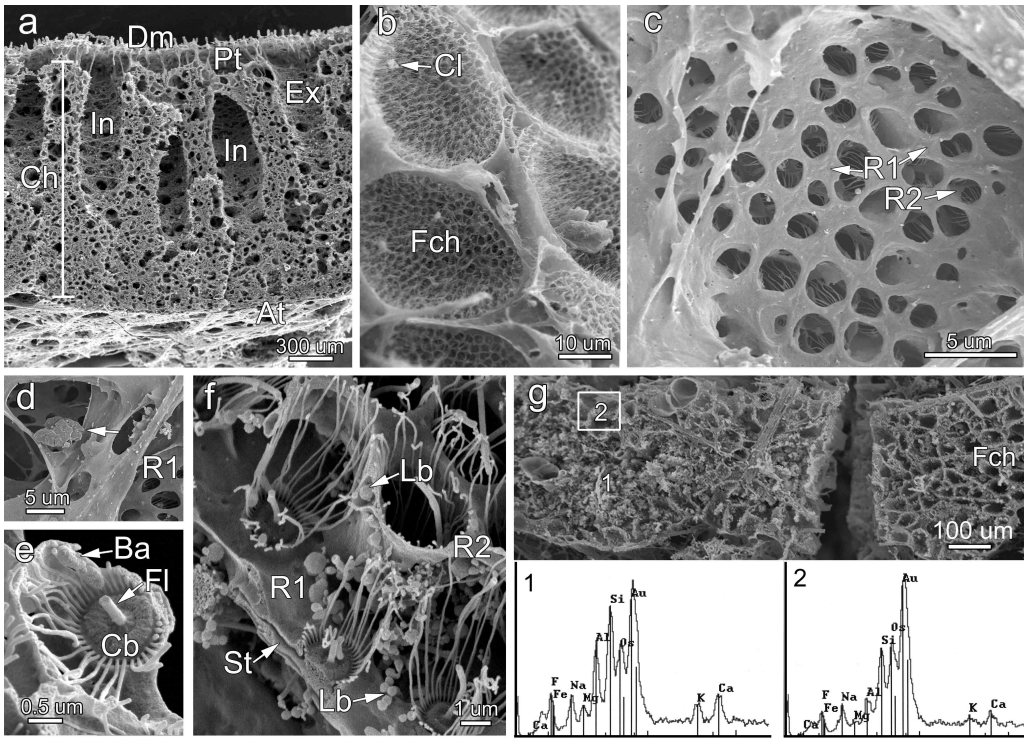
a
Dm
Pt
Ex
In
In
Ch
At
300 um
b
Cl
Fch
10 um
c
R1
R2
5 um
d
R1
5 um
e
Ba
Fl
Cb
0.5 um
f
Lb
R2
R1
St
Lb
1 um
g
2
1
Fch
100 um
1
Si
Au
Al
Os
F
Fe
Na
Mg
K
Ca
2
Au
Os
Si
F
Fe
Na
Al
Mg
K
Ca

2.6 References

Albert, J. (1999) Computational modeling of an early evolutionary stage of the nervous system. *BioSystems* **54**, 77-90.

Alldredge, A. L. and Silver, M. W. (1988) Characteristics, dynamics and significance of marine snow. *Progress in Oceanography* **20**, 41-82.

Anthony, K. R. N. (2000) Enhanced particle-feeding capacity of corals on turbid reefs (Great Barrier Reef, Australia). *Coral Reefs* **19**, 59-67.

Barthel, D. (1995) Tissue composition of sponges from the Weddell Sea Antarctica: not much meat on the bones. *Marine Ecology Progress Series* **123**, 149-153.

Bavestrello, G., Arillo, A. and Calcinai, B. (2003) The aquiferous system of *Scolymastra joubini* (Porifera, Hexactinellida) studied by corrosion casts. *Zoomorphology* **122,** 119-123.

Bavestrello, G., Burlando, B. and Sarà, M. (1988) The architecture of the canal systems of *Petrosia ficiformis* and *Chondrosia reniformis* studied by corrosion casts (Porifera, Demospongiae). *Zoomorphology* **108**, 161-166.

Beaulieu, S. E. (2001) Life on glass houses: sponge stalk communities in the deep sea. *Marine Biology* **138**, 803-817.

Bergles, D. and Tamm, S. (1992) Control of cilia in the branchial basket of *Ciona intestinalis* (Ascidiacea). *Biological Bulletin* **182**, 382-390.

Bett, B. J. and Rice, A. L. (1992) The influence of hexactinellid sponge *Pheronema carpenteri* spicules on the patchy distribution of macrobenthos in the porcupine seabright (Bathyl NE Atlantic). *Ophelia* **36**, 217-226.

Bock, M. J. and Miller, D. C. (1996) Fluid flow and suspended particulates as determinants of polychaete feeding behavior. *Journal of Marine Research* **54**, 565-588.

Burns, D. O. and Bingham, B. L. (2002) Epibiotic sponges on the scallops *Chlamys hastata* and *Chlamys rubida*: increased survival in a high-sediment environment. *Journal of the Marine Biological Association of the United Kingdom* **82**,: 961-966.

Corey, D. P. and Hudspeth, A. J. (1979). Ionic basis of the receptor potential in a vertebrate hair cell. *Nature* **281,** 675-677.

Chan, S.-A., Chow, R. and Smith, C. (2003) Calcium dependence of action potential-induced endocytosis in chromaffin cells. *European Journal of Physiology* **445**, 540-546.

Conway, K. W., Barrie, J. V., Austin, W. C., and Luternauer, L. (1991) Holocene sponge bioherms on the western Canadian continental shelf. *Continental Shelf Research* **11**, 771-790.

Conway. K. W., Barrie, J. V. and Krautter, M. (2004) Modern siliceous sponge reefs in a turbid, siliclastic setting: Fraser River delta, British Columbia, Canada. *N. Jb. Geol. Palaont. Mh.* **6**, 335-350.

Elliott, G. R. D. and Leys, S. P. (2007) Coordinated contractions effectively expel water from the aquiferous system of a freshwater sponge. *Journal of Experimental Biology* **210**, 3736-3748.

Ellis, J., Cummings, V., Hewitt, J., Thrush, A.S., and Norkko, A. (2002) Determining effects of suspended sediment on condition of a suspension feeding bivalve (*Atrina zelandica*): results of a survey, a laboratory experiment and a field transplant experiment. *Journal of Experimental Marine Biology and Ecology* **267,** 147-174.

Ellwanger, K. Eich, A. and Nickel, M. (2006) GABA and glutamate specifically induce contractions in the sponge *Tethya wilhelma*. *Journal of Comparative Physiology A* **193:** 1-11.

Gerrodette, T. and Flechsig, A.O. (1979) Sediment-induced reduction in the pumping rate of the tropical sponge *Verongia lacunosa*. *Marine Biology* **55,** 103-110.

Grigoriev, N. and Spencer, A. N. (1995) A mechanism for fatigue of epithelial action potentials in the hydromedusa *Polyorchis penicillatus:* a case of non-neuronal habituation. *Marine and Freshwwater Behavior and Physiology* **25**, 1-13.

Ilan, M. and Abelson, A. (1995) The life of a sponge in a sandy lagoon. *Biological Bulletin* **189**, 363-369.

Josephson, R. K. (1985) Communication by conducting epithelia. In: Strumwasser F, Strumwasser MJ (eds) Comparative neurobiology: modes of

communication in the nervous system. Wiley-Interscience, New York, pp 133-148

Lawn, I. D., Mackie, G. O. and Silver, G. (1981) Conduction system in a sponge. *Science* **211**, 1169-1171.

Leys, S. P. (1995) Cytoskeletal architecture and organelle transport in giant syncytia formed by fusion of hexactinellid sponge tissues. *Biological Bulletin* **188**, 241-254.

Leys, S. P. (1999) The choanosome of hexactinellid sponges. *Invertebrate Biology* **118**, 221-235.

Leys, S. P. and Eerkes-Medrano, I. (2006) Feeding in a Calcareous sponge: particle uptake by pseudopodia. *Biological Bulletin.* **211**, 157-171.

Leys, S. P. and Lauzon, N. R. J. (1998) Hexactinellid sponge ecology: growth rates and seasonality in deep water sponges. *Journal of Experimental Marine Biology and Ecology* **230**, 111-129.

Leys, S. P. and Mackie, G. O. (1997) Electrical recording from a glass sponge. *Nature* **387**, 29-30.

Leys, S. P. (1999).The choanosome of hexactinellid sponges. *Invertebrate Biology* **118,** 221-235.

Leys, S. P., Mackie, G. O. and Meech, R. W. (1999) Impulse conduction in a sponge. *Journal of Experimental Biology* **202**, 1139-1150.

Leys S. P., Mackie, G. O. and Reiswig, H. M. (2007) The biology of glass sponges. *Advances in Marine Biology* **52**, 1-145.

Leys, S. P. and Meech R. W. (2006) Physiology and coordination in sponges. *Canadian Journal of Zoology* **84**, 288-306.

Leys, S. P., Wilson, K., Holeton, C., Reiswig, H. M., Austin, W. C. and Tunnicliffe, V. (2004) Patterns of glass sponge (Porifera, Hexactinellida) distribution in coastal waters of British Columbia, Canada. *Marine Ecology Progress Series* **283**, 133-149.

Mackie, G. O. (1979) Is there a conduction system in sponges? *Colloques Internationaux du Centree National de la Recherche Scientifique* **291**, 145-151

Mackie, G. O., Lawn, I. D. and Pavans de Ceccatty, M. (1983) Studies on hexactinellid sponges. II. Excitability, conduction and coordination of responses in *Rhabdocalyptus dawsoni* (Lambe, 1873). *Philosophical Transactions of the Royal Society of London* B **301**, 401-418.

Mackie, G. O., Paul, D. H., Singla, C. M., Sleigh, M. A. and Williams, D. E. (1974) Branchial innervation and ciliary control in the ascidian *Corella*. *Proceedings of the Royal Society of London B* **187**, 1-35.

Mackie, G. O. and Singla, C. L. (1983) Studies on hexactinellid sponges. I. Histology of *Rhabdocalyptus dawsoni* (Lambe, 1873). *Philosophical Transactions of the Royal Society of London B* **301**, 365-400.

Nickel, M. (2004) Kinetics and rhythm of body contractions in the sponge *Tethya wilhelma* (Porifera: Demospongiae). *Journal of Experimental Biology* **207**, 4515-4524.

Nickel, M., Donath, T., Schweikert, M. and Beckmann, F. (2006) Functional morphology of *Tethya* species (Porifera): 1. Quantitative 3D-analysis

of *Tethya willhelma* by synchrotron radiation based X-ray microtomography *Zoomorphology* **125**, 209-223.

Pile, A. J. and Young, C. M. (2006) The natural diet of a hexactinellid sponge: Benthic-pelagic coupling in a deep-sea microbial food web. *Deep-Sea Research* **53**, 1148-1156.

Reiswig, H. M. (1971) In situ pumping activities of tropical Demospongiae. *Marine Biology* **9**, 38-50.

Shimmen, T. (2001). Involvement of receptor potentials and action potentials in mechano-perception in plants. *Australian Journal of Plant Physiology* **28,** 567 - 576.

Turon, X., Galera, J. and M. J. Uriz (1998). Clearance rates and aquiferous systems in two sponges with contrasting life-history strategies. *Journal of Experimental Zoology A* **278,** 22-36.

Urrutia, M. B., Iglesias, J. I. P. and Navarro, E. (1997) Feeding behaviour of *Cerastoderma edule* in a turbid environment: physiological adaptations and derived benefit. *Hydrobiologia* **355,** 173-180.

van Soest, R. W. M. (1993) Distribution of sponges on the Mauritian continental shelf. *Hydrobiologia* **258**, 95-106.

Walter, M. F., Satir P (1978) Calcium control of ciliary arrest in mussel gill cells. *Journal of Cell Biology*.**79,** 110-120.

Whitney F, Conway C, Thomson R, Barrie V, Krautter M, Mungove G (2005) Oceanographic habitat of sponge reefs on the western Canadian continental shelf. *Continental Shelf Research* **25**, 211-226.

Wyeth, R. C. (1999). Video and electron microscopy of particle feeding in sandwich cultures of the hexactinellid sponge, *Rhabdocalyptus dawsoni*. *Invertebrate Biology* **118**, 236-242.

Yahel G, Eerkes-Medrano DI, Leys SP (2006) Size independent selective filtration of ultraplankton by hexactinellid glass sponges *Aquatic Microbial Ecology* **45**, 181-194.

Yahel G, Whitney F, Reiswig HM, Eerkes-Medrano DI, Leys SP (2007) *In situ* feeding and metabolism of glass sponges (Hexactinellida, Porifera) studied in a deep temperate fjord with a remotely operated submersible. *Limnology and Oceanography* **52**, 428-440.

Chapter Three: CLONING AND CHARACTERIZATION OF INWARD RECTIFIER POTASSIUM CHANNELS FROM THE DEMOSPONGE *AMPHIMEDON QUEENSLANDICA*[2]

3.1 Introduction

Progress in understanding the ionic currents of sponges has been limited. Block of *Rhabdocalyptus dawsoni* (Porifera: Hexactinellida) action potentials by the calcium channel blockers Co^{2+}, Mn^{2+} and nimodipine suggests that propagation depends on calcium influx (Leys et al., 1999). Patch-clamp recordings from *Xenopus* oocytes injected with total RNA from *R. dawsoni* indicate the presence of depolarization activated potassium current (Leys, personal communication); but without intracellular or patch recordings from sponge tissues the contribution of specific ionic currents to the action potential or resting membrane potential remains unknown.

The complex glycocalyx on sponge cells (Müller, 1982) had hindered formation of tight seals between the membrane and recording electrodes. Recently Carpaneto et al. (2003) surmounted these difficulties and obtained a high percentage of gigaohm seals (65-100%), suitable for patch-clamp recordings, by bathing *Axinella polypoides* (Porifera: Demospongiae) cells in solution containing trivalent cations (100 μM - 1 mM La^{3+} and 10 μM - 300 μM Gd^{3+}). Their recordings reveal an outward rectifying cation current that is gated by heat,

---

2 *A version of this chapter has been published. Tompkins-MacDonald et al. 2009. Journal of Experimental Biology 212: 761-767.*

negative mechanical pressure and arachadonic acid (Zocchi et al., 2001). The profile is similar to the S-type channel in the sea slug *Aplysia californica* and TREK-1 in mammals (J.Patel et al., 1998; Maingret et al., 2000; Patel et al., 1998) but without clones of the channel sequence a definitive link between ionic currents and particular ion channels cannot be made. Moreover without cloned channels we cannot determine how the molecules underlying ionic currents have been modified over evolutionary time during acquisition of nervous and rapid conduction systems.

The absence of ion channel clones from the Porifera is notable considering their key position at the base of the Metazoa. Relationships among the earliest diverging animal groups are still unstable with recent molecular evidence supporting one of placozoans, ctenophores or sponges as the sister group to all other metazoans (Dellaporta et al., 2006; Dunn et al., 2008; Philippe et al., 2009; Srivastava et al., 2008). Most phylogenies however, place sponges as the most ancient multicellular metazoans. Analyses based on 18s rDNA suggest that sponges arose first, but are paraphyletic; that is, a sponge-like animal gave rise to other metazoans (Borchiellini et al., 2001; Medina et al., 2001; Sperling et al., 2007).

The need for direct analysis of sponge ion channels has been highlighted by Hille (2001), in his compendium on ion channels. Cloning ion channels from sponges however is challenging due to the absence of sequences on which to base

cloning efforts, the difficulty of designing degenerate primers for an organism which as undergone 600 million years of independent evolution; and the presence of contaminating symbionts in most sponge tissue. Boyd (1981) has documented a diverse fauna inhabiting the outer spicule coat of *Rhabdocalyptus dawsoni*, and I have observed colonial hydroids intertwined with the sponge tissue. Degenerate primers may conceivably amplify symbiont cDNAs if intact sponge tissues are used. To confirm whether sequences are of sponge origin primers must be tested against genomic DNA of sponge aggregates – tissue preparations that may not express the full cDNA complement but which are purified of symbionts. As a testament to the challenging nature of this work, I have cloned fragments of Shaker-like voltage gated channels from cDNA extracted from slices of *R. dawsoni.* However Shaker clones were not detected in aggregates – suggesting that initial clones were from a contaminant. A suite of degenerate primers for Shaker channels were tested against demosponge and hexactinellid tissue. These experiments are summarized in Appendix A.1.

Sequencing the genome of the sponge *Amphimedon queenslandica* (formerly *Reniera sp.*) has allowed ion channel cloning to progress. This demosponge is native to the southern Great Barrier Reef, reproductive year round (Hooper and Soest, 2006) and has large brood chambers up to 1cm in diameter each containing 20-150 larvae (Leys and Degnan, 2001). Larvae contain only bacterial symbionts, compared to adult sponges which may harbour a variety of invertebrate symbionts. As such, larvae are considered a relatively clean source of starting material suitable for molecular biology. Searches of the genome trace

files by Sakarya et al. (2007), and by me indicate the absence of Shaker like channels, further supporting the notion that at least some sponge ion channels are sufficiently different from other metazoan channels so that approaches using degenerate primers are less effective. Genome searches have however revealed the presence of many homologues typically associated with synapses. Among these are a number of potassium channels including inward rectifier potassium (Kir) channels.

Architecturally, Kir channels are the simplest potassium channels, with only two transmembrane domains but also the most fundamental as they stabilize the membrane potential. Individual Kir channels subunits are typically 372-501 amino acids long with two transmembrane domains (M1 and M2) flanking a central pore-forming loop that is highly conserved among potassium channels and forms the filter for K^+ selectivity (Doupnik et al., 1995). Functional channels form as tetramers of four identical (homomers) or distinct (heteromers) subunits surrounding a central pore that is lined by M2 and P loops (Doyle et al., 1998; Jiang et al., 2002; Kuo et al., 2003; Nishida et al., 2007). We know this from X-ray crystallographic studies on prokaryotic K^+ channels and a mouse G-protein gated Kir channel. These studies have also provided significant insight into the permeation properties of other K channels as two pore potassium channels (4TM), calcium activated, cyclic nucleotide-gated and voltage-gated potassium channels (6TM) are elaborations of the 2TM architecture (Gallin and Spencer, 2001). Despite these conserved pore properties Kir channels are unique in that they preferentially conduct potassium into the cell as described below.

As expected for a K^+ selective channel, when the inside of the cell is more negative than the equilibrium potential for potassium (E_K), large amounts of potassium enter the cell, moving down the electrochemical gradient – thus returning the resting membrane potential to E_K. Excitatory stimuli that depolarize the membrane just positive to the potassium equilibrium potential are offset by outward current through Kir channels, however at more depolarized potentials outward current through Kir channels is blocked, allowing the membrane to further depolarize and electric signals to propagate. Block of outward current is attributed to intracellular cations including Mg^{2+} and polyamines which block the cytoplasmic portion of the pore, preventing efflux of potassium. Inward potassium flow is favoured as potassium entering the cell can displace blocking ions. Further, conductance is higher at more hyperpolarized potentials due to weaker internal block (Doupnik et al., 1995; Nichols and Lopatin, 1997; Oliver et al., 2000a).

In summary, Kir channels stabilize the membrane potential by passing inward K^+ current at potentials hyperpolarized to E_K and outward current at slightly depolarized potentials. Block of outward K^+ current at potentials significantly depolarized to E_K allows the membrane to depolarize past the excitation threshold in response to excitatory stimuli. A sharp excitation threshold, beyond which outward current through Kir channels no longer offsets depolarizing currents, is most effectively established by strong inward rectifier channels (i.e. vertebrate Kir2 and Kir3). Almost no outward current passes through these channels at potentials 50 mV positive to E_K because they are

additionally blocked by polyvalent amines (polyamines), including intracellular spermine (+3) and spermidine (+4), conferring steep voltage dependence. These channels are typically expressed in cells of the heart, skeletal muscle, nervous system and other tissues which conduct electric signals (Oliver et al., 2000).

Weak rectifiers (i.e. vertebrate Kir1 channels) by contrast are blocked by Mg^{2+} but not higher valence polyamines. The weaker and less voltage dependent block allows outward current to pass even at 80 mV more depolarized than E_K (Oliver et al., 2000a). Passage of a higher portion of outward current through apical Kir1.1 channels in renal epithelia is advantageous as it mediates export of K^+ into the nephron distal tubule – a necessary process in urine formation (Lu and MacKinnon, 1994a). Strong and weak rectifiers are regulated by both external signals and by indicators of the metabolic state of the cell, including G-proteins, pH, ATP, and transmitters (Baukrowitz, 2000; Doupnik et al., 1995; Ruppersberg, 2000).

Characterization of Kir channels has to date focused on vertebrate Kir channels; revealing 7 Kir subfamilies, Kir1 through Kir7 that underlie the diversity of inward rectifier current. Knowledge of how membrane conduction properties changed during the evolution of multicellularity however would be aided by comparative analysis of Kir channels from phyla occupying early branching positions within the Metazoa. This evolutionary approach to understanding ion channels moreover can help clarify structure-function relationships. As pointed out by Anderson and Greenberg (2001), taking advantage of the phylogenetic distance between mammals and basal metazoans

allows us to improve the signal-to-noise ratio, since conserved function can be attributed to residues conserved over evolutionary time.

I report the cloning and functional characterization of the first ion channels isolated from a sponge (*Amphimedon queenslandica*, Demospongiae, Porifera). Two clones, AmqKirA and AmqKirB, were obtained using sequences predicted by Onur Sakarya and Ken Kosik (University of California at Santa Barbara) as bases for primer design. Cloned channels were expressed in *Xenopus* oocytes and their functional properties investigated in collaboration with Linda Boland (University of Richmond). Sponge Kir channels were found to share the phenotype and critical residues that regulate strong inward rectification with vertebrate Kir2 channels, which are typically expressed in excitable cells (Doupnik et al., 1995). Phylogenetic analysis was completed together with Warren Gallin and Sally Leys and suggests that Kir channels in sponges, cnidarians, and triploblastic metazoans each arose from a single channel and that duplications arose independently in the different groups. Diversification into the channel subfamilies Kir1 through Kir7 occurred independently in the chordates.

3.2 Materials and Methods

3.2.1 Isolation of cDNAs and DNA sequencing

3.2.1.1 RNA extraction

Larvae of mixed developmental stages of *Amphimedon queenslandica* preserved in RNAlater® (Ambion, Inc.) were kindly provided by BM Degnan

from Heron Island, Queensland. Total RNA was extracted with TRIZOL® according to Invitrogen specifications. After removal of RNAlater® 50-100 larvae were homogenized in 1 mL of TRIzol using a plastic pestle. Cellular debris was removed by centrifugation at 12000 x g for 10 minutes. After a 5 minute room temperature incubation the supernatant was added to 0.2 ml chloroform, mixed vigorously, incubated 3 minutes then centrifuged at 12000 x g for 15 minutes at 4°C. The RNA in the upper aqueous phase was transferred to a new tube and precipitated with 0.5 ml isopropyl alcohol, incubated at room temperature for 10 minutes, then centrifuged at 12000 x g for 10 minutes at 4°C. After removal of the supernatant the pellet was washed with 1 mL 75% ethanol, vortexed and centrifuged at 7500 x g for 5 minutes. The pellet was then air dried and RNA dissolved in 20 µl RNase-free water. A Novapec II was used to quantify RNA – a total of 10 µg was obtained.

Full-length cDNA was prepared in two ways: with the GeneRacer kit (Invitrogen) and by rolling circle amplification (RCA) (Polidoros et al., 2006).

3.2.1.2 cDNA synthesis

3.2.1.2.1 Rolling Circle Amplified cDNA

RCA cDNA was synthesized from 5 µg total RNA using the Superscript III Reverse Transcriptase Module (Invitrogen) with a 5' phosphorylated OligodT(18) primer. RNA was mixed with 1 µl primer, 1 µl 10mM dNTP mix to a final volume of 10 µl, incubated at 65°C for 5 minutes to remove RNA secondary structure, chilled on ice for 1 min and centrifuged to collect liquid. To

this, 4 µl 5X First Strand Buffer, 1 µl 0.1 M dithiothreitol (DTT), 1 µl RNaseOut (40 U/µl), 1 µl SuperScript III RT (200 U/µl) were added. This was mixed by pipetting, briefly centrifuged and incubated at 50ºC for 60 minutes to allow transcription of cDNA to proceed. The reaction was inactivated at 70°C for 15 minutes, chilled on ice for 2 minutes and centrifuged to collect fluid. RNA was removed by adding 1 µl RNase H (2 U) and incubating at 37°C for 20 minutes.

The reaction was purified with the QIAquick PCR purification kit. Full length transcripts were circularized with 150 units CircLigase enzyme (Epicentre) in 1x Circligase Buffer with 50µM ATP. The reaction was incubated for 1 hour at 60ºC, inactivated at 80ºC for 10 minutes and purified as above. Circularized templates were amplified using 10 units of Phi29 DNA polymerase in 1x Phi29 Reaction Buffer (New England Biolabs). The reaction was supplemented with 200 $\mu g \cdot ml^{-1}$ bovine serum albumin, 200 µM dNTPs and 10 µM random heptamers made resistant to Phi29 exonuclease activity by addition of 3'phosphothiote linkages. Amplification proceeded for 20 hours at 30˚C and was inactivated by incubation at 70˚C for 10 min.

3.2.1.2.2 GeneRACE cDNA

GeneRace ready cDNA was prepared according to Invitrogen kit specifications. Generation of full length cDNA from 2 µg RNA was ensured by adding Calf Intestinal Phosphatase (CIP) to remove 5' phosphates which are exposed on truncated mRNA. The reaction, including 2.5 µg RNA (5 µl), 1 µl 10X CIP Buffer, 1 µl RNaseOut (40 U/µl), 1 µl CIP (10U/µl) and 2 µl DEPC

water, was incubated at 50ºC for 1 hour. This removes truncated messages from the amplification pool.

RNA was precipitated by adding 90 µl DEPC and 100 µl phenol:chloroform, vortexing for 30 seconds then centrifuging at maximum speed for 5 minutes. The upper aqueous phase, containing RNA, was transferred to a new tube, to which 2 µl 10 mg/ml mussel glycogen and 10 µl 3 M sodium acetate, pH 5.2 was added and mixed; 220 µl 95% ethanol was added, the sample vortexed and then frozen on dry ice for 10 minutes. RNA was pelleted by centrifugation at maximum speed for 20 minutes at 4ºC. After removal of the supernatant the pellet was washed by adding 500 µl 70% ethanol, vortexing briefly, then centrifuging at maximum speed for two minutes at 4ºC. The supernatant was removed, the pellet was air dried and then resuspended in 7 µl DEPC water.

The 5' cap structure on full length mRNA was then removed with tobacco acid pyrophosphatase (TAP), exposing a 5' phosphate to which a 5' oligonucleotide of known sequence could be ligated. The RNA was mixed with 1 µl 10X TAP Buffer, 1 µl RNaseOut (40U/µl) and 1µl TAP (0.5U/µl). Following incubation at 37ºC for 1 hour the RNA was precipitated as above. The decapped RNA was resuspended in 7 µl DEPC water and the GeneRacer 5' RNA Oligo was ligated to the 5' end. RNA was mixed with 0.25 µg GeneRacer RNA Oligo, incubated at 65ºC for 5 min to relax the RNA secondary structure, mixed with 1 µl 10X Ligase Buffer, 1 µl 10 mM ATP, 1 µl RNaseOut (40U/µl) and 1 µl T4 RNA ligase (5U/µl) and incubated at 37ºC for 1 hour.

Following precipitation first strand cDNA was synthesized using the Superscript III module as outlined above for preparation of RCA cDNA. However instead of priming reverse transcription with a 5' phosphorylated OligodT(18) primer, the reaction was primed with the GeneRacer Oligo dT Primer which is preceded by an oligonucleotide sequence with known priming sites for subsequent amplification reactions.

3.2.2 Amplification of ion channel sequences

Ion channel sequences, including two putative potassium inward rectifier channel sequences, "AmqKirA" and "AmqKirB" assembled from unannotated trace files of the *Amphimedon queenslandica* (formerly *Reniera sp.*) genome, were generously shared by Onur Sakarya and Kenneth S. Kosik (University of California, Santa Barbara). Initial fragments were amplified using specific primers designed against the 5' and 3' ends of these sequences. Primer sequences are listed in Appendix A.2 The forward, 5', primers for both AmqKirA (Kir1F) and AmqKirB (Kir2F) started with the sequence **GGCTCGAGCCACC**. This included a 5' clamp (GG), an Xho1 restriction site (CTCGAG), and a Kozak consensus sequence (GCCACC) which is recognized by protein synthesis machinery in the *Xenopus* oocytes. The 3', reverse, primer for AmqKirA (Kir1R) included a 5' clamp (GG), and an SpeI restriction site (ACTAGT). Because AmqKirB contained internal SpeI cut sites the reverse primer (Kir2R2) was instead designed with a BglII restriction site (AGATCT). Restriction sites were included so that cloned sequences could be cut out of the cloning vector PCR4-

TOPO (Figure 3-1) used in my experiments and ligated into the pxt7 vector (Figure 3-2) for expression.

Amplification reactions included 5 µl GoTaq Buffer (Promega), 1.5 µl 25 mM $MgCl_2$, 0.2 µl 25 mM dNTPs, 0.4 µl each 50 µM forward and reverse primer, 0.125 µl GoTaq® Flexi, 13.175 µl dH2O and 1 µl GeneRace-ready cDNA. Cycling parameters were 94ºC 2 min, 34x (94ºC 30 s, 56ºC 30 s, 72ºC 10 min) 72ºC 30 min for AmqKirA and 94ºC 2 min, 34x (94ºC 30 s, 53.5ºC 30 s, 72ºC 10 min) 72ºC 30 min for AmqKirB. Products were separated by electrophoresis on 1% agarose gels in 1x TAE (50x stock contains 242 g Tris base, 57.1 ml glacial acetic acid, 100 ml 50 mM EDTA, pH 8, in 1 L) supplemented with 0.5 $\mu g \cdot ml^{-1}$ ethidium bromide. 20 µl samples mixed with 4 µl 6x load dye were run simultaneous with a 1 µg 2-Log DNA ladder (New England Biolabs). Gels bathed in TAE were run at 125 V for 30 minutes to 1 hour. Ethidium bromide stained DNA bands were visualized on a transilluminator and images captured with a digital camera. Bands of the expected size (1071 for AmqKirA and 1095 for AmqKirB) were cut from the gel and purified with the QIAquick Gel Extraction Kit.

Products were cloned using the TOPO TA Cloning Kit for sequencing (Invitrogen). The products were first ligated into a cloning vector: 4ul purified PCR product was mixed with 1 µl pcr4-TOPO vector and 1 µl salt solution, and then incubated at room temperature for 5 minutes and overnight at 4ºC. The vector, containing the PCR product was then transformed into TOP10 chemically competent *Escherichia coli* cells. Cells thawed on ice were mixed with 2 µl

ligation reaction. After 10 minutes the cells were heat shocked at 42ºC for 30 seconds, returned to ice, mixed with 250 µl warm SOC medium, then incubated at 37ºC for 1 hour while shaking at 200 rpm. Cells were plated on LB plates supplemented with 100 µg/ml ampicillin, in volumes of 10 µl, 50 µl and "the rest" (~200 µl).

After 18 hours incubation at 37ºC, plates were analyzed for growth. Since ligation of a PCR product into pcr4-TOPO disrupts the lethal gene *ccd*B, only transformed cells containing the recombinant vector grow. Colonies were screened for the presence of the desired insert by creating a new streak of each colony for future use, mixing the remainder of the colony in 50 µl sterile water and adding 1µl of this mixture to a PCR reaction containing 20 µl T1.1x PCR buffer (50 mM Tris-HCl pH 9.2, 1.5 mM $MgCl_2$, 0.4 mM β-Mercaptoethanol, 0.1 µg/µl BSA, 10 mM $NH_4SO_{4,}$ 0.2 mM dNTPs), 0.5 µl each 50 µM T3 and T7 which prime against pcr4-TOPO sequence flanking the insert (Figure 3-1) and 0.5 µl Taq 9 (Department of Biological Sciences, University of Alberta). The PCR cycling parameters were 94ºC 2 min, 30x (94ºC 30s / 58ºC 30s/ 72ºC 1.5 min), 72ºC 2 min. Products were analyzed by running 20 µl on agarose gels. Products of the expected size, 1175 (AmqKirA) and 1199 (AmqKirB) including 104 bp of flanking pcr4-TOPO sequence, were identified. Corresponding colonies were then cultured to provide sufficient starting material for sequencing. 5 mL LB broth supplemented with 100 µg/mL ampicillin was inoculated with a streak corresponding to each positive colony and incubated at 37^{o}C for 18 hours while shaking at 250 rpm.

Plasmid DNA containing the PCR product was purified from 3 ml of bacterial culture using the QIAprep Spin Miniprep Kit. Purified plasmid DNA was subsequently sequenced by mixing 4 µl v3.1 5x Sequencing Buffer (Applied Biosystems), 3 µl 1. 6 µM forward or reverse sequencing primer, 400 ng plasmid template, 1 µl Big Dye premix (Applied Biosystems) and water to 20 µl. Samples were then placed in a thermal cycler for 25 cycles of 96^{o}C for 30s, 50^{o}C for 15s and 60^{o}C for 2min. Reactions were stopped by mixing samples with 2 µl NaOAc/EDTA. DNA was precipitated on ice for 15 minutes with 80 µl ethanol and by centrifuging for 15 minutes at 4^{o}C. After discarding the supernatant DNA pellets were washed with 500 µl cold 70% ethanol centrifuged for 5minutes at 4^{o}C. Supernatants were removed, pellets dried and samples brought to the Molecular Biology Service Unit (University of Alberta) to run on a sequencing gel. Sequence data were downloaded as ABI files and analyzed using sequence analyses software, Staden Package 1.7.0.

3.2.3 Inverse and RACE-PCR

Complete cDNA sequences were determined using a combination of inverse PCR on RCA cDNA template (Polidoros et al., 2006) and RACE-PCR on GeneRACE ready cDNA, which has known priming sites at the 5' and 3' ends. For inverse PCR primer sets includes Kir1inv5' with Kir1inv3' (AmqKirA) and Kir2inv5' with Kir2inv3' (AmqKirB). Reactions included 5µl Go Taq Buffer, 1.5 µl 25 mM $MgCl_2$, 0.2 µl 25 mM dNTPs, 0.4 µl each 50 µM primer, 0.125 µl Taq Flexi, 1 µl RCA cDNA and water to 25 µl with cycling conditions 94ºC 2 min,

34x (94ºC 30 s, annealing 30 s, 72ºC 10 min) 72ºC 30 min. Annealing temperatures were 46ºC for AmqKirA and 55ºC for AmqKirB. To obtain the 5' ends by RACE the cDNA was amplified using the GeneRacer 5' primer and reverse gene specific primer, Kir1RevGR (AmqKirA) and Kir2RevGR (AmqKirB). Nested PCR involved a GeneRacer 5' nested primer and nested reverse gene specific primers Kir1RevNGR (AmqKirA) and Kir2RevNGR (AmqKirB). Sequences were amplified, cloned and sequenced as above. The 5' PCR the reaction included 3 µl 10 µM GeneRacer 5' primer, 1 µl 10 µM reverse primer, 5 µl GoTaq buffer, 1.5 µl 25 mM $MgCl_2$, 0.2 µl 25 mM dNTPs, 0.125 µl TaqFlexi and 0.5 µl GeneRACE ready cDNA and water to 25 µl. Cycling parameters were 95°C 2 min, 35x (95°C 30 s, anneal 30 s, 72°C 3 min) 72°C 10 min. Annealing temperatures were 56 and 52ºC for AmqKirA and AmqKirB respectively. Serial dilutions of 5' RACE product were amplified with GeneRACE nested 5' primer and nested reverse primers (1 µl each 10 µM primer and 54.8 or 53.6°C annealing).

Amplified sequences were analyzed by electrophoresis, cloned and sequenced as above. The 5' ends was determined by identifying a start codon downstream of the GeneRACE 5' Oligo and in frame with the inward rectifier sequence. The stop codons predicted by sequences assembled by Onur Sakarya were found to be in frame with the start site and were confirmed by PCR. RACE PCR was therefore unnecessary for the 3' end of the two putative Kir channels. Since the primer sets used to originally amplify AmqKirA and AmqKirB encompassed the 5' and 3' ends, clones produced from original amplification

already contained the full open reading frame. The full sequence was confirmed from uncloned PCR products from at least two independent PCR reactions. Clones free of PCR errors, judged by comparison with unclined PCR products, were selected for expression and archived by adding 0.65 mL glycerol mix (65% glycerol, 100 mM $MgSO_4$, and 25 mM Tris-HCl pH 8, 0.2 µM filtered) to 1.3 mL overnight culture and freezing at -80ºC in Corning® 2 ml cryogenic vials.

3.2.4 Amino acid sequence and phylogenetic analysis

Sponge inward rectifier sequences, AmqKirA and AmqKirB were subject to Kyte-Doolittle hydropathy analysis by entering amino acid sequences in the online entry form at http://gcat.davidson.edu/rakarnik/kyte-doolittle.htm with a window size of 9. Predicted transmembrane domains were also checked at http://www.cbs.dtu.dk/services/TMHMM/. AmqKirA and AmqKirB were aligned and compared with amino acid sequences of both invertebrate and vertebrate inward rectifier sequences compiled from NCBI, Joint Genome Institute (http://www.jgi.doe.gov/sequencing/why/3161.html) and Ensemble databases. To determine pairwise identity values, AmqKirA and AmqKirB amino acid sequences were each in turn aligned using LALIGN online software (http://www.ch.embnet.org/software/LALIGN_form.html) and default parameters for global alignments. Multiple alignments were generated using MUSCLE (Edgar, 2004). Alignments used for phylogenetic analysis were manually adjusted in MacClade (Maddison and Maddison, 2003) and a PERL script was used to remove characters with more than 2% gaps to produce a trimmed alignment of

122 sequences and 280 positions. Sequences included in phylogenetic analysis are given in Appendix A.3. All data sets are available on request. The optimal tree topology and Bayesian posterior values were obtained using MrBayes v3.1.2 (Ronquist and Huelsenbeck, 2003) with the default parameters for amino acid sequences. The same dataset was also analyzed with RaxML (Stamatakis, 2006), as implemented on the CIPRES server (http://www.phylo.org/) to obtain maximum likelihood bootstrap values.

3.2.5 Functional Expression in Oocytes

3.2.5.1 Ligation into expression vector

Open reading frames of the two putative inward rectifiers, AmqKirA and AmqKirB were digested out of the pcr4-TOPO cloning vector at XhoI and SpeI cut sites for AmqKirA and XhoI and BglII cut sites for AmqKirB and ligated into pxt7 vectors which were digested with the same restriction enzymes. Restriction digest of AmqKirA from pcr4-TOPO using New England Biolabs reagents included 3-6 µg AmqKirA plasmid template, 4 µl Buffer 2, 0.4 µl BSA, 1 µl XhoI, 1 µl SpeI and water to 40 µl. The digest reaction for AmqKirB included 3-6 µg template, 4 µl Buffer 3, 1 µl XhoI, 1.5 µl BglII, 0.4 µl BSA and water to 40 µl. The same digests were completed with 3 µg pxt7. All digests were incubated at 37ºC for 3 hours then separated on 1% agarose gels. Bands corresponding to AmqKir and digested pxt7 sequences were purified with the QIAquick Gel Extraction Kit. In order to ensure sufficient yield for subsequent ligation

reactions, 30 µl water applied to elute DNA was allowed to sit on the QIAquick column membrane for 30 minutes before spinning through.

Ligation reactions included 2 µl Ligase 10X Buffer, 0.5 µl T4 DNA Ligase (Promega), digested pxt7 vector and insert in 3:1, 1:1 and 1:3 ratios, and nuclease free water to a volume of 20 µl. Reactions were incubated at 15ºC for 12-18 hours and heat inactivated at 65ºC for 10 minutes. Pxt7 expression plasmid containing the Kir inserts were subsequently cloned by transforming TOP10 chemically competent cells as above.

Clones were screened for the presence of insert in the proper orientation using reverse gene specific primers (Kir1R and Kir2R2 for AmqKirA and AmqKirB respectively) and a forward pxt7 specific primer that binds 53 bp upstream of Kir start sites. Reactions included 20 µl T1.1x buffer, 0.5 µl each 50 µM forward and reverse primer, 0.4 µl Taq16 (in house Taq, Biological Sciences Department, University of Alberta) and 1 µl template. Cycling parameters were 94ºC 2 min, 30x (94ºC 30s / 58ºC 30s/ 72ºC 1.5 min), 72ºC 2 min. Minipreps of positive clones were prepared as before and eluted in 30 µl nuclease free water.

3.2.5.2 cRNA synthesis

To prepare RNA 25-30 µl plasmid containing Kir cDNA was digested for 1 hour at 37^{o}C with 1 µl XbaI in 5 µl 10x buffer 2 (both New England Biolabs) and RNase-free water to 50 µl. The linearized plasmid-vector construct was isolated by electrophoresis, purified with a QIAquick Gel Extraction Kit, or purified directly from the linearization using the GeneClean Turbo Kit, and used

as a template for synthesis of complementary RNA. RNAs, capped with an analog of the 5' 7-methyl guanosine cap of eukaryotic mRNA were synthesized *in vitro* using Ambion (Austin, TX) mMessage mMachine RNA polymerase kits. Briefly 6 µl linearized plasmid was mixed with 10 µl NTP/CAP, 2 µl Reaction Buffer and 2 µl T7 polymerase and incubated at 37 ^{o}C for 2 hours. DNA was removed by incubating with 5 µl Turbo DNase for 15 min at 37 ^{o}C. RNA was purified by lithium chloride precipitation (mMessage, mMachine kit, Ambion) or with the RNAid kit (Bio 101, Vista, CA) and concentrations were determined by spectrophotometry. RNA quality was further confirmed by running 1 µl on an agarose gel.

3.2.5.3 Oocyte preparation

Oocytes were surgically harvested from female *Xenopus laevis* (*Xenopus* I, Dexter, MI or Biological Sciences Animal Services) frogs on ice after 5 minutes anaesthesia in buffered 0.1-0.17% 3-aminobenzoic acid ethyl ester (MS-222) (Sigma Chemical). The ovarian lobe was separated into half centimetre sections with forceps and oocytes were released and defolliculated by gentle agitation for 1 hour or less in 0.5 mg/ml collagenase A (Sigma-Aldrich) dissolved in either a Ca^{2+}-free solution (in mM: 96 NaCl, 2 KCl, 1 $MgCl_2$, 5 HEPES, pH 7.4 with NaOH), or MBM (in mM: NaCl 88, KCl 1, $Ca(NO_3)_2$ 0.33, $CaCl_2$ 0.41, $MgSO_4$ 0.82, $NaHCO_3$ 2.4, HEPES 10, sodium pyruvate 2.5, penicillin G 0.1 g/L and gentamycin sulphate 0.05 g/L, pHed to 7.5 with Tris base). Oocytes were then washed three times and maintained at 19ºC in MBM or frog Ringer's solution (in

mM: 96 NaCl, 1 KCl, 1 $CaCl_2$, 2 $MgCl_2$, 10 HEPES, 5 sucrose, and 2 Na pyruvate, pH 7.4 with NaOH with 50 U/ml penicillin G). Stage V/VI oocytes were injected with 2.3-50.6 nl of cRNA dissolved in DEPC-treated water (5-45 ng cRNA/oocyte). Storage medium was refreshed daily and electrophysiological recordings were done 1-6 days post-injection.

3.2.5.4 Electrophysiology

Potassium currents were recorded from *Xenopus* oocytes. The benefits of recording from oocytes include large cell size for ease of manipulation during injection and electrode insertion, macroscopic currents owing to the extensive surface area, and minimal endogenous current (Kusano et al., 1982). Recordings were performed using standard methods of two-electrode voltage clamp (Boland et al., 2003). Voltage clamp is a technique used to measure the amount of current that crosses the membrane while holding the membrane potential at a set level, the command voltage. This approach gives an idea of the amount of current passing through the complement of expressed channels in the oocyte membrane at a given membrane potential. In the two electrode configuration, one electrode records the membrane voltage (Vm). Current proportional to the difference between Vm and the command voltage (Vcmd; voltage set by experimenter) is then forced through the second electrode, bringing Vm closer to Vcmd (Figure 3-3).

Glass microelectrodes were pulled from borosilicate glass. Voltage measuring and current passing electrodes were backfilled with 3 M KCl and had resistances between 0.2 and 1.7 MOhm. We used a Geneclamp 500B amplifier

(Axon Instruments, Foster City, CA) and an OC-725C amplifier (Warner Instruments, Hamden, CT). Currents were sampled at 5-10 kHz and filtered at 1-2 kHz. Recordings were done at room temperature (about 23ºC), and oocytes were perfused continuously during recordings. Solution composition varied by experiment.

Like other authors (Dibb et al., 2003; Krapivinsky et al., 1998; Silverman et al., 1998) we could not use P/N leak subtraction to subtract endogenous currents as Kir channels are known to pass current over the range of command potentials used. P/N subtraction might therefore inadvertently subtract Kir current. Overall endogenous currents in *Xenopus* oocytes are known to be low (Kusano et al., 1982). Endogenous chloride currents were minimized by using low chloride solutions in which chloride salts are replaced by the equivalent methanesulfonate salt. The standard, low chloride, external solution contained (in mM): 5 K methane sulfonate (MES), 95 NMDG-MES, 2 $CaCl_2$, 2 $MgCl_2$, 10 HEPES, pH 7.3 with methanesulfonic acid. K^+ concentrations were adjusted by changing the ratios of K^+ and $NMDG^+$ containing solutions using either the methanesulfonate or chloride salt of K^+. For selectivity experiments permeability to K^+, Na^+ and Rb^+ were compared. Since Rb-MES salts were unavailable 10mM Cl^- salts were used for K, Na and Rb. Chloride currents in this experiment were minimized by adding the blocker niflumic acid. Other solutions are noted in figure legends. Data were recorded on Pentium computers equipped with Digidata 1320A (Axon Instruments) A/D hardware. Axon's Clampex acquisition and Clampfit analysis software (version 9) were used. Data were also transferred to

Microsoft Excel and Microcal Origin (Northampton, MA, USA) for additional analysis, curve-fitting, and the production of figures. Results were calculated from cells with negligible background currents and only for stable cells with membrane potentials not more depolarized than –50 mV in 5 mM external K^+. A portion of recordings were completed on a separate electrophysiology setup with the same components. With this set up, traces displayed in Clampex were consistently offset from the current displayed on the amplifier. To correct for this artefact, the difference between the current displayed in Clampex and on the amplifier display at the holding potential was determined and then added to each trace. Adjusted traces were consistent with those obtained on the main electrophysiology set up.

3.3 Results and Discussion

3.3.1 Cloning and sequencing AmqKirA and AmqKirB

Two inward rectifier potassium channels, AmqKirA and AmqKirB, were cloned from the demosponge *Amphimedon queenslandica.* Initial sequences were amplified with gene specific primers and separated by electrophoresis (Figure 3-4A). Products were gel purified and cloned. Clones positive for the insert were identified by colony PCR and sequenced. 5'ends of AmqKirA and AmqKirB were confirmed by RACE PCR (Figure 3-4B). RACE results confirmed that the initial cloned Kir sequences were the full cDNA sequences. 3'RACE was not necessary as a stop codon in frame with the 5' start site was amplified in the original open reading frame. Inverse PCR on rolling circle amplified cDNA was also attempted to determining sequence of 5' and 3' ends, however sequencing results indicated

that there was some crossover or concatamerization in the template cDNA. This was thought to be the case because identical regions of the AmqKirB sequence were linked in duplicate. Inverse PCR products were not further analyzed.

The AmqKir cDNAs had open reading frames of 1047 and 1071 bp respectively (Appendix A.4), corresponding to predicted amino acid sequences of 349 and 357 residues with 68% shared identity (Figure 3-5). Analysis of the genome assembly indicated that these are single exon, tandemly-duplicated genes.

3.3.2 Phylogenetic Analysis and Primary Structure

As in other Kir channels, AmqKirA and AmqKirB each contain two transmembrane helices M1 and M2 flanking a conserved pore structure containing the TXGYG signature sequence for K^+ channels. These domains were inferred by Kyte-Doolittle hydrophathy plots (Figure 3-6) and were consistent with mapped domains of vertebrate Kir channels. I identified 5 and 4 consensus protein kinase A (PKA) phosphorylation sites in the cytoplasmic domains of AmqKirA and AmqKirB, respectively (Figure 3-5). Additionally, in AmqKirB, there are 2 consensus protein kinase C (PKC) phosphorylation sites. Sequence identity for the full length clones was 29-35% with *Nematostella vectensis* (Cnidaria) and 23-30% with mammalian Kirs, well below the identity levels found across known Kir subfamilies (50-60% with the exception of Kir7 which shares only 38% identity with other mammalian subfamilies) (Doupnik et al., 1995; Krapivinsky et al., 1998). The channel core (M1, P, and M2) had higher amino acid identity with

mammalian (38-51%) and cnidarian (48-54%) inward rectifiers, Table 3-1 and Figure 3-7.

The phylogenetic relationships between sponge and other metazoan inward rectifiers are shown in Figure 3-8. The overall tree topology based on the alignment of the full channel sequences shows that Kir diversification occurred independently in sponges, cnidarians, invertebrates, and chordates and indicates that a single ancestral gene gave rise to inward rectifiers in the Metazoa.

We rooted the tree between Poriferan and Cnidarian sequences based on current knowledge of relationships among metazoan phyla (Borchiellini et al., 2001; Collins, 1998; Sperling et al., 2007). Computer-predicted inward rectifier sequences from the choanoflagellate *Monosiga brevicolis* (gi167515450 and gi167522960) were highly divergent and their inclusion in the analysis destabilized all branches suggesting that protozoan and metazoan Kir sequences are distinct. The bacterial Kir sequence Kirbac1.1 was not included. Lack of available sequences for ctenophores prevented a test of the recent hypothesis that this group is the sister to other metazoans (Dunn et al., 2008).

The order of branching of vertebrate Kir subfamilies is consistent with previous analyses (Okamura et al., 2005; Tanaka-Kunishima et al., 2007) – with the exception of Kir6 which in Bayesian analysis branches before triploblastic invertebrates, but with very low support. Also, as shown previously, we find that diversification of Kir channel subfamilies occurred in vertebrates, and urochordate Kirs lie at the base of this diversification.

3.3.3 Expression in oocytes

To study the functional characteristics of AmqKirA and AmqKirB channels, we cloned full-length cDNAs into the pxt7 expression plasmid, prepared cRNAs by *in vitro* transcription, and injected purified cRNAs into frog oocytes. AmqKirA and AmqKirB were digested from the pCR4-TOPO vector with the same pair of restriction enzymes used to linearize the pxt7 expression vector (Figure 3-9A). Digested Kir and pxt7 were ligated together and the recombinant vector cloned. Clones positive for the Kir insert in the proper orientation were identified by colony PCR (Figure 3-9B) and sequencing. Positive clones were miniprepped, linearized (Figure 3-9C) and cRNA prepared. Figure 3-9D shows purified cRNA which was subsequently used for injection into oocytes.

3.3.3.1 Electrophysiological properties

From a holding potential of -50 or 0 mV, voltage steps or a ramp protocol were used to change the membrane potential. Oocytes injected with either AmqKirA or AmqKirB cRNAs demonstrated prominent inward currents (negative current) which did not inactivate during 2 sec voltage pulses (Figure 3-10). Outward (positive) currents were minimal. Because we injected oocytes with only a single cRNA species, it is clear that AmqKir channels can exist as homo-multimers. Whether they naturally co-assemble with other Kir subunits is not yet known.

Sponge channels were constitutively active without the addition of activators such as G-proteins or ATP, although we cannot rule out a requirement

for an activator that is endogenous to the oocytes. A suggestion for an as yet unknown modulatory mechanism was found for AmqKirB currents which demonstrated an unusual phenomenon of run-up of current amplitude during recordings. The example (Figure 3-10B) shows 5-fold growth of the inward current without a significant change in the reversal potential and without an increase in the outward current over nearly 2 hours. Similar results were obtained from all cells injected with AmqKirB although the rate of increase of inward current varied from cell to cell. Run-up has been reported for vertebrate Kir2.1 and Kir2.2 currents and may be explained by PKA activity whereas these currents were down-regulated by activation of PKC (Fakler et al., 1994; Scherer et al., 2007; Zitron et al., 2004).

The current-voltage relationship for AmqKirA and AmqKirB is strongly rectifying with large inward currents at membrane potentials hyperpolarized to the equilibrium potential for potassium (E_K) and very small currents positive to E_K (Figure 3-10). In mammalian cells, this phenotype is characteristic of Kir3 channels which are activated by G proteins, and Kir2 channels which are constitutively active. Strong rectification is determined by pore-lining residues which facilitate voltage-dependent block by internal Mg^{2+} and polyamines. In the M2 region of Kir2.1 S165 binds Mg^{2+} and D172 binds Mg^{2+} and polyamines (Lopatin et al., 1994; Lu and MacKinnon, 1994b; Stanfield et al., 1994; Wible et al., 1994). The C-terminus forms the cytoplasmic portion of the pore. Negatively charged C-terminal residues including E224, D255, D259 and E299 attract Mg^{2+} and polyamines to the transmembrane plugging (Bichet et al., 2003; Kubo and

Murata, 2001; Lu, 2004; Taglialatela et al., 1995). Interestingly despite the phylogenetic distance between sponge and vertebrate Kir subfamilies these residues were conserved in AmqKirA and AmqKirB - with the exception of S165, which maps to a cysteine (C157), another polar residue, in AmqKirA (Figure 3-7).

3.3.3.2 Selectivity for K^+

Consistent with other inward rectifiers, when external potassium concentration, $[K^+]_o$, was altered, either from low to high or high to low concentration, AmqKir reversal potentials, defined as the zero current membrane potential, shifted in accordance with the equilibrium potential for potassium, E_K, and current amplitude increased in as $[K^+]_o$ increased (Fig 3-10C). Theoretical values for E_K were calculated at various $[K^+]_o$ using the Nernst equation: $E_K=(RT/F)\ln([K^+]_o/[K^+]_i)$, where R is the gas constant, T is the temperature in Kelvin and F is the Faraday constant. Assuming internal K^+ concentrations, $[K^+]_i$ of 140 mM, E_K values at 2, 5, 10, 25 and 50mM would be -100.0, -78,4, -62.1, -40,6 and -24.2. These are in close agreement with the recorded values for reversal potential: -117± 3.10 (n=13), -94.46 ± 2.59 (n=13), -77.75 ± 2.75 (n=12), -49.20 ± 3.30 (n=10) and -38 ± 1.5 (n=5) for AmqKirA; and -112.91 ± 4.36 (n=11), 8-1.73 ± 3.62 (n=15), -78.8 ± 3.28 (n=3.28), -59 ± 3.06 (n=3) and -47.5 ± 1.5 (n=2) for AmqKirB. The relationship between reversal potential and $[K^+]_o$ was linear; the reversal potential for AmqKirA, for example, was depolarized by 49 mV for each 10x increase in external K (i.e. Figure 3-10C, inset). This is close to the

theoretical value of 58 for a perfectly K selective channel. Results were calculated from cells with negligible background currents and only for stable cells with membrane potentials not more depolarized than –50 mM in 5 mM external K.

We further tested selectivity of AmqKirA and AmqKirB by comparing inward current amplitude in K^+, Na^+, Rb^+ and $NMDG^+$ containing solutions, and found both channels to be highly K^+ selective (Figure 3-11). $NMDG^+$ (radius 4.5 Å) was used as an impermeable counter ion (i.e. 10 mM X^+ in 90 mM $NMDG^+$), and as expected currents in $NMDG^+$ alone were negligible. Currents were also negligible in 10 or 100 mM Na^+. This is consistent with almost all other K channels (Hille, 1992) and the close-fit model in which K^+ (radius 2.66 Å) is coordinated through the pore by snug interactions with carbonyl side chains, replacing the shell of water molecules around K^+ (Doyle et al., 1998). Na^+ (radius 1.90 Å) is too small to be coordinated by these side chains (Bezanilla and Armstrong, 1972; Hille, 1973; Mullins, 1959).

Unlike most potassium channels which have similar or greater permeability to Rb^+ than to K^+ (Doyle et al., 1998), current through AmqKirB in 10mM Rb^+ at -140mV was only 14.6 ± 1.6% (n=5) the current in 10 mM K^+ (Figure 3-11B). We cannot confirm that the observed AmqKir currents are from passage of Rb^+ as RbCl solution applied to AmqKirA contained 2.25 mM K^+ from pHing with KOH. Nonetheless the low permeability to Rb highlights the selectivity of both AmqKir channels. Permeability of AmqKirA to Rb^+ was tested by Linda Boland and also found to be minimal (<20% K^+ current). In vertebrate Kir2.1, a threonine

in the selectivity filter (T141) is linked to low Rb^+ permeability. This residue is thought to narrow the selectivity filter such that conductance of smaller K^+ (radius 2.66 Å) is favored over larger Rb^+ (radius 2.96 Å) (Choe et al., 2000). In AmqKirA and AmqKirB however, this is a valine, a residue linked to high Rb^+ permeability in Kir1.1 (Figure 3-11C). This suggests that other residues contribute to high selectivity in AmqKir channels.

3.3.3.3 Block by external Cs^+, and Ba^{2+} and Na^+

To further characterize the electrophysiology of AmqKir channels we tested the effect of Cs^+ and Ba^{2+}, monovalent and divalent cations which block K current in other inward rectifiers. Both AmqKirA and AmqKirB currents were blocked by Cs^+ and Ba^{2+} but we analyzed data for AmqKirA only because continual current run-up (Figure 3-10B) precluded accurate measurement of the percent block in AmqKirB. Oocytes expressing AmqKirA were perfused with solution containing 0.03 – 3mM Cs^+ and 0.01 – 1mM Ba^{2+} (Figure 3-12A and B), and current inhibition was assessed using voltage step and ramp protocols. As with other cloned and native Kir channels, block by Cs^+ and Ba^{2+} was time and voltage dependent and was largely reversible upon washout (Figure 3-12C). Block by Cs^+ showed prominent voltage-dependence in that hyperpolarization intensified the block and depolarization relieved it. This was first noticed for Cs^+ block of Kir currents in starfish eggs (Hagiwara et al., 1976). Raab-Graham et al. (1994) found that Cs^+ produced rapid interruption of K current which became more frequent at

more negative membrane potentials - a pattern consistent with open channel block.

Block of AmqKirA currents in 5mM K^+ was concentration dependent with an IC_{50} of 37uM for Ba^{2+} and 173 µM for Cs^+. High affinity Ba^{2+} block in vertebrate Kir2.1 (IC50 2.7 ±0.1 µM at -80 mV) is linked to two residues: E125 and T141 (Alagem et al., 2001). The negatively charged residue E125 in the outer channel vestibule is thought to mediate Ba^{2+} entry into the pore either by electrostatic attraction or facilitating dehydration of entering ions. T141 is just two positions N terminal of GYG and is thought to stabilize Ba^{2+} binding within the selectivity filter. This is supported by x-ray crystallography of KcsA, a bacterial 2TM K channel, equilibrated with $BaCl_2$ solution. The crystal structure shows a Ba^{2+} ion bound to the intracellular end of the selectivity filter, close to residue corresponding to T141 in Kir2.1 (Jiang and MacKinnon, 2000).

In AmqKirA the residues corresponding to E125 and T141 are N117 and V133 respectively. Other channels with N and V at these positions were still blocked by Ba^{2+} but with lower affinity than Kir2.1 – comparable to AmqKir channels. The mutation V121T in Kir1.2 at the site corresponding to Kir2.1 T141 increased Ba^{2+} sensitivity (Zhou et al., 1996) as did the mutating N125 in chick Kir2.1 to E, the corresponding residue in human and mouse Kir2.1 (Navaratnam et al., 1995).

T141 in vertebrate Kir2.1 has also been linked to Cs^+ block. Mutation of T141 to valine, the residue in AmqKir channels reduced but did not abolish Cs^+ block

(Thompson et al. 2000). The residue S165, corresponding to the polar residue, C157, in AmqKirA, also confers Cs^+ sensitivity to Kir2.1 (Thompson et al., 2000).

The inset in Figure 3-11A also shows results of AmqKirA block by addition of 0.03-1mM Na^+ (NaCl) to oocytes bathed in 5 mM K^+.

3.3.3.4 Block by tertiapin-Q

Tertiapin-Q, a nonoxidizable form of honey bee toxin has been shown to selectively inhibit a subset of Kir channels and is one of only a few blockers available to discriminate between the contributions of different Kir channels *in situ* (Ramu et al., 2004). In the hopes that this might be a tool applicable to studying Kir in sponge tissues we tested the ability of TPN-Q to block AmqKirA, relative to toxin sensitive rat Kir1.1b and toxin insensitive mouse Kir2.1 (Figure 3-12 D to F). Because the block of Kir1.1b by TPN-Q was pH sensitive, as reported by Ramu et al. (2004), we performed these experiments at an external pH of 7.6. In our experiments rat Kir1.1 b currents were blocked as expected in a concentration dependent manner with 80% block at 100 nM (n=2). By contrast, AmqKirA, like mKir2.1, was insensitive to 100 nM TPN-Q. TPN-Q will therefore not be useful for deciphering *in situ* the contributions of AmqKirA to the membrane potential. The structural basis of TPN-Q selectivity is a variable region in the N-terminal part of the linker region between M1 and M2. It has been suggested that the variable region in Kir1.1 (11 residues) and Kir3.4 (10 residues) forms an alpha helix which interacts with the helical portion of TPN-Q.

Insensitivity of Kir2.1 channels may be explained by a shorter variable region (8 residues) as a complete helical turn may not form (Jin et al., 1999; Ramu et al., 2004). As with KirBac1.1 which lacks this region and is insensitive to TPN-Q (Ramu et al. 2004), the corresponding region in AmqKir channels is only four residues and not likely long enough to confer sensitivity (Figure 3-12G). The variable region is similarly short or absent in predicted *Nematostella vectensis* Kir channels indicating that the variable region may not have been present in Kir channels of early branching metazoans.

3.4 Concluding remarks and directions for future research

I have cloned and functionally expressed the first ion channels from the Phylum Porifera, prioritizing inward rectifier potassium channels for their simple architecture and fundamental role in setting the membrane potential. The electrophysiological properties of sponge Kir channels including the absence of substantial outward current at membrane potentials positive to E_K, the high selectivity for K^+ and the voltage-dependent block by Ba^{2+} and Cs^+ indicate that these key features of strong inwardly rectifying K^+ channels are conserved throughout evolution.

3.4.1 Functional significance and mechanism of strong inward rectification

In vertebrates strongly rectifying channels are typically localized to excitable cells including neurons, cardiac muscle and skeletal muscle (Kubo et al., 2005). Strong block of these channels by internal polyamines and Mg^{2+} prevents passage of significant outward current at potentials more positive than equilibrium

for potassium, allowing the cell to depolarize further, and for electrical signals to propagate (Oliver et al., 2000). The presence of strongly rectifying sponge Kir channels is consistent with the idea that some sponge cell membranes are specialized for active signalling. I attempted to confirm the mechanism of rectification by excising oocyte macropatches in inside-out conformation and varying bath (intracellular) concentrations of Mg^{2+} and polyamines. Potassium-selective currents were not detected, however, suggesting inadequate density of channels. Given sufficient current (15 µA whole oocyte current should give detectable 15 pA currents in 4 µm patches) the following should be attempted. Presence of inward rectification should be confirmed by running voltage ramps or steps in cell-attached mode. The patch should then be excised to Mg^{2+} and polyamine-free solution (pipette: 85mM KCl, 0.3 mM $CaCl_2$, 1 mM $MgCl_2$, 5mM K_2HPO_4, 5mM KH_2PO_4, 10 mM NaCl, KOH to pH 7.4 and 100mM K total; and bath: 85mM KCl, 5mM Na_2EDTA, 5mM K_2HPO_4, 5mM KH2PO4, KOH to pH 7.2 and 100 mM total K). Voltage ramps or steps should be repeated at 60 s intervals. If block of outward current is due to an intracellular blocking molecule then the ratio of outward current to inward current should increase as cytosolic components are washed away – that is the inward rectification should disappear. To test whether Mg^{2+} and polyamines may be involved in intracellular block each can in turn be added to the bath (intracellular) solution to see if inward rectification returns. Suggested test concentrations would be 0.1, 0.5, 1, 2, 5 and 10mM Mg^{2+} by adding from a 1 M MgCl2 stock and readjusting the pH; and 1, 10, 100 and 1000 µM spermine or spermidine added directly from 10 mM stocks

adjusted to pH 7.2 with HCl. Because 5mM EDTA is present in the medium to chelate divalent cations some of the Mg^{2+} added will be chelated. Additional Mg^{2+} must therefore be added to get the desired concentration. According to the maxchelator site http://www.stanford.edu/~cpatton/maxc.html $MgCl_2$ concentrations of 4.9, 5.5, 6, 7, 10 and 15 mM would be required to get the desired free Mg^{2+} concentrations. After experiments with a given patch are completed, Mg^{2+} should be added in excess (20 mM) to cause complete block of outward current. Residual current should be considered leak current and subtracted offline to give leak corrected records.

Intracellular block by Mg^{2+} is responsible for inward rectification in the vertebrate Kir subfamilies, excepting Kir7 which has unique pore properties (Krapivinsky et al. 1998). If Mg^{2+} block is confirmed in AmqKir channels this would suggest that this mechanism of gating was present in the earliest metazoan channels. As there is no electrophysiological data on protozoan inward rectifiers and no Mg^{2+} or polyamine data for prokaryote Kirs we cannot say how earlier Kir channels were gated. The two putative choanoflagellate inward rectifiers channels, however, had only a portion of residues associated with Mg^{2+} and polyamine block: residues mapping to Kir2.1 D172 and E299 but not S165, E224, D255 or D259 in *M. brevicolis* gi|167515450; and D172 and E224 but not S165, D255, D259 or E299 in *M. brevicolis* gi167522960. Inward rectifier K channels in plants have a different architecture, with 6 transmembrane domains and are not gated by Mg^{2+} (Hedrich et al., 1995; Zimmermann et al., 1998). Inwardly rectifying currents in plant guard cells are inhibited by polyamines, however it is

unclear if the polyamines act directly on the channel or through a second messenger pathway (Liu et al., 2000).

3.4.2 Future directions

Recordings from sponge cell membranes are still required. Determining contributions of individual Kir channels by knocking down channel activity remains a challenge in vertebrates. Few specific inhibitors are available to distinguish Kir channel subtypes. As a result genetic knockouts (Kofuji et al., 2000) and RNA interference (Kucheryavykh et al., 2007) have been employed to study physiological roles of Kir4.1 channels in glial cells. Tertiapin-Q, which blocks vertebrate Kir1.1 and Kir3.1/3.4 (Ramu et al., 2004) was ineffective as a blocker for AmqKirA. Kir current may, however, be non-specifically inhibited by bathing cells in Cs^{+} or Ba^{2+} containing solutions (Yamoah et al., 1998).

Native inward rectifier currents should be monitored at hyperpolarized potentials to determine if channel activities fluctuate over prolonged periods. We have already seen evidence of current modulation in AmqKirB channels which display a phenomenon of run-up of current amplitude. Presumably *in situ* such modulation would lead to gradual changes in membrane potential and hence excitability over time. Long term changes in membrane potential could underlie, for example, changes in frequencies of rhythmic contractions in demosponges (Nickel, 2004) and of repeated feeding current arrests in hexactinellids (Tompkins-MacDonald and Leys, 2008).

Future work should investigate the types of modulators that act on AmqKir channels to understand the environmental stimuli and metabolic indicators that alter excitability. Understanding the contribution of Kir channels to the resting potential will set the groundwork for future study of ionic currents that depolarize the membrane as part of active signalling. Identification of modulators that alter AmqKir current amplitude will also help to pinpoint residues that mediate regulation of Kir channels. Homology modelling may also help in identifying conserved functional domains. Identifying domains functionally conserved with sponge ion channels may give insight into domains present in Kir channels in ancestral animals prior to diversification. Phylogenetic analyses indicate that the functionally distinct Kir families 1 through 7 diversified in the deuterostome lineage. However the origins of functional domains with these channels remain unknown. Alignments show conservation of residues which confer a strong rectifier phenotype consistent with Kir2 and Kir3 channels. Whether regulatory domains including ATP binding (Kir6), pH sensing (Kir1), and GTP binding (Kir3) domains were also present in basal metazoan Kir channels should be investigated to gain further insight into the evolution of metazoan potassium channels. This approach has given insight into diversification of metazoan receptor molecules. Domains mapping to both glutamate receptors and GABA receptors for example were cloned in a single GABA/glutamate receptor hinting at a common origin for the two receptor families and indicating that many of the functional domains were already present in the earliest metazoans (Perovic et al., 1999).

Overall this work has provided unique insight into the functional properties of a potassium channel cloned from the earliest branching extant metazoans and sets the groundwork for understanding membrane potential in a basal metazoan.

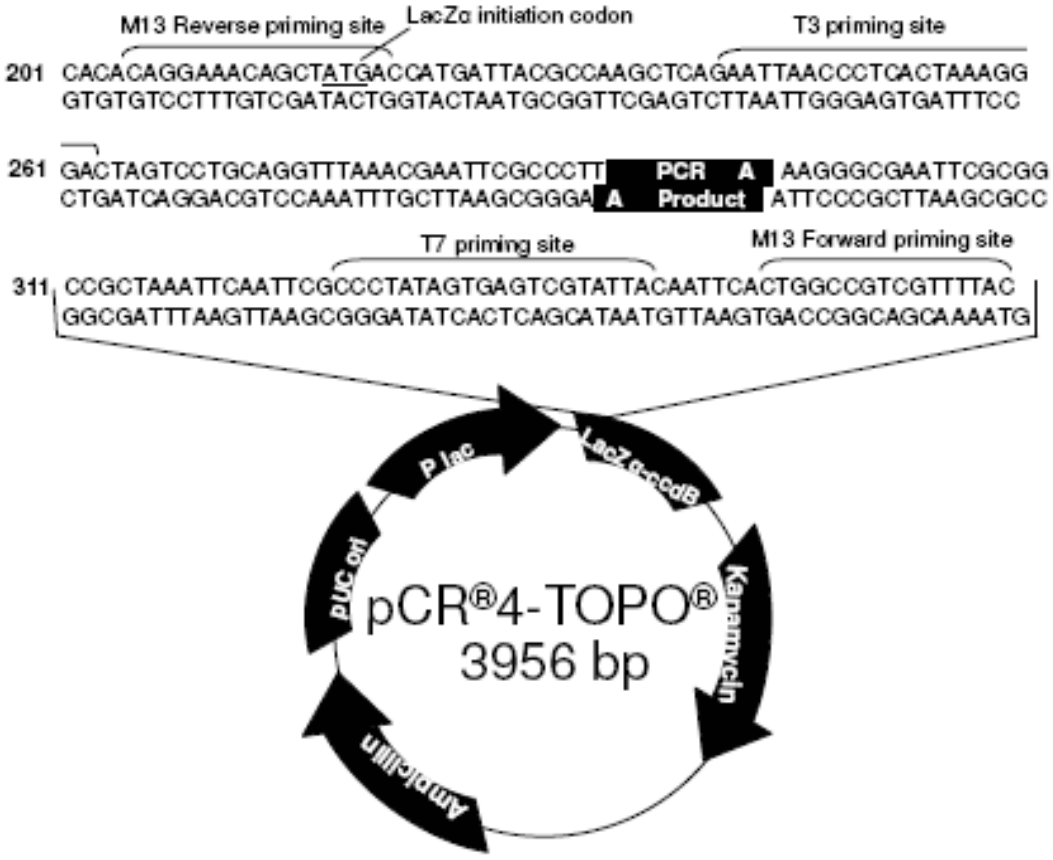

Figure 3-1: Simplified map of PCR4®-TOPO® cloning vector adapted from www.invitrogen.com.

Taq amplified PCR products are ligated into the vector at TA overhangs where indicated. PCR products are amplified and sequenced by adding primers that anneal to either M13 Forward/M13 Reverse or T3/T7 priming sites. Insertion of a PCR product interrupts the lethal lacZ-α-ccdB fusion gene, allowing only positively transformed cells to grow.

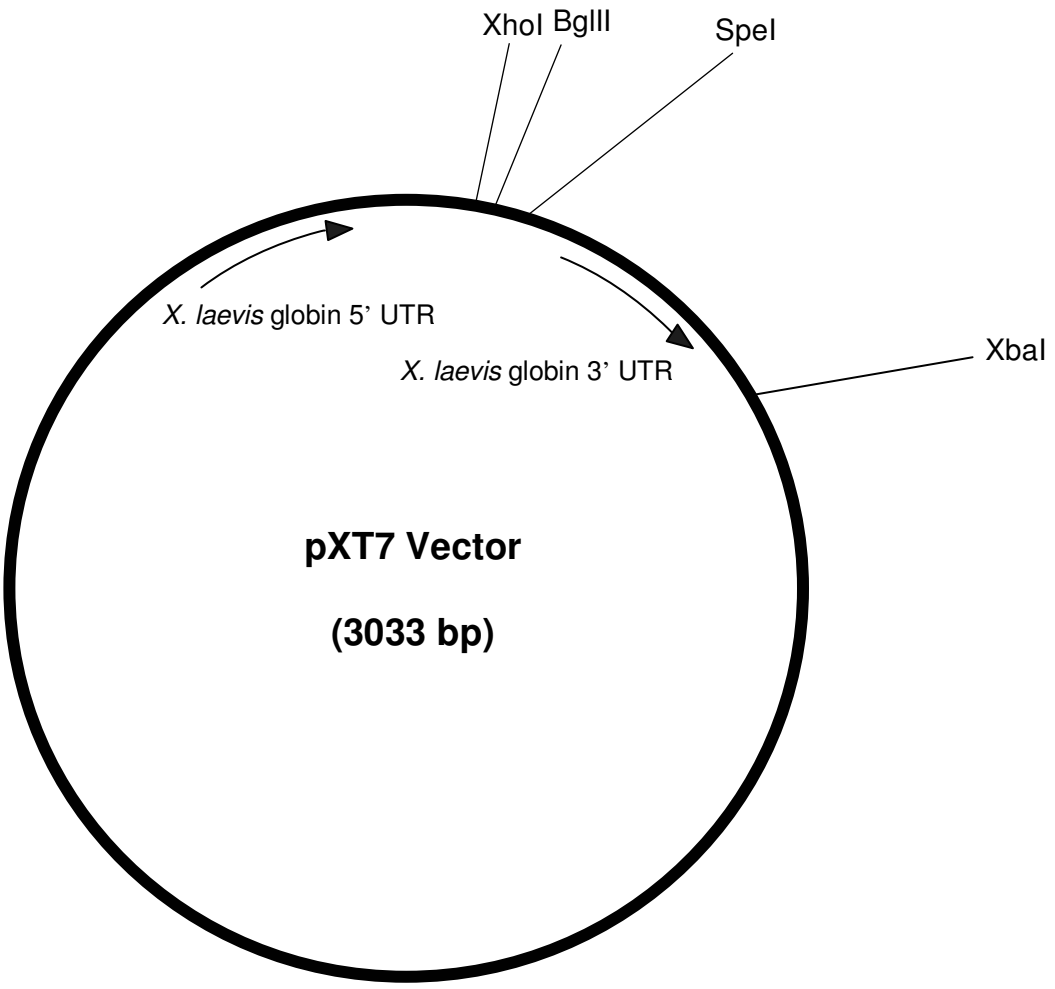

Figure 3-2: Simplified map of the pXT7 expression vector.

Shown are restriction sites compatible with insertion of AmqKirA (XhoI/SpeI) and AmqKirB (XhoI/BglII) open reading frames and linearization of the AmqKir-pXT7 construct (XbaI). The promoter for the *Xenopus laevis* globin enhances expression in *X. laevis* oocytes.

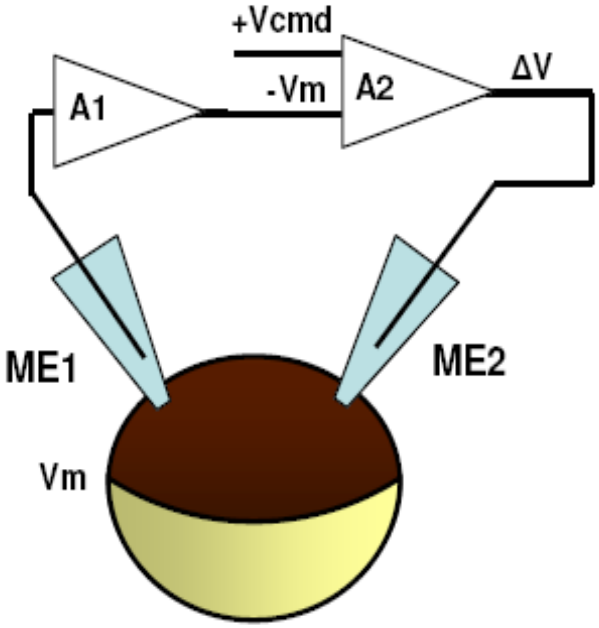

Figure 3-3: Simplified circuit for Two-Electrode Voltage Clamp of oocytes.

Membrane potential (Vm) is recorded by an amplifier (A1) connected to the voltage recording microelectrode (MEI). The difference (ΔV) between Vm and command potential (Vcmd; set by user) is recorded in amplifier 2 (A2). A current proportional to the difference between Vcmd and Vm is then forced through the current-passing microelectrode (ME2), bringing the membrane potential closer to Vcmd.

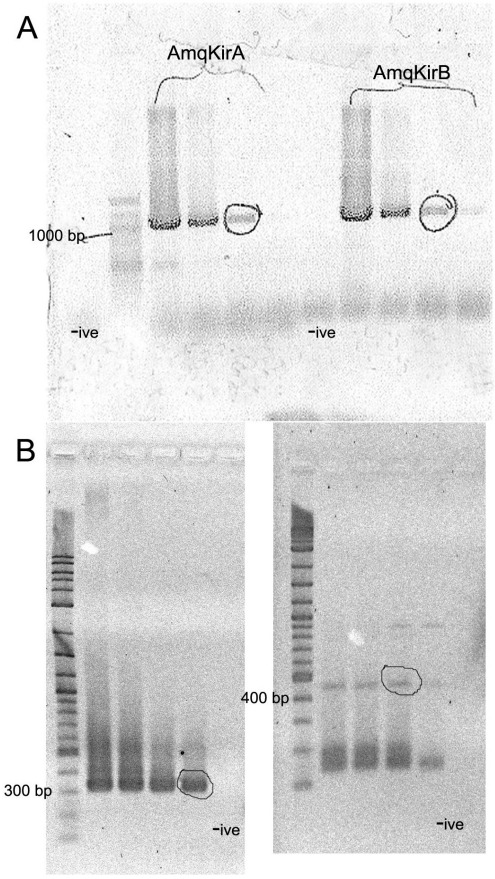

Figure 3-4: Ethidium bromide stained agarose gels (1%) showing AmqKir products.

(A) Amplified open reading frame of AmqKirA and AmqKirB. Products were amplified from 10^{-1} through 10^{-4} dilutions of cDNA. Circled bands were cloned and sequenced. (B) The 5' ends were confirmed by nested 5'-RACE on 10^{-1} through 10^{-4} dilutions of 5' RACE products. The highlighted bands were sequenced and found to have a start site in frame with the remaining Kir sequence. Samples were run against a 100 bp ladder (Promega) (A) or 2-log DNA ladder (New England Biolabs). Samples were mixed with 6x load dye and wells were loaded with 20 µl samples. No template controls (-ive) are shown for each.

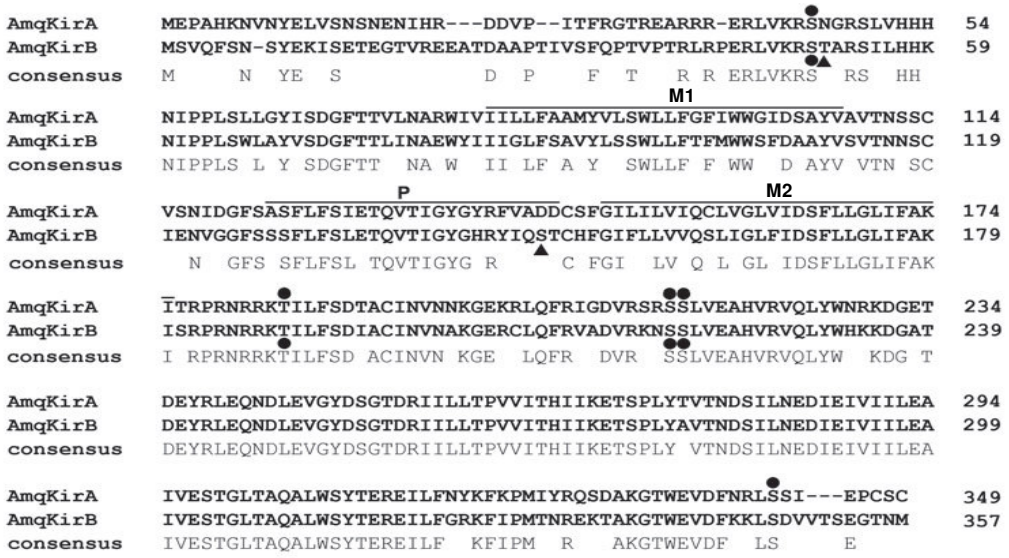

Figure 3-5: LALIGN global alignment of predicted AmqKirA and AmqKirB amino acid sequences.

Putative membrane spanning regions (M1, M2) and pore forming loop (P) deduced from hydropathy analysis and comparison with vertebrate Kir channels are noted by bars. Putative protein kinase A (PKA) (●) and protein kinase C (PKC) (▲) phosphorylation sites were predicted by two out of three prediction programs used (KinasePhos, PredPhospho and Group-based Phosphorylation Scoring).

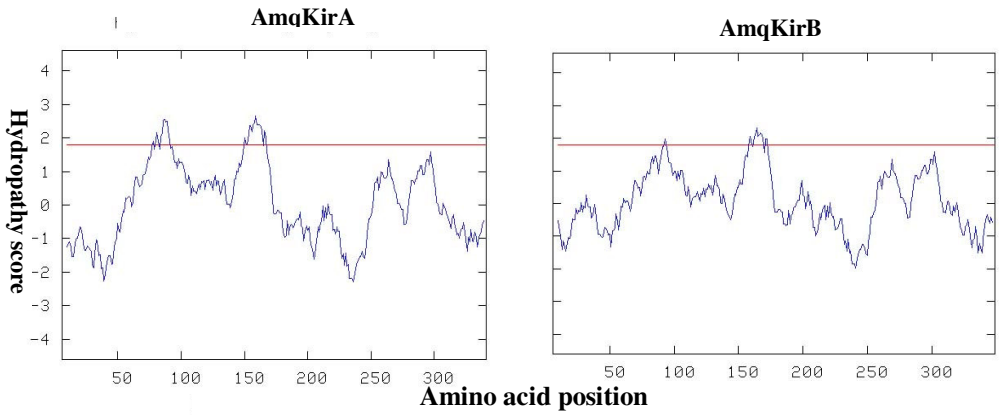

Figure 3-6: Kyte-Doolittle hydropathy plots for AmqKirA and AmqKirB.

Hydropathy scores at each position were produced by averaging the scores of 9 amino acids around that position. The hydrophobic domains, shown above the cutoff (red line) are consistent with the two transmembrane domains of other inward rectifier potassium channels.

Table 3-1: Percentage amino acid identity of AmqKirA and AmqKirB with *Nematostella vectensis* (Nv) and vertebrate Kir channels.

Percent identity was calculated from global alignments with LALIGN online software (http://www.ch.embnet.org/software/LALIGN_form.html) for the overall channel sequence and the channel core (transmembrane regions M1 and M2 and pore region)

	% Identity with AmqKirA		% Identity with AmqKirB	
Sequence	Overall	Core	Overall	Core
AmqKirA	–	–	67.8	69.2
AmqKirB	67.8	69.2	–	–
Nv gi156375411	35.4	46.8	34.6	46.8
Nv gi156372465	29.2	54.4	29.6	50.6
Nv gi156395183	32.7	50.6	33.5	50.6
Nv gi156387460	32.7	51.9	31.7	48.1
rKir1.1	28.4	44.3	28.7	48.1
mKir2.1	29.5	46.8	28.2	38.0
hKir2.2	30.1	51.3	29.5	46.2
hKir2.3	27.9	46.2	28.1	44.9
hKir2.4	26.9	44.9	25.7	38.5
hKir3.1	23.3	39.7	24.5	42.3
hKir3.2	30.2	47.4	28.9	43.6
$hK_ir3.3$	29.1	47.4	27.8	41.0
hKir3.4	29.3	44.9	28.6	44.9
hKir4.1	25.9	38.0	27.1	41.8
hKir4.2	25.3	42.3	26.6	42.3
hKir5.1	24.8	41.0	24.3	37.2
hKir6.1	25.1	43.0	26.6	44.3
hKir6.2	28.7	49.4	28.6	43.0
hKir7.1	25.0	43.6	23.2	39.7

Vertebrate Kir sequences are given for human (hKirx.x), rat (rKir1.1) and mouse (mKir2.1) channels, which were used as controls in our electrophysiology experiments.

Figure 3-7: Multiple alignment of AmqKir with cnidarian and vertebrate Kir sequences.

AmqKirA and AmqKirB were aligned with predicted cnidarian (*Nematostella vectensis,* Nv*)* and selected rat (r), human (h) and mouse (m) Kir channel sequences. Sequences were aligned with ClustalX and analyzed with BOXSHADE. Lines indicate the likely M1 and M2 transmembrane domains and the pore-forming region (P) and variable region (V). Residues mapping to the Kir2.1 residues that determine Mg^{2+} and polyamine block are marked with an asterisk.

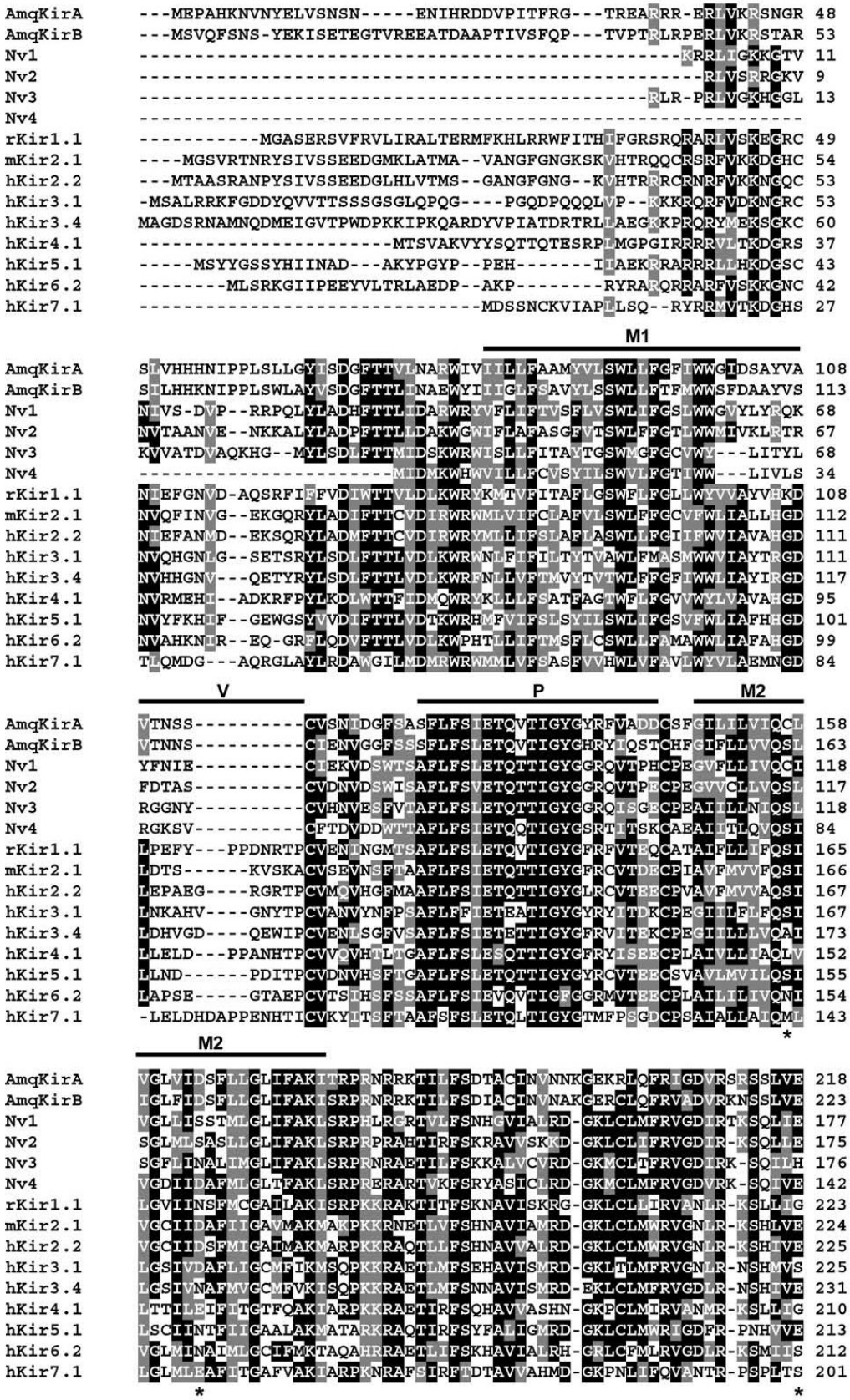
AmqKirA ---MEPAHKNVNYELVSNSN-----ENIHRDDVPITFRG---TREARRR-ERLVKRSNGR 48
AmqKirB ---MSVQFSNS-YEKISETEGTVREEATDAAPTIVSFQP---TVPTRLRPERLVKRSTAR 53
Nv1 ----------KRRLIGKKGTV 11
Nv2 ----------RLVSRRGKV 9
Nv3 ----------RLR-PRLVGKHGGL 13
Nv4
rKir1.1 ----------MGASERSVFRVLIRALTERMFKHLRRWFITHIFGRSRQRARLVSKEGRC 49
mKir2.1 ----MGSVRTNRYSIVSSEEDGMKLATMA--VANGFGNGKSKVHTRQQCRSRFVKKDGHC 54
hKir2.2 ---MTAASRANPYSIVSSEEDGLHLVTMS--GANGFGNG--KVHTRRRCRNRFVKKNGQC 53
hKir3.1 -MSALRRKFGDDYQVVTTSSSGSGLQPQG----PGQDPQQQLVP--KKKRQRFVDKNGRC 53
hKir3.4 MAGDSRNAMNQDMEIGVTPWDPKKIPKQARDYVPIATDRTRLLAEGKKPRQRYMEKSGKC 60
hKir4.1 ----------MTSVAKVYYSQTTQTESRPLMGPGIRRRRVLTKDGRS 37
hKir5.1 -----MSYYGSSYHIINAD---AKYPGYP--PEH-------IIAEKRARRRLLHKDGSC 43
hKir6.2 --------MLSRKGIIPEEYVLTRLAEDP--AKP--------RYRARQRRARFVSKKGNC 42
hKir7.1 ----------MDSSNCKVIAPLLSQ--RYRRMVTKDGHS 27
M1
AmqKirA SLVHHHNIPPLSLLGYISDGFTTVLNARWIVIILLFAAMYVLSWLLFGFIWWGIDSAYVA 108
AmqKirB SILHHKNIPPLSWLAYVSDGFTTLINAEWYIIIGLFSAVYLSSWLLFTFMWWSFDAAYVS 113
Nv1 NIVS-DVP--RRPQLYLADHFTTLIDARWRYVFLIFTVSFLVSWLIFGSLWWGVYLYRQK 68
Nv2 NVTAANVE--NKKALYLADPFTTLLDAKWGWIFLAFASGFVTSWLFFGTLWWMIVKLRTR 67
Nv3 KVVATDVAQKHG--MYLSDLFTTMIDSKWRWISLLFITAYTGSWMGFGCVWY---LITYL 68
Nv4 ----------MIDMKWHWVILLFCVSYILSWVLFGTIWW---LIVLS 34
rKir1.1 NIEFGNVD-AQSRFIFFVDIWTTVLDLKWRYKMTVFITAFLGSWFLFGLLWYVVAYVHKD 108
mKir2.1 NVQFINVG--EKGQRYLADIFTTCVDIRWRWMLVIFCLAFVLSWLFFGCVFWLIALLHGD 112
hKir2.2 NIEFANVD--EKSQRYLADMFTTCVDIRWRYMLLIFSLAFLASWLLFGIIFWVIAVAHGD 111
hKir3.1 NVQHGNLG--SETSRYLSDLFTTLVDLKWRWNLFIFILTYTVAWLFMASMWWVIAYTRGD 111
hKir3.4 NVHHGNV---QETYRYLSDLFTTLVDLKWRFNLLVFTMVYTVTWLFFGFIWWLIAYIRGD 117
hKir4.1 NVRMEHI--ADKRFPYLKDLWTTFIDVQWRYKLLLFSATFAGTWFLFGVVWYLVAVAHGD 95
hKir5.1 NVYFKHIF--GEWGSYVVDIFTTLVDTKWRHMFVIFSLSYILSWLIFGSVFWLIAFHHGD 101
hKir6.2 NVAHKNIR--EQ-GRFLQDVFTTLVDLKWPHTLLIFTMSFLCSWLLFAMAWWLIAFAHGD 99
hKir7.1 TLQMDG---AQRGLAYLRDAWGILMDMRWRWMMLVFSASFVVHWLVFAVLWYVLAEMNGD 84
V P M2
AmqKirA VTNSS----------CVSNIDGFSASFLFSIETQVTIGYGYRFVADDCSFGILILVIQCL 158
AmqKirB VTNNS----------CIENVGGFSSSFLFSLETQVTIGYGHRYIQSTCHFGIFLLVVQSL 163
Nv1 YFNIE----------CIEKVDSWTSAFLFSLETQTTIGYGGRQVTPHCPEGVFLLIVQCI 118
Nv2 FDTAS----------CVDNVDSWISAFLFSVETQTTIGYGGRQVTPECPEGVVCLLVQSL 117
Nv3 RGGNY----------CVHNVESFVTAFLFSLETQTTIGYGGRQISGECPEAIILLNIQSL 118
Nv4 RGKSV----------CFTDVDDWTTAFLFSIETQQTIGYGSRTITSKCAEAIITLQVQSI 84
rKir1.1 LPEFY---PPDNRTPCVENINGMTSAFLFSLETQVTIGYGFRFVTEQCATAIFLLIFQSI 165
mKir2.1 LDTS------KVSKACVSEVNSFTAAFLFSIETQTTIGYGFRCVTDECPIAVFMVVFQSI 166
hKir2.2 LEPAEG----RGRTPCVMQVHGFMAAFLFSIETQTTIGYGLRCVTEECPVAVFMVVAQSI 167
hKir3.1 LNKAHV----GNYTPCVANVYNFPSAFLFFIETEATIGYGYRYITDKCPEGIILFLFQSI 167
hKir3.4 LDHVGD----QEWIPCVENLSGFVSAFLFSIETETTIGYGFRVITEKCPEGIILLLVQAI 173
hKir4.1 LLELD---PPANHTPCVVQVHTLTGAFLFSLESQTTIGYGFRYISEECPLAIVLLIAQLV 152
hKir5.1 LLND------PDITPCVDNVHSFTGAFLFSLETQTTIGYGYRCVTEECSVAVLMVILQSI 155
hKir6.2 LAPSE-----GTAEPCVTSIHSFSSAFLFSIEVQVTIGFGGRMVTEECPLAILILIVQNI 154
hKir7.1 -LELDHDAPPENHTICVKYITSFTAAFSFSLETQLTIGYGTMFPSGDCPSAIALLAIQML 143
M2
M2
AmqKirA VGLVIDSFLLGLIFAKITRPRNRRKTILFSDTACINVNNKGEKRLQFRIGDVRSRSSLVE 218
AmqKirB IGLFIDSFLLGLIFAKISRPRNRRKTILFSDIACINVNAKGERCLQFRVADVRKNSSLVE 223
Nv1 VGLLISSTMLGLIFAKLSRPHLRGRTVLFSNHGVIALRD-GKLCLMFRVGDIRTKSQLIE 177
Nv2 SGLMLSASLLGLIFAKLSRPRPRAHTIRFSKRAVVSKKD-GKLCLIFRVGDIRKSQLLE 175
Nv3 SGFLINALIMGLIFAKLSRPRNRAETILFSKKALVCVRD-GKMCLTFRVGDIRKSQILH 176
Nv4 VGDIIDAFMLGLTFAKLSRPRERARTVKFSRYASICLRD-GKMCLMFRVGDVRKSQIVE 142
rKir1.1 LGVIINSFMCGATLAKISRPKKRAKTITFSKNAVISKRG-GKLCLLIRVANLRKSLLIG 223
mKir2.1 VGCIIDAFIIGAVMAKMAKPKKRNETLVFSHNAVIAMRD-GKLCLMWRVGNLRKSHLVE 224
hKir2.2 VGCIIDSFMIGAIMAKMARPKKRAQTLLFSHNAVVALRD-GKLCLMWRVGNLRKSHIVE 225
hKir3.1 LGSIVDAFLIGCMFIKMSQPKKRAETLMFSEHAVISMRD-GKLTLMFRVGNLRNSHMVS 225
hKir3.4 LGSIVNAFMVGCMFVKISQPKKRAETLMFSNNAVISMRD-EKLCLMFRVGDLRNSHIVE 231
hKir4.1 LTTILEIFITGTFQAKIARPKKRAETIRFSQHAVVASHN-GKPCLMIRVANMRKSLLIG 210
hKir5.1 LSCIINTFIIGAALAKMATARKRAQTIRFSYFALIGMRD-GKLCLMWRIGDFRPNHVVE 213
hKir6.2 VGLMINAIMLGCIFMKTAQAHRRAETLIFSKHAVIALRH-GRLCFMLRVGDLRKSMIIS 212
hKir7.1 LGLMLEAFITGAFVAKIARPKNRAFSIRFTDTAVVAHMD-GKPNLIFQVANTRPSPLTS 201

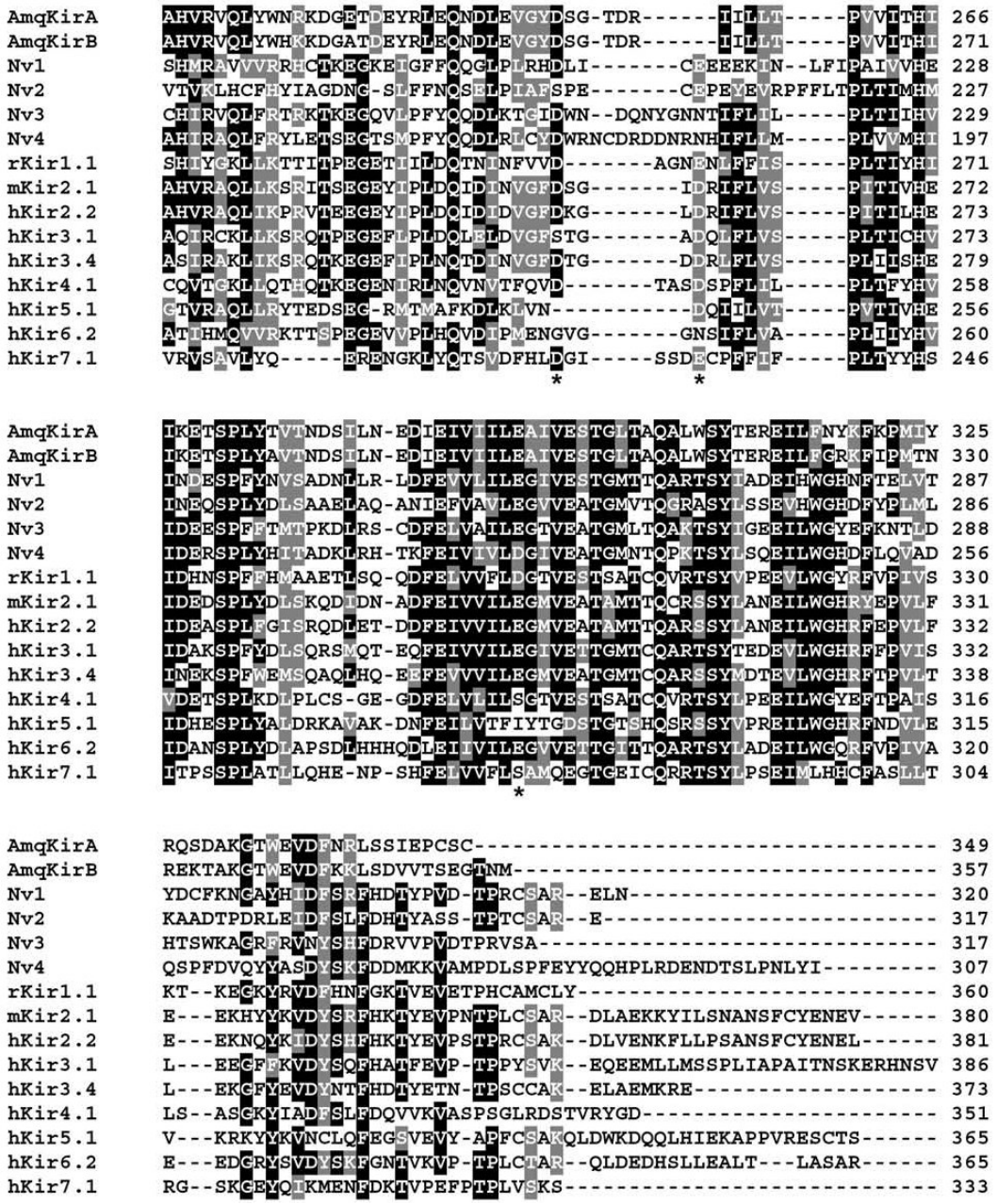
AmqKirA AHVRVQLYWNRKDGETDEYRLEQNDLEVGYDSG-TDR------IILLT-----PVVITHI 266
AmqKirB AHVRVQLYWHKKDGATDEYRLEQNDLEVGYDSG-TDR------IILLT-----PVVITHI 271
Nv1 SHMRAVVVRRHCTKEGKEIGFFQQGLPLRHDLI-------CEEEEKIN--LFIPAIVVHE 228
Nv2 VTVKLHCFHYIAGDNG-SIFFNQSHLPIAFSPE-------CEPEYEVRPFFLTPLTIMHM 227
Nv3 CHIRVQLFRTRKIKEGQVLPFYQQDLKTGIDWN--DQNYGNNTIFLIL-----PLTIIHV 229
Nv4 AHIRAQLFRYLETSEGTSMPFYQQDLRLCYDWRNCDRDDNRNHIFLLM-----PLVVMHI 197
rKir1.1 SHIYGKLLKTTITPEGETIILDQTNINFVVD-------AGNENLFFIS-----PLTIYHI 271
mKir2.1 AHVRAQLLKSRITSEGEYIPLDQIDINVGFDSG-------IDRIFLVS-----PITIVHE 272
hKir2.2 AHVRAQLIKPRVTEEGEYIPLDQIDIDVGFDKG-------LDRIFLVS-----PITILHE 273
hKir3.1 AQIRCKLLKSRQTPEGEFLPLDQLDLDVGFSTG-------ADQLFLVS-----PLTICHV 273
hKir3.4 ASIRAKLIKSRQTKEGEFIPLNQTDINVGFDTG-------DDRLFLVS-----PLIISHE 279
hKir4.1 CQVTGKLLQTHQTKEGENIRLNQVNVTFQVD-------TASDSPFLIL-----PLTFYHV 258
hKir5.1 GTVRAQLLRYTEDSEG-RMTMAFKDLKLVN-----------DQIILVT-----PVTIVHE 256
hKir6.2 ATIHMQVVRKTTSPEGEVVPLHQVDIPMENGVG-------GNSIFLVA-----PLIIYHV 260
hKir7.1 VRVSAVLYQ-----ERENGKLYQTSVDFHLDGI-----SSDECPFFIF-----PLTYYHS 246
AmqKirA IKETSPLYTVTNDSILN-EDIEIVIILEAIVESTGLTAQALWSYTEREILFNYKFKPMIY 325
AmqKirB IKETSPLYAVTNDSILN-EDIEIVIILEAIVESTGLTAQALWSYTEREILFGRKFIPMTN 330
Nv1 INDESPFYNVSADNLLR-LDFEVVLILEGIVESTGMTTQARTSYIADEIHWGHNFTELVT 287
Nv2 INEQSPLYDLSAAELAQ-ANIEFVAVLEGVVEATGMVTQGRASYLSSEVHWGHDFYPLML 286
Nv3 IDEESPFFTMTPKDLRS-CDFELVAILEGTVEATGMLTQAKTSYIGEEILWGYEFKNTLD 288
Nv4 IDERSPLYHITADKLRH-TKFEIVIVLDGIVEATGMNTQPKTSYLSQEILWGHDFLQVAD 256
rKir1.1 IDHNSPFFHMAAETLSQ-QDFELVVFLDGTVESTSATCQVRTSYVPEEVLWGYRFVPIVS 330
mKir2.1 IDEDSPLYDLSKQDIDN-ADFEIVVILEGMVEATAMTTQCRSSYLANEILWGHRYEPVLF 331
hKir2.2 IDEASPLFGISRQDLET-DDFEIVVILEGMVEATAMTTQARSSYLANEILWGHRFEPVLF 332
hKir3.1 IDAKSPFYDLSQRSMQT-EQFEIVVILEGIVETTGMTCQARTSYTEDEVLWGHRFFPVIS 332
hKir3.4 INEKSPFWEMSQAQLHQ-EEFEVVVILEGMVEATGMTCQARSSYMDTEVLWGHRFTPVLT 338
hKir4.1 VDETSPLKDLPLCS-GE-GDFELVLILSGTVESTSATCQVRTSYLPEEILWGYEFTPAIS 316
hKir5.1 IDHESPLYALDRKAVAK-DNFEILVTFIYTGDSTGTSHQSRSSYVPREILWGHRFNDVLE 315
hKir6.2 IDANSPLYDLAPSDLHHHQDLEIIVILEGVVETTGITTQARTSYLADEILWGQRFVPIVA 320
hKir7.1 ITPSSPLATLLQHE-NP-SHFELVVFLSAMQEGTGEICQRRTSYLPSEIMLHHCFASLLT 304
AmqKirA RQSDAKGTWEVDENRLSSIEPCSC---------- 349
AmqKirB REKTAKGTWEVDFKKLSDVVTSEGTNM---------- 357
Nv1 YDCFKNGAYHIDFSRFHDTYPVD-TPRCSAR--ELN---------- 320
Nv2 KAADTPDRLEIDFSLFDHTYASS-TPTCSAR--E---------- 317
Nv3 HTSWKAGRFRVNYSHFDRVVPVDTPRVSA---------- 317
Nv4 QSPFDVQYYASDYSKFDDMKKVAMPDLSPFEYYQQHPLRDENDTSLPNLYI---------- 307
rKir1.1 KT--KEGKYRVDFHNFGKTVEVETPHCAMCLY---------- 360
mKir2.1 E---EKHYYKVDYSRFHKTYEVPNTPLCSAR--DLAEKKYILSNANSFCYENEV------ 380
hKir2.2 E---EKNQYKIDYSHFHKTYEVPSTPRCSAK--DLVENKFLLPSANSFCYENEL------ 381
hKir3.1 L---EEGFFKVDYSQFHATFEVP-TPPYSVK--EQEEMLLMSSPLIAPAITNSKERHNSV 386
hKir3.4 L---EKGFYEVDYNTFHDTYETN-TPSCCAK--ELAEMKRE---------- 373
hKir4.1 LS--ASGKYIADFSLFDQVVKVASPSGLRDSTVRYGD---------- 351
hKir5.1 V---KRKYYKVNCLQFEGSVEVY-APFCSAKQLDWKDQQLHIEKAPPVRESCTS------ 365
hKir6.2 E---EDGRYSVDYSKFGNTVKVP-TPLCTAR--QLDEDHSLLEALT---LASAR------ 365
hKir7.1 RG--SKGEYQIKMENFDKTVPEFPTPLVSKS---------- 333

Figure 3-8: Phylogenetic relationships between AmqKir channels and other metazoan inward-rectifier potassium (Kir) channels.

The phylogenetic relationship was derived as described in Materials and methods. The best Maximum Likelihood tree is shown with Bayesian support values above and RaxML maximum likelihood bootstrap support values below each node. Relationships not recovered in the RaxML analysis are indicated by nf. The tree was simplified by collapsing vertebrate Kir subfamilies from one through to seven and urochordate, arthropod and nematode clades of inward-rectifiers (represented by open triangles).

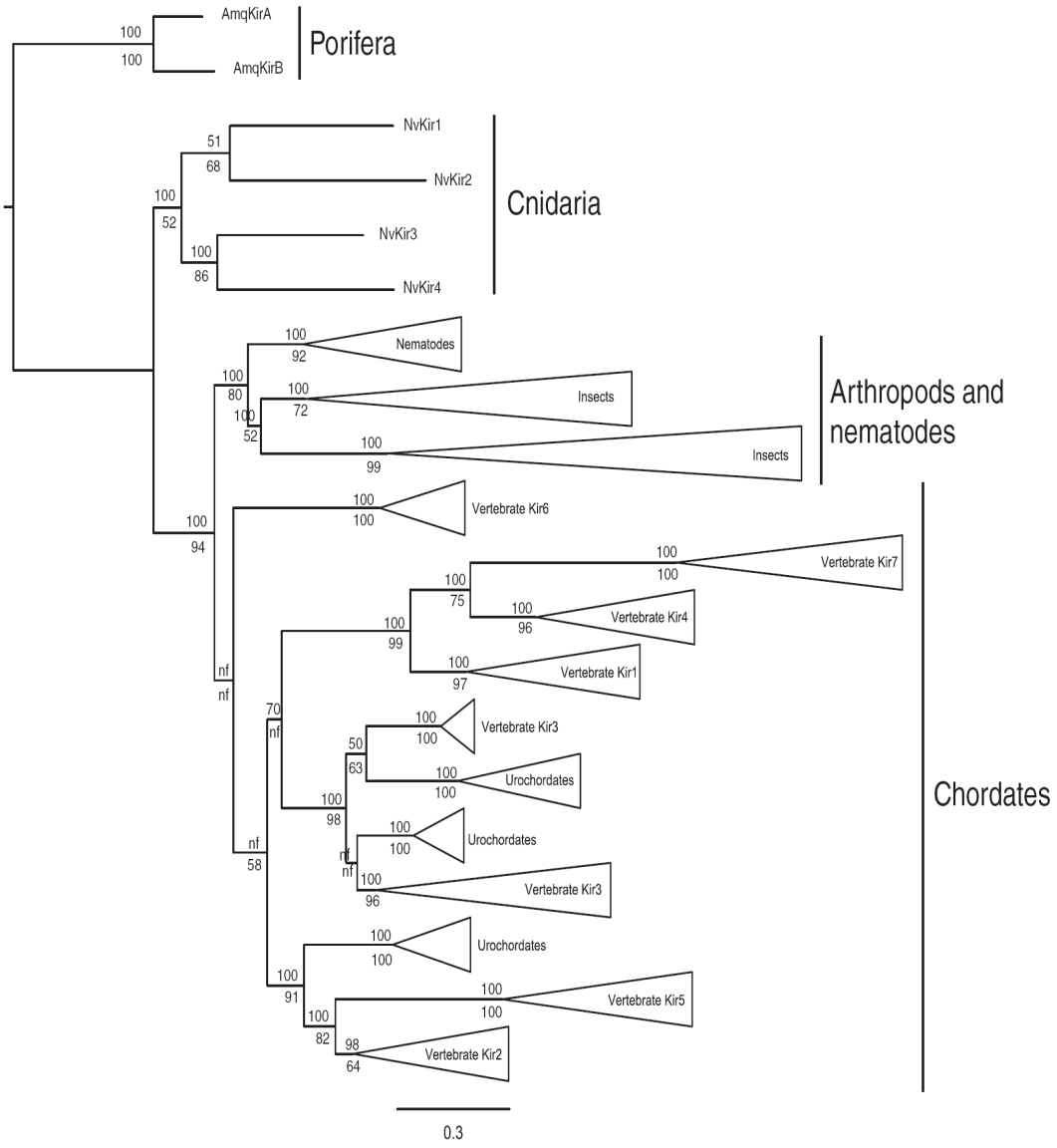
AmqKirA
AmqKirB
Porifera
NvKir1
NvKir2
NvKir3
NvKir4
Cnidaria
Nematodes
Insects
Insects
Arthropods and nematodes
Vertebrate Kir6
Vertebrate Kir7
Vertebrate Kir4
Vertebrate Kir1
Vertebrate Kir3
Urochordates
Urochordates
Vertebrate Kir3
Urochordates
Vertebrate Kir5
Vertebrate Kir2
Chordates
0.3

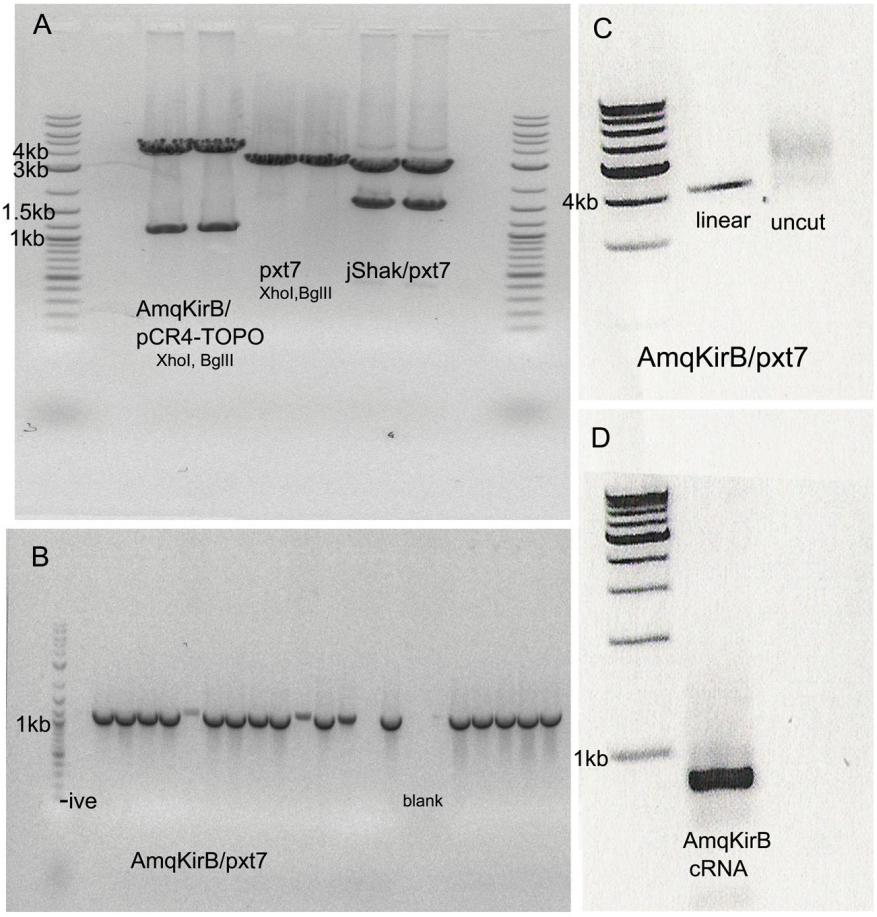

Figure 3-9: Ethidium bromide stained agarose gels (1%) showing procedure to obtain AmqKir cRNA.

(A) AmqKirB digested out of pcr4-TOPO; pxt7 digested with the same sets of restriction enzymes to give compatible ends. As a positive control the digest was also run on pxt7 containing jShak, a jellyfish Shaker potassium channel of known size. (B) Colony PCR to confirm the presence of AmqKirB sequences in the pxt7 expression vector. Colonies were screened with a forward pXT7 primer and reverse AmqKirB primer. (C) Linearization of the AmqKirB/pxt7 construct with XbaI. (D) Sample gel showing cRNA quality

Figure 3-10: Heterologous expression of sponge inward-rectifier potassium (Kir) channels.

Strongly rectifying currents in 5 mM external K^+ (KMES) recorded from (A) AmqKirA using 2 s voltage steps from –150 to +100 mV in +20mV increments from a holding potential –50 mV and (B) AmqKirB using a voltage ramp from a holding potential of –50 mV. Current–voltage plots for AmqKirB were taken at 10 (#1), 30 (#2), 60 (#3) and 90 (#4) mins. The inset shows, in the same cell, the time-dependent change in the normalized current at –140mV (until the recording ended). (C) Effect of increasing external K^+ on AmqKirA currents. Solutions of 2, 5, 10, 25 and 50 mM KMES were used. The inset is a semi-log plot of the reversal potential versus external K^+ concentration for AmqKirA (N = 6–28 per concentration, means ± s.e.m.). The fitted line has a slope of 49 mV.

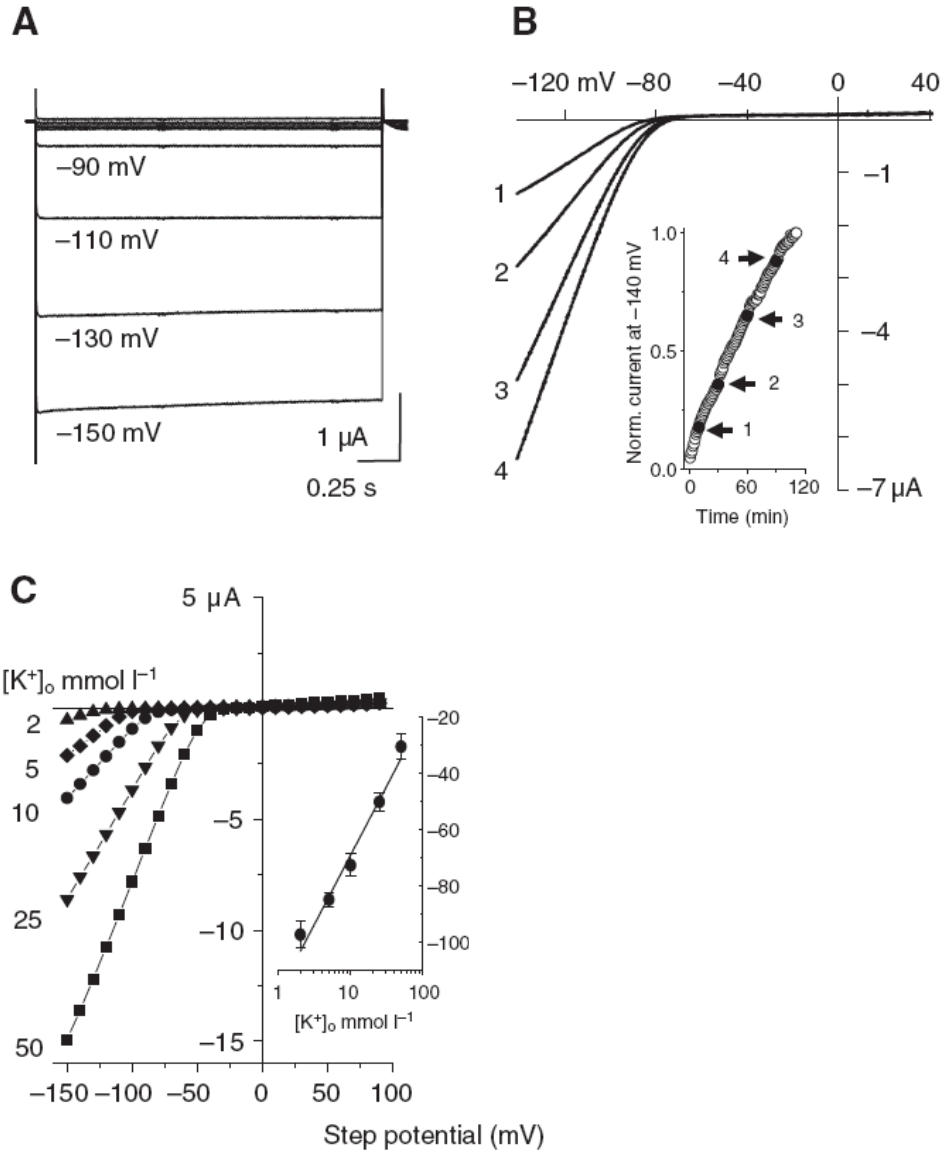
A
–90 mV
–110 mV
–130 mV
–150 mV
1 µA
0.25 s
B
–120 mV –80 –40 0 40
1
2
3
4
–1
–4
–7 µA
Norm. current at –140 mV
1.0
0.5
0.0
0 60 120
Time (min)
C
5 µA
[K+]o mmol l–1
2
5
10
25
50
–5
–10
–15
–20
–40
–60
–80
–100
1 10 100
[K+]o mmol l–1
–150 –100 –50 0 50 100
Step potential (mV)

Figure 3-11: Test of selectivity for K^+ over other monovalent cations.

Representative AmqKirA (A) and AmqKirB (B) current–voltage relationships recorded in the presence of K^+, $NMDG^+$ and Na^+ (all used as MES salts), showing no permeability to Na^+ or $NMDG^+$. The inset shows results of the test of Na (0.03–1 mM NaCl) block of 5 mM KMES currents (N=5, means ± s.e.m.). (B) also shows limited Rb^+ permeability. The highlighted residue (T) in Kir2.1 is typically associated with low Rb permeability (C). V, the corresponding residue in AmqKir channels is associated with high Rb permeability in Kir1.1, indicating that other AmqKir residues are responsible for high selectivity.

A

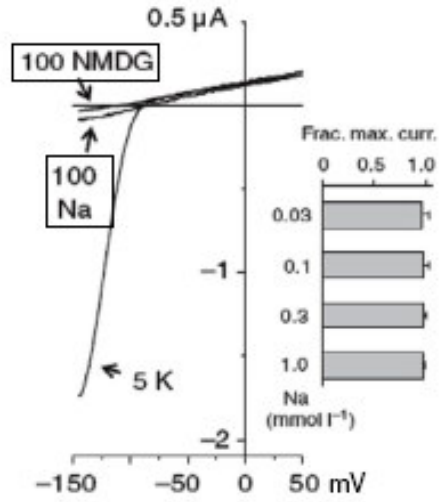

B

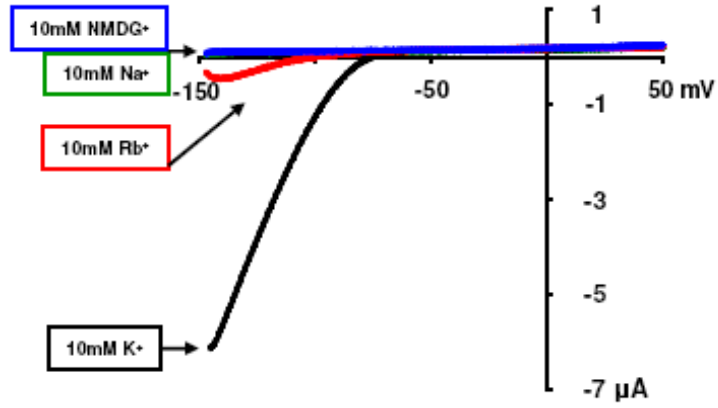

C

AmqKirA	FLFSIETQ**V**TIGYGYR
AmqKirB	FLFSLETQ**V**TIGYGHR
Kir1.1 (HIGH Rb permeability)	FLFSLETQ**V**TIGYGFR
Kir2.1 (LOW Rb permeability)	FLFSIETQ**T**TIGYGFR

.

Figure 3-12: Test of channel block of AmqKirA.

Representative current–voltage relationships in 5mM KMES with increasing concentrations of (A) CsCl or (B) $BaCl_2$. (C) The normalized Kir current at –140 mV is plotted versus blocking ion concentration. The data were fit by a logistic equation with an IC_{50} of 37 μM for Ba^{2+} (N=5–8) and 173 μmol l^{-1} for Cs^{+} (N=8, means ± s.e.m.). Test for tertiapin-Q (TPN-Q) toxin block of (D) AmqKirA, (E) mKir2.1 (mouse Kir) and (F) rKir1.1b (rat Kir) in the absence (0 nmol l^{-1}) or presence of 10 and 100 nmol l^{-1} TPN-Q. Recordings were done in 5mmol^{l-1} KMES, pH 7.6. Currents were measured using 500 ms voltage ramps from a holding potential of –50 mV. The block of rKir1.1b was reversible. (G) Alignment showing that TPN-Q insensitive channels, including AmqKirA and AmqKirB have a shorter variable region. Outward currents in (D) were larger than normal as a result of using a leaky cell for this specific experiment.

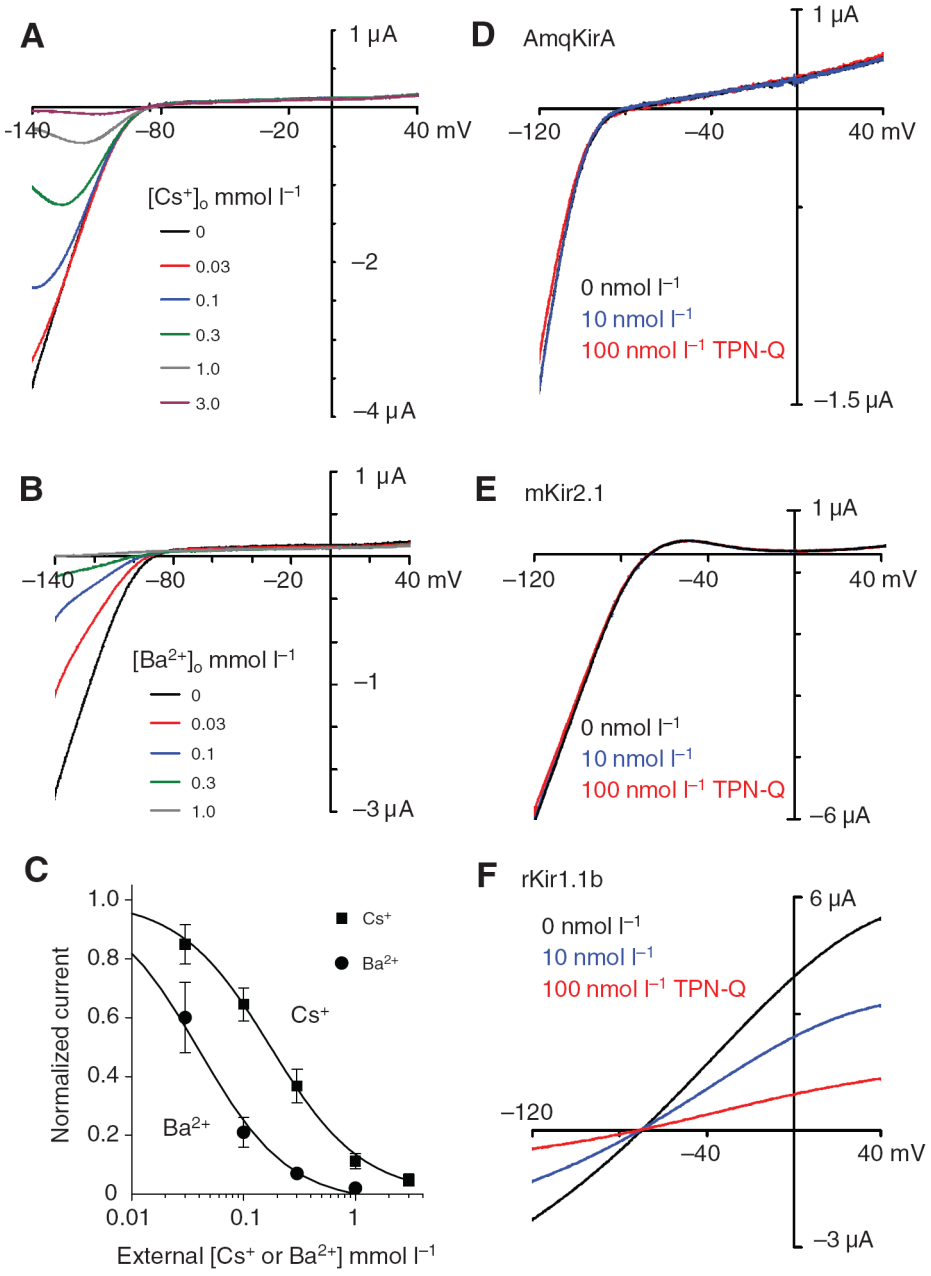

G

```
AmqKirA   AVT------NS-SCV   115 ┐
AmqKirB   SVT------NN-SCI   120 ┘  TPN-Q insensitive
mKir2.1   DLDT---SKVSKACV   123 ┐
rKir1.1   DLPEFYPPDNRTPCV   122 ┘  TPN-Q sensitive
mKir3.4   DLD-HVGDQEWIPCV   130
```

3.5 References

Alagem, N., Dvir, M. and Reuveny, E. (2001). Mechanism of Ba^{2+} block of a mouse inwardly rectifying K^+ channel: differential contribution by two discrete residues. *Journal of Physiology* **534**, 381-393.

Anderson, P. A. V. and Greenberg, R. M. (2001). Phylogeny of ion channels: clues to structure and function. *Comparative Biochemistry and Physiology Part B* **129**, 17-18.

Baukrowitz, T. (2000). Inward rectifier potassium channels and a multitude of intracellular gating molecules. *European Journal of Biochemistry* **267**, 5823.

Bezanilla, F. and Armstrong, C. M. (1972). Negative conductance caused by entry of sodium and cesium ions into the potassium channels of squid axons. *Journal of General Physiology* **60**, 588–608.

Bichet, D., A.Haass, F. and Jan, L. Y. (2003). Merging functional studies with structures of inward rectifier K^+ channels. *Nature Reviews Neuroscience* **4**, 957-967.

Boland, L., Jiang, M., Lee, S., Fahrenkrug, S., Harnett, M. and O'Grady, S. (2003). Functional properties of a brain-specific NH2-terminally spliced modulator of Kv4 channels. *American Journal of Physiology - Cell Physiology* **285**, C161-C170.

Borchiellini, C., Manuel, M., Alivon, E., Boury-Esnault, N., Vacelet, J. and Parco, Y. L. (2001). Sponge paraphyly and the origin of Metazoa. *Journal of Evolutionary Biology* **14**, 171-179.

Boyd, I. (1981). The spicule jungle of *Rhabdocalyptus dawsoni*: A unique microhabitat. BSc thesis. University of Victoria, British Columbia.

Carpaneto, A., Magrassi, R., Zocchi, E., Cerrano, C. and Usai, C. (2003). Patch-clamp recordings in isolated sponge cells (*Axinella polypoides*). *Journal of Biochemical and Biophysical Methods* **55** 179-189.

Choe, H., Sackin, H. and Palmer, L. G. (2000). Permeation properties of inward-rectifier potassium channels and their molecular determinants. *Journal of General Physiology* **115**, 391-404.

Collins, A. G. (1998). Evaluating multiple alternative hypotheses for the origin of Bilateria: An analysis of 18S rRNA molecular evidence. *Proceedings of the National Academy of Sciences* **95**, 15458-15463.

Dellaporta, S. L., Xu, A., Sagasser, S., Jakob, W., Moreno, M. A., Buss, L. W. and Schierwater, B. (2006). Mitochondrial genome of *Trichoplax adhaerens* supports Placozoa as the basal lower metazoan phylum *Proceedings of the National Academy of Sciences* **103**, 8751-8756.

Dibb, K. M., Rose, T., Makary, S. Y., Claydon, T. W., Enkvetchakul, D., Leach, R., Nichols, C. G. and Boyett, M. R. (2003). Molecular Basis of Ion Selectivity, Block, and Rectification of the Inward Rectifier Kir3.1/Kir3.4 K^+ Channel. *Journal of Biological Chemistry* **278**, 49537-49548.

Doupnik, C. A., Davidson, N. and Lester, H. A. (1995). The inward rectifier potassium channel family. *Current Opinion in Neurobiology* **5**. 268-277.

Doyle, D. A., Cabral, J. M., Pfuetzner, R. A., Kuo, A., Gulbis, J. M., Cohen, S. L., Chait, B. T. and MacKinnon, R. (1998). The Structure of the

potassium channel: molecular basis of K^+ conduction and selectivity *Science* **280**, 69-77.

Dunn, C. W., Hejnol, A., Matus, D. Q., Pang, K., Browne, W. E., Smith, S. A., Seaver, E., Rouse, G. W., Obst, M., Edgecombe, G. D. et al. (2008). Broad phylogenomic sampling improves resolution of the animal tree of life. *Nature* **452,** 745-750.

Edgar, R. C. (2004). Muscle: a multiple sequence alignment method with reduced time and space complexity. *BMC Bioinformatics* **5**, 113.

Fakler, B., Brändlea, U., Glowatzkia, E., Zennera, H.-P. and Ruppersberga, J. P. (1994). Kir2.1 inward rectifier K^+ channels are regulated independently by protein kinases and ATP hydrolysis. *Neuron* **13**, 1413-1420.

Gallin, W. J. and Spencer, A. N. (2001). Evolution of potassium channel proteins. In *Potassium channels in cardiovascular biology*, (ed. A. a. Rusch), pp. 3-16. New York: Kluwer Academic/Plenum Publishers.

Hagiwara, S., Miyazaki, S. and Rosenthal, N. P. (1976). Potassium current and the effect of cesium on this current during anomalous rectification of the egg cell membrane of a starfish. *The Journal of General Physiology* **67**, 621-638.

Hedrich, R., Moran, O., Conti, F., Busch, H., Becker, D., Gambale, F., Dreyer, I., Kiich, A., Neuwinger, K. and Palme, K. (1995). Inward rectifier potassium channels in plants differ from their animal counterparts in response to voltage and channel modulators. *European Biophysics Journal* **24**, 107-115.

Hille, B. (1973). Potassium channels in myelinated nerve. Selective permeability to small cations. *Journal of General Physiology* **61**, 669–686.

Hille, B. (2001). Ionic channels of excitable membranes. Sunderland, MA.: Sinauer Associates, Inc.

Hooper, J. N. A. and Soest, R. W. M. V. (2006). A new species of *Amphimedon* (Porifera, Demospongiae, Haplosclerida, Niphatidae) from the Capricorn-Bunker Group of Islands, Great Barrier Reef, Australia: target species for the 'sponge genome project'. *Zootaxa* **1314**, 31-39.

J.Patel, A., Honoré, E., Maingret, F., Lesage, F., Fink, M., Duprat, F. and Lazdunski, M. (1998). A mammalian two pore domain mechano-gated S-like K^+ channel. *The EMBO Journal* **17**, 4283-4290.

Jiang, Y. and MacKinnon, R. (2000). The barium site in a potassium channel by X-ray crystallography. *Journal of General Physiology* **115**, 269-272.

Jin, W., Klem, A. M., Lewis, J. H. and Lu, Z. (1999). Mechanisms of inward-rectifier K^+ channel inhibition by tertiapin-Q. *Biochemistry* **38**, 14294-14301.

Kofuji, P., Ceelen, P., Zahs, K. R., Surbeck, L. W., Lester, H. A. and Newman, E. A. (2000). Genetic inactivation of an inwardly rectifying potassium channel (Kir4.1 subunit) in mice: phenotypic impact in retina. *Journal of Neuroscience* **20**, 5733–5740.

Krapivinsky, G., Medina, I., Eng, L., Krapivinsky, L., Yang, Y. and Clapham, D. E. (1998). A novel inward rectifier K^+ channel with unique pore properties. *Neuron* **20**, 995-1005.

Kubo, Y., Adelman, J., Clapham, D., Jan, L., Karschin, A., Kurachi, Y., Lazdunski, M., Nichols, C., Seino, S. and Vandenberg, C. (2005). International Union of Pharmacology. LIV. Nomenclature and molecular relationships of inwardly rectifying potassium channels. *Pharmacological Reviews* **57**, 509-526.

Kubo, Y. and Murata, Y. (2001). Control of rectification and permeation by two distinct sites after the second transmembrane region in Kir2.1 K^+ channel. *Journal of Physiology* **531**, 645-660.

Kucheryavykh, Y. V., Kucheryavykh, L. Y., Nichols, C. G., Maldonado, H. M., Baksi, K., Reichenbach, A., Skatchkov, S. N. and Eaton, M. J. (2007). Downregulation of Kir4.1 inward rectifying potassium channel subunits by RNAi impairs potassium transfer and glutamate uptake by cultured cortical astrocytes. *Glia* **55**, 274 –281.

Kusano, K., Miledi, R. and Stinnakre, J. (1982). Cholinergic and catecholaminergic receptors in the *Xenopus* oocyte membrane. *Journal of Physiology* **328**, 143-170.

Leys, S., Mackie, G. and Meech, R. (1999). Impulse conduction in a sponge. *Journal of Experimental Biology* **202**, 1139-1150.

Leys, S. P. and Degnan, B. M. (2001). Cytological basis of photoresponsive behavior in a sponge larva. *Biological Bulletin* **201**, 323-338.

Liu, K., Fu, H., Bei, Q. and Luan, S. (2000). Inward potassium channel in guard cells as a target for polyamine regulation of stomatal movements. *Plant Physiology* **124**, 1315-1325.

Lopatin, A. N., Makhina, E. N. and Nichols, C. G. (1994). Potassium channel block by cytoplasmic polyamines as the mechanism of intrinsic rectification *Nature* **372**, 366-369.

Lu, Z. (2004). Mechanism of rectification in inward-rectifier K^+ channels. *Annual Review of Physiology* **66**, 103-129.

Lu, Z. and MacKinnon, R. (1994a). A conductance maximum observed in an inward rectifier potassium channel. *Journal of General Physiology* **104**, 477-486.

Lu, Z. and MacKinnon, R. (1994b). Electrostatic tuning of Mg^{2+} affinity in an inward-rectifier K^+ channel. *Nature* **371**, 243-246.

Maddison, D. R. and Maddison, W. P. (2003). MacClade 4: analysis of phylogeny and character evolution. Sunderland, MA: Sinauer Associates.

Maingret, F., Lauritzen, I., Patel, A. J., Heurteaux, C., Reyes, R., Lesage, F., M., L. and Honore`, E. (2000). TREK-1 is a heat-activated background K^+ channel. *The EMBO Journal* **19**, 2483-2491.

Medina, M., Collins, A. G., Silberman, J. D. and Sogin, M. L. (2001). Evaluating hypotheses of basal animal phylogeny using complete sequences of large and small subunit rRNA *Proceeding of the National Academy of Sciences* **98**, 9707-9712.

Müller, W. (1982). Cell membranes in sponges. *International Review of Cytology* **77**, 129-181.

Mullins, L. J. (1959). The penetration of some cations into muscle. *Journal of General Physiology* **42**, 817–829.

Navaratnam, D. S., Escobar, L., Covarrubias, M. and Oberholtzer, J. C. (1995). Permeation properties and differential expression across the auditory receptor epithelium of an inward rectifier K^+ channel cloned from the chick inner ear. *Journal of Biological Chemistry* **270**, 19238-19245.

Nichols, C. G. and Lopatin, A. N. (1997). Inward rectifier potassium channels. *Annual Review of Physiology* **59**, 171-191.

Nickel, M. (2004). Kinetics and rhythm of body contractions in the sponge *Tethya wilhelma* (Porifera: Demospongiae) *Journal of Experimental Biology* **207**, 4515-4524.

Okamura, Y., Nishino, A., Murata, Y., Nakajo, K., Iwasaki, H., Ohtsuka, Y., Tanaka-Kunishima, M., Takahashi, N., Hara, Y., Yoshida, T. et al. (2005). Comprehensive analysis of the ascidian genome reveals novel insights into the molecular evolution of ion channel genes. *Physiological Genomics* **22**, 269-282.

Oliver, D., Baukrowitz, T. and Fakler, B. (2000). Polyamines as gating molecules of inward-rectifier K^+ channels. *European Journal of Biochemistry* **267**, 5824-5829.

Patel, A. J., Honoré, E., Maingret, F., Lesage, F., Fink, M., Duprat, F. and Lazdunski, M. (1998). A mammalian two pore domain mechano-gated S-like K^+ channel. *The EMBO Journal* **17**, 4283-4290.

Perovic, S., Krasko, A., Prokic, I., Mueller, I. and Mueller, W. (1999). Origin of neuronal-like receptors in Metazoa: cloning of a metabotropic

glutamate/GABA-like receptor from the marine sponge *Geodia cydonium*. *Cell and Tissue Research* **296**, 395-404.

Philippe, H., Derelle, R., Lopez, P., Pick, K., Borchiellini, C., Boury-Esnault, N., Vacelet, J., Renard, E., Houliston, E., Quéinnec, E. et al. (2009). Phylogenomics revives traditional views on deep animal relationships. *Current Biology* **19**, 706-712.

Polidoros, A. N., Pasentsis, K. and Tsaftaris, A. S. (2006). Rolling circle amplification-RACE: a method for simultaneous isolation of 5' and 3' cDNA ends from amplified cDNA templates. *BioTechniques* **41**, 35-36; 38; 40 passim.

Raab-Graham, F., K., Radeke, C. M. and Vandenberg, C. A. (1994). Molecular cloning and expression of a human heart inward rectifier potassium channel. *Neuroreport* **5**, 2501-2505.

Ramu, Y., Klem, A. and Lu, Z. (2004). Short variable sequence acquired in evolution enables selective inhibition of various inward-rectifier K^+ channels. *Biochemistry* **43**, 10701-10709.

Ronquist, F. and Huelsenbeck, J. P. (2003). MrBayes 3, Bayesian phylogenetic inference under mixed models. *Bioinformatics* **19**, 1572-1574.

Ruppersberg, J. (2000). Intracellular regulation of inward rectifier K^+ channels. *European Journal of Physiology* **441**, 1-11.

Sakarya, O., Armstrong, K. A., Adamska, M., Adamski, M., Wang, I.-F., Tidor, B., Degnan, B. M., Oakley, T. H. and Kosik, K. S. (2007). A post-synaptic scaffold at the origin of the animal kingdom. *PLoS ONE* **6**, 1-9.

Scherer, D., Kiesecker, C., Kulzer, M., Gunth, M., Scholz, E. P., Kathofer, S., Thomas, D., Maurer, M., Kreuzer, J. and Bauer, A. (2007). Activation of inwardly rectifying Kir2.x potassium channels by β3-adrenoceptors is mediated via different signaling pathways with a predominant role of PKC for Kir2.1 and of PKA for Kir2.2. *Naunyn Schmiedeberg's Archives of Pharmacology* **375**, 311-322.

Silverman, S., Lester, H. A. and Dougherty, D. A. (1998) Asymmetrical contributions of subunit pore regions to ion selectivity in an inward rectifier K^+ channel. *Biophysical Journal* **75**, 1330-1339.

Sperling, E. A., Pisani, D. and Peterson, K. J. (2007). Poriferan paraphyly and its implications for precambrian palaeobiology. *Geological Society of London - Special Publication* **286**, 355–368.

Srivastava, M., Begovic, E., Chapman, J., Putnam, N. H., Hellsten, U., Kawashima, T., Kuo, A., Mitros, T., Salamov, A., Carpenter, M. L. et al. (2008). The *Trichoplax* genome and the nature of placozoans. *Nature* **454,** 955-960.

Stamatakis, A. (2006). RAxML-VI-HPC: maximum likelihood-based phylogenetic analyses with thousands of taxa and mixed models *Bioinformatics* **22**, 2688.

Stanfield, P. R., Davies, N. W., Shelton, P. A., Sutcliffe, M. J., Khan, I. A., Brammar, W. J. and Conley, E. C. (1994). A single aspartate residue is involved in both intrinsic gating and blockage by Mg^{2+} of the inward rectifier, IRK1. *Journal of Physiology* **478**, 1-6.

Taglialatela, M., Ficker, E., Wible, B. A. and Brown, A. M. (1995). C-terminus determinants for Mg^{2+} and polyamine block of the inward rectifier K^+ channel IRK1. *EMBO Journal* **14**, 5532-5541.

Tanaka-Kunishima, M., Ishida, Y., Kunitaro Takahashi, Honda, M. and Oonuma, T. (2007). Ancient intron insertion sites and palindromic genomic duplication evolutionally shapes an elementally functioning membrane protein family. *BMC Evolutionary Biology* **7**, doi:10.1186/1471-2148-7-143.

Thompson, G. A., Leyland, M. L., Ashmole, I., Sutcliffe, M. J. and Stanfield, P. R. (2000). Residues beyond the selectivity filter of the K^+ channel Kir2.1 regulate permeation and block by external Rb^+ and Cs^+. *Journal of Physiology* **526**, 231-240.

Tompkins-MacDonald, G. J. and Leys, S. P. (2008). Glass sponges arrest pumping in response to sediment: implications for the physiology of the hexactinellid conduction system *Marine Biology* **154**, 973-984.

Wible, B. A., Taglialatela, M., Ficker, E. and Brown, A. M. (1994). Gating of inwardly rectifying K^+ channels localized to a single negatively charged residue. *Nature* **361**, 246-249.

Yamoah, E. N., Matzel, L. and Crow, T. (1998). Expression of different types of inward rectifier currents confers specificity of light and dark responses in type A and B photoreceptors of Hermissenda. *The Journal of Neuroscience* **18**, 6501-6511.

Zhou, H., Chepilko, S., Schutt, W., Choe, H., Palmer, L. G. and Sackin, H. (1996). Mutations in the pore region of ROMK enhance Ba^{2+} block. *American Journal of Physiology - Cell Physiology* **271**, C1949-C1956.

Zimmermann, S., Talke, I., Ehrhardt, T., Nast, G. and Müller-Röber, B. (1998). Characterization of SKT1, an inwardly rectifying potassium channel from potato, by heterologous expression in insect cells. *Plant Physiology* **116**, 879-890.

Zitron, E., Kiesecker, C., Luck, S., Kathofer, S., Thomas, D., Kreye, V. A., Kiehn, J., Katus, H. A., Schoels, W. and Karle, C. A. (2004). Human cardiac inwardly rectifying current IKir2.2 is upregulated by activation of protein kinase A. *Cardiovasc. Res.* **63,** 520-527.

Zocchi, E., Carpaneto, A., Cerrano, C., Bavestrello, G., Giovine, M., Bruzzone, S., Guida, L., Franco, L. and Usai, C. (2001). The temperature-signaling cascade in sponges involves a heat-gated cation channel, abscisic acid and cyclic ADP-ribose. *Proceeding of the National Academy of Sciences* **98,** 14859-14864.

Chapter Four: *AMPHIMEDON QUEENSLANDICA* POTASSIUM CHANNELS: EVIDENCE FROM CLONING AND ASSEMBLY FROM THE GENOME TRACE FILES

4.1 Introduction

The first potassium channels were cloned almost 25 years ago (Kamb et al., 1987; Papazian et al., 1987; Stuhmer et al., 1988; Takumi et al., 1988; Tempel et al., 1987). Since then, cloning and genome sequencing have revealed an impressive diversity of channels in both prokaryotes and eukaryotes (Jan and Jan, 1997; Rudy, 1988). Potassium channels are present in all sequenced genomes and they form the largest contingent of channels. Genomes of *Drosophila*, *C. elegans* and humans, for example, contain 30-100 potassium channel genes.

Potassium channels can most simply be delineated into groups by the predicted membrane topology of the principle (α) or "pore-forming" subunits (Coetzee et al., 1999; Jan and Jan, 1997; Rudy, 1988; Shieh et al., 2000). Typically subunits have either 2, 4 or 6 transmembrane domains (TMD) (Figure 4-2). Two transmembrane (2TM) domain potassium channels are the dominant topology in prokaryotes. In metazoans, 2TM subunits form inward rectifier potassium channels. The two transmembrane domains M1 and M2 are separated by a pore-forming loop with a selectivity filter (GYG or GFG) that is conserved among all potassium channels. A potassium-selective ion conduction pathway is formed by assembly of four pore-forming loops (one from each of four subunits) lining a central pore. Six TM channels (domains S1-S6) also assemble as tetramers. These include voltage gated potassium channels, Ca^{2+}-activated

potassium channels and KCNQ channels. The S5-pore-S6 portion is homologous to M1-pore-M2 of inward rectifier (2TM) channels. Four TM channels are like two 2TM subunits arranged end to end. Instead of having one pore lining-loop per subunit, 4TM subunits have two pores in tandem. Presumably each channel is formed by two subunits, each contributing two out of four pore-forming loops. Further diversity in each channel type is introduced by alternative splicing (Miller, 2000) or heteromeric assembly of subunits (Isacoff et al., 1990).

Gating stimuli are similarly diverse and allow potassium channels to respond to voltage and to the metabolic state of the cell. Broadly speaking, K^+ channel subfamilies correspond to the mechanisms by which they are gated – for example, voltage, calcium, sodium, G-proteins and polyamines (Coetzee et al., 1999; Miller, 2000) . Together the ensemble channel complement, under control of physiological signals, regulates membrane potential for homeostasis, cell volume regulation, cell proliferation and electrical signalling.

Most potassium channel physiology is understood from expression work in heterologous systems. For example, expression of Shaker voltage gated potassium channels in *Xenopus* oocytes confirmed that channel subunits assemble as tetramers and that distinct subunits can coassemble as heteromultimers (Isacoff et al., 1990). The heterogeneous nature of channel assembly and multiplicity of K channels, however, make it difficult to distinguish contributions of individual channels *in situ*. Moreover, in vertebrates many redundancies in channel function

exist as a result of full genome duplication in a chordate ancestor (Okamura et al., 2005).

A phylogenetic approach can help to decipher the channel complements necessary for regulation of membrane potential. Anderson and Greenberg (2001) (2001) have advocated comparing ion channels from phylogenetically distant groups as a means of improving the signal to noise ratio inherent in sequencing information. Those residues that remain conserved over evolutionary time are likely to be critical to channel function. The same rationale may apply to deciphering the channel complement critical for regulation of the membrane potential. Representatives of the Shaker superfamily of potassium channels, for example, have been identified in mammals, and in cnidarians (Jegla et al., 1995; Wei et al., 1990).

Potassium channel diversity is certainly not restricted to the Metazoa. A random genome sequencing project for *Paramecium tetraurelia* suggests that upwards of 1% of the genome may encode potassium channels, compared to 0.25% in humans (Haynes et al., 2003). All of these channels, however, formed one closely related group of proteins within *Paramecium*, distinct from Metazoan channels. In plants, a genome wide survey of rice (*Oryza sativa*), revealed 3 genes for 2 pore 4 transmembrane (TM) domain K channels and 11 for 1 pore 6 transmembrane K channels (Amrutha et al., 2007). The latter was subdivided into 5 voltage sensitive groups based on sequence similarity and functional properties (Adams et al., 1982), however, again, these groups were found to be phylogenetically distinct from Metazoan channels. Moreover, although tissues of

certain plants can conduct electrical impulses like animals the mechanisms appear to be distinct. For example plant cells are depolarized by Cl^- efflux rather than Na^+ or Ca^{2+} influx (Wacke and Thiel, 2001). These phylogenetically distinct aspects of membrane physiology intimate that excitability and its molecular underpinnings arose separately in Metazoans and other eukaryotic lineages. In contrast, conservation of ion channel families throughout the animal kingdom indicates that there may be a Metazoan specific ion channel complement. Consistent with this idea, the genome of the sea anemone *Nematostella vectensis* (Anthozoa, Cnidaria) contains a diversity of potassium channels homologous to those of higher animals. These include inward rectifier K channels (personal observation), voltage gated K^+ channels and slowpoke and large conductance calcium activated potassium channels (Putnam et al., 2007). Searches of trace files from the *Amphimedon queenslandica* genome suggest a comparable diversity of K channels in the Porifera, supporting the idea that the building blocks of metazoan excitability preceded evolution of the nervous system. A void in the literature remains to characterize the ion channel physiology of the Porifera, and from this to infer the complement of channels and membrane physiology of the first animals. The cloning and characterization of sponge inward rectifier potassium channels (Chapter 3) and patch clamp recordings from *Axinella polypoides* (Carpaneto et al., 2003) are major inroads to this end goal. Further ion channel characterization depends on the availability of sequences on which to base cloning efforts.

In this chapter I present partial sequences for a number of putative potassium channels from *A. queenslandica* as well as putative full length clones for two pore potassium channels. For each sequence I propose affiliations with known channel families and give suggestions for obtaining full length sequences and characterizing channels. I finish with speculations on potassium channel complements of Porifera and ancestral metazoans.

4.2 Materials and methods

4.2.1 Searching the Amphimedon queenslandica genome for K^+ channel sequences

Amphimedon queenslandica genomic DNA sequences stored at the National Centre for Biotechnology Information (NCBI) were searched with the tblastn sequence alignment program using metazoan Shaker family (Kv1, Kv2, Kv3 and Kv4) protein sequences from the voltage-gated potassium channel (Kv) database (VKCDB) (Li and Gallin, 2004). Sequences used in the search were from *Polyorchis penicillatus* (Cnidaria), *Schistosoma mansoni* and *Notoplana atomata* (Platyhelminthes), *Caenorhabditis elegans* (Nematoda), *Hirudo medicinalis* and *Haemopis marmorata* (Annelida), *Loligo Pealei*, *Aplysia californica* and *Aplysia sp.* (Mollusca), *Drosophila melanogaster*, *Panulirus interruptus* and *Limulus polyphemus* (Arthropoda), *Halocynthia roretzi* (Urochordata), and *Rattus norvegicus* (Vertebrata) (Appendix B.1). *A. queenslandica* blast hits were saved as a list of non-redundant accession numbers

and Batch Entrez was used to retrieve trace files, including raw sequence data, from the trace archive database at NCBI.

Staden Package 1.7 was used to assemble overlapping *A. queenslandica* sequences into longer contiguous sequences. Sequence strength was checked by translating the nucleotide sequences in 6 frames and doing a reverse search against the VKCDB database using the VKCBLAST tool. *A. queenslandica* nucleotide sequences which matched Kv channels at expected values less than 0.05 were then used to re-search the *A. queenslandica* trace archives at NCBI using the nucleotide blast program. Notably, while the *A. queenslandica* sequences were initially retrieved by blasting with sequences of Kv channels, the initial intended target of our search, the majority of the retrieved sequences had greater identity with other K channel families. A more exhaustive search using sequences from additional potassium channel families would undoubtedly recover many additional potassium channel hits.

A. queenslandica predicted K channel sequences were also generously shared by Onur Sakarya and Ken Kosik at the University of California at Santa Barbara (Appendix B.2). These sequences were generated as part of a large scale search of the sponge genome for putative post-synaptic molecules (Sakarya et al., 2007). Portions of some of these sequences are highlighted to show fragments that were independently recovered through my search and assembly efforts.

Some of the sequences were cloned fully or partially. The methods for cloning inward rectifier potassium (Kir) channels were outlined in Chapter 3. Methods for cloning or partial cloning are given below for putative two pore

potassium channels, potassium tetramerization domain containing proteins and tetrameric potassium selective cyclic nucleotide gated channels. Attempts at cloning the putative potassium channel from the Slo family are also summarized though they were unsuccessful. Sequences of GeneRace primers and sequencing primers T3 and T7 can be found in Appendix A.2 where their use was reported for cloning Kir channels. Remaining primer sequences are listed in Appendix B.3. Detailed methods for standard procedures including electrophoresis, synthesis of cDNA, preparation of circularized cDNA and GeneRACE cDNA, gel and plasmid purification, cloning and sequencing, cRNA synthesis, expression in oocytes, and electrophysiology were provided in Chapter 3 and are not repeated here.

4.2.2 Two pore potassium (K2P) channels

4.2.2.1 Cloning K2P channels

Putative two pore potassium channel sequences were amplified using primers K2P1F and K2P1R designed to amplify the open reading frame predicted by the Kosik lab, assuming that the predicted sequence contained the correct start and stop sites. As with primers for amplification of Kir channels (Chapter 3), forward and reverse primers were preceded by a 5' clamp and restriction sites compatible with insertion into the pxt7 expression vector. In the forward primer this is followed by a Kozak consensus sequence. PCR reactions contained 5 µl GoTaq buffer, 1.5 µl 25 mM $MgCl_2$, 0.2 µl 25 mM dNTPs, 0.4 µl each 50 µM primer, 0.125 µl Taq flexi, 13.175 µl water and 1 µl cDNA. Cycling parameters were 94°C 2 min, 34x (94°C 30 s, 53.5°C 30 s, 72°C 10 min) 72°C 30 min. Bands

of the expected size, 1083 bp including primer sequence, were cleaned with the QIAGEN Gel Extraction Kit, ligated into the pcr4-TOPO vector and transformed into TOP10 chemically competent cells. Positive transformants were detected by colony PCR with 20 µl T1.1x buffer, 0.5 µl 50 µM T3 and T7, 0.5 µl Taq16 (house Taq, University of Alberta) and 1ul template and cycling parameters of 94°C 2 min, 34x (94°C 30s, 58°C 30s, 72°C 1.5min) 72°C 2 min. Positive colonies were minicultured, miniprepped and sequenced. To confirm that we had amplified the true 5' end, RACE PCR was performed on geneRACE ready cDNA. Each reaction included 3 µl 10 µM GeneRACE 5' primer, 1µl 10uM K2PRevGR, 5 µl HiFi buffer, 2 µl 50mM MgSO4, 0.4 µl 25mM dNTPs, 0.5 µl Platinum HiFi Taq, 1 µl template and water to 50 µl. Cycling conditions were 94°C 2 min, 30x (94°C 30s, 58°C 30s, 68°C 7 min) 68°C 20 min. Amplified sequences were analyzed by electrophoresis, cloned and sequenced. The start site was found to be the same as that predicted by Onur Sakarya and amplified in my initial PCR reaction. The stop codon (3' end) predicted by Onur Sakarya was found to be in frame with the start site and was confirmed by PCR. We had already cloned the full open reading frame using primers K2P1F and K2P1R. Clones free of PCR errors were identified by comparison with uncloned PCR products. These clones were used for expression work and archived as glycerol stocks at -80°C.

4.2.2.2 Preparation of K2P complementary RNA

The open reading frame was digested out of pcr4-TOPO at XhoI and SpeI cut sites and ligated into pxt7 vectors which were digested with the same restriction enzymes. Digests included 3-6 µg K2P or pxt7 plasmid template, 4 µl Buffer 2, 0.4 µl BSA, 1 µl XhoI, 1 µl SpeI (New England Biolabs) and water to 40µl. These were incubated at 37°C for 3 hours and separated on 1% agarose gels. Purified products corresponding to K2P and digested pxt7 were ligated in 3:1, 1:1 and 1:3 ratios in reactions containing 2 µl Ligase 10X Buffer, 0.5 µl T4 DNA Ligase (Promega) and nuclease free water to 20 µl. Reactions were incubated at 15°C for 12-18 hours and heat inactivated at 65°C for 10 minutes. Products were transformed into TOP10 chemically competent cells.

Clones were screened for the presence of insert in the proper orientation using the reverse gene specific primer K2P1R and the forward pxt7 specific primer as described in Chapter 3. Minipreps (25-30 µl) of positive clones were then linearized with XbaI. The linearized plasmid-vector construct was isolated by electrophoresis, purified and used as a template for synthesis of complementary RNA (cRNA) using the Ambion (Austin, TX) mMessage mMachine RNA polymerase kit. Concentrations were determined by spectrophotometry and RNA quality was confirmed by running 1 µl on an agarose gel.

I attempted to increase the concentration of linear template in the cRNA synthesis reaction as a means of improving cRNA yield, since K2P currents were not observed in oocytes injected with 30 ng cRNA. Steps to increase template

concentration included pooling and precipitating product from multiple gel extractions or minipreps, allowing DNA to sit on gel extraction or miniprep column membranes for 20 minutes before eluting, and recovering DNA in concentrated form with QIAGEN MinElute Gel Extraction Kit.

4.2.2.3 K2P functional expression in oocytes

Oocytes surgically harvested from anaesthetized female *Xenopus laevis* (Xenopus I, Dexter, MI or University of Alberta Biological Sciences Animal Services) and prepared as indicated in Chapter 3. Stage V/VI oocytes maintained in MBM or frog Ringer's solution were injected with 50.6 nl of cRNA dissolved in DEPC-treated water (55-70 ng cRNA/oocyte). Negative controls were injected with DEPC-treated water. For positive controls oocytes were injected with 2-30 ng mouse two-pore potassium channel cRNA including TREK-1 and TRAAK; both generously shared by Doug Bayliss (University of Virginia). Oocytes were maintained at 19°C and storage medium was refreshed daily. Electrophysiological recordings were done 1-6 days post-injection.

Currents were recorded from oocytes using standard methods of two-electrode voltage clamp as outlined in Chapter 3 (Boland et al., 2003). Recordings were completed at the University of Richmond in collaboration with Linda M. Boland with the exception of pH experiments which were completed at the University of Alberta. Membrane voltage was altered by applying voltage ramps between -100 and +100 mV or steps at 10 mV increments. We did not apply P/N leak subtraction since K2P channels are known to pass current over a broad range of potentials (Lotshaw, 2007; O'Connell et al., 2002; Patel and Honore, 2001).

Endogenous chloride currents (Kusano et al., 1982) were minimized by using low chloride solutions in which chloride salts are replaced by the equivalent methanesulfonate salt. The standard, low chloride, external solution contained (in mM): 5 K methane sulfonate (MES), 95 NMDG-MES, 2 $CaCl_2$, 2 $MgCl_2$, 10 HEPES, pH 7.3 with methanesulfonic acid. In an unrelated set of experiments with the same batch of uninjected oocytes we did not observe a difference in currents in low chloride solution, versus 10mM chloride with the chloride channel blocker niflumic acid. K^+ concentrations were adjusted by changing the ratios of K^+ and NMDG containing solutions. Other solutions varied by experiment. Effects of polyunsaturated fatty acids were tested by L.M. Boland. Oocytes were perfused with recording solution supplemented with 100 µM arachadonic acid (AA) or docosahexaenoic acid (DHA), both of which create mechanical tension by altering membrane curvature. Positive controls for stretch effects introduced by AA, DHA or swelling (below) were mouse TREK1 and mouse TRAAK.

To determine the effect of tonicity, oocytes were perfused with 110, 160, 210, 260 and 310 mOsM solutions. Standard recording solution had an osmolarity of 210 mOsM and contained (in mM): 2 KMES, 98 NMDG, 2 $CaCl_2$, 2 $MgCl_2$, and 10 HEPES. Osmolarity was reduced by adjusting the NMDG-MES content to 48 and 23 mM. To increase osmolarity to 260 and 310 mOsM, 50 and 100mM sucrose was added.

Finally, to determine if channel activity was pH dependent, K2P injected oocytes were perfused with standard recording solutions pHed to 6.5, 6.9, 7.3, 7.7 and 8.1 with methanesulfonic acid. For pH 6.5-7.3 10 mM HEPES was replaced

with PIPES, while 10mM HEPES was used from pH 7.3-8.1. The overlap at pH 7.3 was employed to test whether differences in current are introduced by using two different buffers.

Data were visualized with Axon's Clampex acquisition and Clampfit analysis software (version 9). Qualitative evaluation of the cells showed that of stable cells there was no difference in current phenotype compared to uninjected or water injected cells. It is unknown whether the lack of current phenotype is due to lack of expression or trafficking channels to the membrane or inappropriate conditions for current activation. Data were not analyzed further.

4.2.3 Cloning of potassium tetramerization domain containing genes

Two distinct sequence fragments which returned BLAST hits against 'potassium tetramerization domain containing" (KCTD) proteins were assembled from the trace files of *A. queenslandica* and are listed in Appendix B.4 along with other sequence fragments showing similarity to potassium channels. Inverse primers designed to amplify the 5' and 3' end were respectively Kinv7-5' and Kinv7-3'. Initial PCR products were generated by inverse PCR on 10^{-1}, 10^{-2}, 10^{-3} and 10^{-4} dilutions of *A. queenslandica* rolling circle amplified (RCA) circularized cDNA (Polidoros et al., 2006). Reactions included 5 µl GoTaq buffer, 1.5 µl 25 mM $MgCl_2$, 0.2 µl 25 mM dNTPs, 0.5 µl each 50 µM 5' and 3' primer, 0.125 µl Taq Flexi, 1 µl template and water to 25 µl. Cycling parameters were 94°C 2 min, 34x (94°C 30 s, 50.1°C 30 s, 72°C 10 min) 72°C 30 min. Products were analyzed by gel electrophoresis, cloned and sequenced as described previously. Two

partial sequences were obtained – 232 and 354 bp respectively. Overall identity between the two sequences was 36.5% (http://www.ch.embnet.org/software/LALIGN_form.html). However, both contained GGGCATACCTCATTGACAGGAGTCCTGAATATTTTGAGCCACTTCTCA ACTTC corresponding to the putative amino acid sequence AYLIDRSPEYFEPLLNF. While part of this sequence matched the primer sequence used to amplify it, the sequence was considered legitimate as it matched sequences in the *A. queenslandica* trace files. Primers for 5' and 3' RACE were designed against the sequence above. 5'RACE reactions included 3 µl 10 µM GeneRacer 5' primer, 1 µl 10 µM KtetRevGR primer, 5 µl GoTaq buffer, 1.5 µl 25 mM $MgCl_2$, 0.2 µl 25 mM dNTPs, 0.125 µl TaqFlexi and 0.5 µl GeneRACE ready cDNA and water to 25 µl. Cycling parameters were 95°C 2 min, 35x (95°C 30 s, 58°C 30 s, 72°C 3 min) 72°C 10 min. A 10^{-2} dilution of 5' RACE product was amplified with GeneRACE nested 5' primer and KtetNRevGR (1 µl each 10 µM primer and 53°C annealing). The 3' RACE reaction included 3µl 10 µM GeneRACE 3' primer, 1 µl 10 µM KtetFwdGR, 5 µl 10x HiFi buffer, 2 µl 50 mM $MgSO_4$, 37.1 µl water, 0.4 µl 25 mM dNTPs, 0.5 µl Platinum HiFi Taq and 1 µl GeneRACE ready cDNA. Cycling parameters were 94°C 2 min, 30x (94°C 30 s, 56.1°C 30 s, 68°C 7 min), 68°C 20 min. Nested 3' RACE on serial dilutions of the first round product and included 1 µl each 10 µM GeneRACE 3' nested primer, KtetFwdNGR and template with an annealing temperature of 58°C. Amplified products were isolated on 1% agarose gels, purified with the QIAquick

Gel Extraction kit, ligated into the pcr4-TOPO cloning vector and cloned. Positive clones were identified by colony PCR, and sequenced.

4.2.4 Partial cloning of a putative cyclic nucleotide gated potassium channel

Several primer sets were used to attempt amplification of the Kosik lab sequence labelled SubH_Kv (Appendix B.2). These included primers Kv1F with Kv1R which span the predicted open reading frame (1737 bp) or the internal primer set Kv2F with Kv2R designed to amplify a predicted 1257 bp sequence. Reactions included 5 µl GoTaq buffer, 1.5 µl 25 mM dNTPs, 0.4 µl each 50 µM primer, 0.125 µl Taq Flexi, 1 µl template (10^{-1} through 10^{-4} dilutions of *A. queenslandica* RCA cDNA) and water to 25 µl. For both primer sets cycling parameters were 94°C 2min, 34x (94°C 30 s, annealling 30 s, 72°C 10 min) 72°C 30min. Annealling temperatures were 48.3°C for Kv2F and Kv2R and 40.4°C, 41.7°C, 43.5°C, 45.8°C, 51.1°C, 53.8°C, 56.2°C and 58.1°C for Kv1F and Kv1R. A third nested set of primers was designed to target only those regions that were conserved against potassium channels (expected value < 10^{-12}). Primers were Kv3Fwd and Kv3Rev and the nested primer was Kv3NFwd. Bands were amplified from 10^{-3} and 10^{-4} dilutions of RCA cDNA using reactions containing 12.5 µl 2x GoTaq Green master mix, 2 µl each 10 µM Kv3Fwd and Kv3Rev, 0.5 µl template and water to 25 µl and cycling parameters of 95°C 2min, 35x (95°C 30s, 58°C 30s, 72°C 3min) 72°C 10min. Products were analyzed on 1% agarose gels, cloned and sequenced.

Primers for RACE PCR were designed against sequences amplified with Kv3Fwd and Kv3Rev. These included the reverse specific primer AqKvRevGR2, the forward specific primer AqKvFwdGR and nested forward primers AqKvFwdNGR1 and AqKvFwdNGR2.

5' RACE reactions included 3 µl 10 µM GeneRACE 5' primer, 1 µl 10 µM AqKvRevGR2, 5µl 10xHiFi buffer, 1µl 10mM dNTP, 1µl GeneRACE ready cDNA, 0.5µl HiFi Taq (Platinum HiFi), 2µl 50mM MgSO4 and water to 50 µl. Reactions were cycled at 94°C 2 min, 30x (94°C 30 s, 60°C 30 s, 68°C 10 min) 68°C 30 min. For 3'RACE primers were replaced with 3 µl 10 µM GeneRACE 3' primer and 1 µl 10 µM AqKvFwdGR. Nested RACE reactions included 1µl each 10 µM GeneRACE 3' nested primer and either AqKvFwdNGR1 or AqKvFwdNGR2 and were annealed at 52°C. Products from nested 3'RACE were isolated by gel electrophoresis, purified and reamplified using the same reaction conditions and 35 amplification cycles. RACE products were not processed through the sequencing stage.

4.2.5 Attempted cloning of a putative slo family potassium channel

A putative nucleotide sequence for an *A. queenslandica* channel was assembled by Onur Sakarya and Ken Kosik and named SubT_KCa (Appendix B.2). My tblastx searches of the NCBI database indicate that the sequence is more similar to sodium-activated potassium channels (KNa) than to a calcium-activated potassium channel (KCa); both KNa and KCa are members of the Slo family of potassium channels; however primers were named to be consistent with Kosik's

naming scheme. The primer set KCa1F with Kca1R was designed to amplify the predicted full length sequence. Reactions included 5µl GoTaq Buffer, 1.5µl 25 mM MgCl2, 0.2 µl 25 mM dNTPs, 0.4 µl each 50 µM primer, 0.125 µl TaqFlexi, 16.375 µl water and 1 µl template, either 10^{-1}, 10^{-2}, 10^{-3} or 10^{-4} dilutions of RCA cDNA. Cycling parameters were 94°C 2 min, 34x (94°C 30 s, 54.9°C 30 s, 72°C 10 min), 72°C 30 min. When no products were recovered PCR was repeated with a temperature gradient from 40-60°C and exact annealing temperatures of 40.4°C, 41.7°C, 43.5°C, 45.8°C, 48.4°C, 51.1°C, 53.8°C, 56.2°C and 58.1°C. While a faint band corresponding to a 1500 bp product was visualized on 1% agarose gels this product was not successfully cloned and was considerably smaller than the anticipated product, which is 3558 bp. A second primer set was designed using the Primer3 program (http://frodo.wi.mit.edu/primer3/) to select the optimal set of PCR primers by considering the entire putative sequence. The primers KCa2F and KCa2R were used with the same reaction conditions and an annealing temperature of 51°C and did not result in a product. A third set of primers was designed by considering only those portions of the putative sequence which blasted as conserved against other metazoan potassium channels. The primers were KCa3Fwd and KCa3Rev and the nested primer set KCa3NFwd and KCa3NRev. The primer set KCa3Fwd and KCa3Rev was tested on dilutions of *A. queenslandica* RCA cDNA using the reaction conditions above and annealing temperatures of 48°C and 58°C – however no products were visible by electrophoresis. The nested primer set was not tested.

4.2.6 Amino acid sequence and phylogenetic analysis

Transmembrane domains of two pore potassium channels were estimated by entering amino acid sequences in the online entry form at http://www.cbs.dtu.dk/services/TMHMM/ or http://gcat.davidson.edu/rakarnik/kyte-doolittle.htm with a window size of 9. AmqK2PA and AmqK2PB were aligned and compared with amino acid sequences of both invertebrate and vertebrate two pore potassium channel sequences compiled from NCBI, Joint Genome Institute (http://www.jgi.doe.gov/sequencing/why/3161.html) and Ensemble databases. To determine pairwise identity values sequences were aligned using LALIGN online software (http://www.ch.embnet.org/software/LALIGN_form.html) and default parameters for global alignments. Multiple alignments were generated with MEGA 4.0 software using ClustalW. Alignments used for phylogenetic analysis were manually adjusted. Phylogenetic trees were generated with MEGA software using Maximum Parsimony analysis with 500 bootstrap replicates and the close-neighbour-interchange algorithm and default parameters.

4.3 Results and Discussion

I present sequences, speculations on channel identity and suggestions for extending analysis of multiple putative potassium channels from the demosponge *Amphimedon queenslandica*. Combined results and discussion are given for each putative sequence in turn.

4.3.1 Sequences retrieved by blast searches of Amphimedon queenslandica genome trace files

Searches of *A. queenslandica* trace files returned a number of nucleotide sequences for putative potassium channels. *A. queenslandica* hits matching other metazoan K channels with expected values less than 0.05 (meaning there is less than 5% chance that the match is due to chance alone) were used for a second round of searching to retrieve adjacent portions of the same sequence. At the time these sequences were compiled cloning vector sequences were not yet removed from the trace files, and limited access to information on the genome project (genome not publicly released) meant that I was unable to manually trim vector from my list of sequences. Without trimming vector sequence I retrieved growing numbers of sequences when I researched the trace files with initial fragments of putative potassium channels. Many of the returned sequences were matched only to vector. Rather than continuing searches for contiguous sequences I instead attempted to extend sequences by RACE PCR on generace ready cDNA or inverse PCR on circularized cDNA.

Contiguous *A. queenslandica* sequences which matched metazoan K channel sequences at expected values less than 1e-10 are summarized in Table 4-1 and listed in full in Appendix B.4. Table 4-1 includes the identity of the most similar sequence retrieved by searching NCBI using the tblastx search query. I have also indicated which sequences match those predicted by Onur Sakarya and Ken Kosik. Inverse primer sets were designed for each of these sequences in order to amplify 5' and 3' ends from circularized cDNA generated by rolling circle

amplification. Primer set Kinv7-5' and Kinv7-3' amplified a sequence that was most similar to potassium tetramerization domain containing proteins. These results are summarized in section 4.3.2.2. Other cloned sequences were obtained by designing primers against Kosik lab sequences. These include putative 2 pore potassium channels (K2P) (section 4.3.2.1) and a partial sequence of a putative tetrameric potassium selective cyclic nucleotide gated channel (Section 4.3.3.2). Putative sodium or calcium-activated potassium channels (KNa or KCa) were not successfully cloned, however sequences assembled from trace files are presented along with suggestions for cloning and analysis.

4.3.2 Sequences cloned from A. queenslandica cDNA

4.3.2.1 Two pore potassium channels

4.3.2.1.1 Cloning of two pore potassium channels

Primers designed to amplify the predicted K2P open reading frame amplified a product of the expected size, ~ 1000 bp (Figure 4-2A). When I used the *A. queenslandica* nucleotide sequence to search translated nucleotide databases at NCBI the most similar sequence was a *Danio rerio* TASK-2 acid sensitive K2P channel (accession NP_956927.1; expected value 2e-34) while 8 out the top 10 hits were TREK-2 mechanosensitive K2P channels. RACE PCR to confirm the 5' sequence returned a 150 bp product. The sequence aligned with the 5' end initially predicted by Kosik. RACE to amplify the 3' end was not necessary as a TGA stop site in frame with the start site was already confirmed by

sequencing. Two sequences, AmqK2PA and AmqK2PB, (Appendix B.5) were confirmed by cloning; each being 1062 bp long. Most nucleotide differences between the two sequences were synonymous, however nonsynonymous changes resulted in amino acid differences at positions 273 (S/T) and 313 (K/E) (Figure 4-3A).

4.3.2.1.2 Primary structure

Two pore potassium channels (K2P), also known as tandem domain potassium channels were first identified in the yeast *Saccharomyces cerevisae* (Ketchum et al., 1995). The yeast TOK1 channel has 8 transmembrane (8TM) domains and could be likened to a 6TM channel (with a pore between the 5th and 6th TM domains), and a 2TM channel in tandem. Metazoan two pore potassium channels on the other hand have four transmembrane domains (4TM) and are architecturally arranged like two inward rectifier potassium channels (2TM) in tandem (Figure 4-3B) (O'Connell et al., 2002; Patel and Honore, 2001). Each 4TM subunit bears two pore loops. Presumably these channels assemble as dimers where the central pore is lined by four pore-forming loops (2 from each subunit). This differs from other K channels which have only one pore-forming loop per subunit and assemble as tetramers.

The two *A. queenslandica* sequences differ from each other by only 2/353 amino acids and appear to share the metazoan 4TM topology. Hydropathy plots (Figure 4-3C) show four 23 amino acid stretches with hydropathy values above 1.8, indicating that they are membrane spanning domains. As with hydropathy

plots for other metazoan K2P channels (Bang et al., 2000; Reyes et al., 1998) there are two additional peaks in hydropathy corresponding to the pore-forming (P) domains. Membrane spanning and pore-forming regions were further estimated by alignment with human K2P channels with published hydropathy profiles. The predicted AmqK2P pore regions (P1 and P2) share 82% and 64% identity with those predicted for TREK-2 (Bang et al., 2000).

As with most K2P channels the second pore has a phenylalanine (F) in the GXG motif instead of a tyrosine (Y). Loss of tyrosine would normally lead to loss of K selectivity. However interaction between tyrosine and an aspartate (D) downstream of F (GFGD) in the adjoining subunit stabilizes the pore and may introduce flexibility in permeation and selectivity (Chapman et al., 2001).
Two pore potassium channels have weak intrinsic voltage sensitivity, lacking the S4 voltage sensor of voltage gated channels. Weak voltage dependence complements the leak phenotype of these channels - passing current down the electrochemical gradient (normally out of cells under resting conditions) and across a broad range of membrane potentials (Lesage, 2003).

4.3.2.1.3 Physiology of K2P channels

Current magnitude and degree of rectification in K2P channels are not, however, invariant but rather modulated in vivo by a variety of physicochemical factors and neurochemicals, depending on the channel subfamily (Goldstein, 2001; Honore, 2007; Kim, 2005; Lesage and Lazdunski, 2000; Patel and Honore, 2001; Talley and al., 2003). Inhibiting K2P channels reduces outward flux of K^+

which leads to membrane depolarization and increase in excitability.

Activating or opening K2P further depresses or hyperpolarizes the membrane, reducing excitability (Bayliss and Barrett, 2008). K2P channels have been broadly dubbed cellular sensors as a result of the diversity of stimuli which regulate their activity, including pH, anaesthetics, stretch, temperature, second messengers, oxygen tension and lipid signalling (O'Connell et al., 2002). Details of channel regulation have been resolved primarily in heterologous expression systems and have helped to create pharmacological and biophysical profiles for the six mammalian K2P subfamilies: TWIK, TREK, TASK, TALK, THIK and TRESK (Lotshaw, 2007). TREK-1 channels, for example, are activated by stretch and increase in temperature, and TREK-1, TREK-2 and TRAAK by arachadonic acid and other polyunsaturated fatty acids applied internally. Many K2P channels are sensitive to anaesthetics and TASK channels are inhibited by external acidification. Likely many K2P channels contribute to the resting potential of a given cell.

Abbreviated profiles of some of the best characterized channels are given in Table 4-2 (adapted from O'Connell et al. 2002). Such reviews and complementary literature (Barriere et al., 2003; L'Hoste et al., 2007; Morton et al., 2005; Niemeyer et al., 2001; Reyes et al., 1998) were helpful to us in designing experiments where we attempted to activate AmqK2P currents.

4.3.2.1.4 Attempts to record from AmqK2P channels

We ran voltage ramp and voltage step protocols (-100 to 100 mV) using two electrode voltage clamp to record from *Xenopus* oocytes injected with AmqK2PA and AmqK2PB cRNA (30-50 ng). Bathing solutions were adjusted to vary pH, tonicity or to include the polyunsaturated fatty acids arachadonic acid (AA) or docosahexaenoic acid (DHA), both of which activate TREK-1 channels by modifying the curvature of the membrane. Despite these manipulations we did not observe currents distinct from those in uninjected or water-injected oocytes. There are a number of potential reasons that we would not have observed currents. These may include lack of expression, problems with folding or targeting the channels to the oocyte membrane, or incorrect conditions for current activation.

4.3.2.1.5 Phylogenetic relationships of K2P channels

Genome surveys and physiological recordings from invertebrates indicate that K2P channels are ubiquitous throughout the Metazoa and diversified into subfamilies homologous to those described in vertebrates (Buckingham et al., 2005). S-type leak currents, well described in the mollusc *Aplysia*, appear to match the pharmacological profile of mammalian TREK-1 channels (Jezzini et al., 2006; Patel et al., 1998). Eleven putative K2P genes, including several vertebrate homologues have been identified from the *Drosophila melanogaster* genome, including ORK-1, the first metazoan K2P channel to be cloned. And the *Caenorhabditis elegans* genome contains 50 putative K2P channels – over half the complement of K channels – including homologues of all vertebrate K2P

subfamilies. The abundance of K2P channels in *C. elegans* is thought to augment the integrative capacity of the small number of neurons by allowing 'fine tuning' of the firing of individual cells (Salkoff et al., 2001).

There is little information on the K2P channel complement of early branching metazoans, however TREK-1 like currents have been recorded from cells of the demosponge *Axinella polypoides* (Zocchi et al., 2003; Zocchi et al., 2001). Moreover, the presence of five genes for 4TM K2P channels in the *Arabidopsis thaliana* genome (Becker et al., 2004; Gobert et al., 2007) indicates that K2P genes of this architecture were present in eukaryotes ancestral to both plants and metazoans.

To gain more information on the relationships among metazoan K2P channels and to attempt to determine affiliation of AmqK2P channels with known K2P channel families I aligned K2P sequences from both invertebrates and vertebrates (Figure 4-4 shows alignment with human K2P sequences) and ran maximum parsimony analysis with MEGA 4. AmqK2P sequences were used to root the tree. Sequences used in the analysis are listed in Appendix B.6.

I recovered relationships among vertebrate K2P subtypes which were consistent with those published by others (Bayliss and Barrett, 2008; Honoré, 2007; Lesage, 2003). For example, mechano-gated TREK1, TREK2 and TRAAK channels formed a clade as did the weak inward rectifiers TWIK1, TWIK2 and KCNK7. Several invertebrate sequences were found to be similar to vertebrate THIK and vertebrate TASK3 and TASK5 channels. In contrast to the analyses of Buckingham et al. (2005) however, even with a low cut-off of 20%, relationships

among most invertebrate K2P sequences including AmqK2P were unresolved. Our analyses only included invertebrate sequences from *C. elegans*, *Drosophila melanogaster*, *Aplysia californica* and *Lymnaea stagnalis.* Inclusion of additional sequences would strengthen the analysis, however sequences should be confirmed by cloning.

4.3.2.1.6 Suggestions for additional analyses of AmqK2P channels

The non-specific nature of stimuli, coupled with the absence of specific pharmacological agents has restricted our understanding of native K2P channels. Links between cloned and native channels are primarily established by localizing channel expression to particular cells or tissues and comparing endogenous currents to those obtained in heterologous expression systems (Buckingham et al., 2005). For example, oxygen sensitive TASK-1 channels have been localized to the carotid body where oxygen sensitive potassium currents have been described. Knock-outs (null mutants) have also been informative (Alloui and al., 2006; Bayliss and Barrett, 2008).

Knock-out technology has not been developed in the Porifera, but endogenous K2P-like currents have been described in isolated cells of the demosponge *Axinella polypoides* (Zocchi et al., 2001). The unitary currents recorded by Zocchi et al. (2001) were reminiscent of TREK-1 channels in mammals and S-type currents in the sea slug *Aplysia.* TREK-1 and S-type channel currents are known to be activated by mechanical tension and increase in temperature and have been implicated in central and peripheral thermosensing and

mechanosensation (Honoré, 2007; Maingret et al., 2000). The comparable channel in *A. polypoides* was activated by heat stress (increase from 14 to 26°C) and by arachidonic acid, which mimics mechanical tension by modifying the membrane curvature. Downstream of this channel, a signalling cascade leads to an increase in filtration rate, oxygen consumption and protein synthesis (amino acid incorporation) (Zocchi et al., 2003).

I suggest cloning K2P channels from *A. polypoides* using AmqK2P channels as bases for degenerate primer design. Channel electrophysiology can then be determined in oocyte expression systems and compared to described *A. polypoides* currents to determine if channel profiles are similar. To this end current amplitude should be recorded over a range of voltages in the presence of arachadonic acid, which activated native currents, and over a range of temperatures. A link has already been established between activity of a native K2P-like channel and filtration and respiration rates in *A. polypoides.* Characterizing cloned *A. polypoides* K2P channels may provide an opportunity to connect physiology of an individual channel with a defined whole animal physiology outcome.

4.3.2.2 Potassium channel tetramerization domain containing (KCTD) proteins)

4.3.2.2.1 Cloning of a putative KCTD protein

Using inverse primers designed against a putative potassium channel sequence from the *A. queenslandica* trace files, a 232 bp product was amplified from cDNA that had been circularized with the CircLigase enzyme (Figure 4-6).

A blastx search of NCBI databases found the sequence to be most similar to potassium channel tetramerization domain containing protein (KCTD). I had anticipated that the circularized cDNA template would provide the sequences of the 5' and 3' ends. I decided, however, to proceed with conventional 5' and 3' RACE, since some recombination was suspected in the circularized template, based on other amplifications. A single sequence was amplified. The final sequence was found to be 1359 bp long (including the stop codon), corresponding to a predicted open reading frame of 451 amino acids (Appendix B.7). The most similar sequence retrieved by blastx was a *Danio rerio* potassium channel tetramerisation domain containing 9 (KCTD9), mRNA, (accession NM_001002738.1; expected value 3e-92). This sequence was determined from cloned PCR products. To rule out the possibility of PCR-introduced errors the sequence should still be confirmed from uncloned PCR products from at least two independent amplifications from cDNA.

A second partial KCTD sequence (AmqKCTDB) identified from trace files but not cloned is listed in Appendix B.4 as well. Note, the trace file sequences have not been corrected for the presence of non-coding regions or sequencing vector.

4.3.2.2.2 Primary structure

In Kv channels the N-terminal region, known as the tetramerization domain, mediates assembly of 4 Kv subunits around the central ion conduction pathway via Velcro-like interactions of BTB (bric-a-brac, tram-track, broad

complex) sites (Zollman et al., 1994) in neighbouring subunits. The *A. queenslandica* AmqKCTDA sequence described here has a domain sharing 20-29% identity with the tetramerization domain of Kv channels and is approximately as long as a Kv channel (>1000 bp); however no transmembrane domains were highlighted by hydropathy analyses, suggesting that AmqKCTDA is not a channel-forming protein.

Potassium channel tetramerization domain containing (KCTD) proteins are a poorly understood group named for homology of their N-terminal sequence with that of Kv channels (Dementieva et al., 2009). Analysis of the crystal structure of human KCTD5 indicates, however, that the BTB domain mediates assembly into pentamers, rather than tetramers as in Kv channels. The central cavity formed by the circular arrangement of KCTD5 subunits is continuous, spanning 110 Å but is variable in diameter (4.5-20 Å). Dementieva et al. (2009) indicated that water molecules were apparent within the cavity and suggested that cations could potentially fit where the cavity narrows to 4.5 Å. However, pentamers were formed in aqueous solution; not in membranes where ion conduction would serve to regulate membrane potential.

Dementieva et al. (2009) aligned N-termini of human KCTD (KCTD 1-19 and 21) and Kv proteins to highlight conservation of the tetramerization domains. I have adapted their alignment to show that the N-terminus of AmqKCTDA is conserved with the T1 domain of Kv channels and N-terminus of other KCTD proteins (Figure 4-7). Overall identity with human KCTDs ranged from 11.1 to 42.3%. Identity was higher, however, when considering the N-terminus in

isolation (up to 51.9%). Human KCTD group I, including KCTD2, KCTD5, KCTD9 and KCTD17, was most similar to AmqKCTDA. Comparison of AmqKCTDA and human KCTD proteins (full length and N-termini only) by maximum parsimony analysis (Appendix B.8) similarly placed AmqKCTDA within group I, closest to KCTD9. Inclusion of the putative N-terminus of AmqKCTDB suggests that it is also similar to human group I KCTD proteins, albeit more related to KCTD2, 5 and 17. KCTD sequences from other metazoans, including invertebrates, were initially included however when aligned with clustalW no significant similarities were found. This unexpected output was likely a result of including sequences that were erroneously predicted to be KCTD proteins by automated computational analysis using programs such as GNOMON. These predicted sequences were found in NCBI databases. Since a full group of KCTD sequences confirmed by cloning was only available for humans, only human and sponge KCTD sequences were included in my analyses.

Because AmqKCTDA and B share sequence with KCTD5, information from the KCTD5 crystal structure can be used to make inferences on structural domains of AmqKCTD proteins. Each individual KCTD5 subunit has a core comprised of 6 α helices and 6 β sheets, a variable C-terminus and a conserved N-terminus - residues 44-149 for KCTD5. In KCTD5 and Kv channels this region contains the BTB domain and is comprised of a 3 stranded β sheet and 5 α helices. Interaction between KCTD5 BTB domains is mediated by acidic residues hydrogen bonding with basic residues in neighbouring subunits. KCTD5 acidic residues Asp 93, Asp 95 and Glu 124 interact via H-bonds with the basic residues

Arg107 and Lys110. With the exception of Asp 95 these residues are also found in AmqKCTDA (Figure 4-7) (and all but Glu 124 in the translated trace file sequence for AmqKCTDB), suggesting a common mechanism of interaction of domains.

4.3.2.2.3 Physiology of KCTD proteins

Given their mutual property of assembly via BTB domains KCTD proteins were expected to bind to and modulate Kv channels. There is, however, no electrophysiological support for this to date. When KCTD5 was coexpressed with Kv1.2, Kv2.1, Kv3.4 or Kv4.2 no differences in Kv currents were observed (Dementieva et al., 2009). KCTD expression levels are elevated in fetal tissues, indicating a developmental role (Gamse et al., 2005), however their function remains unclear. To date there is no electrophysiological evidence that KCTD proteins pass current. KCTD5 instead binds to GRASP55, a protein that contributes to Golgi stacking and protein trafficking (Shorter et al., 1999). KCTD12 is thought to function in maturation of inner ear neurons (Resendes et al., 2004); a defect in KCTD7 is associated with neurodegeneration (Van Bogaert et al., 2007); and KCTD11 was found to suppress sonic hedgehog signalling and to promote tumour growth associated with medullablastoma (Di Marcotullio et al., 2004; Zawlik et al., 2006). Given the diversity of functions implied to date it is clear that functional data on KCTD proteins from phylogenetically disperse groups is required before conclusions about the biological significance can be

made. Moreover given the available data we cannot speculate on AmqKCTD function without functional characterization of these particular proteins.

4.3.2.2.4 Suggestions for further analyses of AmqKCTDA

Function of AmqKCTDA proteins could be tested by first expressing the proteins in *Xenopus* oocytes to determine whether they pass current. To do this, the full AmqKCTDA sequence must be confirmed from uncloned PCR products amplified with primers that flank the full open reading frame. Suggested primers are GGCTCGAGCCACCATGGCTGCCGCAAGG (forward) and GGACTAGTTCAGTCATTGTTATCATTGC (reverse). Like primers used to amplify the open reading frame of Kir and K2P channels (methods), the forward primer is preceded by a GG clamp, an XhoI restriction site and a Kozak consensus sequence. The reverse primer is preceded by GG clamp and SpeI restriction site. Individual clones that are free of PCR errors can then be ligated into the pxt7 vector for expression as described previously. Expression studies may, however, be premature particularly if sponge KCTD proteins function to modulate channels. Assuming a modulating role a better log of the complement of sponge ion channels and their baseline physiology is first required. We can then co-express AmqKCTDA with each channel to determine if it modulates the currents in any way.

4.3.3 Putative A. queenslandica K channels. Partially cloned sequences

4.3.3.1 Cyclic nucleotide gated channels

Cyclic nucleotide gated (CNG) channels are typically nonselective – passing Na^+ and K^+ and even Ca^{2+}. They are gated by 3',5'-cyclic monophosphates (cNMPs) including cAMP or cGMP binding to a site at their C-terminal end. CNG channels are part of the S4-superfamily of ion channels, characterized by 6 transmembrane domains per subunit, with a pore between domains S5 and S6 (Kaupp and Seifert, 2002; Miller, 2000). They also have repeating positively charged residues in the S4 domain. Note, that the S4 domain in Kv channels is the voltage sensor, which mediates gating in Kv channels. CNG channels, however, are not gated by voltage. S4 conservation in both CNG and Kv channels indicates that it is part of the core structure of this superfamily (Jan and Jan, 1990). Like other six transmembrane channels, CNG channels assemble as homo or heteromeric tetramers, with each of the four subunits contributing a pore forming loop to line a central water filled cavity (Kaupp and Seifert, 2002).

4.3.3.2 Putative tetrameric potassium selective cyclic nucleotide gated channel (KCNG)

The assembled sequence designated by Kosik as SubH_Kv (Appendix B.2), however, was found to be most similar to a unique type of cyclic nucleotide gated channel when the translated sequence was used to search NCBI translated nucleotide databases (tblastx). The most similar sequence with an expected value of 7e-65 was a tetrameric potassium-selective cyclic nucleotide gated channel from the echinoderm *Strongylocentrotus purpuratus* (accession NM_001081964.1). The *S. purpuratus* channel was the first of its kind cloned and

is unique in that it is potassium selective (Galindo et al., 2007). The tetrameric structure is also unique among potassium channels. Rather than having 4 subunits, each with six transmembrane domains and a pore forming loop, the Sp-tetraKCNG channel has four 6TM domains in tandem, each containing a pore forming loop (Figure 4-8). This channel structure is typical of voltage gated sodium and calcium channels which are thought to have arisen after a 6TM K channels underwent a duplication to produce a 12TM sequence containing two 6TM repeats. After a period of sequence divergence the 12TM sequence is thought to have duplicated, giving rise to four 6TM repeats (Hille, 2001; Strong et al., 1993). These 24 TM channels function as monomers where the four pore-forming loops within the single peptide associate to surround an ion conducting pathway.

Closer comparison of the Kosik SubH_Kv sequence and Sp-tetraKCNG shows that the highest match was against Sp-tetraKCNG pore and S6 (sixth transmembrane) domains and against the cyclic nucleotide binding domains in each of the four repeats (Table 4-3). Slightly higher expected values show that the degree of match against the first repeat was not as significant as that for repeats II-IV. This may be a result of a missing domain in the Kosik sequence. The translated Kosik sequence contains only 3 out of an expected 4 conserved pore forming sequences containing the GYG motif. Since there are no known channels with three pore-forming loops in a single subunit it is likely that the Kosik sequence is not accurate and needs to be extended.

4.3.3.2.1 Partial cloning of a putative tetrameric potassium selective cyclic nucleotide gated channel

I was unable to amplify the predicted Kosik SubH_Kv sequence using primer sets Kv1F and Kv1R or Kv2F and Kv2R. These were designed to amplify sequences 1737 and 1257 long respectively. Primer set Kv3Fwd and Kv3Rev, however, was designed to target regions with similarity to Sp-tetraKCNG pore domains in the forward direction and cyclic nucleotide binding domains in the reverse direction. With these primers I cloned and sequenced an 878 bp product (Figure 4-9). This sequence contains one of an expected four K^+ selective pore forming loops. Three more are expected assuming this is a tetrameric channel. Stretches of this sequence 56 bp, 190 bp, and 131 bp in length matched the Kosik sequence; however intervening sequences of 56 bp, 389 bp and 57 bp do not match (Appendix B.8). Moreover, the regions which match the Kosik sequence are not in frame with each other, and the 878 bp sequence does not form an open reading frame. The sequence was amplified from *A. queenslandica* cDNA prepared with the Invitrogen Superscript III kit. Since I did not treat the sample with DNase prior to reverse transcription I cannot rule out the possibility that I have amplified a genomic DNA product where coding sequences are interrupted by introns. Consistent with this, the corresponding genomic DNA sequence from the trace files contains the same intervening sequence. It is also possible that the sequence is non-coding and that I have instead amplified a pseudogene. Pseudogenes, or defunct genes, are typically duplicates of existing genes that have been disabled either by damage during the copying process or by accumulated

mutations that render them non-functional (Gerstein and Zheng, 2006). In order to determine the full sequence and whether it is functional RACE will be required to determine the 5' and 3' ends. Due to time constraints I did not complete RACE for this sequence. Following RACE, primers spanning the full sequence should be used to determine whether the sequence is an open reading frame. The full reading frame for Sp-tetraKCNG could not be amplified in one step as the sequence was too long (6714 bp). Galindo et al. (2007) confirmed the sequence by assembling overlapping sequences attained from cDNA and from trace files in the *S. purpuratus* genome database.

The putative *A. queenslandica* sequence, which I designate Amq-tetraKCNG should also be verified by comparison with trace file sequences. I have assembled three additional sequences with similarity to Sp-tetraKCNG or to the comparable channel in the urchin *Arbacia punctulata* (expected value <2e-21) and which share some sequence with Kosik SubH_Kv). These sequences are listed in Appendix B.4 and should be considered both when designing additional primers and when revising the predicted open reading frame. Again, I have not corrected trace file sequences for introns or vector sequence.

4.3.3.3 Functional and phylogenetic significance of tetrameric potassium selective cyclic nucleotide gated channels

Physiology of this unique channel is to date known only from echinoderms, where the channel has been localized to sperm and is thought to mediate chemotactically guiding sperm to the egg. In *S. purpuratus* the egg-derived peptide Speract activates a guanylyl cyclase in turn increasing cGMP

(Garbers, 1989; Yuen and Garbers, 1992). Sp-tetraKCNG is activated by cGMP. It is thought that this channel hyperpolarizes the membrane, relieving inactivation from voltage gated Ca^{2+} channels (Galindo et al., 2007). The comparable channel in *Arbacia punctulata* can be activated by a single molecule of cGMP binding to the third repeat of the tetrameric channel (Bönigk et al., 2009). Downstream Ca^{2+} influx through Ca_v channels is thought to regulate sperm trajectory. Wood et al (2007) found that increases in flagellar Ca^{2+} caused a transient increase in flagellar asymmetry, leading to a turn. Opening of Sp-tetraKCNG in the absence of cGMP in planar bilayers suggests these channels may also regulate potential of the resting membrane (Galindo et al., 2007).

Galindo et al. (2007) compared Sp-tetraKCNG domains 1 through 4 with 6 transmembrane domain channels. Their analysis places the Sp-tetraKCNG channel within the S4-superfamily, but on a separate branch between two groups with which it shares properties: K^+-selective and voltage-dependent EAG channels, and voltage-independent CNG cation channels; both families which possess cyclic nucleotide binding domains.

Confirmation of the *A. queenslandica* sequence will be needed to determine whether tetrameric K selective CNG channels are a novelty within echinoderms or if they are present in early branching metazoans. Given the indirect role of these channels in regulating flagellar beat it would be interesting to determine the contribution to the sponge feeding current which is generated by beating of flagella.

4.3.4 Putative K^+ channel sequences from A. queenslandica trace files

4.3.4.1 Slo family of potassium channels

The Slo family of potassium channels are structurally similar to the S4-superfamily of Kv and CNG channels having 6 transmembrane domains, with pore forming loop between domains S5 and S6. Slo family members include BK (Big K) or large conductance calcium-activated potassium channels (KCa; slo1), sodium dependent potassium channels (KNa; slo2) and pH-sensitive potassium channels (slo3). Partial sequences from the *A. queenslandica* trace files were found to be similar to KNa or KCa channels. These sequences are presented and further information on these channel types provided.

4.3.4.1.1 Putative KNa sequences in the *A. queenslandica* genome

A tblastx search of translated nucleotide databases at NCBI revealed that the highest degree of similarity with the Kosik sequence SubT_KCa was not with a KCa but rather a KNa, a sodium dependent potassium channel (accession BC103950.1; expected value2 e-77). I attempted to clone this sequence using four different primer sets (Appendix B.3) but failed to amplify a product. This raises the possibility that the predicted sequence is not accurate or that it is not expressed in larvae. To improve the chances of amplifying a coding region, primers should be designed to span regions that are conserved against KNa channels. Additionally, I have assembled seven sequences from the *A. queenslandica* trace files – all of which share sequence with Kosik SubT_KCa. I have redesignated SubT_KCa as AmqKNaA and have designated the trace file

sequences AmqKNaB through AmqKNaG (Appendix B.4). These sequences were originally grouped into two contigs containing 5 and 12 clones respectively. Contigs were split to sequences AmqKNaB through AmqKNaD (contig 1) and AmqKNaE through AmqKNaG (contig 2) since sequences within these contigs differed by ~ 4% in aligned regions. These sequences should be considered when revising the predicted sequence and designing new primer sets.

4.3.4.1.1.1 Physiology of KNa channels

In rat, KNa channels, including *Slick* (slo2.1) and *Slack* (slo2.2) have been localized to the heart and nervous system (Bhattacharjee et al., 2002; Bhattacharjee et al., 2003; Yuan et al., 2003). KNa channels are activated or opened by elevated cytosolic Na^+, and less so Cl^-, repolarizing or hyperpolarizing the membrane. Activation of *Slick* channels is additionally augmented under low ATP conditions, in effect reducing firing of nerves and other excitable cells under low energy conditions. KNa channels are believed to play a protective role during ischemia when oxygen and ATP are limited (Dryer, 1991; Haddad, 1993; Kameyama et al., 1984; Luk and Carmeliet, 1990; Mitani, 1992). Under these conditions intracellular Na^+ increases due to reduced activity of the Na^+/K^+ ATPase. Elevated Na^+ leads to action potential shortening or to propagation of fewer action potentials – owing to repolarizing effects of currents through KNa channels. KNa channels are also known to contribute to afterhyperpolarization, the hyperpolarized phase following an action potential (Kim and MacCormick, 1998).

Interestingly the slo2 homologue in *Caenorhabditis elegans* is activated by Ca^{2+} and Cl^- rather than by Na^+ and Cl^- as seen in mammals (Yuan, 2000). It may be that activation by Na^+ is a specialization in vertebrates where Na^+ is the primary charge carrier in the depolorization phase of the action potential. It will be interesting to see whether slo2 channels are more sensitive to gating by Ca^{2+} than Na^+ in invertebrates in general, where Ca^{2+} action potentials are more ubiquitous (Jeziorski et al., 2000).

4.3.4.1.2 Putative KCa sequences in the *Amphimedon queenslandica* genome

My searches of the *A. queenslandica* trace files also returned nucleotide sequences with similarity to calcium activated potassium (KCa) channels. The most similar sequence retrieved by a tblastx search of translated nucleotide databases was a BK, or high conductance, calcium activated potassium channel from *Aplysia californica* (accession AY372117.1; expected value 6e-44). Contiguous sequences assembled in Staden Package are listed in Appendix B.4 and denoted AmqKCaA, and AmqKCaB. The latter sequence differs by addition of a single 13 bp nucleotide sequence. Translations in all three forward frames are also given for each sequence. Stretches of 439 and 193 amino acids in frame with the pore region (MTTVGYGDV) are seen in the +2 and +1 frames for translations of AmqKCaA and AmqKCaB nucleotide sequences respectively. The 439 amino acid sequence for AmqKCaA aligns with high conductance calcium activated potassium channels along its entire length. However, without data from cDNA we cannot verify the AmqKCa sequences. Moreover it is unclear whether the stop

codons upstream and downstream of the 439 bp *A. queenslandica* sequence are introduced by alternating introns and exons or sequence from a sequencing vector. Full length clones will also be required to confirm that the trace files are portions of a coding sequence rather than a pseudogene.

4.3.4.1.2.1 Structure and physiology of BK or high conductance calcium activated potassium channels

Metazoan pore forming or α subunits of high conductance or BK KCa channels are encoded by the *Slo1* or *slowpoke* gene and functional variation is introduced by alternative splicing. Structurally, BK channels are similar to voltage gated K channels, through domains S1-S6, including homology among charged redsidues in the S4 domain (Vergara et al., 1998). In addition, BK channels have a seventh transmembrane domain (S0) at the N-terminal end of the channel. Additionally 4 hydrophobic segments in the cytoplasmic portion of the C-terminus are proposed (Figure 4-10) (Meera et al., 1997; Wei et al., 1994).

BK (Big K) channels are named for their large unitary conductances – typically 200-400 pS (Marty, 1981). They are also voltage dependent, with greater sensitivity to Ca^{2+} at depolarized than at resting potentials (Latorre et al., 1989). Because BK channels are more sensitive to calcium at depolarized potentials they activate rapidly on the upstroke of an action potential (Adams et al., 1982), initiating repolarization, and close rapidly at negative membrane potentials (Cui et al., 1997) making for a short afterhyperpolarization and ultimately shortening the interval between action potentials. Other types of KCa channels including SK (small K) and IK (intermediate K) may extend the interval between action

potentials as they are voltage insensitive and continue to pass current at negative membrane potentials, contributing to prolonged afterhyperpolarizations (Faber and Sah, 2003; Latorre et al., 1989).

4.3.4.1.2.2 Phylogenetic distribution of calcium activated potassium channels

Calcium-gated potassium channels have been identified in both prokaryotes and eukaryotes. The bacterial potassium channel MthK is structurally distinct from metazoan KCa channels, having only two transmembrane spanning domains per subunit; but is opened by elevated internal calcium (Jiang et al., 2002). Several calcium activated potassium currents have been described in *Paramecium* where they mediate repolarization (Hennessey and Kung, 1987), and the first calcium activated potassium currents in the Metazoa were recorded from the invertebrate *Aplysia* (Mollusca: Gastropoda) (Meech and Strumwasser, 1970). It is reasonable to expect sponges, early branching metazoans, to have KCa channels given KCa ubiquity across phyla.

4.3.4.1.2.3 Suggestions for analyses of sponge calcium activated potassium channels

AmqKCa channels once cloned can be compared with BK channel sequences and characterized in *Xenopus* oocytes to determine their affiliation. AmqKCa channels can be treated with known blockers of BK channels to determine how their pharmacological profiles compare. Candidate blockers include tetraethylammonium (TEA), charybdotoxin, penitrem A, paxilline and iberiotoxin where the latter two are selective for BK channels.

Dehydrosoyasaponin-1 (DHS-1) may be used to activate BK currents (Faber and Sah, 2003).

It is worthwhile probing the role of KCa channels in the sponge membrane particularly since there is reason to believe that coordinated events are initiated by a rise in calcium. *Rhabdocalyptus dawsoni* (Porifera: Hexactinellida) action potentials are blocked by 24 µM nimodipine, a calcium channel blocker, indicating that they are Ca^{2+}-based potentials (Leys et al., 1999). Action potentials have not yet been recorded from demosponges, however repolarizing currents, or alternatively Ca^{2+} pumps or buffers, are anticipated in resetting sponge membranes after rapid straightening of posterior cilia in *A. queenslandica* (Leys et al., 2002; Leys and Degnan, 2001) and after propagation of contractile waves in the freshwater demosponge *Ephydatia muelleri* (Elliott and Leys, 2007). In the latter, cells in the mesohyl arrest crawling when contractile waves pass, indicating a diffusible substance, possibly calcium, mediates the event. Elliott and Leys (2010) also found that contractions could not be triggered in medium free of Ca^{2+} and other divalent ions.

The role of KCa channels in setting the interval between events should also be explored. Rhythmic contractions with a periodicity of 0.1-1 per hour are seen in the demosponge *Tethya willhelma* (Nickel, 2004) and in glass sponges (Porifera: Hexactinellida) action potentials may fire at regular intervals leading to repeated flagellar arrests. While Leys et al. (1999) have confirmed that action potential frequency in the glass sponge *Rhabdocalyptus* is limited by absolute (30 s) and relative refractory periods (150 s), the currents dictating the interspike

interval are to date unknown. Dissection of calcium activated potassium currents may help to resolve the mechanics.

4.3.4.2 Putative voltage gated K channels

Remaining sequences assembled from the *A. queenslandica* trace files returned top blast hits against voltage gated potassium channels (Table 4-1), however each of these sequences appeared only once in searches of the *A. queenslandica* trace files – less frequent than expected given that the protocol for genome sequencing through the Joint Genome Institute is designed for multiple coverage. Sequences under-represented in the trace files could be non-native DNA from contaminating tissue, or these sequences may just not be sequenced as easily due to secondary structure limiting access to those regions of DNA. Or, these regions may have been under-represented by as a result of random sampling, despite multiple coverage. Numerous attempts were made to clone voltage gated potassium channels from the glass sponge *R. dawsoni* using degenerate primers designed against metazoan voltage gated potassium channels from the Shaker family (Appendix A.1). Representatives of this family were expected in sponges since they are already diversified into the four subfamilies Shak, Shab, Shaw and Shal in cnidarians (Jegla et al., 1995). Moreover, Leys and Meech recorded potassium currents with voltage sensitivity from sponge aggregates grafted to *R. dawsoni* (Leys, personal communication). Before abandoning the search for voltage gated potassium channels in the Porifera additional efforts should be made to assemble a Kv sequence from the trace files

by identifying overlapping sequences in the database. Inverse primers designed against sequences AmqKvA-C and AmqKvE did not return products.

4.4 Summary and conclusions

4.4.1 The potassium channel complement of A. queenslandica

I have presented sequence information for a variety of putative *A. queenslandica* potassium channels and have speculated on functional significance by indicating roles of related channels in other metazoans. To summarize I will recap *A. queenslandica* sequence information in the context of potassium currents required for an action potential. While action potentials have not yet been described from demosponges, the collection of sequences presented in this chapter indicate a complement of channels that could 1) set the resting membrane potential (Kir and K2P channels), 2) repolarize the membrane after a spike in membrane potential (KCa, KNa and possibly Kv) 3) hyperpolarize the membrane (KCa or KNa) and 4) return the membrane to rest (Kir and K2P). For reference purposes Box 1 includes an action potential schematic with descriptions of the phases above, and the potassium channels involved at each stage.

4.4.1.1 Summary of cloned potassium channel sequences

To summarize, I have cloned full length *A. queenslandica* sequences for inward rectifier (Kir) and two pore potassium (K2P) channels, both of which are known to maintain the resting membrane potential, including correcting afterhyperpolarization, and to regulate excitability by bringing the membrane toward or away from threshold.

Our expression work in *Xenopus* oocytes (Chapter 3) indicates that AmqKir channels are strongly rectifying, a phenotype typical of inward rectifiers found in excitable cells. This type of channel stabilizes the membrane potential by passing inward K^+ current at potentials hyperpolarized to the equilibrium potential for potassium (Ek). However, above E_K outward K^+ currents, which could offset depolarizing currents, are blocked allowing the membrane to depolarize past the excitation threshold in response to excitatory stimuli (Oliver et al., 2000).

K2P channels are modulated by a variety of physical and chemical stimuli, many of which couple channel activity to the metabolic state of the cell. We were unable to record AmqK2P currents; however mechano and temperature sensitive K2P-like currents are described in the demosponge *Axinella polypoides* (Carpaneto et al., 2003; Zocchi et al., 2003; Zocchi et al., 2001). Activation of these currents leads to a downstream increase in filtration and respiration rates. Future work on sponge K2P channels should involve linking physiology of cloned K2P channels to the above described physiology. AmqK2P sequences can serve as bases for cloning K2P homologues in *A. polypoides.*

A putative full length potassium tetramerization domain containing (KCTD) protein was also cloned. While these proteins were initially thought to regulate voltage gated K channels by mutual association of their tetramerization domains there is to date no electrophysiological evidence for this, nor evidence that ions are conducted through the water filled cavity formed by circular arrangement of KCTD subunits. Functionally KCTD proteins remain enigmatic.

4.4.1.2 Summary of expected channels based on genome searching and partially cloned sequences

Cloned sequences confirm the presence in sponges of inward rectifier and two pore potassium channels, which regulate the resting membrane potential and return the membrane to rest following afterhyperpolarization.

Sequences similar to the *S. purpuratus* channel, Sp-tetraKCNG, may indicate the presence of an additional channel regulating membrane potential. Constitutive or cGMP induced opening of the *S. purpuratus* channel hyperpolarizes the membrane. Partial sequences from the *A. queenslandica* genome also indicate the presence of channels that could contribute to the repolarization phase of an action potential. These include voltage gated potassium channels, Ca^{2+}- activated and Na^{+}- activated potassium channels. The latter two may also contribute to afterhyperpolarization.

4.4.2 Directions for future ion channel research

My conclusions on the potassium channel complement of *A. queenslandica* are tentative since confirmation of molecular identity requires full length clones as well as biophysical characterization. Nonetheless, the available data suggests that the genome of sponges encodes a diversity of potassium channel sequences which together could allow the membrane to depolarize and then return to resting potential. Additional attempts to extend sequences by cloning and trace file assembly are required.

Moreover, the trace file sequences listed in Appendix B.4 were generated solely by searching for Kv-like sequences. Likely additional potassium channel

sequences would be recovered with an exhaustive search, using representative sequences from other K channel families and subfamilies. *A. queenslandica* sequences can also be used as bases for degenerate primer design to extend cloning to other sponges and other basal metazoans. K channels of distantly related sponges can be compared to infer the channel complement of ancestral sponges. Comparison with other basal metazoans and with unicellular eukaryotes (outgroups) will provide insight into the membrane physiology of ancestral metazoans. Further insight will come from determining contributions of individual channels to the membrane potential. Channels should first be characterized in heterologous expression systems, such as *Xenopus* oocytes, and then efforts made to record and modulate channel activity *in situ.* Species with stereotypical physiology should be considered for ongoing work so that deviations in physiology downstream of channel modulation can be recognized. Examples of stereotypical physiology include coordinated contractions in the freshwater demosponge *Ephydatia muelleri* (Elliott and Leys, 2007) and action potentials and resultant flagellar arrests in the glass sponge *Rhabdocalyptus dawsoni* (Leys et al., 1999). In the demosponge *Axinella polypoides* activation of heat and mechano sensitive currents reminiscent of mammalian TREK-1 K2P currents leads to a downstream increase in filtration and respiration rates (Zocchi et al., 2003; Zocchi et al., 2001). I recommend using AmqK2P sequences as bases for primer design to amplify K2P channels from *A. polypoides.* An exciting opportunity exists to link physiology of a specific potassium channel with a defined change in animal physiology.

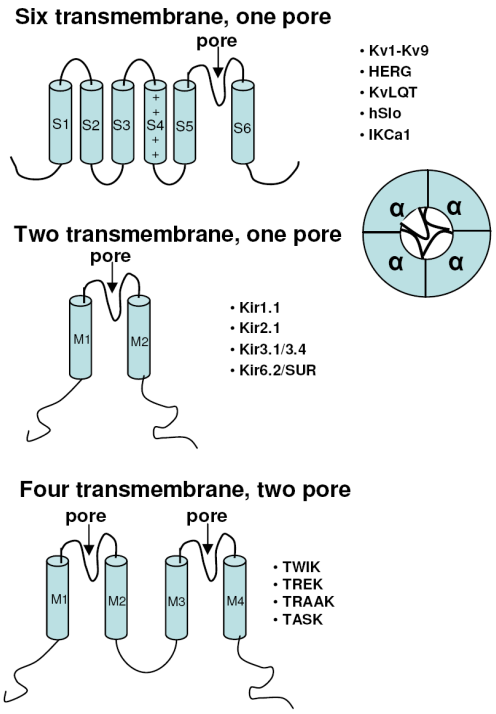

Figure 4-1: Summary of potassium channel types.

Schematic representation of the three structural types of potassium channels; adapted from Shieh et al. (2000). Six transmembrane (6 TM) domain channels with domains S1-S6 and a pore forming loop between domains S5 and S6. Positively charged residues in the S4 domain mediate voltage sensing. 6TM channels (and 2TM channels) assemble as tetramers of four α subunits, each with their pore-forming loop (P) lining the conducting pore (inset). Two TM domain subunits with transmembrane domains M1 and M2 flanking a pore forming loop. Four TM subunits with two pore-forming loops: one between M1 and M2 and a second between M3 and M4. Two α subunits assemble to form a channel with four pore-forming loops.

Table 4-1: Summary of partial putative potassium channel sequences assembled from the *Amphimedon queenslandica* genome trace files.

Sequences are given in Appendix B.4 and are the consensus of overlapping clones. Below I have indicated the ID assigned to the sequence, the list of clones included in the consensus sequence, top BLAST hit from the NCBI database and the expected value, which indicates the probability that the similarity with the blast hit is due to chance alone. I have also indicated whether the assembled trace file sequences match any of the potassium channel sequences assembled by Onur Sakarya and Ken Kosik.

Assigned name	Clones in consensus	Length (introns and vector not trimmed)	Most similar sequence retrieved by tblastx search	Expected value	Matching regions in Kosik channels (bp)
AmqKCTDA	CABF15367.g1 CABF2444		PREDICTED: Strongylocentrotus purpuratus similar to K channel tetramerisation domain containing 5 XM_001192661.1	2e-24	n/a
AmqKCTDB	CAYH6722.b1	851	BTB/POZ domain-containing protein KCTD9 [Rattus norvegicus]NP_001102341.1	1e-33	n/a
Amq-tetraKCNGC	BAYB232386.b1 BAYA65925.y1	1239	S. purpuratus tetrameric K-selective cyclic nucleotide gated channel (TetraKCNG), mRNA NM_001081964.1	2e-21	SubH_Kv 666-770; 827-1015
Amq-tetraKCNGD	BAYB290435.g1 BAYA494664.y4	907	Arbacia punctulata putative cNMP-gated K channel mRNA, partial cds, DQ822203.1	3e-22	SubH_Kv 639-683; 734-874

Amq-tetraKCNGE	BAYA25784.x1 BAYB332077.b1 BAYB16073.b1 BAYB67633.b1 BAYA320287.b1 BAYA320287.b1 BAYB149972.b1	1578	A. punctulata putative cNMP-gated K channel mRNA, partial cds, DQ822203.1	1e-34	SubH_Kv 749-793; 854-994; 1073-1247
AmqKNaB	BAYB228725 BAYA193722	1090 bp	K channel subfamily T member 2 (Na^+-activated K channel) [Rattus norvegicus] NP_942057.1	1e-13	SubTKCa 783-987; 1045-1090
AmqKNaC	BAYB442502 BAYB366268	878 bp	K channel subfamily T member 2 [R. norvegicus] NP_942057.1	2e-18	SubTKCa 444-647; 705-825
AmqKNaD	BAYB79925	848 bp	PREDICTED: similar to K channel subfamily T member 1 [Ciona intestinalis] XP_002120561.1	4e-16	SubTKCa 1-147; 205-269
AmqKNaE	BAYA222360.y1 BAYB494011.b1 BAYB111824.b1 BAYB269389.b1 BAYA42973.y1	1468	PREDICTED: K channel, subfamily T, member 2 [Taeniopygia guttata] XP_002192224.1	2e-24	SubTKCa 509-713; 771-891; 951-1087
AmqKNaF	BAYB368280.b1 BAYB575793.g1 BAYB166920.b1 BAYA24883.y1 BAYA376968.x1 BAYA430446.b1	1471	PREDICTED: Bos taurus K channel subfamily T member 1 XR_083872.1	1e-31	SubTKCa 514-718
AmqKNaG	BAYA386058.x1		Same as above	3e-28	SubTKCa 20-224
AmqKCa_A	BAYA563557.x2 BAYA330024.y1 BAYB373746.b1 BAYB125094.b1 BAYB125094.g1		Aplysia californica high conductance Ca^{2+}-activated K channel, AY372117.1	6e-44	n/a
AmqKCa_B	BAYA442637.y1 BAYB117607.b1 BAYB28391.b1 BAYB242155.g1		Same as above	4e-49	n/a
AmqKvA	BAYB571575.b1	690	Nephila clavata spKv3 mRNA for potassium channel Kv3, complete cds, AB212763.1	2e-24	n/a
AmqKvB	BAYB600936.b1	741	A. californica (clone Akv5.1) noninactivating potassium channel	9e-21; 7e-21	n/a

			mRNA, complete cds; Mesobuthus martensii shaker cognate b (Shab) gene, exon 2 and partial L35766.1; EU642903.1		
AmqKvC	BAYB227340.g1 (no overlapping sequences found)	786	A. californica K channel mRNA, complete cds, M95914.1; Xenopus laevis Kv channel, shaker-related subfamily	9e-113; 4e-98	n/a
AmqKvD	BAYB235512.b1 BAYB432185.g1	1047	A. californica Shaw K channel Kv3.1a mRNA, complete Cds	2e-103	n/a
AmqKvE	BAYB37212.b1 BAYB571575.g1	1227	Notoplana atomata K channel Kv3.2 mRNA, complete cds AY186794.1	1e-24	n/a

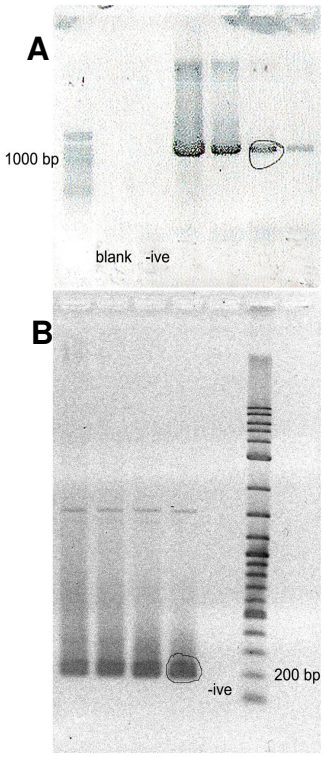

Figure 4-2: Ethidium bromide stained agarose gels (1%) showing AmqK2P products.

(A) AmqK2P sequences were amplified from 10^{-1} through 10^{-4} dilutions of cDNA using primers spanning the predicted full length *A. queenslandica* K2P channel. The circled band was cloned and sequenced. (B) The 5' ends were confirmed by nested 5'-RACE on 10^{-1} through 10^{-4} dilutions of the 5' RACE product. The circled band was cloned and sequenced and found to have a start site in frame with the remaining K2P sequence. No template (-ive) controls are indicated.

Figure 4-3: Primary structure and predicted topology of AmqK2P channel subunits.

(A) Predicted amino acid sequences of *A. queenslandica* two pore potassium channels AmqK2PA and AmqK2PB. Since the two sequences differed by only 2 amino acids a single sequence is given below. Amino acid differences between the two are shown as (AmqK2PA/AmqK2PB). The four predicted membrane spanning domains are boxed and the two pore-forming regions are underlined. B) Schematic of predicted secondary structure of K2P pore-forming subunit adapted from O'Connell et al. (2002). Transmembrane domains (M1 through M4), pore-forming domains (P1 and P2) and N and C termini are indicated. Two pore-forming subunits are predicted to assemble such that four pore-forming domains surround a central pore. C) Kyte-Doolittle Hydropathy plot for AmqK2P channels. A single plot is shown as the two amino acid differences between AmqK2PA and AmqK2PB did not change the hydropathy profile. Stretches of amino acids with hydropathy values greater than 1.8 were predicted to be membrane spanning. The peak at position 160, however, corresponds to the first pore forming region. Predicted transmembrane (M1-M4) are indicated.

A

MEKEVESEIPAVASDREDSESRELTEKPQEDTAEDEEPEDTGFECSRAYFT

RLFCNLNIYNQAFILFALVMTYILVGGAIFLAFELPAETKRNEAITAANETY

IRAFNNIVDQLVNFTNLTEEEAMALVRRVAQSAIDASNNQPTNNWEYGS

AIFFATTVITTIGYGSIAPETDGGRGFFIPYALVGIPLTLIFLGFLGQVTLNKG

VDRATRCLRRRVTFDWGQILVVFTIGLVSFIFIPAIIFAIIDDWTYFEAVYFT

FVSLTTVGFGDFVP(S/T)APKTFRGLYRFSLICWLFLGLAFIALIIAQTQERI

ENVR(K/E)SVKKCRKCIKRTGGKLMLRKKNKESSKDNEKTEETEVEKE

B

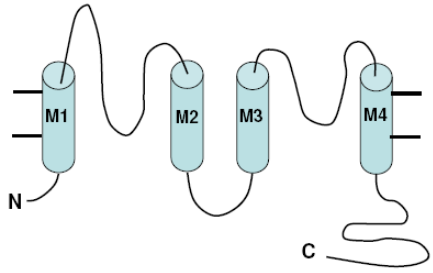

C

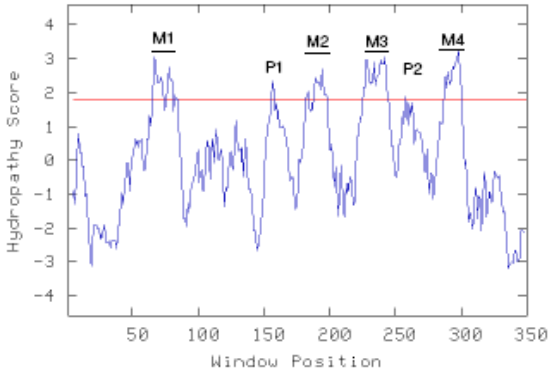

Table 4-2: Electrophysiological properties of mammalian two pore potassium channels adapted from O'Connell et al. (2002).

Responses to reagents are: ↑ (increase 30% or more); ↓ (decrease 30% or more) or X (no significant change). TEA = tetraethyammonium; AA = arachadonic acid; 4-AP = 4-amino pyridine; PKC=phosphokinase C; IBMX = 1-methyl-3-isobuyylxanthine; PMA=phorbol-12-myristate-acetate.

Properties of K2P channels														
Name	Classical blockers					Physiological sensitivity				PKA activators				PKC activators
	Quinine 100 µM	TEA+ 1 mM	4-AP 1 mM	Cs+ 100 µM	Ba2+ 100 µM	Stretch	AA 10 µM	Acid internal pH 6	Acid external pH 6	IBMX 1 mM	Forskolin 10 µM	IBMX + Forskolin	cAMP	PMA 40 nM
TASK1	X	X	X	↓	X	X	X	X	↓	X	X			X
TASK2	↓	X	X	X	↓		X	X	↓	X	X	X	X	X
TASK3	↓			X	X		X	X	↓			X		X or ↓
TASK4	X	X	X	X	↓		X	X	↓			X		X
TWIK1	↓	↓	X	X	↓		X	↓	X		X		X	↑
TWIK2	X				↓			↓	X			X	X	↑
TREK1	X	X		X	↓	↑	↑	↑				↓		↓
TREK2		X			↓	↑	↑	↑		↓			↓	X
TRAAK		X	X	X	X	↑	↑	X	X	X	X	X		X
THIK1							↑	X	↓					
TALK1	↓	X	X	X	↓		X	X	↓	X	X	X	X	X
TALK2	↑	X	X	X	↓		X	X	↓	X	X	X	X	X

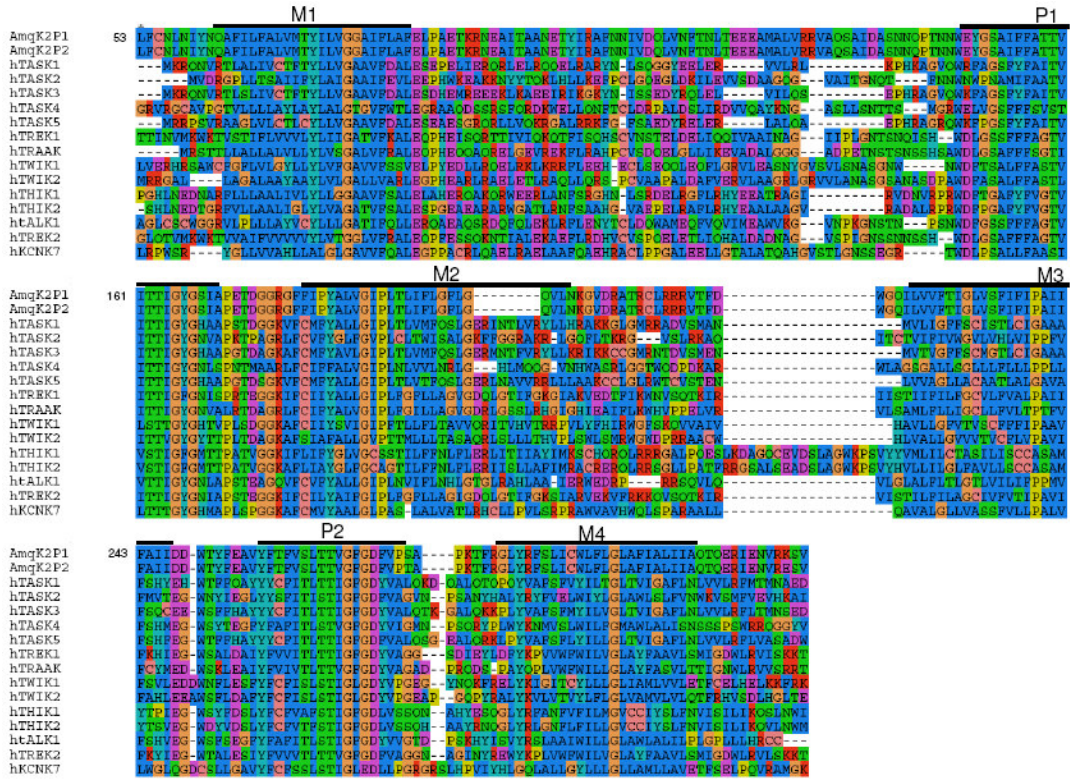

Figure 4-4: Partial clustalW alignment of predicted AmqK2P amino acid sequences with human K2P amino acid sequences.

Predicted AmqK2P transmembrane domains M1-M4 and pore P1 and P2 are indicated.

Figure 4-5: Evolutionary relationships of metazoan two pore potassium channels inferred using Maximum Parsimony analysis in MEGA 4.

The bootstrap consensus tree shows branches which are supported in greater than 20% of replicates (500 replicates). The tree was obtained using the Close-Neighbor-Interchange algorithm with search level 3. Analysis is based on 85 sequences with 162 positions; 152 of which are informative. Sequences were compiled from *C. elegans* (twk), *Drosophila melanogaster*, *Lymnaea stagnalis* and *Aplysia californica* and vertebrates. Relationships among most invertebrate sequences were unresolved. Instead of showing each sequence on its own branch, the sequences were collapsed into one polytomy.

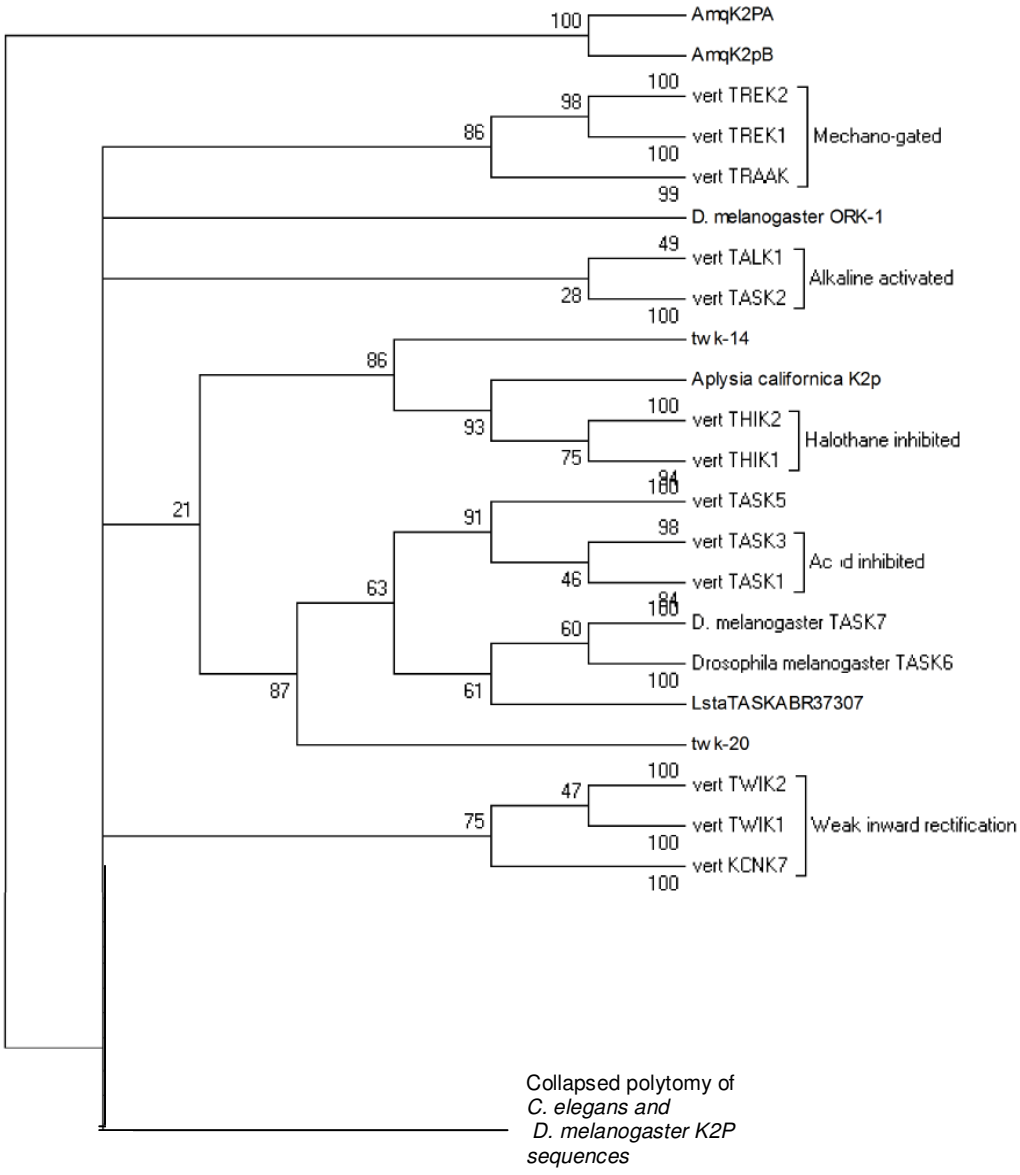
AmqK2PA
AmqK2pB
vert TREK2
vert TREK1
vert TRAAK
Mechano-gated
D. melanogaster ORK-1
vert TALK1
vert TASK2
Alkaline activated
twk-14
Aplysia californica K2p
vert THIK2
vert THIK1
Halothane inhibited
vert TASK5
vert TASK3
vert TASK1
Acid inhibited
D. melanogaster TASK7
Drosophila melanogaster TASK6
LstaTASKABR37307
twk-20
vert TWIK2
vert TWIK1
vert KCNK7
Weak inward rectification
Collapsed polytomy of
C. elegans and
D. melanogaster K2P
sequences

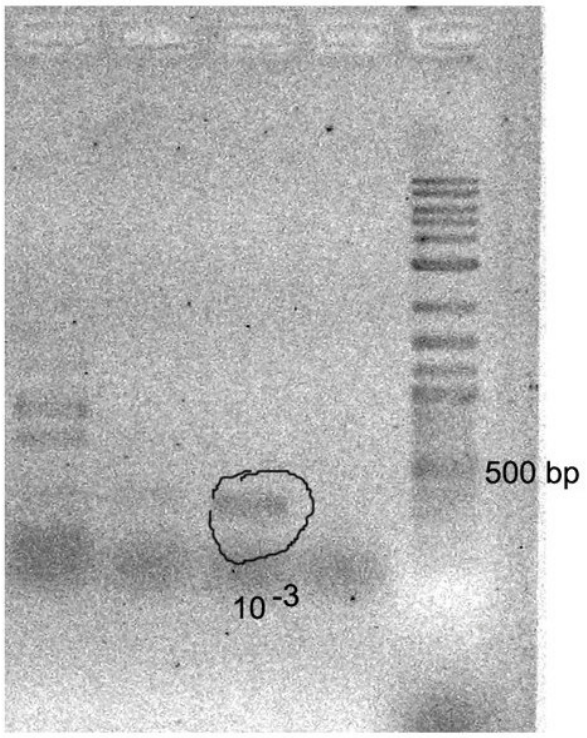

Figure 4-6: Ethidium bromide stained agarose gel (1%) showing the initial AmqKCTD product.

The circled product was amplified from circularized *A. queenslandica* cDNA using the inverse primer set Kinv7-5' and Kinv7-3'.

Figure 4-7: Alignment of BTB domains of AmqKCTDA and group I human KCTD proteins with the tetramerization domains of Kv channels.

Percent identity with AmqKCTDA is given for the displayed portion of each sequence. Structural elements identified from the crystal structure of KCTD5 are mapped onto the alignment of KCTD sequences. Assembly of KCTD subunits is mediated by hydrogen bonding of KCTD5 acidic residues (+) to basic residues (-) on adjoining subunits. Many of these residues are conserved in AmqKCTDA.

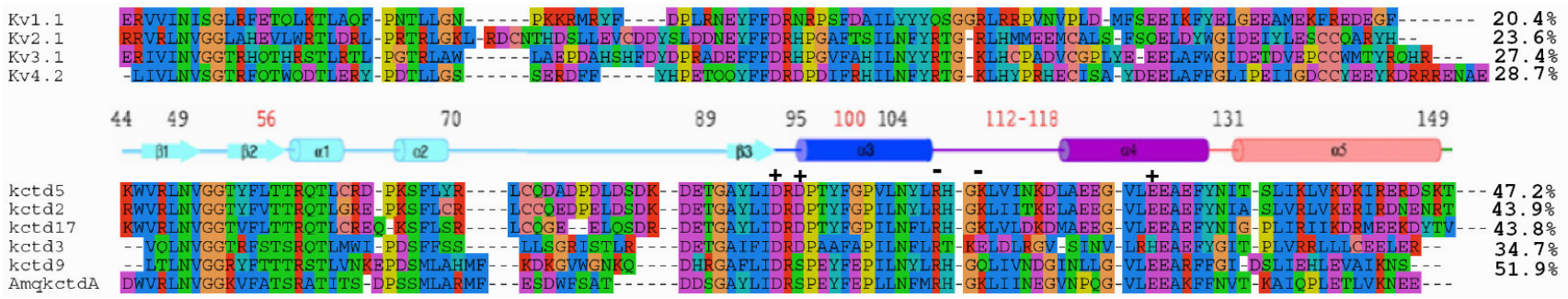
Kv1.1 20.4%
Kv2.1 23.6%
Kv3.1 27.4%
Kv4.2 28.7%
44 49 56 70 89 95 100 104 112-118 131 149
β1 β2 α1 α2 β3 α3 α4 α5
kctd5 47.2%
kctd2 43.9%
kctd17 43.8%
kctd3 34.7%
kctd9 51.9%
AmqkctdA

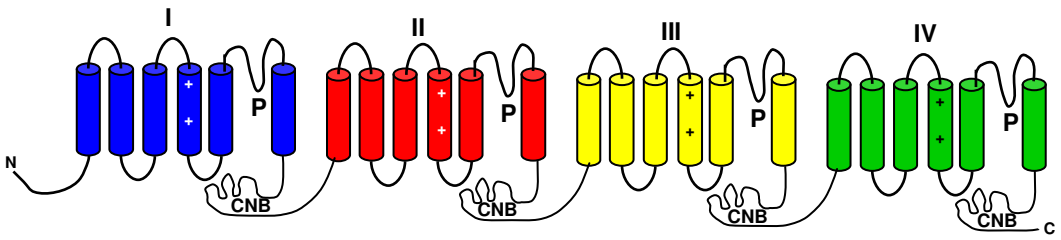

Figure 4-8: Schematic representation of the *Strongylocentrotus purpuratus* tetrameric potassium selective cyclic nucleotide gated channel, Sp-tetraKCNG.

Each of the four KCNG domains (I–IV) is composed of six transmembrane segments (S1–S6) with a pore loop (P) between S5 and S6, and a cyclic nucleotide-binding domain (CNBD) after S6.

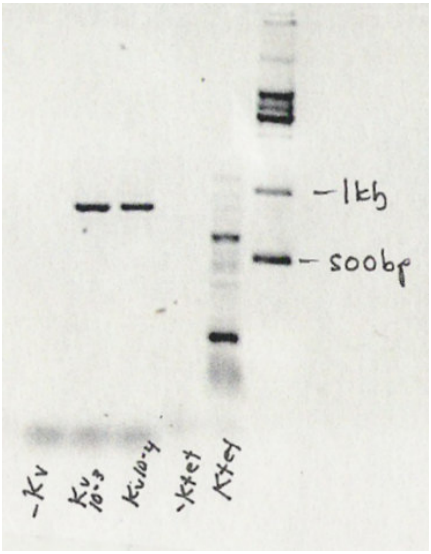

Figure 4-9: Ethidium bromide stained 1% agarose gel showing putative Amq-tetraKCNG fragment.

Bands were amplified from 10^{-3} and 10^{-4} dilutions of *A.. queenslandica* cDNA using primers Kv3Fwd and Kv3Rev. The lane next to the ladder is the product of 5' RACE to amplify AmqKCTDA. No template (-Kv and –Ktet) controls are shown for each.

Table 4-3: Comparison of SubH_Kv and Sp-tetraKCNG sequences.

The SubH_Hv (Appendix B.2) nucleotide sequence was used to search NCBI translated nucleotide databases using the tblastx search algorithm. The most similar sequence was found to be the *S. purpuratus* tetrameric potassium selective cyclic nucleotide gated channel. The table below indicates the regions of greatest match between SubH_Kv and Sp-tetraKCNG. The expected value is the probability that the match between the two sequences is due to chance alone.

Sp-tetraKCNG Domains		Matching region of SubH_Kv translated sequence (bp)	Expected value
Repeat	Domain		
I	Pore + S6	13-53	2e-46
	S6	218-274	2e-21
	CNBD	325-391	2e-21
II	S6	12-72	7e-65
	Pore + S6	218-312	2e-46
	CNBD	335-399	2e-46
	CNBD	306-325	2e-46
	S6	451-511	2e-21
III	Pore + S6	218-305	7e-65
	CNBD	332-393	7e-65
	S6	447-551	2e-46
	S6	5-65	2e-21
IV	S6	444-551	7e-65
	S6	218-306	2e-21

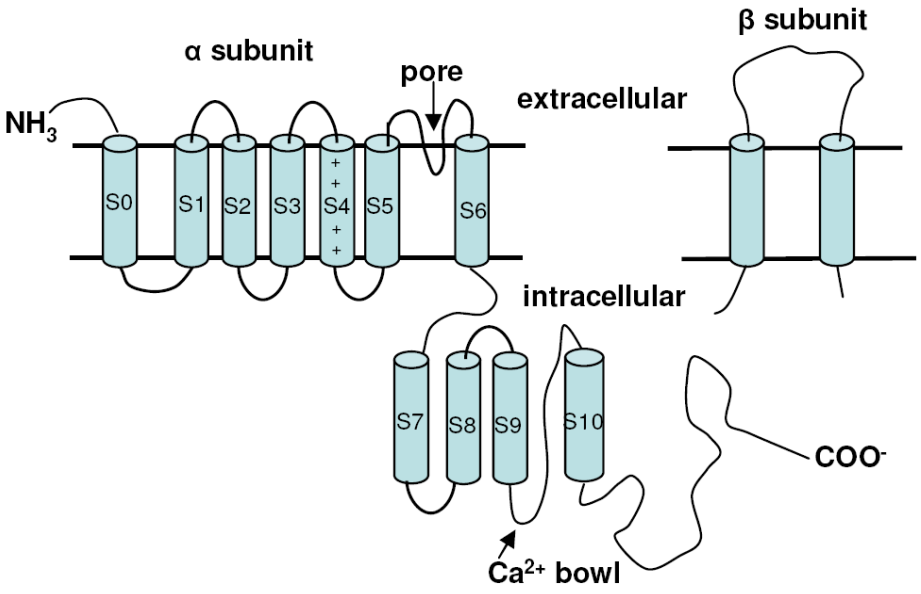

Figure 4-10: Proposed topology of large conductance (BK) calcium-activated potassium channels, adapted from Faber (2003).

BK channels are formed from alpha and beta subunits. The alpha subunit has 6 transmembrane domains S1-S6 and an S4 domain with positively charged residues, like voltage gated channels. Additionally BK channels are proposed to have a seventh transmembrane domain, S0, at the N-terminal end. Ca^{2+} is thought to bind within the extended C-terminus which is proposed to contain four hydropohobic domains (S7-S10).

Box 1: Action potential schematic with phases and contributing K+ channels identified

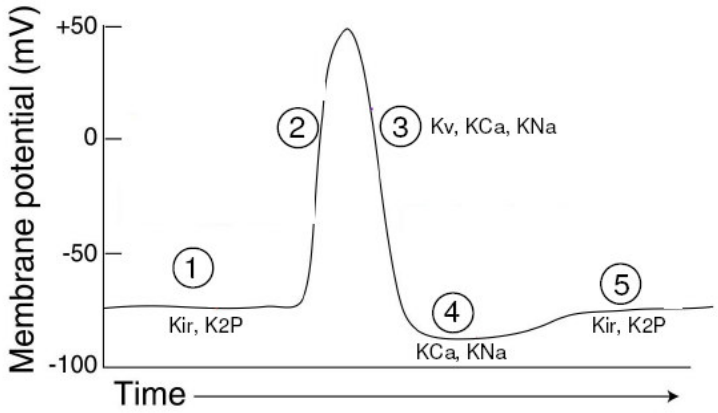

(1) **Resting membrane**
At rest K^+ is higher inside the cell than out. This is largely due to the electrogenic Na+K+ATPase which continuously pumps K^+ into the cell in exchange for Na^+ in a 2:3 ratio. K^+ is also attracted to the inside of the cell by large organic anions and enters through two pore potassium (K2P) and inward rectifier potassium channels (Kir).

(2) **Depolarization**
Excitatory stimuli, depolarize the membrane away from the resting membrane potential. If the depolarization is sufficient, voltage-sensitive ion channels open allowing influx of Na^+ or Ca^{2+} causing further depolarization

(3) **Repolarization**
Membrane potential is returned to rest by the opening of potassium channels, allowing K^+, which is held at high levels in resting cells, to flood out, repolarizing the cell. A variety of K channels mediate repolarization. Voltage gated potassium channels (Kv) are opened by depolarization. Ca^{2+}- or Na^+-activated potassium channels (KCa or KNa) may be opened by elevated cytosolic Ca^{2+} or Na^+ in the rising phase of the action potential.

(4) **Afterhyperpolarization**
Afterhyperpolarization (AHP) is the phase following an action potential where the membrane potential is more negative than the resting membrane potential. Hyperpolarization may be mediated by both KCa and KNa currents, with the latter contributing to the prolonged, later phase of the AHP (Kim and MacCormick, 1998). Hyperpolarization is important for relieving inactivation from ion channels including voltage gated calcium channels (Krasznai, Marian et al. 2000). The time course of afterhyperpolarization can govern the length of the refractory period.

(5) **Return to resting potential**
As already mentioned, inward rectifier (Kir) and two pore potassium channels maintain the resting membrane potential near equilibrium for potassium. Kir channels are pivotal in returning the membrane potential to rest following afterhyperpolarization as these channels conduct largest inward (depolarizing) currents at potentials hyperpolarized to equilibrium for potassium

4.5 References

Adams, P. R., Constanti, A., Brown, D. A. and Clark, R. B. (1982). Intracellular Ca^{2+} activates a fast voltage-sensitive K^+ current in vertebrate sensory neurons. *Nature* **296**, 746-749.

Alloui, A. and al., e. (2006). TREK-1, a K^+ channel involved in polymodal pain perception. *EMBO Journal* **25**, 2368-2376.

Amrutha, R. N., Sekhar, P. N., Varshney, R. K. and Kishor, P. B. K. (2007). Genome-wide analysis and identification of genes related to potassium transporter families in rice (*Oryza sativa* L.). *Plant Science* **172**, 708–721.

Anderson, P. A. V. and Greenberg, R. M. (2001). Phylogeny of ion channels: clues to structure and function. *Comparative Biochemistry and Physiology Part B* **129**, 17-18.

Bang, H., Kim, Y. and Kim, D. (2000). TREK-2, a new member of the mechanosenitive tandem-pore K^+ channel family. *The Journal of Biological Chemistry* **275**, 17412-17419.

Barriere, H., Belfodil, R., Rubera, I., Tauc, M., Lesage, F., Poujeol, C., Guy, N., Barhanin, J. and Poujeol, P. (2003). Role of TASK2 potassium channels regarding volume regulation in primary cultures of mouse proximal tubules. *Journal of General Physiology* **122**, 177-190.

Bayliss, D. A. and Barrett, P. Q. (2008). Emerging roles for two-pore domain potassium channels and their potential therapeutic impact. *Trends in Pharmacological Sciences* **29**, 566-575.

Becker, D., Geiger, D., Dunkel, M., Roller, A., Bertl, A., Latz, A., Carpaneto, A., Dietrich, P., Roelfsema, M. R. G., Voelker, C. et al. (2004). AtTPK4, an *Arabidopsis* tandem-pore K^+ channel, poised to control the pollen membrane voltage in a pH- and Ca^{2+}-dependent manner. *Proceeding of the National Academy of Sciences U. S. A.* **101**, 15621-15626.

Bhattacharjee, A., Gan, L. and Kaczmarek, L. K. (2002). Localization of the Slack potassium channel in the rat central nervous system. *Journal of Comparative Neurology* **454**, 241-254.

Bhattacharjee, A., Joiner, W. J., Wu, M., Yang, Y., Sigworth, F. J. and Kaczmarek, L. K. (2003). Slick (Slo2.1), a rapidly-gating sodium-activated potassium channel inhibited by ATP. *The Journal of Neuroscience* **23**, 11681-11691.

Boland, L., Jiang, M., Lee, S., Fahrenkrug, S., Harnett, M. and O'Grady, S. (2003). Functional properties of a brain-specific NH_2-terminally spliced modulator of Kv4 channels. *American Journal of Physiology - Cell Physiology* **285**, C161-C170.

Bönigk, W., Loogen, A., Seifert, R., Kashikar, N., Klemm, C., Krause, E., Hagen, V., Kremmer, E., Strünker, T. and Kaupp, U. B. (2009). An Atypical CNG Channel Activated by a Single cGMP Molecule Controls Sperm Chemotaxis. *Science Signalling* **2**, ra68.

Buckingham, S. D., Kidd, J. F., Law, R. J., Franks, C. J. and Sattelle, D. B. (2005). Structure and function of two-pore-domain K+ channels:

contributions from genetic model organisms. *Trends in Pharmacological Sciences* **26**, 362-367.

Carpaneto, A., Magrassi, R., Zocchi, E., Cerrano, C. and Usai, C. (2003). Patch-clamp recordings in isolated sponge cells (*Axinella polypoides*). *Journal of Biochemical and Biophysical Methods* **55** 179-189.

Chapman, M. L., Krovetz, H. S. and Vandongen, A. M. (2001). GYGD pore motifs in neighbouring potassium channel subunits interact to determine ion selectivity. *Journal of Physiology* **530**, 21-33.

Coetzee, W. A., Amarillo, Y., Chiu, J., Chow, A., Lau, D., MacCormack, T., Moreno, H., Nadal, M. S., Ozaita, A., Poutney, D. et al. (1999). Molecular Diversity of K^+ Channels. *Annals New York Academy of Sciences* **868,** 233-285.

Cui, J., Cox, D. H. and Aldrich, R. W. (1997). Intrinsic voltage dependence and Ca^{2+} regulation of mslo large conductance Ca-activated K^+ channels. *Journal of General Physiology* **109**, 647-673.

Dementieva, I. S., Tereshko, V., McCrossan, Z. A., Solomaha, E., Araki, D., Xu, C., Grigorieff, N. and Goldstein, S. A. N. (2009). Pentameric assembly of potassium channel tetramerization domain-containing protein 5. *Journal of Molecular Biology* **387**, 175-191.

Di Marcotullio, L., Ferretti, E., De Smaele, E., Argenti, B., Mincione, C., Zazzeroni, F. and al., e. (2004). REN/KCTD11 is a suppressor of Hedgehog signaling and is deleted in human medulloblastoma. *Proceeding of the National Academy of Sciences U. S. A.* **101**, 10833-10838.

Dryer, S. E. (1991). Na(+)-activated K^+ channels and voltage-evoked ionic currents in brain stem and parasympathetic neurones of the chick. *Journal of Physiology* **435**, 513–532.

Elliott, G. R. D. and Leys, S. P. (2007). Coordinated contractions effectively expel water from the aquiferous system of a freshwater sponge. *Journal of Experimental Biology* **210**, 3736-3748.

Elliott, G. R. D. and Leys, S. P. (2010). Evidence for glutamate, GABA and NO in coordinating behaviour in the sponge, *Ephydatia muelleri* (Demospongiae, Spongillidae) *Journal of Experimental Biology* **213**, 2310-2321.

Faber, E. S. L. and Sah, P. (2003). Calcium-activated potassium channels: multiple contributions to neuronal function. *The Neuroscientist* **9**, 181-194.

Galindo, B. E., Vega-Beltrán, J. L. d. l., Labarca, P., Vacquierc, V. D. and Darszon, A. (2007). Sp-tetraKCNG: A novel cyclic nucleotide gated K+ channel *Biochemical and Biophysical Research Communications* **354**, 668-675.

Gamse, J. T., Kuan, Y.-S., Macurak, M., Brosamle, C., Thisse, B., Thisse, C. and al., e. (2005). Directional assymetry of the zebrafish epithalamus guides dorsoventral innervation of the midbrain target. *Development* **132**, 4869-4881.

Garbers, D. L. (1989). Molecular basis of fertilization. *Annual Review of Biochemistry* **58**, 719–742.

Gerstein, M. and Zheng, D. (2006). The real life of pseudogenes. In *Scientific American*, vol. August 2006, pp. 49-55.

Gobert, A., Isayenkov, S., Voelker, C., Czempinski, K. and Maathuis, F. J. M. (2007). The two-pore channel TPK1 gene encodes the vacuolar K+ conductance and plays a role in K+ homeostasis. *Proceeding of the National Academy of Sciences U. S. A.* **104**, 10726-10731.

Goldstein, S. A. N. (2001). Potassium leak channels and the KCNK family of two-P-domain subunits. *Nature Reviews Neuroscience* **2**, 175-184.

Haddad, G. G., and Jiang, C. (1993). O_2 deprivation in the central nervous system: on mechanisms of neuronal response, differential sensitivity and injury. *Progress in Neurobiology* **40**, 277–318.

Haynes, W. J., Ling, K.-Y., Saimi, Y. and Kung, C. (2003). PAK paradox: *Paramecium* appears to have more K+-channel genes than humans. *Eukaryotic Cell* **2**, 737-745.

Hennessey, T. M. and Kung, C. (1987). A calcium-dependent potassium current is increased by a single-gene mutation in *Paramecium*. *The Journal of Membrane Biology* **98**, 145-155.

Hille, B. (2001). Ionic channels of excitable membranes. Sunderland, MA.: Sinauer Associates, Inc.

Honore, E. (2007). The neuronal background K2P channels: focus on TREK1. *Nature Reviews Neuroscience* **8**, 251-261.

Honoré, E. (2007). The neuronal background K2P channels: focus on TREK1. *Nature Reviews Neuroscience* **8**, 241-261.

Isacoff, E. Y., Jan, Y. N. and Jan, L. Y. (1990). Evidence for the formation of heteromultimeric potassium channels in *Xenopus* oocytes. *Nature* **345**, 530-534.

Jan, L. Y. and Jan, Y. N. (1990). A superfamily of ion channels. *Nature* **345**, 672.

Jan, L. Y. and Jan, Y. N. (1997). Cloned potassium channels from eukaryotes and prokaryotes. *Annual Review of Neuroscience* **20**, 91-123.

Jegla, T., Grigoriev, N., Gallin, W. J., Salkoff, L. and Andrew N. Spencer. (1995). Multiple *Shaker* potassium channels in a primitive metazoan. *The Journal of Neuroscience* **15**, 7989-7999.

Jeziorski, M., Greenberg, R. and Anderson, P. (2000). The molecular biology of invertebrate voltage-gated Ca(2+) channels. *Journal of Experimental Biology* **203**, 841-856.

Jezzini, S. H., Reagin, S., Hohn, A. and Moroz, L. L. (2006). Molecular characterization and expression of a two-pore domain potassium channel in the CNS of *Aplysia californica*. *Brain Research* **1094**, 47-56.

Jiang, Y., Lee, A., Chen, J., Cadene, M., Chait, B. T. and MacKinnon, R. (2002). Crystal structure and mechanism of a calcium-gated potassium channel. *Nature* **417**, 515-522.

Kamb, A., Iverson, L. E. and Tanouye, M. A. (1987). Molecular characterization of Shaker, a *Drosophila* gene that encodes a potassium channel. *Cell* **50**, 405-413.

Kameyama, M., Kakei, M., Sato, R., Shibasaki, T., Matsuda, H. and Irisawa, H. (1984). Intracellular Na+ activates a K+ channel in mammalian cardiac cells. *Nature* **309**, 354-356.

Kaupp, U. B. and Seifert, R. (2002). Cyclic Nucleotide-Gated Ion Channels. *Physiological Reviews* **82**, 769-824.

Ketchum, K. A., Joiner, W. J., Sellers, A. J., Kaczmarek, L. K. and Goldstein, S. A. N. (1995). A new family of outwardly rectifying potassium channel proteins with two pore domains in tandem. *Nature* **376**, 690-695.

Kim, D. (2005). Physiology and pharmacology of two-pore domain potassium channels. *Current Pharmaceutical Design* **11**, 2717-2736.

Kim, U. and MacCormick, D. A. (1998). Functional and ionic properties of a slow afterhyperpolarization in ferret perigeniculate neurons in vitro. *Journal of Neurophysiology* **80**, 1222-1235.

Kusano, K., Miledi, R. and Stinnakre, J. (1982). Cholinergic and catecholaminergic receptors in the *Xenopus* oocyte membrane. *Journal of Physiology* **328**, 143-170.

L'Hoste, S., Barriere, H., Belfodil, R., Rubera, I., Duranton, C., Taue, M., Poujeol, C., Barhanin, J. and Poujeol, P. (2007). Extracellular pH alkalinization by Cl^-/HCO_3^- exchanger is crucial for TASK2 activation by hypotonic shock in proximal cell lines from mouse kidney. *American Journal of Physiology - Renal Physiology* **292**, F628-F638.

Latorre, R., Oberhauser, A., Labarca, P. and Alvarez, O. (1989). Varieties of calcium-activated potassium channels. *Annual Review of Physiology* **51**, 385–399.

Lesage, F. (2003). Pharmacology of neuronal background potassium channels. *Neuropharmacology* **44**, 1-7.

Lesage, F. and Lazdunski, M. (2000). Molecular and functional properties of two-pore domain potassium channels. *American Journal of Physiology - Renal Physiology* **279**, F793-F801.

Leys, S., Mackie, G. and Meech, R. (1999). Impulse conduction in a sponge. *Journal of Experimental Biology* **202**, 1139-1150.

Leys, S. P., Cronin, T. W., Degnan, B. M. and Marshall, J. N. (2002). Spectral sensitivity in a sponge larva. *Journal of Comparative Physiology A* **188**, 199-202.

Leys, S. P. and Degnan, B. M. (2001). Cytological basis of photoresponsive behavior in a sponge larva. *Biological Bulletin* **201**, 323-338.

Li, B. and Gallin, W. J. (2004). VKCDB: Voltage-gated potassium channel database. *BMC Bioinformatics* **5**, 3.

Lotshaw, D. P. (2007). Biophysical, pharmacological, and functional characteristics of cloned and native mammalian two-pore domain K+ channels. *Cell Biochemistry and Biophysics* **47**, 209-256.

Luk, H. N. and Carmeliet, E. (1990). Na(+)-activated K+ current in cardiac cells: rectification, open probability, block and role in digitalis toxicity. *European Journal of Physiology.* **416,** 766–768.

Maingret, F., Lauritzen, I., Patel, A. J., Heurteaux, C., Reyes, R., Lesage, F., M., L. and Honore`, E. (2000). TREK-1 is a heat-activated background K+ channel. *The EMBO Journal* **19**, 2483-2491.

Marty, A. (1981). Ca-dependent K channels with large unitary conductance in chromaffin cell membranes. *Nature* **291**, 497–500.

Meech, R. W. and Strumwasser, F. (1970). Intracellular calcium injection activates potassium conductance in *Aplysia* nerve cells. *Federation Proceedings* **29**, 834.

Meera, P., Wallner, M., Song, M. and Toro, L. (1997). Large conductance voltage- and calcium-dependent K+ channel, a distinct member of voltage dependent ion channels with seven N-terminus transmembrane segments (S0-S6) and extracellular N-terminus, and an intracellular (S9-S10) C terminus. *Proceedings of the National Academy of Sciences U S A* **94**, 14066-14071.

Miller, C. (2000). An overview of the potassium channel family. *Genome Biology* **1**, 1-5.

Mitani, A., and Shattock, M.J. (1992). Role of Na-activated K channel, Na-K-Cl cotransport, and Na-K pump in [K]e changes during ischemia in rat heart. *American Journal of Physiology* **263**, H333–H340.

Morton, M. J., Abohamed, A., Sivaprasadarao, A. and Hunter, M. (2005). pH sensing in the two-pore domain K+ channel, TASK2. *Proceeding of the National Academy of Sciences U. S. A.* **102**, 16102-16106.

Nickel, M. (2004). Kinetics and rhythm of body contractions in the sponge *Tethya wilhelma* (Porifera: Demospongiae) *Journal of Experimental Biology* **207**, 4515-4524.

Niemeyer, M. I., Cid, L. P., Barros, L. F. and Sepulveda, F. V. (2001). Modulation of the two-pore domain acid-sensitive K+ channel TASK-2 (KCNK5) by changes in cell volume. *Journal of Biological Chemistry* **276**, 43166-43174.

O'Connell, A. D., Morton, M. J. and Hunter, M. (2002). Two-pore domain K+ channels - molecular sensors. *Biochimica et Biophysica Acta* **1566**, 152-161.

Okamura, Y., Nishino, A., Murata, Y., Nakajo, K., Iwasaki, H., Ohtsuka, Y., Tanaka-Kunishima, M., Takahashi, N., Hara, Y., Yoshida, T. et al. (2005). Comprehensive analysis of the ascidian genome reveals novel insights into the molecular evolution of ion channel genes. *Physiological Genomics* **22**, 269-282.

Oliver, D., Baukrowitz, T. and Fakler, B. (2000). Polyamines as gating molecules of inward-rectifier K+ channels. *European Journal of Biochemistry* **267**, 5824-5829.

Papazian, D. M., Schwarz, T. L., Tempel, B. L., Jan, Y. N. and Jan, L. Y. (1987). Cloning of genomic and complimentary DNA from *Shaker,* a putative potassium channel gene from *Drosophila*. *Science* **237**, 739-754.

Patel, A. J. and Honore, E. (2001). Properties and modulation of mammalian 2P domain K+ channels. *TRENDS in Neurosciences* **24**, 339-346.

Patel, A. J., Honoré, E., Maingret, F., Lesage, F., Fink, M., Duprat, F. and Lazdunski, M. (1998). A mammalian two pore domain mechano-gated S-like K+ channel. *The EMBO Journal* **17**, 4283-4290.

Polidoros, A. N., Pasentsis, K. and Tsaftaris, A. S. (2006). Rolling circle amplification-RACE: a method for simultaneous isolation of 5' and 3' cDNA ends from amplified cDNA templates. *BioTechniques* **41**, 35-36; 38; 40 passim.

Putnam, N. H., Srivastava, M., Hellsten, U., Dirks, B., Chapman, J., Salamov, A., Terry, A., Shapiro, H., Lindquist, E., Kapitonov, V. V. et al. (2007). Sea anemone genome reveals ancestral Eumetazoan gene repertoire and genomic organization. *Science* **317**, 86-94.

Resendes, B. L., Kuo, S. F., Robertson, N. G., Giersch, A. B. S., Honrubia, D., Ohara, O. and al., e. (2004). Isolation from cochlea of a novel human intronless gene with predominant fetal expression. *Journal of the. Association for Research in Otolaryngology* **5**, 185–202.

Reyes, R., Duprat, F., Lesage, F., Fink, M., Salinas, M., Farman, N. and Lazdunski, M. (1998). Cloning and expression of a novel pH-sensitive two pore domain K+ channel from human kidney. *Journal of Biological Chemistry* **273**, 30863-30869.

Rudy, B. (1988). Diversity and ubiquity of K channels. *Neuroscience* **25**, 729-749.

Sakarya, O., Armstrong, K. A., Adamska, M., Adamski, M., Wang, I.-F., Tidor, B., Degnan, B. M., Oakley, T. H. and Kosik, K. S. (2007). A post-synaptic scaffold at the origin of the animal kingdom. *PLoS ONE* **6**, 1-9.

Salkoff, L., Butlera, A., Fawcett, G., Kunkela, M., McArdlea, C., Paz-y-Minoa, G., Noneta, M., Waltona, N., Wanga, Z.-w., Yuana, A. et al. (2001). Evolution tunes the excitability of individual neurons. *Neuroscience* **103**, 853-859.

Shieh, C.-C., Coghlan, M., Sullivan, J. P. and Gopalakrishnan, M. (2000). Potassium channels: molecular defects, diseases, and therapeutic opportunities. *Pharmacological Reviews* **52**, 557-593.

Shorter, J., Watson, R., Giannakou, M. E., Clarke, M., Warren, G. and Barr, F. A. (1999). GRASP55, a second mammalian GRASP protein involved in the stacking of Golgo cisternae in a cell-free system. *EMBO Journal* **18**, 4949-4960.

Strong, M., Chandy, K. G. and Gutmany, G. A. (1993). Molecular evolution of voltage-sensitive ion channel genes: on the origins of electrical excitability. *Moecular Biology and Evolution* **10**, 221-242.

Stuhmer, W., Stocker, M., Sakmann, B., Seeburg, P., Baumann, A., Grupe, A. and Pongs, O. (1988). Potassium channels expressed from rat brain cDNA have delayed rectifier properties. *FEBS letters* **242**, 199-206.

Takumi, T., H., O. and Nakanishi, S. (1988). Cloning of a membrane protein that induces a slow voltage-gated potassium current. *Science* **242**, 1042-1045.

Talley, E. M., Sirois, J. E., Lei, Q. And Bayliss, D. (2003). Two-pore domain (KCNK) potassium channels: dynamic roles in neuronal function. *The Neuroscientist* **9**, 46-56.

Tempel, B. L., Papazian, D. M., Schwarz, T. L., Jan, Y. N. and Jan, L. Y. (1987). Sequence of a probable potassium channel component encoded at Shaker locus of *Drosophila*. *Science* **237**, 770-775.

Van Bogaert, P., Azizieh, R., Désir, J., Aeby, A., De Meirleir, L., Florence, J.-F. and al., e. (2007). Mutation of a potassium channel-related gene in progressive myoclonic epilepsy. *Annals of Neurology* **61**, 579–586.

Vergara, C., Latorre, R., Marrion, N. V., and Adelman, J. P. (1998). Calcium activated potassium channels. *Current Opinion in Neurobiology* **8:** 321-329.

Wacke, M. and Thiel, G. (2001). Electrically triggered all-or-none Ca^{2+}-liberation during action potential in the giant alga *Chara*. *Journal of General Physiology* **118**, 11-21.

Wei, A., Covarrubias, M., Butler, A., Baker, K., Pak, M. and Salkoff, L. (1990). K+ current diversity is produced by an extended gene family conserved in *Drosophila* and mouse. *Science* **248**, 599-603.

Wei, A., Solaro, C., Lingle, C. and Salkoff, L. (1994). Calcium sensitivity of BK-type KCa channels determined by a seperable domain. *Neuron* **13**, 671-681.

Wood, C. D., Nishigaki, T., Tatsu, Y., Yumoto, N., Baba, S. A., Whitaker, M. and Darszon, A. (2007). Altering the speract-induced ion

permeability changes that generate flagellar Ca2+ spikes regulates their kinetics and sea urchin sperm motility *Developmental Biology* **306**, 525-537.

Yuan, A., Dourado, M., Butler, A., Walton, N., Wei, A., and Salkoff,. (2000). SLO-2, a K+ channel with an unusual Cl^- dependence. *Nature Neuroscience* **3**, 771–779.

Yuan, A., Santi, C. M., Wei, A., Wang, Z.-W., Pollak, K., Nonet, M., Kaczmarek, L. K., Crowder, C. M. and Salkoff, L. (2003). The sodium-activated potassium channel is encoded by a member of the *Slo* gene family. *Neuron* **37**, 765-773.

Yuen, P. S. and Garbers, D. L. (1992). Guanylyl cyclase-linked receptors. *Annual Review of Neuroscience* **15**, 193–225

Zawlik, I., Zakrzewska, M., Witusik, M., Golanska, E., Kulczycka-Wojdala, D., Szybka, M. and al., e. (2006). KCTD11 expression in medulloblastoma is lower than in adult cerebellum and higher than in neural stem cells. *Cancer Genetics and Cytogenetics.* **170**, 24–28.

Zocchi, E., Basile, G., Cerrano, C., Bavestrello, G., Giovine, M., Bruzzone, S., Guida, L., Carpaneto, A., Magrassi, R. and Usai, C. (2003). ABA- and cADPR-mediated effects on respiration and filtration downstream of the temperature-signaling cascade in sponges. *Journal of Cell Science* **116**, 629-636.

Zocchi, E., Carpaneto, A., Cerrano, C., Bavestrello, G., Giovine, M., Bruzzone, S., Guida, L., Franco, L. and Usai, C. (2001). The temperature-signaling cascade in sponges involves a heat-gated cation channel, abscisic acid

and cyclic ADP-ribose. *Proceeding of the National Academy of Sciences* **98**, 14859-14864.

Zollman, S., Godt, D., Prive, G. G., Couderc, J. and Laski, F. A. (1994). The BTB domain, found primarily in zinc finger proteins, defines an evolutionarily conserved family that includes several developmentally regulated genes in *Drosophila*. *Proceedings of the National Academy of Sciences* **91**, 10717–10721.

Chapter Five: CONCLUSIONS AND DIRECTIONS FOR FUTURE RESEARCH

5.1 Sponges and the origin of conduction systems

The nervous system is thought to have evolved in eumetazoans after the lineages giving rise to sponges and eumetazoans diverged. Nonetheless, sponges display integrated responses in the absence of nerves. For example, glass sponges (Hexactinellida) propagate action potentials through their syncytial tissues at 0.27 $cm \cdot s^{-1}$ and some cellular sponges (Demospongiae and Calcareae) undergo coordinated contractions. I am broadly interested in understanding the basis of coordination in these early branching animals for two reasons: 1) To garner insight into the mechanisms by which the first multicellular animals would have sensed and responded to their environment prior to the emergence of the nerves, and 2) by documenting ion channels underlying excitability in sponges, to gain an appreciation of the complement of membrane proteins that might have been available for incorporation into and modification in early neurosensory systems.

5.2 Overview of multifaceted approach

I have taken a multifaceted approach to glean information on both the functional context of coordination in sponges and underlying membrane physiology, since difficulties in maintaining specimens and obtaining tight seals for electrophysiology preclude directly cataloguing and characterizing sponge membrane currents. I began my thesis working with *Rhabdocalyptus dawsoni*, a glass sponge from which action potentials are known (Leys et al., 1999). Flagellar

arrests coincide with propagated action potentials in *R. dawsoni* allowing for immediate cessation of the feeding current. In Chapter 2 I described arrest patterns as a proxy for electrical activity in the sponge and described arrest responses to mechanical and sediment stimuli to provide a context for the coordination system.

I had anticipated then identifying ion channels native to *R. dawsoni* as a next step in understanding membrane physiology in a sponge with stereotypical behaviour. However, my attempts to clone voltage gated potassium channels were unsuccessful in part due to the absence of ion channel sequences on which to base primer design for degenerate PCR. I instead proceeded with cloning ion channels from *Amphimedon queenslandica*, since availability of the genome for this sponge facilitated design of primers specific for ion channels. I prioritized potassium channels for their role in regulating the membrane potential. In Chapter 3 I described the cloning and characterization of *A. queenslandica* inward rectifier potassium channels and speculated on their role *in situ*. Chapter 4 describes the cloning of a second type of potassium channel, the two pore potassium channel. I then bring together sequence information from partial cloning and search and assembly of sequences from the *A. queenslandica* genome to propose a putative complement of ion channels available to regulate membrane potential in the Porifera. I summarize the salient findings of each of these three chapters (2, 3 and 4) in the sections below, and then give suggestions for future research directions.

5.3 Chapter 2 – Physiology of the glass sponge conduction system. Insights from the arrest response

In Chapter 2 I described patterns of feeding current arrests in the glass sponges *Rhabdocalyptus dawsoni* and *Aphrocallistes vastus.* Arrests coincide with the arrival of action potentials within the tissue (Leys et al., 1999) and can be triggered electrically or mechanically, including by sediment in the incurrent water. Since electrical recordings are difficult to obtain, feeding current arrests served as a convenient proxy for electrical activity within the sponge. My finding that sediment triggers arrests is consistent with a protective role wherein feeding cessation prevents excessive sediment uptake. Under continued barrage and with repeated doses, however, sponges were less likely to arrest. By adapting to the repeated stimuli sponges were able to continue to refresh their incurrent water, although pumping level was gradually depressed, presumably by clogging. The distinct arrest-recovery patterns of the two species seemed fitting to their niches. The *R. dawsoni* arrest response was more sensitive and arrests were prolonged, sometimes exceeding 1 hour. Full shut down of pumping could minimize clogging of the sponge tissue following resuspension of sediment by passing fish – a regular occurrence during our *in situ* observations. *A. vastus* however, project into the water column where they are exposed to sediment in ambient currents on an ongoing basis. These sponges arrested in the presence of sediment but resumed pumping immediately, allowing the aquiferous system to be more continuously perfused. In both species return to full pumping level following sediment exposure was marked by repeated arrests with a defined periodicity indicative of

pacemaker activity. Visualization of particulate levels in a flume tank would be needed to determine whether this repeated arrest-recovery pattern helps to relieve clogging.

This work gives a functional context for propagation of electric signals in glass sponges – to stop the feeding current in response to noxious environmental conditions. Comparably, coordinated contractions in cellular sponges are also thought to clear the sponge of sediment (Elliott and Leys, 2007). My work has also highlighted a number of features of the conduction system. These include distinct excitability thresholds; reduced responsiveness to repeated stimuli – a form of adaptation; and mechanosensitivity. Additional work completed by myself and Bob Meech, but not described in this thesis found propagation of feeding current arrests to be highly temperature sensitive with a temperature coefficient (Q_{10}) of 3, where Q_{10} is a measure of how the rate changes over a 10ºC increase in temperature.

The above listed conduction system properties are a reflection of the ionic currents governing membrane physiology. I attempted to clone ion channels from *R. dawsoni* with intentions of correlating channel properties with ionic currents underlying action potentials. I prioritized searching for voltage gated potassium (Kv) channels for their anticipated role in repolarization. Since Kv channels are already diversified into Shaker subfamilies in Cnidarians (Jegla et al., 1995), the most basal animals with a nervous system, Shaker-like sequences were expected in sponges. My attempts to clone homologous channels with degenerate primers, however, were unsuccessful. A survey of the genome of *Amphimedon*

queenslandica for post-synaptic molecules by Sakarya et al. (2007) did not return sequences for voltage gated potassium channels. My searches of the *A. queenslandica* trace files returned several Kv-like sequences, however they were present in lower numbers than expected for a genome sequenced multiple times – raising the possibility that they are from contaminating tissue.

5.4 Chapter 3 - Cloning and characterization of inward rectifier potassium channels

Cloning of K^+ channels progressed with the use of sequences from the *A. queenslandica* genome as bases for primer design. Inward rectifier (Kir) and two pore potassium (K2P) channels were prioritized for their fundamental role of setting the membrane potential and regulating cell excitability (Doupnik et al., 1995; Lesage and Lazdunski, 2000; Lotshaw, 2007; Nichols and Lopatin, 1997; O'Connell et al., 2002). Cloning and functional expression of inward rectifier potassium channels are described in Chapter 3. Phylogenetic comparison of sponge inward rectifiers with those of other metazoans indicates that sponge and metazoan inward rectifiers each arose from individual channels and that diversification occurred independently within the different groups. Nonetheless, expression work showed that AmqKir channels were strongly rectifying, like vertebrate Kir2 and Kir3 channels. Channels of this phenotype are typically expressed in excitable cells where they set the excitation threshold (Oliver et al., 2000). They pass large inward currents, down the potassium electrochemical gradient when the inside of the cell is more negative (hyperpolarized) than equilibrium for potassium (E_k). Driving forces for hyperpolarization in sponge

cells are unknown, however in other metazoans gating of chloride or potassium channels by inhibitory neurotransmitters can lead to hyperpolarization in post-synaptic via Cl^- influx and/or K^+ efflux (Fagg and Foster, 1983). Upon depolarization, intracellular Mg^{2+} and polyamines plug these channels, preventing short-circuiting of action potentials by blocking outward K+ current. Experiments to test the mechanism of block as outlined in Chapter 3 will be required; however, most of the residues involved in polyamine and Mg^{2+} block in vertebrate Kir2 and Kir3 are also found in AmqKir, and polyamines, including spermine and spermidine, occur naturally in sponge cells (Zahn et al., 1981). In situ recordings of AmqKir channels will be needed to determine whether these channels regulate cellular excitability.

5.5 Chapter 4 - Two pore potassium channels and other channels – clues to the potassium channel complement of an early branching metazoan

Two pore potassium channels (Chapter 4) were also cloned. Phylogenetic comparison confirmed published relationships among vertebrate K2P channels, and indicated that homologues of some vertebrate K2P channels are present in invertebrates, however relationships among most invertebrate K2P channels, including those of *A. queenslandica*, were unresolved. Expression was also attempted however currents distinct from those observed in uninjected or water injected oocytes were not observed.

Signal transduction work on the demosponge *Axinella polypoides* indicates the presence of a heat and mechano-gated K channel with properties similar to the vertebrate K2P channel TREK-1 (Zocchi et al., 2001). Activation of

this channel leads to an increase in intracellular Ca^{2+} via a signal transduction pathway and this in turn leads to an increase in filtration and respiration rate (Zocchi et al., 2003). I recommend using AmqK2P sequences as bases for designing primers to amplify K2P channels from *A. polypoides* and then comparing native K2P-like currents with those recording in oocyte expression systems. There is an opportunity to link properties of an individual channel with a defined outcome in whole animal physiology.

The role of K2P currents in the temperature-dependent increase in conduction velocity in *R. dawsoni* should also be explored. Activation of K2P currents with increase in temperature would hyperpolarize the membrane. A plausible explanation for increase in conduction velocity could be the availability of a larger pool of voltage gated calcium channels to depolarize the membrane. Hyperpolarization is known to relieve inactivation on voltage gated calcium channels (Krasznai et al., 2000).

A collection of partial sequences (Chapter 4) also indicate a diversity of potassium channels within *A. queenslandica.* Without cloned cDNA sequences and expression data my conclusions are tentative. However, collectively my results indicate a potassium channel complement that could maintain and regulate the resting potential (Kir and K2P), repolarize the membrane (Ca^{2+}- activated, Na^{+}- activated and potentially voltage gated K^{+} channels), hyperpolarize the membrane after an action potential (Na^{+}-activated K^{+} channels) and correct afterhyperpolarization (Kir and K2P).

Action potentials to date have only been recorded from *R. dawsoni*, where they propagate through syncytial tissues. They are most likely Ca^{2+}-based potentials (Leys et al., 1999). In the absence of Kv channels, which I was unable to amplify, Ca^{2+}-activated K^+ channels (KCa) could repolarize the membrane following increase in intracellular Ca^{2+}. In cellular sponges electrical signalling seems unlikely since there are no known low resistance pathways for passage of current, with the possible exception of cytoplasmic bridges between posterior ciliated cells of some larvae (Maldonado et al., 2003). However, intracellular Ca^{2+} may increase via signal transduction, downstream of mechanical tension or increase in temperature (Zocchi et al., 2001) or activation of metabotropic glutamate (Perovic et al., 1999) or integrin receptors . KCa channels could, again, repolarize the membrane following increase in intracellular Ca^{2+}.

5.6 Directions for future research

Additional attempts to extend sequences by cloning and trace file assembly are required. Moreover, an exhaustive genome search, using representative sequences from all K^+ channel families should be conducted to recover a more complete potassium channel complement of *A. queenslandica.* Once confirmed potassium channel sequences can be compared with those of other metazoans and with outgroup unicellular eukaryotes to provide insight into the collection of molecules that might have mediated coordination in the earliest animals.

Electrophysiological profiles should be determined by expression of channels in heterologous systems and ideally output should be used to inform experiments wherein channel activity is recorded directly in the sponge membrane. Preliminary work by Leys and Degnan (2001) has already implied a role for potassium channels in setting the resting membrane potential in *A. queenslandica* larvae. They found that increasing external K^+ caused a reversible arrest of cilia. When we increased external potassium in our inward rectifier experiments, membrane potential shifted to the new equilibrium for potassium, at more depolarized voltages. Presumably depolarization of the *A. queenslandica* membrane would bring the membrane closer to threshold, possibly leading to influx of Ca^{2+}, which is known to contribute to ciliary arrest in other invertebrates (Walter and Satir, 1978).

In expanding ion channel work, species with well characterized physiology should be considered. This way, downstream effects can more readily be detected. Candidates may include *R. dawsoni*, for which extracellular recording techniques are established and action potential kinetics described (Leys et al., 1999); or *Ephydatia muelleri*, with kinetics of contractions described (Elliott and Leys, 2007). Two pore potassium channels, from *A. polypoides* specifically, should be cloned and characterized as Zocchi et al. (2003; Zocchi et al., 2001) found that intracellular Ca^{2+} and respiration and filtration rates increased downstream of activation of a channel akin to a K2P channel.

Finally, expression patterns of channels can help to identify cells or tissues that might function in signal reception, conduction or response to stimuli. In glass

sponges presumably any region of the syncytial trabecular tissue will depolarize when stimulated, as light touches to any region of the outer body wall elicited flagellar arrests

In cellular sponges various sensory tissues have been suggested. Leys and Elliott (personal communication) have described isolated cells with paired cilia in the osculum of juvenile *E. muelleri.* Since water moves through the relatively narrow osculum at high velocity it makes sense to locate sensors here (Meech, 2007). It is unclear how signals from the sensors would communicate with the contractile apparatus, however nitric oxide synthase has been detected in the pinacoderm (Elliott and Leys, 2010), the tent-like epithelia like covering, indicating a role for nitric oxide in mediating contractions. Western blots performed by Ramoino et al. (2007) showed staining for molecules involved in GABA signalling in the pinacoderm, choanocyte chambers, and scattered archaeocytes. Choanocytes could potentially serve both receptor and effector roles – sensing an environmental change and altering flagellar beat. They are structurally similar to vertebrate mechanosensory cells, leading some authors (Jacobs et al., 2007) to propose that choanocyte-like cells gave rise to eumetazoan sensory cells. Other potential receptor-effector cells include pigmented posterior ciliated cells of *Amphimedon queenslandica* larvae. These cells mediate responses to change in ambient light via abrupt straightening or folding over of cilia.

Expression patterns of post-synaptic genes highlight another cell type in *A. queenslandica* larvae (Sakarya et al., 2007). Five genes identified in the post-synaptic scaffold were labelled in ciliated globular cells, referred to as flask cells,

which are interspersed in the columnar epithelium. Presumably these genes cluster together via identified PDZ binding domains. Additionally, components of the notch-delta signalling pathway for neuronal specification and a homologue of the proneural molecules basic helix loop helix (bHLH) have been detected (Richards et al., 2008).

The globular cells are rich in small vesicles and membranous tubules consistent with a role in synthesis and exocytosis of molecules. The cell apices protrude beyond the margin of the larva and the cilia lack rootlets, suggesting a sensory rather than a locomotory role (Leys and Degnan, 2001; Richards et al., 2008). Richards et al. have suggested that the globular cells are akin to "proto-neural" cells. Conceivably cell apices sense environmental stimuli and then release substances from vesicles to relay information throughout the larva. Such signals could induce a larva to settle, metamorphose, or release substances to mediate attachment to a substrate. Under this scenario an intriguing link between ion channel physiology and organismal behaviour remains to be explored.

The partially cloned *A. queenslandica* sequence designated Amq-tetraKCNG was found to be most similar to an echinoderm tetrameric cyclic nucleotide gated K+ channel. In urchin sperm these channels were opened after egg-derived peptides triggered an increase in endogenous cGMP (Garbers, 1989; Yuen and Garbers, 1992). Channels were highly sensitive, opening upon binding a single molecule of cGMP (Bönigk et al., 2009). Downstream of channel opening, sperm altered their trajectory. Presumably hyperpolarization resulting from channel opening relieve inactivation on voltage gated calcium channels and

resulting calcium influx altered flagellar beat, allowing sperm to track toward nanomolar concentration of egg peptide in the ambient environment (Bönigk et al., 2009; Galindo et al., 2007). Confirmation of a comparable channel and its expression pattern in *A. queenslandica* larvae waits further cloning to extend available sequences. Investigating the role of this channel in larval response to settlement cues represents a potential area of research interfacing between channel biophysics and environmental physiology and providing insight into early mechanisms of coordination.

5.7 References

Bönigk, W., Loogen, A., Seifert, R., Kashikar, N., Klemm, C., Krause, E., Hagen, V., Kremmer, E., Strünker, T. and Kaupp, U. B. (2009). An Atypical CNG Channel Activated by a Single cGMP Molecule Controls Sperm Chemotaxis. *Science Signalling* **2**, ra68.

Doupnik, C. A., Davidson, N. and Lester, H. A. (1995). The inward rectifier potassium channel family. *Current Opinion in Neurobiology* **5,** 268-277.

Elliott, G. R. D. and Leys, S. P. (2007). Coordinated contractions effectively expel water from the aquiferous system of a freshwater sponge. *Journal of Experimental Biology* **210**, 3736-3748.

Elliott, G. R. D. and Leys, S. P. (2010). Evidence for glutamate, GABA and NO in coordinating behaviour in the sponge, *Ephydatia muelleri* (Demospongiae, Spongillidae) *Journal of Experimental Biology* **213**, 2310-2321.

Galindo, B. E., Vega-Beltrán, J. L. d. l., Labarca, P., Vacquierc, V. D. and Darszon, A. (2007). Sp-tetraKCNG: A novel cyclic nucleotide gated K+ channel *Biochemical and Biophysical Research Communications* **354**, 668-675.

Garbers, D. L. (1989). Molecular basis of fertilization. *Annual Review of Biochemistry* **58**, 719–742.

Jacobs, D., Nakanishi, N., Yuan, D., Camara, A., Nichols, S. and Hartenstein, V. (2007). Evolution of sensory structures in basal metazoa. *Integrative and Comparative Biology* **47**, 712–723.

Jegla, T., Grigoriev, N., Gallin, W. J., Salkoff, L. and Andrew N. Spencer. (1995). Multiple *Shaker* potassium channels in a primitive metazoan. *The Journal of Neuroscience* **15**, 7989-7999.

Krasznai, Z., Marian, T., Izumi, i., Damjanovich, S., Balkay, L., Tron, L. and Morisawa, M. (2000). Membrane hyperpolarization removes inactivation of Ca2+ channels, leading to Ca2+ influx and subsequent initiation of sperm motility in the common carp. *Proceeding of the National Academy of Sciences U. S. A.* **97**, 2052-2057.

Lesage, F. and Lazdunski, M. (2000). Molecular and functional properties of two-pore domain potassium channels. *American Journal of Physiology - Renal Physiology* **279**, F793-F801.

Leys, S., Mackie, G. and Meech, R. (1999). Impulse conduction in a sponge. *Journal of Experimental Biology* **202**, 1139-1150.

Leys, S. P. and Degnan, B. M. (2001). Cytological basis of photoresponsive behavior in a sponge larva. *Biological Bulletin* **201**, 323-338.

Lotshaw, D. P. (2007). Biophysical, pharmacological, and functional characteristics of cloned and native mammalian two-pore domain K+ channels. *Cell Biochem Biophys* **47**, 209-256.

Maldonado, M., Durfort, M., McCarthy, D. A. and Young, C. M. (2003). The cellular basis of photobehavior in the tufted parenchymella larva of demosponges. *Marine Biology* **143**, 427–441.

Meech, R. W. (2007). Non-Neural Reflexes: Sponges and the Origins of Behaviour. *Current Biology* **18**, R70-R72.

Nichols, C. G. and Lopatin, A. N. (1997). Inward rectifier potassium channels. *Annual Review of Physiology* **59**, 171-191.

O'Connell, A. D., Morton, M. J. and Hunter, M. (2002). Two-pore domain K+ channels - molecular sensors. *Biochimica et Biophysica Acta* **1566**, 152-161.

Oliver, D., Baukrowitz, T. and Fakler, B. (2000). Polyamines as gating molecules of inward-rectifier K+ channels. *European Journal of Biochemistry* **267**, 5824-5829.

Perovic, S., Krasko, A., Prokic, I., Mueller, I. and Mueller, W. (1999). Origin of neuronal-like receptors in Metazoa: cloning of a metabotropic glutamate/GABA-like receptor from the marine sponge *Geodia cydonium*. *Cell and Tissue Research* **296**, 395-404.

Ramoino, P., Lorenzo, G., Paluzzi, S., Raiteri, L. and al., e. (2007). The GABAergic-like system in the marine demosponge *Chondrilla nucula*. *Microscopy Research Technique* **70**, 944-951.

Richards, G. S., Simionato, E., Perron, M., Adamska, M., Vervoort, M. and Degnan, B. M. (2008). Sponge genes provide new insight into the evolutionary origin of the neurogenic circuit. *Current Biology* **18**, 1156-1161.

Sakarya, O., Armstrong, K. A., Adamska, M., Adamski, M., Wang, I.-F., Tidor, B., Degnan, B. M., Oakley, T. H. and Kosik, K. S. (2007). A post-synaptic scaffold at the origin of the animal kingdom. *PLoS ONE* **6**, 1-9.

Walter, M. F. and Satir, P. (1978). Calcium control of ciliary arrest in mussel gill cells. *Journal of Cell Biology* **79**, 110-120.

Yuen, P. S. and Garbers, D. L. (1992). Guanylyl cyclase-linked receptors. *Annual Review of Neuroscience*

15, 193–225

Zahn, R. K., Zahn, G., Muller, W. E. G., Kurelec, B., Rijavec, M., Batel, R. and Given, R. (1981). Assessing consequences of marine pollution by hydrocarbons using sponges as model organisms. *The Science of the total environment* **20**, 147-169.

Zocchi, E., Basile, G., Cerrano, C., Bavestrello, G., Giovine, M., Bruzzone, S., Guida, L., Carpaneto, A., Magrassi, R. and Usai, C. (2003). ABA- and cADPR-mediated effects on respiration and filtration downstream of the temperature-signaling cascade in sponges. *Journal of Cell Science* **116**, 629-636.

Zocchi, E., Carpaneto, A., Cerrano, C., Bavestrello, G., Giovine, M., Bruzzone, S., Guida, L., Franco, L. and Usai, C. (2001). The temperature-signaling cascade in sponges involves a heat-gated cation channel, abscisic acid and cyclic ADP-ribose. *Proceeding of the National Academy of Sciences* **98,** 14859-14864.

APPENDIX A:

A.1. Summary of attempts to clone sponge voltage gated potassium channel sequences

Degenerate primers were designed against conserved regions in metazoan voltage gated potassium channels. Different primer sets were designed for each of the four families Kv1, Kv2, Kv3 and Kv4. Primer sequences are given in the table below. Combinations of these primers were tested on *Rhabdocalyptus dawsoni* cDNA and aggregate DNA, *Aphrocallistes vastus* DNA and *Ephydatia muelleri* DNA and cDNA. Specific primers were tested on *Amphimedon queenslandica* cDNA..

A putative potassium channel fragment from Rhabdocalyptus dawsoni

A fragment found to be most similar to *Aplysia californica* Kv3 in a tblastx search (NCBI) was amplified from *Rhabdocalyptus dawsoni* cDNA using the following primer combinations below:

1st amplification from cDNA:

Sense primers (designed against Kv T1 region):	**Antisense:**
1819	GeneRacer 3' Race Primer

2nd amplification *(template is 2/40ul dilution of 1st amp):*

Sense primers (designed against S4):	**Antisense (designed against S5-pore-S6):**
1820	1822
1820	1823

(The above two primer sets are overlapping such that the product with the second primer set will be 18 nucleotides longer)

The above primer combinations gave respectively bands labeled b and c in lanes 3 and 5 in the scanned gel below. Lane 1 is a 100 bp standard and lanes 4 and 6 are no template controls.

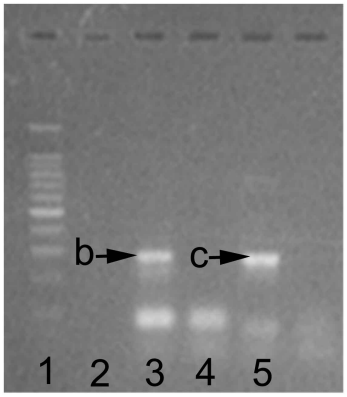

Clean sequence from the above band was 280-300 bp however there appeared to be multiple isoforms. In both an NCBI Blast search and a VKCDB search the sequence came up as a Potassium channel closest to the Shaw channel in *Aplysia.*

Cloning the K channel fragments:
The PCR was replicated and each of the two products b and c cloned into electrocompetent *E. coli* with the TOPO TA cloning kit. Crack PCR was performed on 12 single colonies from each of reactions 'b' and 'c' and the PCR products were sequenced.

Two main sequences were obtained:

b7 *(the only colony with this sequence):*
gnnnncatgatatccaagcgaattctcccttcgagtggttcgagtat
tccgagttttcaagttaaccaggcactcagtgggtcttaagattctc
tggcatactctccacgccagcatgaaagagctgacaattctctcgat
cttcatgtttctgggtgtggtgatcttcgccagtttgatatactacg
cagagaagttgtcagatgattatatggggaaggagggtgaggataaa
tccccgtttattgacataccagtcggattatggtgggcaatagttac
catgactacagtgggctacgaagggcgaattcgtttaaacctgcagg
actagtccctttagtgagggttaata

Gene specific primers 1924 (sense) and 1923 (antisense) were designed to amplify the 168bp portion above highlighted in yellow.

b10 *(several colonies have this sequence):*
cgtagcccactgtagtcatggtaactacagcccaccagaacccg
actgggatatcgataaacgggctcggcgtgtaatccaggctcgt
cttgtccacgtaatattcctcgctcagtttctccgcgtagtaga
tgaggctcgcgaagatgaccacgcccaggaacatgaagatgctt
aagatcatgagctccttcatactcgcgtgtagcgtgtgccagag
gatcttcaggcccaccgagtgtctcgtgaacttcaanactcgga
atactcgaaccactcg

Gene specific primers 1918 (sense) and 1916 (antisense) were designed to amplify the 184 bp fragment highlighted in yellow above.

New primers were designed and priming sites for 2097 & 2098 (b7) and 2099 and are highlighted in pink.

For b7 we expect a 179 bp fragment
For b10 we expect a 198 bp fragment.

Testing for the presence of K channel in Genomic DNA

Gene specific primers for the above clones were tried on genomic DNA. This was done because cDNA made from sponge RNA (extracted from whole sponge) could be contaminated with cDNA from symbionts. The hydroid in the photo below, for example, lives intertwined with the tissue of *R. dawsoni.*Genomic DNA was extracted from 3-day old sponge aggregates (see schematic below), since they are expected to be free of contaminants.

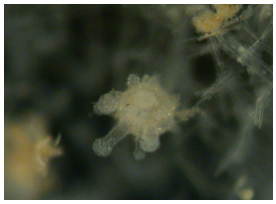

hydroid in *Rhabdocalyptus* tissue

Preparation of aggregates (pure sponge)

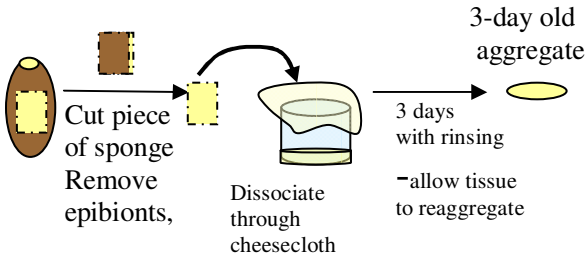

Despite extensive optimization of PCR, genomic dot blots, and genomic southerns **Neither K channel fragment was in aggregate genomic DNA**

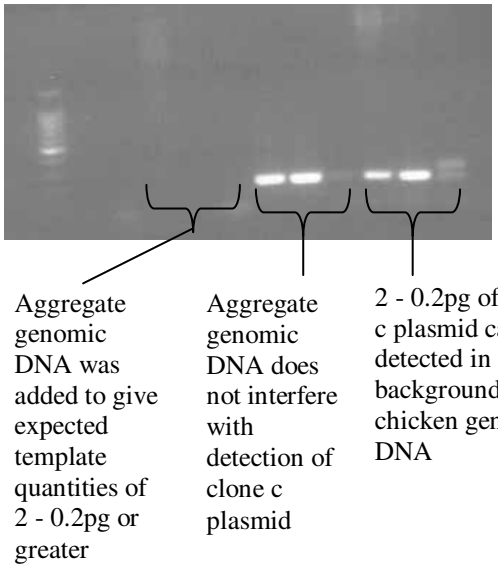

Appendix A.1 Table 1: Sequences of primers used to attempt amplification of sponge voltage gated potassium channels. Degenerate primers were designed to match sequences conserved with metazoan voltage gated channels. Specific primers were designed against putative voltage gated K channel sequences idebtified from *Amphimedon queenslandica* genome trace files.

Primer name	**Sequence 5'-3'**	**Target**	**Direction Sense (S) Antisense (A)**
WJG1819	CGATCCACTGAGGAACGAGTACttyttygwnmg	Kv1 T1	S
aWJG1820	CGAGTGGTTCGAGTATTCCGArtnttyaaryt	KV1 S4	S
WJG1821	AGCCCCTTAGAATGCCGAswnaryttraa	Kv1S4	A
WJG1822	CGTAGCCCACTGTAGTCATGGTAACTayngcccacca	Kv1S5S6	A
WJG1823	CATGGTAACTACAgcccaccaraa	Kv1S5S6	A
WJG1824	GGGGATCGATGAGATATACCTAGAGwsntgytgyca	Kv2 T1	S
WJG1825	ACGAGTCGTTCAGATATTTCGAathatgmgnrt	Kv2 S4	S
WJG1826	CGTGCTAGTTTTAGAATTCGCAGTaynckcatdat	Kv2 S4	A
WJG1827	CGTGATTGTGgcccaccaraa	Kv2 S5S6	A
WJG1828	TGTTGGAGGCATCCGAcaysaracnta	Kv3 T1	S
WJG1829	AAGGGGTATGTGTCATGtggttyacnht	Kv3 S2	S
WJG1830	AAATAAACCGCATTAGGAATTCAadngtraacca	Kv3 S2	A
WJG1831	TCGCCGTACCCTAGCgtngtcatngt	Kv3 S5S6	A
WJG1832	GCATACCACTACTATGGCTCTGTGTytntaytaydt	Kv4 T1	S
WJG1833	CCATACCGGCGGCCwbntggtaytayac	Kv4 S5S6	S
WJG1834	CTTCCCTGCTATGGTTTTTggnacnayrtc	Kv4 S5S6	A
WJG1118	TCGGAATTCTATGACTACTGTTGGNTAYGGNGA	Kv pore	S
WJG1119	ACTTCTAGAGGTAGTGCTATTRYNAGNACNCC	Kv S5S6	A
GJT1	GTNTTYMGNATHTTYAA	Kv1 S4	S
GJT2	TANCCNACNGTNGTCAT	Kv1 S5S6	A
GJT3	ACNACNGCCCACCARAA	Kv1 S4	A
GJT4	TTYMGNATHATGMGNAT	Kv2 S4	S
GJT5	ACNGTNGTCATNGTDAT	Kv2 S5S6	A
GJT6	TTYAARYTNACNMGNCA	Kv3 S4	S
GJT7	GCNCCNACNARCATNCC	Kv3 S5S6	A
GJT8	TTYMGNATHTTYAART	Kv4 S4	S
GJT9	GGNACCATRTCNCCRTA	Kv4 S5S6	A
DADNRVI-F	GAYGCNGAYAAYMGNGTNAT	Putative *A. queenslandica* Kv'	S
ALDEPY-R	TANGGYTCRTCRAANARNGC	"	A
FKL(S/T)RH	TTYAARYTNWSNRGNCAY	"…… "..	S
MTTVGYGD	TCNCCNTANCCNACNGTNGTC	"…… "	A
KvPinv5'	ARISWIGTGATGTAICSIGT	Amq pore region	A inverse
KvPinv3'	TACTGGGCIGTIACIATG	Amq pore region	S inverse
Kinv3-5'	AAAGCTGGGCCTATTTCGAT	AmqKvC RNRPSF	A inverse

Kinv3-3’	TTACCAAAGTGGTGGCAGGT	AmqKvC YQSGGR	S inverse
Kinv4-5’	GGTTCCGGAATAGCGTATCA	AmqKvE DTLFRN	A inverse
Kinv4-3’	TTTTTCGATAGAGATCCCAATGT	AmqKvE FFDRDP N	S inverse
Kinv6-5’	TGCCTGTGGTATGGATGAAA	AmqKvB SSIPQA	A inverse
Kinv6-3’	GACGACTGTGGGATATGGTG	AmqKvB TTYVGY	S inverse
Kinv8-5’	TCGCGATCAAAGAAATATTCA	AmqKvA EYFFDR	A inverse
Kinv8-3’	TCTGTTCTTCAATACCTCAGAACC	AmqKvA SVLYQRT	S inverse

A.2. Primers used to amplify inward rectifier potassium channel sequences from *Amphimedon queenslandica.*

Primer name	Sequence	Description	Tm (ºC)
Kir1F	Xho1 **GGCTCGAGCCACC**ATGGAGCCAGCCCATAAAAAC 5' clamp Kozak consensus sequence	Forward Kir1 primer	68.8
Kir2F	Xho1 **GGCTCGAGCCACC**ATGTCTGTCCAGTTCTCTAATAGC 5' clamp Kozak consensus sequence	Forward Kir2 primer	66.5
Kir1R	SpeI **GGACTAGT**CTAGCAAGAGCAAGGCTCTATG 5' clamp	Reverse Kir1 primer	60.9
Kir2R2	BglII **GGAGATCT**TTACATGTTTGTTCCTTCGC 5' clamp	Reverse Kir2 primer	57.9
T3	ATTAACCCTCACTAAAGGGA	Forward sequencing primer	48
T7	TAATACGACTCACTATAGGG	Reverse sequencing primer	48
GeneRacer™ 5′ Primer	5′-CGACTGGAGCACGAGGACACTGA-3′	Forward primer for 5' RACE	74
Kir1RevGR	GTTGGTTACGGCCACGTAAGCTGAATC	Reverse AmqKirA primer for 5' RACE	61.5
Kir2RevGR	GTACAGTAGGCTGGAAGCTCACTAT	Reverse AmqKirB primer for 5' RACE	57.7
GeneRacer™ 5′ Nested Primer	5′-GGACACTGACATGGACTGAAGGAGTA-3′	Nested forward primer for 5' RACE	78
Kir1RevNGR	AGTACTGTAGTGAAGCCGTCGCTAATG	Nested reverse AmqKirA primer for 5' RACE	59.8

Kir2RevNGR	GCATCTGTAGCTTCTTCTCGAACTGTT	Nested reverse primer for 5' RACE	58.6
Kir1inv5'	GACACTGCTTGCATCAATGTTAAC	Reverse Kir1 primer to amplify 5' end from circularized cDNA	55.0
Kir1inv3'	CACTGAATGACAAGGATTAGTATAC	Forward Kir1 primer to amplify 5' end from circularized cDNA	51.1
Kir2inv5'	GTACAGTAGGCTGGAAGCTCACTATTGTTG	Reverse Kir1 primer to amplify 5' end from circularized cDNA	60.1
Kir2inv3'	GACCAACAGGGAAAAAACGGCTAAAGG	Forward Kir1 primer to amplify 5' end from circularized cDNA	60.2
1174	TGCTTGTTCTTTTTGCAGAAG	Forward pxt7 primer	49

A.3. Metazoan inward rectifier potassium channel protein sequences included in phylogenetic analyses.

>Tcas~Kir2~1~XP~970557
>Tcas~Kir~XP~970630
>Dmel~Kir~CAC87640
>Dpse~Kir~XP~001357041
>Agam~Kir~XP~555705
>Aaeg~Kir~XP~001653741
>Cpip~Kir~EDS26599
>Mmus~Kir7~1~NP~001103697
>Hsap~Kir7~1~BAA28271
>Drer~Kir7~1~BAF03613
>Trub~Kcnj13~AR~SINFRUP00000157298
>Tdub~Kir7~1~BAF73699
>Aque~Kir1~1
>Aque~Kir2~1
>Ajap~Kir~BAA76936
>Xlae~Kir5~1~NP~001079187
>Mmus~Kir5~1~BAA34723
>Hsap~Kir5~1~NP~061128
>Xlae~Kir1~1~NP~001080002
>Ggal~Kir4~2~XP~425554
>Oana~Kir4~2~XP~001509904
>Mmus~Kir4~2~O88932
>Hsap~Kir4~2~NP~002234
>Hsap~Kir4~1~AAB07046
>Mmus~Kir4~1~Q9JM63
>Trub~Kcnj10~1~AR~SINFRUP00000158178
>Trub~Kcnj10~2~AR~SINFRUP00000157232
>Omas~Kir~BAA12009
>Drer~Kir1~1~NP~957329
>Drer~Kcnj1~2~AR~ENSDARP00000032987
>Ggal~Kcnj1~AR~XP~425795
>Mmus~Kir1~1~NP~062633
>Hsap~Kir1~1~NP~000211
>Nvec~Kir~XP~001630074
>Nvec~Kir~XP~001629058
>Nvec~Kir~XP~001634221
>Nvec~Kir~XP~001636991
>Drer~Kir6~2~NP~001012387
>Trub~Kcnj11A~AS~SINFRUP00000142891
>Oana~Kir6~2~XP~001509905
>Mmus~Kir6~2~NP~034732
>Hsap~Kcnj11~AS~NP~000516

>Drer~Kir6~1~NP~001025324
>Ggal~Kcnj8~AS~ENSGALP00000021601
>Hsap~Kir6~1~Q15842
>Mmus~Kir6~1~P97794
>Cele~Irk1~NP~509138
>Cbri~XP~001676969
>Hror~GIRKB~BAB56015
>Csav~ENSCSAVP00000004317
>Cint~GIRKB~G~ci0100132443
>Cint~ENSCINP00000005467
>Cint~ENSCINP00000005450
>Cint~ENSCINP00000005482
>Drer~Kir3~4~XP~690493
>Ggal~KcnjEX~G~ENSGALP00000011203
>Trub~Kcnj3~G~SINFRUP00000142587
>Ggal~Kir3~1~Q90854
>Oana~Kir3~1~XP~001508825
>Mmus~Kir3~1~BAA08079
>Hsap~Kir3~1~AAB42176
>Trub~Kcnj3A2~G~SINFRUP00000145066
>Ggal~Kcnj3A~G~ENSGALP00000016136
>Drer~Kir3~1~XP~698251
>Trub~Kcnj3A1~G~SINFRUP00000161686
>Hror~GIRKA~BAB56014
>Cint~GIRKA~G~ci0100138554
>Csav~ENSCSAVP00000019853
>Trub~Kcnj9~G~SINFRUP00000131396
>Oana~Kir3~3~XP~001516278
>Mmus~Kir3~3~P48543
>Hsap~Kir3~3~AAB07043
>Ggal~Kcnj5~G~ENSGALP00000001788
>Mmus~Kir3~4~AAB01687
>Hsap~Kir3~4~P48544
>Trub~Kcnj6~G~SINFRUP00000131474
>Hsap~Kir3~2~AAC50258
>Mmus~Kir3~2~P48542
>Hror~Kir~BAB78515
>Cint~ENSCINP00000016903
>Csav~ENSCSAVP00000008943
>Mmus~Kir2~4~NP~666075
>Hsap~Kir2~4~NP~037480
>Ggal~Kir2~3~XP~416263
>Hsap~Kir2~3P48050
>Mmus~Kir2~3~P52189
>Omyk~Kir2~2~ABE02698

>Ggal~Kcnj12~ENSGALP00000007506
>Mmus~Kir2~2~P52187
>Hsap~Kir2~2~AAH27982
>Drer~Kir2~1~XP~692193
>Trub~Kcnj2~SINFRUP00000137388
>Xlae~Kir2~1~ABQ44516
>Ggal~Kir2~1~AAB88799
>Mmus~Kir2~1~P35561
>Hsap~Kir2~1~P63252
>Omyk~Kir2~1~ABE02696
>Drer~Kcnj2~ENSDARP00000020190
>Cele~irk~2~NP~508143
>Cbri~Kir~XP~001666945
>Tcas~Kir~XP~974236
>Tcas~Kir~XP~974211
>Tcas~Kir~XP~974184
>Nvit~Kir~XP~001607604
>Amel~Kir~XP~392010
>Dmel~Kir2~1~CAC87637
>Dpse~Kir~XP~001358357
>Aaeg~Kir~EAT39259
>Agam~Kir~XP~321870
>Cpip~Kir~EDS45181
>Aaeg~XP~001653528
>Cpip~Kir~EDS45186
>Amel~Kir~XP~392011
>Nvit~Kir~XP~001607609
>Dmel~Kir~CAC87638
>Dpse~Kir~XP~001357808
>Agam~Kir~XP~321867
>Aaeg~XP~001653529
>Cpip~Kir~EDS45184

A.4. Nucleotide sequences of inward rectifier potassium channels cloned from *Amphimedon queenslandica.*

A.4.1. Nucleotide sequence of AmqKirA

```
   1 atggagccag cccataaaaa cgtcaactat gaattagtat cgaattctaa tgagaatatc
  61 catcgtgatg acgttcccat aacattcaga ggaactcgtg aagcgagaag acgcgagagg
 121 ttagtaaaga ggtccaatgg ccgctcgttg gtgcaccatc acaacatacc gccgctgagc
 181 ttgctggggt acattagcga cggcttcact acagtactta atgcaaggtg gatcgttata
 241 atactgctgt ttgcagctat gtacgtatta tcatggctgc tctttggatt catatggtgg
 301 gggattgatt cagcttacgt ggccgtaacc aactcatctt gcgtttctaa tatcgatgga
 361 ttctcagcat ctttcctgtt ctcaatagag actcaggtaa caattgggta cgggtatcgc
 421 tttgtcgcag acgactgctc ctttggtata ctaatccttg tcattcagtg tttggttggg
 481 ctcgttatag actcattcct actgggtctg atattcgcta aaatcaccag acccaggaac
 541 aggcgtaaga cgatcctctt cagtgacact gcttgcatca atgttaacaa taaaggagag
 601 aagaggcttc agtttcgtat tggtgatgtt aggagcagat catcgctagt ggaggcacac
 661 gtacgtgtac aactatactg gaatagaaaa gatggggaga ctgatgaata caggttggaa
 721 cagaatgact tggaagttgg ctatgatagt ggcactgatc gcattatatt attaacccca
 781 gtggtaataa cacacattat aaaggagaca agccctcttt atacagtaac aaatgatagc
 841 atattaaatg aagacattga gattgtcatt atactggaag ccattgtgga gagtactggc
 901 ctaactgcac aagctctatg gtcttacact gagagagaaa tattgttcaa ttacaaattt
 961 aaacctatga tatacagaca gagtgatgcc aaaggtactt gggaagtgga ttttaataga
1021 cttagctcca tagagccttg ctcttgctag
```

A.4.2. Nucleotide sequence of AmqKirB

```
   1 atgtctgtcc agttctctaa tagctatgaa aaaatctctg aaaccgaagg aacagttcga
  61 gaagaagcta cagatgcagc tccaacaata gtgagcttcc agcctactgt accaacaagg
 121 ctaaggccag agagactagt gaaaaggtct actgctcgct ctatcttgca ccacaagaat
 181 atcccaccac ttagctggtt agcatacgtt agtgacggat ttactacatt gataaatgca
 241 gagtggtaca ttataattgg gttattctca gctgtgtatc tctcatcgtg gctcctgttt
 301 actttcatgt ggtggtcgtt tgatgcagcc tatgtatctg ttacaaacaa ttcttgcatt
 361 gaaaatgttg gaggattctc ttcatcgttt ctcttctcat tagagacaca agtaaccatt
 421 ggctatgggc accgatacat acagagcacc tgtcactttg gcatatttct acttgtggtg
 481 caaagtctta taggactctt tatcgattcg ttcctactgg gtctgatatt tgctaaaatc
 541 tccagaccca gaaacagacg caagacgatc cttttcagtg acattgcttg cattaatgtt
 601 aatgctaaag gggagaggtg cctccagttc cgtgtagctg atgtcaggaa aaattcatca
 661 ctagtggagg cacacgtacg tgtacaactg tactggcata aaaaagatgg tgccactgat
 721 gaatacaggt tggaacagaa tgacttggaa gttggctatg atagtggtac tgatcgtatc
 781 atattattaa ccccagtggt aataacacac attataaagg agacaagccc tctttatgca
 841 gtaactaatg atagcatatt aaatgaagac attgagattg tcattatact ggaagccatt
 901 gtggagagta ctggcctaac tgcacaagct ctatggtcct acactgagag agaaatattg
 961 tttgggcgaa aatttatacc aatgaccaac agggaaaaaa cggctaaagg aacgtgggaa
1021 gtggatttca aaaagctgag cgatgttgtg accagcgaag gaacaaacat gtaa
```

APPENDIX B:

B.1. List of sequences used to search *Amphimedon queenslandica* genome trace files for putative potassium channel sequences.

Sequences were compiled from the Voltage Gated Potassium channel database (VKCDB). VKCDB index numbers and GenBank protein ID numbers are given for each sequence.

VKCDB index	GenBank Protein ID	Description
VKC139	987509	potassium channel homolog [Polyorchis penicillatus].
VKC140	987511	potassium channel homolog [Polyorchis penicillatus].
VKC239	1763619	potassium channel alpha subunit [Polyorchis penicillatus].
VKC285	1763617	potassium channel gamma subunit [Polyorchis penicillatus].
VKC123	510098	potassium channel protein [Schistosoma mansoni]
	29373793	potassium channel Kv3.1 [Notoplana atomata]
	29373795	potassium channel Kv3.2 [Notoplana atomata]
VKC472	3415130	shaker related delayed rectifier potassium channel [Haemopis marmorata].
VKC138	3387822	voltage-gated potassium-channel LKv1; delayed rectifier potassium channel [Hirudo medicinalis].
VKC200	2133555	shaw protein - California spiny lobster [Panulirus interruptus].
VKC205	14190059	potassium channel protein Shal 1.i [Panulirus interruptus].
VKC206	14190051	potassium channel protein Shal 1.e [Panulirus interruptus].
VKC208	14190049	potassium channel protein Shal 1.d [Panulirus interruptus].
VKC209	14190045	potassium channel protein Shal 1.b [Panulirus interruptus].
VKC210	13929491	shal 1 potassium channel [Panulirus interruptus].
VKC211	14190057	potassium channel protein Shal 1.h [Panulirus interruptus].
VKC212	1587846	shal gene [Panulirus interruptus].
VKC213	14190053	potassium channel protein Shal 1.f [Panulirus interruptus].
VKC214	14190055	potassium channel protein Shal 1.g [Panulirus interruptus].
VKC216	14190047	potassium channel protein Shal 1.c [Panulirus interruptus].
VKC277	2959686	potassium channel [Panulirus interruptus].
VKC284	499659	K+ channel protein [Panulirus interruptus].
VKC97	2959684	potassium channel [Panulirus interruptus].
VKC407	29470162	voltage-gated K channel [Limulus polyphemus].
VKC103	85111	potassium channel protein A (clone Sh-beta) - fruit fly (Drosophila melanogaster).
VKC104	85242	potassium channel shaker form epsilon - fruit fly (Drosophila melanogaster).
VKC106	85110	potassium channel protein A (clone Sh-alpha) - fruit fly (Drosophila melanogaster).
VKC107	85115	potassium channel protein A (clone ShC1) - fruit fly (Drosophila melanogaster).
VKC131	85112	potassium channel protein A (clone Sh-delta) - fruit fly (Drosophila melanogaster).
VKC132	85113	potassium channel protein A (clone Sh-epsilon) - fruit fly (Drosophila melanogaster).
VKC186	103308	potassium channel protein shaw2 - fruit fly (Drosophila melanogaster).
VKC207	158459	Shab11 protein (Drosophila melanogaster).
VKC21	13432103	Potassium voltage-gated channel protein Shaker (Drosophila melanogaster).
VKC223	103386	potassium channel protein shab11 - fruit fly (Drosophila melanogaster).
VKC224	103307	potassium channel protein shab11 - fruit fly (Drosophila melanogaster).
VKC25	116444	Potassium voltage-gated channel protein Shaw (Shaw2) (Drosophila melanogaster).
VKC26	116443	Potassium voltage-gated channel protein Shal (Shal2) (Drosophila melanogaster).

VKC27	17380406	Potassium voltage-gated channel protein Shab (Drosophila melanogaster).
VKC153	2218158	voltage-dependent potassium channel alpha subunit [Caenorhabditis elegans].
VKC167	17563264	SHaW family of potassium channels (shw-3) [Caenorhabditis elegans].
VKC331	31249890	K (potassium) voltage-gated sensory channel subunit protein 1, isoform a [Caenorhabditis elegans].
VKC332	25147276	K (potassium) Voltage-gated Sensory channel subunit (kvs-1) [Caenorhabditis elegans].
VKC333	17560924	potassium voltage-gated channel subfamily B member 2 (5J797) [Caenorhabditis elegans].
VKC219	3219511	Shaw potassium channel Kv3.1a [Aplysia californica].
VKC268	688438	noninactivating potassium channel [Aplysia californica].
VKC99	155764	potassium channel [Aplysia californica].
VKC164	7321945	action potential broadening potassium channel [Aplysia sp.].
VKC149	2315214	Kv2 voltage-gated potassium channel [Loligo pealei].
VKC117	1245451	voltage-dependent potassium channel SqKv1A [Loligo opalescens].
VKC113	4996280	TuKvI [Halocynthia roretzi].
VKC230	4519932	Kv2 channel alpha-subunit [Halocynthia roretzi].
VKC420	27530018	Kv4 class voltage-gated potassium channel full-length isoform [Halocynthia roretzi].
VKC421	27530020	Kv4 class voltage-gated potassium channel C-terminus truncated isoform [Halocynthia roretzi].
VKC12	116431	Potassium voltage-gated channel subfamily A member 4 (Potassium channel Kv1.4) (RCK4) (RHK1) (RK4).
VKC15	116433	Potassium voltage-gated channel subfamily A member 5 (Potassium channel Kv1.5) (RCK7).
VKC168	2815400	Kv4.3 [Rattus norvegicus].
VKC169	1658483	Kv4.3 potassium channel [Rattus norvegicus].
VKC170	1050332	voltage-gated K+ channel.
VKC180	13929040	potassium voltage gated channel, Shal-related family, member 3 [Rattus norvegicus].
VKC182	12751419	transient voltage dependent potassium channel Kv4.3 long form [Rattus norvegicus].
VKC19	116435	Potassium voltage-gated channel subfamily A member 6 (Potassium channel Kv1.6) (RCK2) (Kv2).
VKC194	92954	voltage-sensitive potassium channel protein [validated] - rat.
VKC197	13929026	potassium channel Kv4.2 [Rattus norvegicus].
VKC24	24418849	Potassium voltage-gated channel subfamily B member 1 (Potassium channel Kv2.1) (DRK1).
VKC247	112304	potassium channel protein IIIA form 1, shaker-type - rat.
VKC248	112166	potassium channel protein - rat.
VKC249	285134	voltage-gated potassium channel protein Raw1 - rat.
VKC266	16758906	potassium voltage gated channel, Shaw-related subfamily, member 3 [Rattus norvegicus].
VKC272	31543041	potassium voltage-gated channel, delayed-rectifier, subfamily S, member 3 [Rattus norvegicus].
VKC28	24418850	Potassium voltage-gated channel subfamily B member 2 (Potassium channel Kv2.2) (CDRK).
VKC3	27465523	Potassium voltage-gated channel subfamily A member 1 (Potassium channel Kv1.1) (IA) (RBKI) (RCK1).
VKC30	116439	Potassium voltage-gated channel subfamily C member 1 (Potassium channel Kv3.1) (Kv4) (NGK2) (RAW2).
VKC33	3023483	Potassium voltage-gated channel subfamily C member 4 (Potassium channel Kv3.4) (Raw3).
VKC36	116440	Potassium voltage-gated channel subfamily C member 2 (Potassium channel Kv3.2) (KSHIIIA).

VKC38	3023480	Potassium voltage-gated channel subfamily C member 3 (Potassium channel Kv3.3) (KSHIIID).
VKC56	25742772	potassium voltage-gated channel, shaker-related subfamily, member 2 [Rattus norvegicus].
VKC6	116428	Potassium voltage-gated channel subfamily A member 3 (Potassium channel Kv1.3) (RGK5) (RCK3) (KV3).
VKC72	112170	potassium channel KV1.3 - rat.
VKC76	206635	voltage-gated potassium channel protein.
VKC82	6981116	potassium voltage-gated channel, shaker-related subfamily, member 4 [Rattus norvegicus].
VKC95	92635	potassium channel KV1.6 - rat.

B.2. Predicted sequences of putative potassium channels compiled by Onur Sakarya and Ken Kosik, University of California at Santa Barbara.

Yellow highlighting represents sequences that I independently recovered through blast searches of the *A. queenslandica* trace files. Names for sequences were assigned by the Kosik lab based on results of similarity searches but affiliations were not necessarily tested by phylogenetic analysis.

B.2.1. Inward rectifier potassium channel sequences

Predicted inward rectifier potassium channel nucleotide sequences
These predicted sequences was used to design primers to clone AmqKirA (SubJ_Kir1) and AmqKirB (SubJ_Kir2) (Chapter 3). Bases which differed from the cloned sequences are underlined.

Sponge_SubJ_Kir1
ATGGAGCCAGCCCATAAAAACGTCAACTATGAATTAGTATCGAATTCTAATGAGAATATC
CATCGTGATGACGTTCCCATAACATTCAGAGGAACTCGTGAAGCGAGAAGACGCGAGAGG
TTAGTAAAGAGGTCCAATGGCCGCTCGTTGGTGCACCATCACAACATACCGCCGCTGAGC
TTGCTGGGGTACATTAGCGACGGCTTCACTACAGTACTTAATGCAAGGTGGATCGTTATA
ATACTGCTGTTTGCAGCTATGTACGTATTATCATGGCTGCTCTTTGGATTCATATGGTGG
GGGATTGATTCAGCTTACGTGGCCGTAACCAACTCATCTTGCGTTTCTAATATCGATGGA
TTCTCAGCATCTTTCCTGTTCTCAATAGAGACTCAGGTAACAATTGGGTACGGGTATCG**T**
TTTGTCGCAGACGACTGCTCCTTTGGTATACTAATCCTTGTCATTCAGTGTTTGGTTGGG
CTCGTTATAGACTCATTCCTACTGGGTCTGATATTCGCTAAAATCACCAGACCCAGGAAC
AGGCGTAAGACGATCCTCTTCAGTGACACTGCTTGCATCAATGTTAACAATAAAGGAGAG
AAGAGGCTTCAGTTTCG**C**ATTGGTGATGTTAGGAGCAGATCATCGCTAGTGGAGGCACA**T**
GTACGTGTACAACTATACTGGAATAGAAAAGATGGGGAGACTGATGAATACAGGTTGGAA
CAGAATGACTTGGAAGTTGGCTATGATAGTGGCACTGATCGCATTATATTATTAACCCCA
GTGGTAATAACACACATTATAAAGGAGACAAGCCCTCTTTATAC**A**ATAACAAATGATAGC
ATATTAAATGAAGACATTGAGATTGT**G**ATTATA**T**TGGAAGCCATTGTGGAGAGTACTGGC
CTAACTGCACAAGCTCTATGGTCTTACACTGAGAGAGAAATATTGTT**T**AATTACAAATTT
AAACCTATGATATACAGACAGAGTGATGCCAAAGGTACTTGGGAAGTGGATTTTAATAGG
CTTAGCTCCATAGAGCCTTGCTCTTGCTAG

Sponge_SubJ_Kir2
ATGTCTGTCCAGTTCTCTAATAGCTATGAAAAAAT**G**TCTGAAACCGAAGGAACAGTTCGA
GAAGAAGCTACAGATGC**T**GCTCCAACAATAGTGAGCTTCCAGCCTACTGTACCAACAAGG
CT**T**AGGCCAGAGAG**G**CTAGT**A**AAAAGGTCTACTGCTCGCT**C**CATCTTGCACCACAAGAAT
ATCCCACCACTTAGCTGGTTAGCATACGTTAGTGACGG**C**TTTACTACA**C**TGATAAATGCA
GAGTGGTACATTATAATTGGGTTATTCTCAGCTGTGTATCTCTCATC**A**TGGCTCCTGTTT
ACTTTCATGTGGTGGTCGTTTGATGCAGCCTATGTATCTGTTAC**C**AACAATTC**C**TGCATT
GAAAATGTTGGAGGATTCTCTTCATCGTTTCTCTTCTCATTAGAGACACAAGTAACCATT
GG**A**TATGGGCACCGATACATACAGAGCACCTGTCACTTTGGCATATTTCTACTTGTGGTG
CAAAGTCTTATAGGACTCTTTATCGATTCGTTCCTACTGGGTCTGATATTTGCTAAAATC
TCCAGACCCAGAAACAGACGCAAGACGATCCT**C**TTCAGTGACATTGCTTGCATTAATGTT
AATGCTAAAGGGGAGAGGTGCCTCCAGTTCCGTGTAGCTGATGTCAGGAAAAATTCATCA
CTAGT**A**GAA**A**GCACA**T**GTACGTGTACAACTGTACTGGCATAAAAAAGATGGTGC**T**ACTGAT
GAATACAGGTTGGAACAGAATGACTTGGAAGTTGGCTATGATAGTGGTACTGATCGTATC
ATATTATTAACCCCAGTGGTAATAACACACATTATAAAGGAGACAAGCCCTCTTTATGCA
GTAACTAATGATAGCATATTAAATGAAGACATTGAGATTGTCATTATACTGGAAGCCATT
GTGGAGAGTACTGGCCTAACTGCACAAGCTCTATGGTCCTACACTGAGAGAGAAATATTG
TTTGGGCGAAAATTTATACCAATGACCAACAGGGAAAAAACGGCTAAAGGAACGTGGGAA

GTGGATTTCAAAAAGCTGAGCGATGTTGTGACCAGCGAAGGAACAAACATGTAA

Predicted inward rectifier potassium channel amino acid sequences
Differences between predicted and cloned sequences are indicated as, for example, (SubJ_Kir1/AmqKirA).

Sponge_SubJ_Kir1
MEPAHKNVNYELVSNSNENIHRDDVPITFRGTREARRRERLVKRSNGRSLVHHHNIPPLS
LLGYISDGFTTVLNARWIVIILLFAAMYVLSWLLFGFIWWGIDSAYVAVTNSSCVSNIDG
FSASFLFSIETQVTIGYGYRFVADDCSFGILILVIQCLVGLVIDSFLLGLIFAKITRPRN
RRKTILFSDTACINVNNKGEKRLQFRIGDVRSRSSLVEAHVRVQLYWNRKDGETDEYRLE
QNDLEVGYDSGTDRIILLTPVVITHIIKETSPLYT(**I/V**)TNDSILNEDIEIVIILEAIVESTG
LTAQALWSYTEREILFNYKFKPMIYRQSDAKGTWEVDFNRLSSIEPCSC

Sponge_SubJ_Kir2
MSVQFSNSYEK(**M/I**)SETEGTVREEATDAAPTIVSFQPTVPTRLRPERLVKRSTARSILHHKN
IPPLSWLAYVSDGFTTLINAEWYIIIGLFSAVYLSSWLLFTFMWWSFDAAYVSVTNNSCI
ENVGGFSSSFLFSLETQVTIGYGHRYIQSTCHFGIFLLVVQSLIGLFIDSFLLGLIFAKI
SRPRNRRKTILFSDIACINVNAKGERCLQFRVADVRKNSSLVEAHVRVQLYWHKKDGATD
EYRLEQNDLEVGYDSGTDRIILLTPVVITHIIKETSPLYAVTNDSILNEDIEIVIILEAI
VESTGLTAQALWSYTEREILFGRKFIPMTNREKTAKGTWEVDFKKLSDVVTSEGTNM

B.2.2. Two pore potassium channels

Predicted two pore potassium channel nucleotide sequences
These predicted sequences was used to design primers to clone AmqK2PA and AmqK2PB. Bases which differed from the cloned sequences are underlined.

Sponge_SubK_K2p
ATGGAGAAAGAGGTCGAGTCAGAAATTCCTGCTGTTGCTAGCGATAGAGAGGACAGCGAG
AGTCGTGAGCTAACAGAAAAGCCACAAGAAGACACAGCAGAGGATGAAGAGCCAGAGGAT
ACTGGGTTTGAGTGTTCCAGGGCCTACTTCACCCGCTTATTCTGTAACCTGAACATCTAC
AACCAAGCCTTCATCCTATTTGCTCTTGTAATGACATACATACTCGTTGGTGGTGCCATA
TTTCTAGCCTTTGAGCTACCGGCAGAGACAAAACGAAATGAGGCCATAACAGCAGCCAAT
GAAACATACATTAGGGCCTTCAACAATATAGTGGATCAACTGGTGAACTTTACCAACCTA
ACAGAAGAGGAGGCTATGGCTTTAGTAAGGAGGGTAGCACAGTCAGCCATTGATGCATCA
AACAATCAGCCGACTAACAACTGGGAGTATGGATCGGCTATCTTCTTTGCCACAACTGTT
ATTACAACAATCGGTTATGGTTCCATTGCTCCTGAGACTGATGGTGGACGTGGTTTCTTC
ATACCCTATGCACTGGTTGGTATACCCCTCACTTTGATATTCCTTGGGTTCTTGGGACAA
GTACTTAACAAAGGAGTCGACCGAGCCACAAGATGTCTCAGAAGACGAGTTACGTTTGAT
TGGGGACAAATATTGGTCGTATTTACCATCGGATTGGTGAGCTTCATCTTCATACCTGCT
ATTATATTCGCTATCATTGATGACTGGACCTACTTTGAAGCAGTTTATTTCACTTTTGTG
TCTCTCACTACAGTCGGTTTCGGTGATTTTGTTCCATCTGCCCCAAAGACATTCCGTGGG
CTCTATCGGTTTAGTCTTATCTGTTGGTTGTTCCTTGGACTTGCATTCATAGCCCTCATC
ATTGCCCAGACACAGGAACGGATTGAGAATGTGAGAAAGAGTGTTAAGAAATGCAGAAAA
TGCATAAAGAGAACAGGAGGAAAGCTCATGCTGAGGAAAAAGAACAAAGAAAGTAGCAAA
GATAATGAAAAAACAGAAGAGACTGAAGTAGAGAAGGAGTGA

Predicted two pore potassium channel amino acid sequence
Amino acid differences from cloned sequences are indicated as (SubK_K2p/AmqK2PA/AmqK2PB)

Sponge_SubK_K2p

MEKEVESEIPAVASDREDSESRELTEKPQEDTAEDEEPEDTGFECSRAYFTRLFCNLNIY
NQAFILFALVMTYILVGGAIFLAFELPAETKRNEAITAANETYIRAFNNIVDQLVNFTNL
TEEEAMALVRRVAQSAIDASNNQPTNNWEYGSAIFFATTVITTIGYGSIAPETDGGRGFF
IPYALVGIPLTLIFLGFLGQVLNKGVDRATRCLRRRVTFDWGQILVVFTIGLVSFIFIPA
IIFAIIDDWTYFEAVYFTFVSLTTVGFGDFVPSAPKTFRGLYRFSLICWLFLGLAFIALI
IAQTQERIENVRKSVKKCRKCIKRTGGKLMLRKKNKESSKDNEKTEETEVEKE

B.2.3. Putative potassium selective cyclic nucleotide gated channel

Predicted nucleotide sequences

Portions of this sequence were cloned using primers designed against the italicized regions. The underlined sequence was cloned and sequenced. Yellow highlighting indicates areas where sequences I independently assembled from the *A. queenslandica* trace files match the predicted sequence.

Sponge_SubH_Kv – redesignated Amq-tetraKCNGA

ATGAATAACATTGGATACTCCTCCTCTTCAGTCATTCATAACTACATATTATCACTATAC
TGGTCAACAACCACAACCACACTAGTTGGATATGGTGACATTGTACCAGTGAATAATGAT
GAGAGGGTATTAGCAATATGTGTCATGCTACTGGGTATTTGGTGCTATGGGTACATGCTG
GGATCTGCAGCTGCTATCATCACTCATACACTACAACCTAGGATATTTCTTGAATTGGAA
AAAGATGATGATATTTTATCACAATTACTGCACTCCTTCGCCATAGAAAGACTACCACCA
CAGACTAAGAGAATGTCACTAGAAGAAGAAGAAGATTATGTAGCTCATCACTCATTCAAG
AAAGAATACTCAATAGTTGCTGGTCTTGCTGCTGCAATGGTCCCTGCTCTAGCTATAGCT
ACTCCTCGACAGTCACCTCCATTAGTCAATGCTGCACTGTCTTCTGTTGGGCCTAAAGAA
ATGCAATCACAACTAACACCACCTACTCTACTTGATTACTCTCTTAGTGCCAATAATAAG
AAAAGGAAAGACTCTATCAGGCAATATAGTACAAGTGCTATCAGGTATTCCAATAGAGAG
GGGTCTGATGATCCTGCAGTTAGTATACAAGTTAGTAGCTCATTCAGTGTTCAGTATA***TG***
AATTCCCTCTACTGGTCCGTAGCAACAACTGCTTCTGTTGGATATGGCGACATTACTCCT
CATAGAAGTCTTGAG___56 bp intervening sequence in partially cloned sequence and trace files
CGTTTGTATGCAATATGTTTTGAGGTGTTTGGTGTCCTCTTCTATGGCCTGATAGTAGCCT
ATTTCACTGCTAGTTTGGTTAATGATGACATTGGGAGAGCTCAGTATCAAGATAAACTGG
AAATGATTAAGAAATATCTGAAAGAACACAAAGTTGACGGCATCCTAAAGAACAGAGTA
ATAAAGTCA___389 bo intervening sequence in partially cloned sequence (matches final 224 bp of clones
BAYB232386.b1 and BAYA65925.y1) ATGTATTTTATAAGTCAAGGATCAGTTGAGATT
ATTAGTAATGATGGTCATGAAGGTACTAGGCTGACTGTGTTGGACGAGGGAAAGTTCTTTGGA
GAAATAAGTTTGGT***CTTTGATTGCAGCAGAACAGC***ATCTGTGAGGACTCTCAGTAATTGT
GATCTATTTGTGTTAAGTAAATCTGATTTTGAATCAGCTCTTGATAAATATCAGGATGTT
GCTGATCAGATCAAAGTTGTTGCTCTTCAAAGAGCTACTCTCTCAGTTCTGACTGACATG
GTTGTGAATGAATCGTTAGCTAAAGGAAAGACCAAAGATGAAACTATTGAATCAATCTTT
GAAGTAAGTATAATTCTAATTATATTTAAAAATCTTACAGCTGCTGATTCTGATACAACC
CGTTACATCACTAGTT_60 bp intervening sequence in trace files_____ACACTGAGAAACTTT
ATGCAATTTTAATAATGATATTTGGGAAACTGTTCTATGGGTTTCTATTGGGGAGTGTTGC
TTCGATGCTTGCTAATAGGAAAAAGAGACAAGTCATGTTTATGAACAAACTGGACTCCAT
CAAAG____78 bp intervening_sequence in trace files_____ATTATGTTGTTGCTGCTGATGTC
TCAGTTCCACTAGAGCGTAAAGTAATTCATCACTGCAATCACCATTGGTTGGAGTCCAAA
GGTATTGACAGGCAGACACTGTTTGATGACACTCCTTATTGTCTCCAATCGGAAATTGCT
CTAGCCACAACACAGAAATTACTCCAAATGGTGGAAAAATTGTTGGAAGAAGGCCGTCAG
TCAGCTGCTGATCCTCATTCTAGTTCCTTGGCACCATTGTCTACCATCTTAAGCTGA

Predicted amino acid sequence

Sponge_SubH_Kv (Amq-tetraKCNGA)

MNNIGYSSSSVIHNYILSLYWSTTTTTLVGYGDIVPVNNDERVLAICVMLLGIWCYGYML
GSAAAIITHTLQPRIFLELEKDDDILSQLLHSFAIERLPPQTKRMSLEEEEDYVAHHSFK

KEYSIVAGLAAAMVPALAIATPRQSPPLVNAALSSVGPKEMQSQLTPPTLLDYSLSANNK
KRKDSIRQYSTSAIRYSNREGSDDPAVSIQVSSSFSVQYMNSLYWSVATTASVGYGDITP
HRSLERLYAICFEVFGVLFYGLIVAYFTASLVNDDIGRAQYQDKLEMIKKYLKEHKVDGI
LKNRVIKSMYFISQGSVEIISNDGHEGTRLTVLDEGKFFGEISLVFDCSRTASVRTLSNC
DLFVLSKSDFESALDKYQDVADQIKVVALQRATLSVLTDMVVNESLAKGKTKDETIESIF
EVSIILIIFKNLTAADSDTTRYITSLYWAVTTMTTVGYGDIVPQNYTEKLYAILIMIFGK
LFYGFLLGSVASMLANRKKRQVMFMNKLDSIKDYVVAADVSVPLERKVIHHCNHHWLESK
GIDRQTLFDDTPYCLQSEIALATTQKLLQMVEKLLEEGRQSAADPHSSSLAPLSTILS

B.2.4. Putative sodium-activated potassium channel

Predicted nucleotide sequences

Yellow highlighting indicates areas where sequences I independently assembled from the *A. queenslandica* trace files match the predicted sequence.

Sponge_SubT_Kca, redesignated AmqNaA

ATGGCAGACAGAGTAGAGCACCGAATTTCTCAGCAGCACTCTCTCCCAAACTCTCCTCTC
CTTAGGAAGAGGAAGAAGATACGGAGACGGTCCCGTCCTGAGGTGTACGATCAGTCAGCA
CCTGTTCCTGCCTCTCCATCCCTCACTTCCTTGAGCTGTTCCTCCAGCGACAGCGAATGT
GAGAGCAATAGAGAAGAAGAAGAGGACCCTCTGCCTGACAAAGACGGCCAGTCAGTCACA
GTTAAACAAGCCCTGGAAGGTCTATTTTATAACAAAGCTGTCCAACTGGTTCACCACCAT
GAACTCATTATCGTAAAGCGATATTCCCATGGAAAGACATTTGGACAAAGGCTTGCGTAT
GTCCTGTATAAACATCCAAAAACACGTCTCATTGCACATTTTGGCGCACTTTTATTGAAC
ATTATCAGCTGCATCCTCTACGTTGCTGAAGCTATATATATCGATAGATTACTGAAAAGT
GCTGATGAAGAGGAGTTTATACTGGGCTGCTTCAACCAGACATGGGTGAACATAACGGAG
CCTTCTTATCTGTGTCTCATTCATCATTTTGAGCGGCTGGGTAAAAAGATATCTCTGTTT
GATACCTACTGGTTTGTGGTCGTCACCTTCAGTACGGTCGGGTATGGGGACATTAGCCCC
GCCCACTGGACTGGGAAGGTCATTATAACGATATTCATAATAGCGGCTTTGATGTACCTC
CCACCTAAGGTGAGCCACACCCTCTTCACTTGT__intervening 57 bp in trace file sequences___
CACTACAAGCAGTACAACAAAGCTAACATCACTAAGCACGTGGTACTAGCAGCTGTGGAT
CTCAAACCGCTGGTACTGAGGGACTTCCTCAGTGAACTCTACTCCGACCCTGGACAAATGG
__intervening 59 bp sequence in trace files__ATACTCAAGTTGTTGTTCTTATTAAAGAAGAACCTG
CCGATTATATTAAAGCCATTCTATTGCACCCGATATGGTCCCAGAGGGTAGCCATATTGAG
AGGAACTGCTTTGAGACCAAGCGACCTAGCAAGAGTCAAGGGCCGTCGG
TTCAATATTCCGGAGTACAAGAGATATGAGGAGTGCTCACCGGTTGAGATATACCACGTG
AAACTCGGAGAGAGCAGATACTTTCATCGTTTCGCTGGAAAGAACTTTTTATTCACTTCT
GTAGTAGCTTATAGAAAGTTCCACGTCCTCTTGTTAGGGATATGTCCGTCAGGTGGTACT
GATATATTGTTCAACCCTGGGATCAACCACATTATGGATCGTAATGATGAGTGTTACTAC
ATTAGCGACACTCATGAGCATAACTCCGACCATCAGATCATACCTGCTAGCACCTTCCAG
TCCAGTTTATGGAGGACATCAGCTACTCTCGGTCTACTGGCCATGTACATATCTGGTATT
GATCCAGACCAGATGTTCCACCAGACCCAGGAGTATGAGGAGAGGGACTCCGACAACAAG
GGGGGGTTTCCTCGCTCAGCATCCAACGACAGACTCAAGAAGTTGTCATCACCTGATTCT
ATTCCTGAGATACAAGTGGAAGGTGTGGCCAGTGGTGTCTCGTTAACTGAGGAGACGAGG
CTACCATCAATTGGAGAGGAGGAGGAGGTACTTGATGAGCAACTAGCGGTTGAAGTTACG
AACTGGCAGCATGACGTACAACATGGTCTCCAGTTATTGAAGTATCATGGGGAGGGGGAA
CTACCCGAGAGGAAACCATGTGTGAAGCTTTCAGTGAAGAGCCATTTTGAAGGTCACCAT
TCACCACGGTCCCATTCACTACCACTGGCAGCTACTACTTGTACAGTAATGGAGCCACAC
CCCCTGGCACACCCCCTACCATCGCTAGGAGTGATACCGGAGGATGAACCTGATGTGATT
GTGATTGGAGAGGAAGAGCCACACCTCCTGCCCCACCTCCAGAGAGTAGGGGATAAGCAG
CATAGCTCAGGGGGAGGGGTAGGGAAGCACAGGGTTCATAGTCAGCCGGCTTTGTTTCAC
TTTGGATTCAACAAGAGACAGTCGGAGCCTAAACATGACGATCACCTCCTCAAAGCTAAG
AAACACTCTCTCAAACTCCACGACAACACTTCAATGAAGTCCTATGTATCGTCCAATGCG
AGTGTTAAAAGTGACATGTCTAATCACAGCATTGACGATGTGGTATCTCTTGAAGTTGAG
GATCTCTCTGATATTGAGGAACTAGAGGACCTTGAGGAAGGACGTCAGCACGAGACAGAG
GGAGGGTTCATATCTGAAGCAGAGACTGAGTCTATCGGTACCCCGTCAGTCATTGGGTCA
CCATTACATCATCATCATCATCACCATCATCATCATAATAATAATGATGTCTTTAAT

GTTGAGTATAATGAAGATGTACCGCCTATCCCTTACTGTGGCTGTGAGCCACTCAAATGT
CACCTCATGAAGAATGCTAGGACTTATGAGGATATCATTATTGACAGGTCATTTATTGGT
GAAGACATCACAAGGCAGTGGTACCATCATGCCATCATCGTTTATTCTGATGTTGTATCT
GACGGTCTCTTCCACTTCATTACTCCATTAAGAGCGGCTTATCTGCCTCCTTCTTCACTG
AAGCCTATTGTATTTCTACTTGGAAACATTACATCTGACCTGCTAAGAGCTGGTATCATG
GTGGCTGAGAGTTTGGTTGTTTTTTCCTCAAACAAGATGAGACAGTCTGATGAAGGGGAG
CACCTGGCAGACGCTGAACACATTACTGCTATAGAGAAGATAGCCAGGTTCAACATCAGG
TTCATTAGGACGACGCCTTTCGAAGACCTCTGCATGCAGAGGCTGAGACACATGGCTCGT
AAAGTGGATCACTTGACCTACCTCTTCCTACCTCAGTTTGCCTCATCCAAAGCATTCTCC
AGTTCAATGCTGGACACTCTCCTCTACCAGTCTTACCAGAAACCTTACATCATTAAACTC
TTCCGGCAACTCCTCGGCTGTACTCAAGTCAAAGGCTCAGGGTTTCTATGGAAGGTAGTG
CCACATATTATTGGTTTCAGTAACTTTTATTGTTACCAGGTTCCTGTCAATAATGAATTG
GCTAAGCTACACACTTATGTAAGAGTCTTCCAGAGACTCGTCGCTTCATTCAGCTTCACT
TCAATGGCTTTGTATCGGACAGCAAACGTTGATCATAATATTGATCCTCAGTATGTGAAA
GGATATTGTGAGGAAGAGCTGGAAAAGTTGAGACTGTTTTTGATTAGTGAACTCCACAGT
TTAGGGATAAAGAGAAATGGTATTCGTCCTCCCCTTAGCAACAAGCCGCCGCCCCCTAGC
GACGATGTTAAAACCGAGCCTTTCTCCCCACCTCCAGCCAGTCAGATCAGTGAACTGGTT
CGTGCTTACTCAGCATCAGCTTTCTATGGAGGGGGCAGTCCCATACCCACGGCCATGCCC
CTAGGCCCTGGGGGTGTGGTCCTGCAGGATACTAGACTTCATTTTGGTTTAATGCGCAAG
TTCAGTTTCACAGGCTCACTCCCCCAGCAGCATCAGACCAACACTGGGAGCTGCTCCGCT
GATTCTTGCGATATGTGA

Predicted amino acid sequence

Sponge_SubT_Kca (AmqKNaA)

MADRVEHRISQQHSLPNSPLLRKRKKIRRRSRPEVYDQSAPVPASPSLTSLSCSSSDSEC
ESNREEEEDPLPDKDGQSVTVKQALEGLFYNKAVQLVHHHELIIVKRYSHGKTFGQRLAY
VLYKHPKTRLIAHFGALLLNIISCILYVAEAIYIDRLLKSADEEEFILGCFNQTWVNITE
PSYLCLIHHFERLGKKISLFDTYWFVVVTFSTVGYGDISPAHWTGKVIITIFIIAALMYL
PPKVSHTLFTCHYKQYNKANITKHVVLAAVDLKPLVLRDFLSELYSDPGQMDTQVVVLIK
EEPADYIKAILLHPIWSQRVAILRGTALRPSDLARVKGRRFNIPEYKRYEECSPVEIYHV
KLGESRYFHRFAGKNFLFTSVVAYRKFHVLLLGICPSGGTDILFNPGINHIMDRNDECYY
ISDTHEHNSDHQIIPASTFQSSLWRTSATLGLLAMYISGIDPDQMFHQTQEYEERDSDNK
GGFPRSASNDRLKKLSSPDSIPEIQVEGVASGVSLTEETRLPSIGEEEEVLDEQLAVEVT
NWQHDVQHGLQLLKYHGEGELPERKPCVKLSVKSHFEGHHSPRSHSLPLAATTCTVMEPH
PLAHPLPSLGVIPEDEPDVIVIGEEEPHLLPHLQRVGDKQHSSGGGVGKHRVHSQPALFH
FGFNKRQSEPKHDDHLLKAKKHSLKLHDNTSMKSYVSSNASVKSDMSNHSIDDVVSLEVE
DLSDIEELEDLEEGRQHETEGGFISEAETESIGTPSVIGSPLHHHHHHHHHHHHNNNDVFN
VEYNEDVPPIPYCGCEPLKCHLMKNARTYEDIIIDRSFIGEDITRQWYHHAIIVYSDVVS
DGLFHFITPLRAAYLPPSSLKPIVFLLGNITSDLLRAGIMVAESLVVFSSNKMRQSDEGE
HLADAEHITAIEKIARFNIRFIRTTPFEDLCMQRLRHMARKVDHLTYLFLPQFASSKAFS
SSMLDTLLYQSYQKPYIIKLFRQLLGCTQVKGSGFLWKVVPHIIGFSNFYCYQVPVNNEL
AKLHTYVRVFQRLVASFSFTSMALYRTANVDHNIDPQYVKGYCEEELEKLRLFLISELHS
LGIKRNGIRPPLSNKPPPPSDDVKTEPFSPPPASQISELVRAYSASAFYGGGSPIPTAMP
LGPGGVVLQDTRLHFGLMRKFSFTGSLPQQHQTNTGSCSADSCDM

B.3. Primers used to amplify putative potassium channel sequences from *Amphimedon queenslandica*

Primer name	Sequence	Description	Tm (ºC)
K2P1F	XhoI GGCTCGAGCCACCATGGAGAAAGAGGTCGAG 5' clamp Kozak consensus	Forward primer to amplify predicted full length K2P	67.3
K2P1R	SpeI GGACTAGTTCACTCCTTCTCTACTTCAG 5' clamp	Reverse K2P primer	57.4
K2PRevGR	GCGGGTGAAGTAGGCCCTGGA	Reverse K2P primer for 5' RACE	63.9
K2PRevNGR	GGCCCTGGAACACTCAAACC	Nested reverse K2P primer for 5' RACE	58.7
Kinv7-5'	CGCCTACATTCAACCTCACC	Reverse inverse primer to amplify 5' end of putative kctd protein	55.8
Kinv7-3'	GGGCATACCTCATTGACAGG	Forward inverse primer to amplify 3' end of putative kctd protein	55.5
KtetRevGR	TGGGTTCACTCCTTCGTTAATAATG	Reverse kctd primer for 5' RACE	62.44
KtetNRevGR	CTTCGTTAATAATGAGCTTCC	Nested reverse kctd primer for 5' RACE	53.6
KtetFwdGR	GTCAACAAGAGCCACACCCTCCT	forward kctd primer for 3' RACE	61.2
KtetFwdNGR	AACTCGGCCCTCAAACTGATCAAA	nested forward kctd primer for 3' RACE	58.9
Kv1F	ATGAATAACATTGGATACTCCTC	Forward primer to amplify full predicted Kosik SubH_Kv	50.0
Kv1R	TCAGCTTAAGATGGTAGACAATG	Reverse primer to amplify full predicted Kosik SubH_Kv	52.3
Kv2F	TGTTGGGCCTAAAGAAATGC	Internal forward Kosik SubH_Kv primer	53.6
Kv2R	GACAATGGTGCCAAGGAACT	Internal reverse Kosik SubH_Kv primer	55.6
Kv3Fwd	TGAATTCCCTCTACTGGTCCG	Internal forward Kosik SubH_Kv primer	61.38
Kv3Rev	GCTGTTCTGCTGCAATCAAAG	Internal reverse Kosik SubH_Kv primer	61.1
Kv3NFwd	TGGCGACATTACTCCTCATAGAAG	Nested internal forward Kosik SubH_Kv primer	61.8
AqKvFwdGR	TCACTGTGTTGGACGAGGGAAA	Forward SubH_Kv primer for 3' RACE	58.4
AqKvFwdNGR1	TGGACGAGGGAAAGTTCTTTGGA	Nested forward SubH_Kv primer for 3' RACE	52.1
AqKvFwdNGR2	TGGTCTTTGATTGCAGCAGAA	Nested forward SubH_Kv primer for 3' RACE	48.1
AqKvRevGR2	GAATGCCGTCAACTTTGTGTTC	Reverse SubH_Kv primer for 5' RACE	50.2

KCa1F	GGCTCGAGCCACCATGGCAGACAGAGTAGAGCA		69.1
KCa1R	GGACTAGTTCACATATCGCAAGAATCAGC		58.9
KCa2F	TCGTTTCGCTGGAAAGAACT	Internal forward Kosik SubT_KCa primer	54.5
KCa2R	GGGGAGGACGAATACCATTT	Internal reverse Kosik SubT_KCa primer	54.4
KCa3Fwd	CCTTCAGTACGGTCGGGT	Internal forward SubT_KCa primer	58.51
KCa3Rev	CTGGTAAGACTGGTAGAGGAGAG	Internal reverse SubT_KCa primer	56.45
KCa3NFwd	TAAGCACGTGGTACTAGCAGC	Nested forward SubT_KCa primer	58.3
KCa3NRev	TCTCAATATGGCTACCCTCTG	Nested reverse SubT_KCa	56.93

B.4. *Amphimedon queenslandica* nucleotide sequences which match metazoan K channel sequences with expected values less than $1e^{-10}$.

Sequences were retrieved from genome trace files. Overlapping sequences from multiple clones were assembled in Staden Pacakage 1.7 to produce consensus sequences. Clones included in each consensus sequence were indicated in Table 4-1. Sequences are not corrected for the presence of introns or cloning vector.

B.4.1. Putative potassium channel tetramerization domain containing protein sequences

AmqkctdA_1
gcgcgcgagtcagtgagcgaggaagcggccgcataacttcgtatagcatacattatacga
agttatcagtcgacggtaccggacatatgcccgggaattcggccattacggccggggaca
ccacgtgggcgtggtattcaacaaaatggctgccgcaagggtgaccttgtacagttcaat
ggaaagctacaggcaacaaagaaaaggcaaagtcattttagttagggagactttgagcga
aactttagttgctgcatctgagaaactcaaagaaaacgtcgaagagttgcggttactgac
gggtggggtagttgatgacatcactttattaagagaggatgatattctaattgctgttac
ctcaagcacagagtcaacaagagccacaccctcctctccgactatactaagcgacctccc
tgaggaccagctacccgaactcggccctcaaactgatcaaagtcatttcctccttaaaaa
gtgctcaaggctcctttcccctgatgctccttcacgtcatgactgggtgaggttgaatgt
aggcgggaaagtatttgccactagcagggcaaccatcacttctgatccatcctcaatgtt
ggctagaatgtttgagtcagattggttcagtactacggatgactccggggcatacctcat
tgacaggagtcctgaacattttgagccacttctcaacttcatgagacatgggaagctcat
tattaacgaaggagtgaacccacagggagtgctagaggaagccaagttcttcaatgttac
taaagctatccaaccactggaaacacttgttaagaatgaagagttctcattagctggtca
tttaacaagaaaggagttcc

AmqkctdB
gcgctagctcgccgcagccgaacgaccgagcgcagcgagtcagtgagcgaggaagcggcc
gcataacttcgtatagcatacattatacgaagttatcagtcgacggtaccggacatatgc
ccgggaattcggccattacggccggggattaaaagaaaaatggcttccgaggtggcagca
aaagatgaatgggttaagctaaatgtcggaggaactctctttatgaccacaaagaccacc
ctctgcaaggagaagaagtcattcctggccagactctgcttagatgatcctgatttacct
tctttaaaggtaagagagagagatagacccatccttttacccccttcctatccctatgtta
ggatgaaactggtgcttatctcatcgatagagactctcgttactttccagtgatacttaa
ctacctcaggcatggaaagatcattgtagagccaacccttcacattgatggtatggtatg
cgctttaattaaaggcgtgacacattctaccattattaatcttaattaccttaaaattct
aattttaattgcttgtactcatactgaagtactaaattaattactgtcagccaaaaaaaa
aaaaaaaaaaaaaaaaaaaaaccagtcggccgcctcggccctcgagaagctttctagacc
attcgtttggcgcgcgggcccagtaggtaagtgaacatggtccatagctgtttcctagga
gatcctggtcatgactagtgcttggattctcaccaataaaaaacgcccggcggcaaccga
gcgttctgaacaaatccaga

B.4.2. Putative tetrameric potassium selective cyclic nucleotide gated channel sequences

Regions matching Kosik SubH_Kv (redesignated Amq-tetreKCNGA) are highlighted. Regions matching the partially cloned sequence Amq-tetraKCNGB are underlined.

Amq-tetraKCNGC

tggaaaagttgatcgagcaaaccattacattaagtacatattaacatactaaatgtacag
cacatcatttacattatatcattttataataggacaacattcatccttgatgtcattgct
ttattaccaactgaactcatagtatttgctatattctctcctttaggacttggtgagtta
gctacttgttcatgttcatgcacattattatttctttttaaattcttttgaaggtccac
gaactagtttaatgagcttagcaagactgaataggctcgtacatattcacagattggtaa
ttagttttcattttattattaactgtacacgtatttttttaggtcatttttttcaatgata
ttaaaaatttaatgccaaaaatgatttggtaggagcactaaaattatttttaaaattaca
aaattatttacaattatgaaataggttgataaaattactggtctacctgttactcagtac
acatttgattggctgcagttggttcatgatctcctgctcttgcctctcactccacagctg
ctgctctcttggcagctgggccaacagcgggatcttcaaaaatcaatcactaagtatgat
gaggcactctttgataatatggtcactctttttctctctctctttccttcttctcttcct
ctacagttagtagctcattcagtgttcagtatatgaattccctctactggtccgtagcaa
caactgcttctgttggatatggcgacattactcctcatagaagtcttgaggtacatcaac
gtagatgtacttgtatgtttataattattatcatctcatcttgcagcgtttgtatgcaat
atgttttgaggtgtttggtgtcctcttctatggcctgatagtagcctatttcactgctag
tttggttaatgatgacattgggagagctcagtatcaagataaactggaaatgattaagaa
atatctgaaagaacacaaagttgacggcatcctaaagaacagagtaataaagtcagtaag
atagagaaagaaaggattactatacaaattgttccaatagtcattatgagtatatgtggc
agagaaataaagctcttgattttcatgatctcttcaaggatatgcctccatcactccaaa
gcgatgtctcactagctctgtacaagaacgctattgacaaagtacaatagtggattgtac
ttgcagtaattattgttgaatgttgtaggtgcctttatt

Amq-tetraKCNGD

accatcaatt
ttctctttgaaatatattttctgattgaggtacttgtacatgtgcatacttttattaggc
aaatgatgcattcattgtgttaagtcaatcctgttttactagtgtctgcataattgttgc
atcttcttcttgtctagatacttattaagtttcatcttggctatgaagacccttcttctg
gtttgatcgttcgagacttcaagttaactttccttcattacctaaggtctccttttggct
ttacgttggacttcattgcaacattcccgtttcatattctttctgcattcgctgagctta
tcattggctctcattcagtaatgtcaacttatctaaagataccacattttctcaggatgc
taaaattttggagattattcctgatccaggagaagaaactaaaccaaaagtaaaggaaag
aagaattatctttaattgttgtgtgcactttaggacagctctcattcaagcactgaagtt
ctttgttcttacaagtttagcaactcagtttgctgcttgtttctggtacttccttagctg
ctcatcatcctcttgtcatgaagactcttgggctacagccataagtataaaatgataata
ataacaaagttaatagtaatcattctagatcttacagctgctgattctgatacaacccgt
tacatcactagtttatactgggcagtgactacaatgacaactgttggctatggggacatt

gtgccacagaattacactgagaaactttatgcaattttaataatgatatttgggaaactg
ttctatgggtttctattggggagtgttgcttcgatgcttgctaataggaaaaagagacaa
gtcatgtttatgaacaaactggactccatcaaagtacaggaataataagaaacattc

Amq-tetraKCNGE

gcttacattagtgcattctgcctcagttatcaagtacagtacttatatactgcatccttt
catcatgtctcttttagattttcttcttcagtagttcagctggtctatcaaccatcaatt
ttctctttgaaatatattttctgattgaggtacttgtgcatgtgcatacttttattaggc
aaatgatgcatccattaccttaagtcaatcctgttttactagtgtctgcataattgttgcatcttcttcttgtctagatacttatt
aagtttcatcttggctatgaagacccctcttctg
gtttaatcgttcgagacttcaagttaactttccttcattacctaaggtctccttttggct
ttacgttggacttcattgcaacattcccgtttcatattctttctgcattcgctgagctca
tcattggctctcattcggtaatgtcaacttatctaaagataccacattttctcaggatgc
tcaaattttggagattatttctgatccaggagaagaaactaaaccaaaagtaaaggaaag
aagaattatctttaattttagtgtgcacttcaggacagctctcattcaagcactgaagtt
ctttgttcttacaagtttagcaactcagtttgctgcttgtttctggtacttccttagctg
ctcatcatcctcttgtcatgaagactcttgggctacagctataagtataaaatgataata
ataacaaagttaataataatcattctagatcttactgttgctgattctgatacaacccgt
tacatcactagtttatactgggcagtgactacaatgacaactgttggctatggggacatt
gtgccacagaattacactgagaaactctatgcaattttaataatgatatttgggaaactg
ttctatgggttcctgttggggagtgttgcttcgatgcttgctaacaggaaaaagagacaa
gtcatgttcatgaacaaactggactccatcaaagtacaggaataataaaaaacattatta
ttattattattattattgttattattatttttacttttattattgtaggattatatt
gttgctgctgatgtctcagttccactagagcgtaaagtaattcatcactgcaatcaccat
tggttggagtctaaaggtattgacaggcagacactgtttgatgacacccttactgtctc
caatcggaaattgctctagctacaacacagaaattactccaaatggtaaagaacagagca
gtacatgcttatattggagaatttaatgcaattatgatacacctataggtaccagtgctg
aactctgtcagtgggtctttgctctgccaaatatcattacacctgagaccttgctacttc
tcagctggtgagatcattatcagtagaggagacgtaggacatggactgtactttatttat
gacggaattgtgagtatatattcaaaatgacatactataaattactgtacatgtacttca
attgtgcattactgctgtaggtggaaaaattgttggaagaaggccgtcagtcagctgctg
atcctcattctagttcct

B.4.3. Putative sodium activated potassium channel sequences

Partial *Amphimedon queenslandica* nucleotide sequences for putative sodium activated potassium channels. Highlighted sequences match Kosik SubT_KCa (redesignated AmqKNaA).

AmqKNaB
ttctgttggtttgttattgagttgctcttcgtttcttttatgttcttttgtgaacatgttgtctgtaaattttggcatgcatctaaca
gaatagtaacaacaccagtactacaactttgttgttttccctctccccccccctctctctctcctcgattagtttaaatctcc

taattatccctaaagattatactctctggtcattacaggtactgatattctcattaattagtttaatattgttattattattat
tttacagttgtttttattgttattattattattttacagttgtttttagcattgatttgtttaattggagcatttactgtcatttatgtac
accaggagccatacgtgagtagttaattaaccactagttaattaactattattaacagggttcagttcctgttttaagacac
gtctttagatacatgactcacagtattgtcatatgcgtgctaattgggttagcatttttttgtcaccgtaagttattatttatttatt
tattttatttgtttatttattaattctcatagctactaatgccgcagtgtctccatattctgtggattccaacgttcctcttctgttg
gccggcaagacacaactttatgtacatagtacagcagaaaagtgaagtatcattctttaggtccttccacggcttccgc
actacagcaatcagcctggcaaccttcctcctctgttttatgttctcatggtaagctccacccactggtcataccctaaac
cacacccctttccttttagtctgtgtctcattcatcattttgagcggctgggtaaaaagatatctctgtttgatacctactggtt
tgtggtcgtcaccttcagtacggtcgggtatggggacattagccccgcccactggactgggaaggtcattataacgat
attcataatagcggctttgatgtacctcccacctaaggtgagccacaccctcttcacttgtgtctattattagtaacaggtt
gataaactgtggagatccttcacgttacatcgtaagcactacaagcagtacaacaaagctaacatcactaagcacgtg
gtac

AmqKNaC
tcatttatgtacaccaggagccatacgtgagtagttaattaaccaccagttaattaactattattaccagggttcagttcct
gttttaagacatgtctttagatacatgactcacagtattgtcatatgtgtgctaattgggttagcattctttgtcaccgtaagt
tattatttatttatttatttttatttgtttatttattaattctcatagctactaatgccgcagtgtctccatattctttggattccgacgt
tcctcttttgttggccggcaagacacaacttcatgtatatagtacagcagaaaagtgaagtatcgttctttaggtccttcca
cggcttccgtactacagcaatcagcctggcaaccttccttctctgtttcatgttctgatggtaagctccacccctttgaccct
aaaccacacccctttccttttagtctgtgtctcattcatcattttgagcggctgggtaaaaagatatctctgtttgatacctac
tggtttgtggtcgttaccttttagtactgtggggtatggggacattagccccgcccactggacagggaaggtcattataa
cgatattcataatagcggctctgatgtacctcccacctaaggtgagccacaccctcttcacttgtgtctattattagtaaca
ggttgataaactatggagatccttcacgttacatcgtaaacactacaagcagtacaacaaagctaacatcactaaacac
gtggtactagcagctgtggaccttaagccgctcgtactgagggacttcctcagtgaactctactccgaccctggacaa
atggtatggaggaatgaacctttacttttaatggaacaattgagactctctctctctc

AmqKNaD
tactggtttgtggtcgttaccttcagtacggtggggtatggggacattagccccgcccactggactgggaaggtcatta
taacgatattcataatagcggctctgatgtacctcccacctaaggtgagccacaccctcttcacttgtgtctattattagta
acaggttgataaactatggagatccttcacgttacatcgtaaacactacaagcagtacaacaaagctaacattactaaa
cacgtggtactagcagctgtggacctcaagccgctggtactgagggacttcctcagtgaactctactccgaccctgga
caaatggtattgaggaatggacccttactttaatggaacaattgagactctctctttttctctctctgtaggatactcaagtt
gttgttcttattaaagaagaacctgccgattatatcaaagccattctattgcacccgatatggtcccagagggtagccat
attgagaggaactgctttgagaccaagcgacctagcaagagtcaagtgagtgacgtacacttactgtgtacatgatac
agtggagggttctctttggctcaatttttgagaaactttaaaaatttgtaaaaaattcaattttgattggaatcaactcaaact
ttttatgcaacataagaacatgtattatatttatcattaataggctaagaacggctgatgcttgtttccttcattcatcaagaa
ctggcagggcagctgatgctgttagtaattaactaatcatttattaattaactgaaactcctcccacttcctgtaggacca
gcataccatcatgagtgcttggaccgttaagaactatgca

AmqKNaE
ttattgttattattattattttacagttgtttttagcgttgatttgtttaattggagcatttactgtcatttatgtacaccaggagcc
atacgtgagtagttaattaaccaccagttaattaactattattaccagggttcagttcctgttttaagacatgtctttagatac
atgactcacagtattgtcatatgtgtgctaattgggttagcattctttgtcaccgtaagttattatttatttatttatttttatttgttt
atttattaattctcatagctactaatgccgcagtgtctccatattctttggattccgacgttcctcttttgttggccggcaaga
cacaacttcatgtatatagtacagcagaaaagtgaagtatcgttctttaggtccttccacggcttccgtactacagcaatc

agcctggcaaccttccttctctgtttcatgttctcgtggtaagctccacccctttgaccctaaaccacacccctttcctt
tagtctgtgtctcattcatcattttgagcggctgggtaaaaagatatctctgtttgatacctactggtttgtggtcgttaccttt
agtactgtggggtatggggacattagccccgcccactggacagggaaggtcattataacgatattcataatagcggct
ctgatgtacctcccacctaaggtgagccacaccctcttcacttgtgtctatttttagtaacaggttgataaactatggagat
ccttcacgttacatcgtaaacactacaagcagtacaacaaagctaacatcactaaacacgtggtactagcagctgtgg
accttaagccgctcgtactgagggacttcctcagtgaactctactccgaccctggacaaatggtatggaggaatgaac
ctttactttaatggaacaattgagactctctctctctgtaggatactcaagttgttgttcttattaaagaagaacctgccg
attatatcaaagccattctattgcacccgatatggtcccagagggtagccatattgagaggaactgctttgagaccaag
cgacctagcaagagtcaagtgagtgacataatgtgaatggagggttccctttggctcaatttttgagcaactttaaaaat
ttgtaaaaaaattcgattttgattggaatcaactcaaacttttatgcaacataagtacatgtattattattatcattaataggc
taagaacagctgatgcttgtttccttcactcatcaagaactgggagggcagctgatgctgttagtaattaactaatcattt
attaattaactgaaactcctcccacttcctgtaggaccaacacaccatcatgagtgcttggactgttaagaactacgctc
cgaagacacgcctctttgtacacgtcagacaaccagggatcctctagagtcgacctgcagcatgcagctgcact

AmqKNaF

ttattgttattattattattttacagttgtttttagcgttgatttgtttaattggagcatttactgtcatttatgtacaccaggagcc
atacgtgagtagttaattaaccactagttaattaactattattaacagggttcagttcctgttttaagacacgtctttagatac
atgactcacagtattgtcatatgcgtgctaattgggttagcatttttttgtcaccgtaagttattatttatttatttattttatttgttt
atttattaattctcatagctactaatgccgcagtgtctccatattctgtggattccaacgttcctcttctgttggccggcaag
acacaactttatgtacatagtacagcagaaaagtgaagtatcattctttaggtccttccacggcttccgcactacagcaa
tcagcctggcaaccttcctcctctgttttatgttctcatggtaagctccacccactggtcataccctaaaccacacccctttt
cctttagtctgtgtctcattcatcattttgagcggctgggtaaaaagatatctctgtttgatacctactggtttgtggtcgtca
ccttcagtacggtcgggtatggggacattagccccgcccactggactgggaaggtcattataacgatattcataatag
cggctttgatgtacctcccacctaaggtgagccacaccctcttcacttgtgtctattattagtaacaggttgataaactgtg
gagatccttcacgttacatcgtaagcactacaagcagtacaacaaagctaacatcactaagcacgtggtactagcagc
tgtggatctcaaaccgctggtactgagggacttcctcagtgaactctactccgaccctggacaaatggtatggaggaa
tggacctttacttttatagaggaattgaaactctctctctctctgcaggatactcaagttgttgttcttattaaagaagaacct
gccgattatattaaagccattctattgcacccgatatggtcccagagggtagccatattgagaggaactgctttgagac
caagcgacctagcaagagtcaagtgagtgacataatgtgaatggagggttccctttggctcaatttttgagaaactttaa
aaatttgttaaaaatccaattttgatcggaatcaactctaacttttaatgcaacataagaacatgtatatatttatcattaata
ggctaagaacagctgatgcttgtttccttcactcatcaagaactgggagggcagctgatgctgttagtaattaactaatc
atttattaattaactgaaactcctcccacttcctgtaggaccaacacaccatcatgagtgcttggactgttaagaactacg
ctccgaagacacgcctctttgtacacgtcagacaaccagggatcctctagagtcgacctgcagcatgcagctgcact

AmqKNaG

Ccacacccctttcctttagtctgtgtctcattcatcattttgagcggctgggtaaaaagatatctctgtttgatacctactgg
tttgtggtcgttaccttagtactgtggggtatggggacattagccccgcccattggacagggaaggtcattataacgat
attcataatagcggctttgatgtacctcccacctaaggtgagccacaccctcttcacttgtgtctattattagtaacaggtt
gataagctatggagatccttcacgttacatcgtaaacactacaagcagtacaacaaagctaacattactaaacacgtgg
tactagcagctgtggacctcaagccgctcgtactgagggacttccttagtgaactctactccgaccctggacaaatggt
atggaggaatagacctttacttttatagaagaattgaaactctctctctctctctctgtaggatactcaagttgttgttctt
ataaaggaagaacctgccgattatatcaaagccattctattgcatccgatatggtcccagagggtagccatattgagag
gaactgctttgagaccaagtgacctagcaagagtcaagtgagtgacataatgtgaatggagggttccctttggctcaat
ttttgagcaactttaaaaatttgttaaaaatccaattttgatcggaatcaactctagctttttatgcaacataagtacatgtatt
attattatcattaataggctaagaacagctgatgcttgtttccttcactcatcaagaactggcagggcagctgatgccgtt

agtaattaactaatcatttattaattaactgaaactcctcccacttcctgtaggaccaacacaccatcatgagtgctt
ggactgttaagaactacgctccgaagacacgcctctttgtacacgtcagacaaccagggatcctctagagtcgacctg
cagcatgcagctgcact

B.4.4. Putative calcium-activated potassium channel sequences

Partial *Amphimedon queenslandica* nucleotide sequences for putative high conductance calcium activated potassium channels. The sequence underlined in AmqKCaB is not present in AmqKCaA. Translations in frames +2 and +1 are given for AmqKCaA and AmqKCaB and the pore region underlined in each.

AmqKCaA

cctaagctacctctaaccctctaaggacatacctagcacataattatgaacaagtgctga
tgtgacaattaatacaaactgcccaataagcaactgtaacaacatatttgttaacccgtt
atagattgcaccaacactggcaaaatgtccacaaaatgctcattaagtgtctcattattg
caacttactaaagctagtctggctgagtcaaaatgcttaattaattctatttaatgataa
ttataccttcactaagtggctttaaatgagcaagtgccacaatggagtgacccgacgcta
cacattgcatgaggttgtacatactgtccttccctccactgcataatgagaataaatgaa
atacaagttgtgaactgatacactactaaactcacctaattaatcctactactttcattg
ctttattgccttcttatgagggacacgtgggcgaattcaatgaattcatgaatattcatt
agcttggctcatggaggagcaagagcaaggaaactcttcttctccttttttgtctaagtat
aagagctaatcaaggatggtggccatacgcagttacctatacagttttgtttgctactgg
cctcctctcactctctcttattctgacactgacctctgtttccttcaaattcaatagaat
gactatgctagctaattcaaagatagtccctctctttgatctgctctttgacccgcagag
tatgacagggaaagttcactttactcttaccctagtcttcaatacaacctatatcagcat
aatgctctggcgctcttcaacccgtcccctgtatgattgcagcattgctgattccactcc
agtttacttgatagtagagactctatcttcatgctatcttataataaattctattgctag
actaattacagcaaagcatagaataatccggtggatatctcttctcactctcgttgatat
tttcactctctctcatccgtttatctctttattgtgcggctacgactggttgggtctcag
agctctaaggtttctgtggttattcgaggcatcaaaagtcctcaaggctctacctgatac
tattaattctgaagacattgttaagattgcaaagatagtaagtcgtttcattggagtatg
gctatcatctagcggcatgatacagctattggagaattctggtgatccgtgggatgatga
tgatgacatcagcatgagcttctggtctagcacatacttcactatgatcactatgactac
tgtgggttatggtgatgttactgtaggcagtgattgtggtcaaatgtttacaatgttcat
tattgttcttgggtttgtactttacatgttttcattgccgactttactggaaattttatt
gggaactcatcaatcatcaaagtttcgtcaaagctacaataaccttattaaacaggaagg
tctcgtcattgttgtgggtagcatcacagagaaaaacgttagctgtttcctcaaagagtt
acttcatccagacaaacaaggcagaccgacatttagtgtcatccttcttcatccttcatt
tcccactcctggcctcagttctattcttaagtcacactatacacgtgttcagtactatca
aggttctgctttaaattacaatgatctgatgagatgtggcctgtctatagccaagtctgt
tatcgtgttagctgatagtcattgctctaatcccatcaaagaggataatgctaatctatt
aagagttgcttctattaaaacgcactctcctctgtcccaataatccttcagctactaatg
aatgacagcaagaaacttcttaaatgtttacctggctggttccaggtagagatgttccac
tgtgtttatttgagtgt

frame +2
> - 625 codons
LSYL*PSKDIPST*L*TSADVTINTNCPISNCNNIFVNPL*IAPTLAKCPQNAH
*VSHYCNLLKLVWLSQNA*LILFNDNYTFTKWL*MSKCHNGVTRRYTLH
EVVHTVLPSTA**E*MKYKL*TDTLLNSPN*SYYFHCFIAFL*GTRGRIQ*IH
EYSLAWLMEEQEQGNSSSPFCLSIRANQGWWPYAVTYTVLFATGLLSLSL
ILTLTSVSFKFNRMTMLANSKIVPLFDLLFDPQSMTGKVHFTLTLVFNTTY
ISIMLWRSSTRPLYDCSIADSTPVYLIVETLSSCYLIINSIARLITAKHRIIRWI
SLLTLVDIFTLSHPFISLLCGYDWLGLRALRFLWLFEASKVLKALPDTINSE
DIVKIAKIVSRFIGVWLSSSGMIQLLENSGDPWDDDDDISMSFWSSTYFTM
ITMTTVGYGDVTVGSDCGQMFTMFIIVLGFVLYMFSLPTLLEILLGTHQSS
KFRQSYNNLIKQEGLVIVVGSITEKNVSCFLKELLHPDKQGRPTFSVILLHP
SFPTPGLSSILKSHYTRVQYYQGSALNYNDLMRCGLSIAKSVIVLADSHCS
NPIKEDNANLLRVASIKTHSPLSQ*SFSY**MTARNFLNVYLAGSR*RCSTV
FI*V

AmqKCaB
cctaagctacctctaaccctctaaggacatacctagcacataattatgaacaagtgctga
tgtgacaattaatacaaactgcccaataagcaactgtaacaacatatttgttaacccgtt
atagattgcaccaacactggcaaaatgtccacaaaatgctcattaagtgtctcattattg
caacttactaaagctagtctggctgagtcaaaatgcttaattaattctatttaatgataa
ttataccttcactaagtggctttaaatgagcaagtgccacaatggagtgacccgacgcta
cacattgcatgaggttgtacatactgtccttccctccactgcataatgagaataaatgaa
atacaagttgtgaactgatacactactaaactcacctaattaatcctactactttcattg
ctttattgccttcttatgagggacacgtgggcgaattcaatgaattcatgaatattcatt
agcttggctcatggaggagcaagagcaaggaaactcttcttctccttttgtctaagtat
aagagctaatcaaggatggtggccatacgcagttacctatacagttttgtttgctactgg
cctcctctcactctctcttattctgacactgacctctgtttccttcaaattcaatagaat
gactatgctagctaattcaaagatagtccctctctttgatctgctctttgacccgcagag
tatgacagggaaagttcactttactcttaccctagtcttcaatacaacctatatcagcat
aatgctctggcgctcttcaacccgtcccctgtatgattgcagcattgctgattccactcc
agtttacttgatagtagagactctatcttcatgctatcttataataaattctattgctag
actaattacagcaaagcatagaataatccggtggatatctcttctcactctcgttgatat
tttcactctctctcatccgtttatctctttattgtgcggctacgactggttgggtctcag
agctctaaggtttctgtggttattcgaggcatcaaaagtcctcaaggctctacctgatac
tattaattctgaagacattgttaagattgcaaagatagtaagtcgtttcattggagtatg
gctatcatctagcggcatgatacagctattggagaattctggtgatccgtgggatg**ctgtatctgatga**gatgacatca
gcatgagcttctggtctagcacatacttcactatgatcactatgactac
tgtgggttatggtgatgttactgtaggcagtgattgtggtcaaatgtttacaatgttcat
tattgttcttgggtttgtactttacatgttttcattgccgactttactggaaattttatt
gggaactcatcaatcatcaaagtttcgtcaaagctacaataaccttattaaacaggaagg
tctcgtcattgttgtgggtagcatcacagagaaaaacgttagctgtttcctcaaagagtt
acttcatccagacaaacaaggcagaccgacatttagtgtcatccttcttcatccttcatt
tcccactcctggcctcagttctattcttaagtcacactatacacgtgttcagtactatca
aggttctgctttaaattacaatgatctgatgagatgtggcctgtctatagccaagtctgt

tatcgtgttagctgatagtcattgctctaatcccatcaaagaggataatgctaatctatt
aagagttgcttctattaaaacgcactctcctctgtcccaataatccttcagctactaatg
aatgacagcaagaaacttcttaaatgtttacctggctggttccaggtagagatgttccac
tgtgtttatttgagtgt

frame +1
> - 628 codons
PKLPLTL*GHT*HIIMNKC*CDN*YKLPNKQL*QHIC*PVIDCTNTGKMSTK
CSLSVSLLQLTKASLAESKCLINSI***LYLH*VALNEQVPQWSDPTLHIA*
GCTYCPSLHCIMRINEIQVVN*YTTKLT*LILLLSLLYCLLMRDTWANSMN
S*IFISLAHGGARARKLFFSFLSKYKS*SRMVAIRSYLYSFVCYWPPLTLSY
SDTDLCFLQIQ*NDYAS*FKDSPSL*SAL*PAEYDRESSLYSYPSLQYNLYQ
HNALALFNPSPV*LQHC*FHSSLLDSRDSIFMLSYNKFYC*TNYSKA*NNP
VDISSHSR*YFHSLSSVYLFIVRLRLVGSQSSKVSVVIRGIKSPQGST*YY*F
*RHC*DCKDSKSFHWSMAII*RHDTAIGEFW*SVGCCI**DDISMSFWSSTY
FTMITMTTVGYGDVTVGSDCGQMFTMFIIVLGFVLYMFSLPTLLEILLGTH
QSSKFRQSYNNLIKQEGLVIVVGSITEKNVSCFLKELLHPDKQGRPTFSVIL
LHPSFPTPGLSSILKSHYTRVQYYQGSALNYNDLMRCGLSIAKSVIVLADS
HCSNPIKEDNANLLRVASIKTHSPLSQ*SFSY**MTARNFLNVYLAGSR*R
CSTVFI*V

B.4.5. Putative voltage gated potassium channel sequences

AmqKvA
atcggttcaatacagttcatttcttgaaatttgagtgtataccacgtgtatgggtatatn
ataccttttgtgtaaaatctttcttatttttttgtatttcagtctatatgctgtatatgaac
agttctaacataagcacactatgtttgctctacgacatggccagacaatgaatgccttga
tgccaggctacaggctagctaacaatggtaatatattgataaatatgtcaacatccaacg
acaaggtggtgttcaatattggtggcaccaaatttgaaacatataaatctacactacgaa
gaataccacaaagtcccttatcaaatgatagttttctgaacaaatattaccaattagatg
accgtgaatatttctttgatcgcgatcctgacgtgtttaaatctgttcttcaatacctca
gaaccggggagcttcacctcagctcatcactatgtggttctgctgttaaaacggagttgg
atttttggggaatatcagaactgaatatcgaagactgctgttggttgaattataattcct
ggactcaaactcttcagtcactaacaaaactagaagtagatcgaaagaagtctattggac
tgaccaaaaaccatcatagcgaaccccatcctcatcatggacagggcaaatgggaaacac
taaaacatcatgggtgggaatttttgagtaatccgaattggtcgacaagttcanaggtaa
tatatctaattgaaaataaatatagttgttca

AmqKvB
gatggacagcagtgatcgttgatatgtttttcttctttacaggagaattagaaacgttat
tattggctaatgtttcattcggactgcggtgctgttatatattgcgtctcttcaggttct
tccgattgaaggagaaatatatcgggttgaaggtcatgtggctggcgattttacagtcaa
aagacgaattgatgcttttagtcatctcctcgttaattctttccaccatattaggctcca
ccacatattactgtgaattggaaaatcccgtgttttcatccataccacaggcaatatggt

gggccattattaccatgacgactgtgggatatggtgatatatatcctatatcacctatag
ggaaatgtgtgggtacagtatgttcgctctgtggtctgttgataatctccatgcctatag
ccattatagcagctaatttcaaccaatatcaccgccagaataaacaattacagtgtatcc
ttaatgatcgataccgatcacagattaaaactaagaaagagactcacattagtggctgtt
tataaccggggtcgtatcgaccaagactgtaaatagtcatcaatgaccaaaggggggata
actaagtgctttaactgccttgaaatgatttgtaactatagctttaatgaaaggagtata
actttgtatattatgttcgtttaatcgactgatagaactcagaatgaactacgagtagta
cttattgcaatcaaaaacgtttcgttaatccattatatttgacaagacctgttcttctga
aaattgaatgaaatggattatattacactcgtcgttttgttcaataaaaacatgtgc

AmqKvC
agtatggaatgatagcaacaatgtcaataacnattcatgatggttttaaagaaaaccatt
ttacttggacaggaggcaaacctcaccattagctcaaaagtaaaccaaattatacaacat
gtttctatgataaagaagggttcattgaattttggaatatcatcctcttcaatggactcg
gaaccattgagcgtggtgttgaccactctgtaatgcttgaactcgggtaaggtttcaagg
caaaatatcacaatagataataaaatcactacaacagacaaaatagcaatcactctggca
gctgttgaactttcaggatactcaaataaaagccacatgcgtctctggaactcgttatga
ggtaatggcacctcctcttccttaatatatccttcatcctcacgaaatttttcaaatgcc
tgatcacccagttcataaaattttatctcttccgaaaacacatccaagggaacattgaca
ggccggcgtaacctgccaccactttggtaaaagtataaaattgcatcaaagctgggccta
tttcgatcaaagaaatattcatttctcaaagagtcatagtatctgttccttttgaagga
cttcccagtaatgtatgtgggaattgattcaaagtttttaactgagtttcaaaccttaat
ccgctcacatttatcacaactctttcaccacattcgtaatcttctgcagccatgccatca
cctccaggaacattaccctcctccgataatttgggaaaggatctggaatgtggagtagaa
cgattgattaacggtcttgagtaaccagctgggccgccgttgccctcaagtgctaccatg
gcggcctccattttaaaaggagtcctactt

AmqKvD
CAATCACAAGATAGATTGAACGTTACAACTGGAGATAATCACAAATTA
TGTCTTTTGGACGGCTCTTGTGGTGGGGTTCGTTGGTTTGAGGTCAGCT
CTGATGACTTTTGGCGGTGTTTTCAAAGAAATTTTATCAAAAGCAGGA
ATAATCACAATTTTTGTCTTTTTGACAGCTCTTGTGGTGGGGTTCGTCA
ACTTTTAACTTGATGGGGTATCCTAAGTCTTTTGGACATCTCTTTGTGA
ATTTGCAAGACCCAAAGTCGTCTGATTGAAAATTGGAATGGTGCAAAT
TGATGCTGTCAGTCTCCCTGATACACATAAAAAAATTTAGAAAACCAC
TTTAGGTTTTGAATTTCAAATATGACTCTCCTGTCATTAGAGTTAAAAA
TCATACGTTACCTTTGCTCCAGTAGATGAATAAGGCTCATCGAATAAA
GCCCAAATTTTTGGTTGAATTCGTTGCCAACAATTTAATTCTCCCGATT
TATATTCGTCCTCTAGACCAAACTTTTTCATGATATCCTCTTCCGTGGG
TTTATCAGTGTCCAAATCAAGGCGGTCGAGTATGGTGAGGACATCTTG
TGTATCTCGATGGCTGGTGTAAGTCATCCAGCAACACGGTTCAACCTG
GTTGGAGTCCAGTCCCCAGAATTCTAACTCCTCCTCGAAAAGAGGTCC
ACACACGTCTGTCGGGTAGTGAAGTTTCCCTGAACGATAATAATTGAG
AATTTGAGCGAACACGCCCGGATGTCTGTCGAAAAAATATTCGTTTAA
CACGGGGTCGTAGTTGGCTAACGCCTCGGTCAGCCTGGATAAGCGAGT

AGCTGGAATTTTCTTCAGGGTGGCCTTATAAGTTTCGTGCCGGATG
CCCCCTACGTTCAGTATCACACGATTGTCTGCATCAGACATATTACTCG
AGAATTCCATATTCGACATTTTCGCGTTACTATGGAAACCCAATCTTTC
CAAAAATAAATTTCTAAAATTTTACGCCCGTAAGCTTTGCCGTGTTTTG
CTTGGCTTAAGAAATGATTTTGTCATGAACACTTTTTAAAAACACTCTT
TGCATGCAGTTTTTTCACAATTCACTAATGTTGTAGTTCTTACACTATC
ATGTCAGATTTTATCATCCATTACCAAATTTTACACATCCATTTTGAAC
A

AmqKvE

TTCAAGATTATAGGTCATCCAAAGAATTTCCTTATATAATTCGATTGAG
CCTGATTAAAGACGAACCGGGCATAAATGAAGCGACAAATGTGTGGA
CATTCACGAACTGTATCTATGGCTCATCTTTTGTTCTTTTCATCACCCAT
TGTAAATGACTATTTAATTCATCTCATATTTGACCTGATTCTCCTTGAA
GCAGAAGAATATTTCTTATGTTTCAGTTCAGATACATATTCATGGATA
ATTAGGCAAGTGTGTTTTAAGTTTTTATTGGTTGTTTCCGAGAATGGGA
ATGAATTTGACACCATCCATCACTATCTAAAAATAAAACGTCACTTTA
GCATTTCAGATATCGTTGGTACTTTGGTGGAAATAAAATGTCCGGTAA
CAAAACTCACCCCGATTCTCTCAATGCATTGTTGAAGAAGAACCACCC
TAAAAGTAAAATTGCCTTTAATGTTTCTATTTCGACTGAAACACTGCTT
TTTAACGTTGGTGGTGCCAAATTTGAAACATATCGTGATACGCTATTCC
GGAACCCCGACAGTCCCTTGACGGACAATATGTTTTTGAAGAAACACT
TCAGAAAGGAACATGGTGACTATTTTTTCGATAGAGATCCCAATGTAT
TTAAATCAGTTCTGCAATATCTCCGTACCGGGCAGCTCCATCTACCATC
TTCAACTTGTGGATCAGCCATAAAAACCGAGTTGGAATTTTGGGGAGT
CGAAGAATCTACTATCGAGGATTGTTGTTGGTTGAATTATAATTCATG
GTCTCAAACTCTCGATAATCTAAAGAAGTTAGAAAAGGATCGTCAAGT
TACTATGGGGTCTATAAGACACGAGAAGCAACTAATCAGGAAATCGA
GACGTTACCTGAACAATGGTTGGCAATTCCTCAATAATCCTAATTGGA
ATCTGTGGTCAAAGGTAGGTCGCCATTTCCATACCGGTATATCAATAG
TCCATTTACAATTAGAGGTGGTGTAAAAACCCAAATAGAGGATCCGGC
TTGCATCAATCAAGACATAGCAAACCACCCACTTACATATCCATGTAA
GCATGTAAAAAATCATTTCTATTCTATGCTAATATCGCCATTCGTTGCT
TGTATGATATATCATAACAATTTTGGTCTATATTTTCAGATATACGGAG
CTATCTCAGTTATATTTGTATTCCTGTCAATATTTTCTTACGTGGCCTTT
ACTCATGAATA

B.5. Nucleotide sequences of cloned *Amphimedon queenslandica* two pore potassium channels.

Nonsynonymous differences at the two highlighted bases in each sequence result in two amino acid differences between the two sequences.

AmqK2PA

atggagaaagaggtcgagtcagaaattcctgctgttgctagcgatagagaggacagcgagagtcgtgagctaacag
aaaagccacaagaagacacagcagaggatgaagagccagaggatactgggtttgagtgttccagggcctacttcac
ccgcttattctgtaacctgaacatctacaaccaagccttcatcctatttgctcttgtaatgacatacatactcgttggtggtg
ccatatttctagcctttgagctaccggcagagacaaaacgaaatgaggccataacagcagccaatgaaacatacatta
gggccttcaacaatatagtggatcaactggtgaactttaccaacctaacagaagaggaggctatggctttagtaagga
gggtagcacagtcagccattgatgcatcaaacaatcagccgactaacaactgggagtatggatcggctatcttctttgc
cacaactgttattacaacaatcggttatggttccattgctcctgagactgatggtggacgtggtttcttcataccctatgca
ctggttggtataccctcactttgatattccttgggttcttgggacaagtacttaacaaaggagtcgaccgagccacaag
atgtctcagaagacgagttacgtttgattGgggacaaatattggtcgtatttaccatcggattggtgagcttcatcttcat
acctgctattatattcgctatcattgatgactggacctactttgaagcagtttatttcacttttgtgtctctcactacagtcggt
ttcggtgattttgttccatctgccccaaagacattccgtgggctctatcggtttagtcttatctgttggttgttccttggactt
gcattcatagccctcatcattgcccagacacaggaacggattgagaatgtgagaaagagtgttaagaaatgcagaaa
atgcataaagagaacaggaggaaagctcatgctgaggaaaaagaacaaagaaagtagcaaagataatgaaaaaac
agaagagactgaagtagagaaggagtga

AmqK2PB

atggagaaagaggtcgagtcagaaattcctgctgttgctagcgatagagaggacagcgagagtcgtgagctaacag
aaaagccacaagaagacacagcagaggatgaagagccagaggatactgggtttgagtgttccagggcctacttcac
ccgcttattctgtaacctgaacatctacaaccaagccttcatcctatttgctcttgtaatgacatacatactcgttggtggtg
ccatatttctagcctttgagctaccggcagagacaaaacgaaatgaggccataacagcagccaatgaaacatacatta
gggccttcaacaatatagtggatcaactggtgaactttaccaacctaacagaagaggaggctatggctttagtaagga
gggtagcacagtcagccattgatgcatcaaacaatcagccgactaacaactgggagtatggatcggctatcttctttgc
cacaactgttattacaacaatcggttatggttccattgctcctgagactgatggtggacgtggtttcttcataccctatgca
ctggttggtataccctcactttgatattccttgggttcttgggacaagtacttaacaaaggagtcgaccgagccacaag
atgtctcagaagacgagttacgtttgattGgggacaaatattggtcgtatttaccatcggattggtgagcttcatcttcat
acctgctattatattcgctatcattgatgactggacctactttgaagcagtttatttcacttttgtgtctctcactacagtcggt
ttcggtgattttgttccaactgccccaaagacattccgtgggctctatcggtttagtcttatctgttggttgttccttggactt
gcattcatagccctcatcattgcccagacacaggaacggattgagaatgtgagagagagtgttaagaaatgcagaaa
atgcataaagagaacaggaggaaagctcatgctgaggaaaaagaacaaagaaagtagcaaagataatgaaaaaac
agaagagactgaagtagagaaggagtga

B.6. List of two pore potassium channel sequences used in phylogenetic analyses

>AmqK2PA
>AmqK2PB
>Mmus~TASK1~O35111
>Rnor~TASK1~O54912
>Hsap~TASK1~NP~002237
>Mmus~TASK2~AAG35065
>Rnor~TASK2~CAJ76245
>Hsap~TASK2~NP~003731
>Mmus~TASK3~ABA28314
>Rnor~TASK3~AAF60229
>Hsap~TASK3~AAF63708
>Hsap~TASK4~AAK28551
>Mmus~TASK5~NP~001025463
>Rnor~TASK5~Q8R5I0
>Hsap~TASK5~AAG33127
>Dmel~TASK6~CAI72672
>Dmel~TASK7~NP~649891
>Rnor~TREK1~NP~742038
>Hsap~TREK1~NP~055032
>Mmus~TREK2~NP~084187
>Rnor~TREK2~NP~075584
>Mmus~TRAAK~NP~032457
>Hsap~TRAAK~NP~201567
>Mmus~TWIK1~NP~032456
>Rnor~TWIK1~NP~067720
>Hsap~TWIK1~NP~002236
>Mmus~TWIK2~ABA28316
>Rnor~TWIK2~NP~446258
>Hsap~TWIK2~NP~004814
>Hsap~THIK1~Q9HB14
>Rnor~THIK2~Q9ERS1
>Rnor~THIK1~Q9ERS0
>Hsap~THIK2~Q9HB15
>Hsap~TALK1~NP~115491
>Lsta~TASK~ABR37307
>Acal~K2p~AAN62847
>Mmus~KCNK2~ENSMUSP00000078416
>Rnor~KCNK4~ENSRNOP00000028704
>Mmus~KCNK7~ENSMUSP00000051278
>Rnor~KCNK7~ENSRNOP00000028197
>Hsap~KCNK10~ENSP00000310568
>Mmus~KCNK12~ENSMUSP00000053595

>C. elegans twk channels: 2-14, 18, 20, 23-26, 28, 30-37, 40, 42-46
>gi|7299176|gb|AAF54374.1| Task7 [Drosophila melanogaster]
>gi|272476968|gb|AAF54970.2| Task6 [Drosophila melanogaster]
>gi|220901687|gb|ACL82897.1| CG42340 [Drosophila melanogaster]
>gi|272505977|gb|ACZ95205.1| CG42594, isoform B [Drosophila melanogaster]
>gi|7300403|gb|AAF55561.1| CG10864 [Drosophila melanogaster]
>gi|22832064|gb|AAN09276.1| open rectifier K[+] channel 1, isoform A [Drosophila melanogaster]
>gi|157400427|gb|AAF46673.2| CG34396, isoform D [Drosophila melanogaster]
>gi|7292650|gb|AAF48048.1| CG1756 [Drosophila melanogaster]

B.7. Cloned putative potassium tetramerization domain containing (kctd) protein

B.7.1. Nucleotide sequence of AmqkctdA, a putative kctd protein

The highlighted region matches the trace file sequence AmqkctdA_1 listed in Appendix B.4

atggctgccgcaagggtgaccttgtacagttcaatggaaagctacaggcaacaaagaaaaggcaaagtcattttagtt
agggagactttgagcgaaactttagttgctgcatctgagaaactcaaagaaaacgtcgaagagttgcggttactgacg
ggtggggtagttgacgacatcactttattaagagaggatgatattctaattgctattacctcaagcacagagtcaacaag
agccacaccctcctctccgattatactaagcgacctccctgaggaccagctacccgaactcggccctcaaactgatca
aagtcatttcctccttaaaaagtgctcaaggctccttttcccctgatgctccttcacgtcatgactgggtgaggttgaatgt
aggcgggaaagtatttgccactagcagggcaaccatcacttctgatccatcctcaatgttggctagaatgtttgagtca
gattggttcagtgctacggatgactccggggcatacctcattgacaggagtcctgaatattttgagccacttctcaactt
catgagacatgggaagctcattattaacgaaggagtgaacccacagggagtgctagaggaagccaagttcttcaatg
ttactaaagctatccaaccactggaaacacttgttaagaatgaagagttctcattagctggtcatttaacaagaaaggag
ttccttcagatgatcattggttcctcctcttcttccgtccttagatgtcaaggtattaatttggaaggtgtggacctctctaac
ctcgatttaaggaacattaacttcaagtgtgctaatttaagatattgtgatttctctcacagtgatctcaccaactgtgtcctt
gagagagccgatctctcatacgctaccctcaataatgctgttcttcagtgtgttcacatgcccagagtagtcatggaag
gagcttgtttaaagaagtgcataatggatgccagcctaggagtatcgactaaccttgaaggggctaacttgaaggcag
caacttttgataacagtcagatgagttgcgtcaatctccgtcttgcgagtctcaaggggcgtgtctcaggtcctgtaac
ctccgctacgcaataatggcaggaactgatatggagaactgtgatttgcgtggctgtgatttgcagcacgctaatctca
gaggtgctaacttagctggtgttaattttgccgatatcactgccccacttcacatgtctcaaacagtaaatgttaatgtctc
ccagttgatatctcccactgagaatcttcagcaatcactagataacccttaccagatggaagcaatgataacaatgact
ga

B.7.2. Predicted amino acid sequence for AmqkctdA

MAAARVTLYSSMESYRQQRKGKVILVRETLSETLVAASEKLKENVEELR
LLTGGVVDDITLLREDDILIAITSSTESTRATPSSPIILSDLPEDQLPELGPQT
DQSHFLLKKCSRLLSPDAPSRHDWVRLNVGGKVFATSRATITSDPSSMLA
RMFESDWFSATDDSGAYLIDRSPEYFEPLLNFMRHGKLIINEGVNPQGVL
EEAKFFNVTKAIQPLETLVKNEEFSLAGHLTRKEFLQMIIGSSSSSVLRCQG
INLEGVDLSNLDLRNINFKCANLRYCDFSHSDLTNCVLERADLSYATLNN
AVLQCVHMPRVVMEGACLKKCIMDASLGVSTNLEGANLKAATFDNSQM
SCVNLRLASLKGACLRSCNLRYAIMAGTDMENCDLRGCDLQHANLRGA
NLAGVNFADITAPLHMSQTVNVNVSQLISPTENLQQSLDNPLPDGSNDNN
D

B.8. Evolutionary relationships of human potassium channel tetramerization domain containing proteins (kctd 1-21) and Amqkctd

Phylogenetic relationships were inferred using the Maximum Parsimony method with MEGA 4 software. The percentage of 500 replicate trees with the topology below is given for each branch. The tree was obtained using the Close-Neighbor-Interchange algorithm with search level 3. A) Tree inferred from full length sequences. B) Tree inferred from N-terminus only.

A

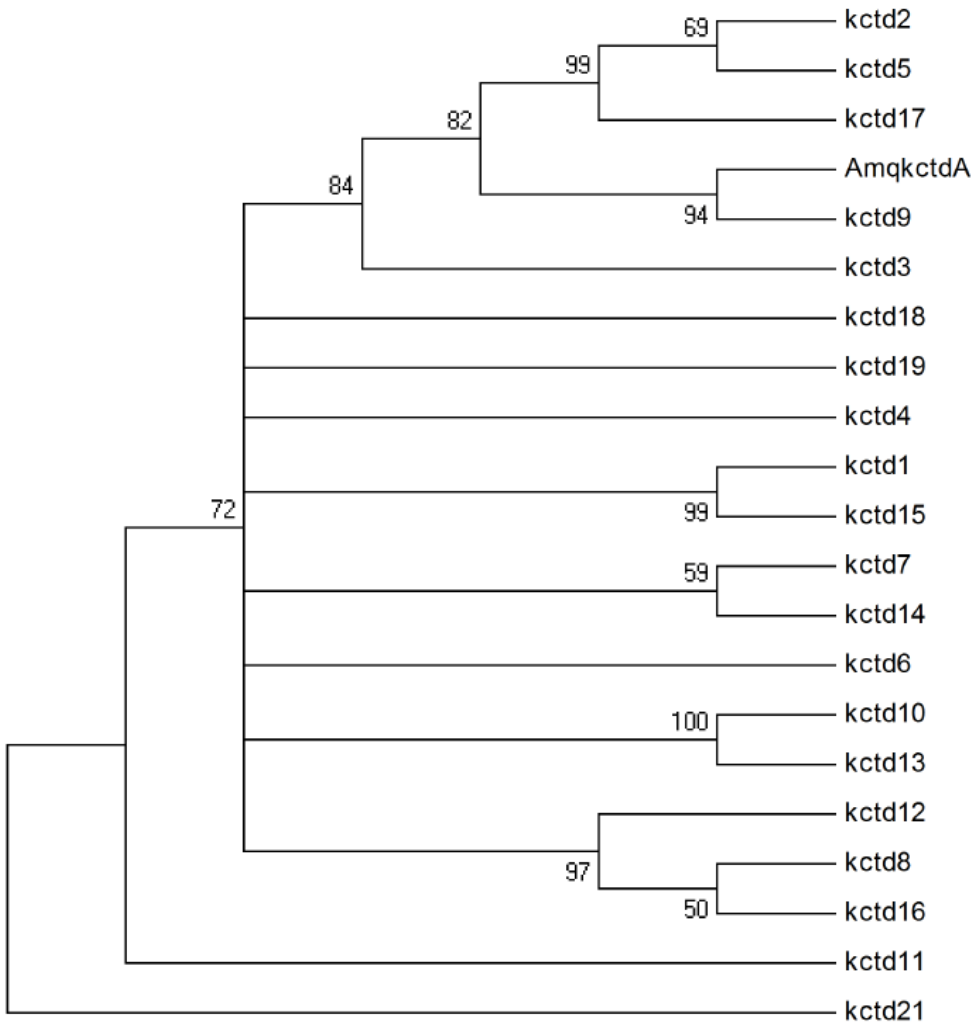

B

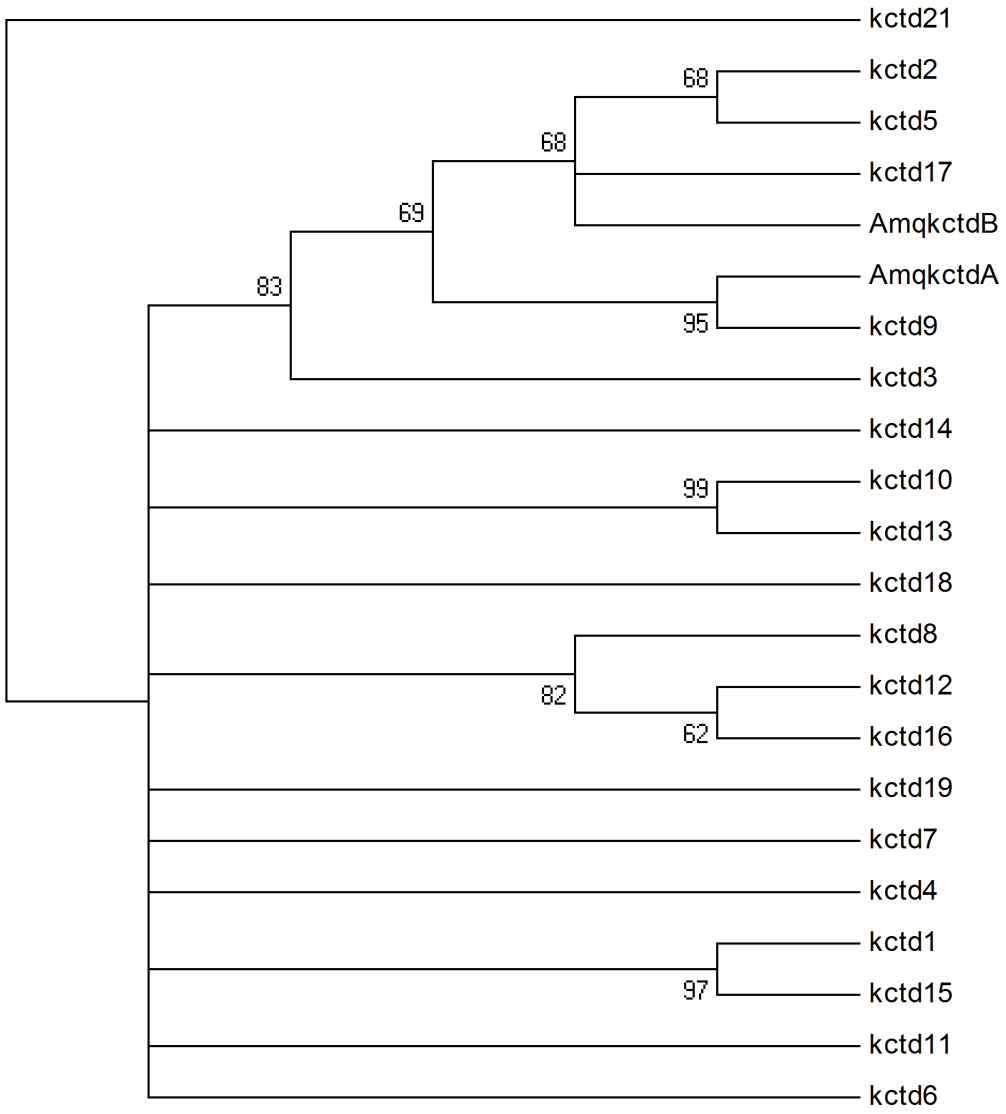
kctd21
kctd2
kctd5
kctd17
AmqkctdB
AmqkctdA
kctd9
kctd3
kctd14
kctd10
kctd13
kctd18
kctd8
kctd12
kctd16
kctd19
kctd7
kctd4
kctd1
kctd15
kctd11
kctd6
68
68
69
83
95
99
82
62
97